Physiographic Controls over Water Quality State for the Northland Region

Clint Rissmann and Lisa Pearson

Land and Water Science Report 2020/05
September 2020

Physiographic Controls over Water Quality State for the Northland Region

Prepared by
Rissmann, C., and Pearson, L.

Land and Water Science Ltd.
www.landwaterscience.co.nz
Invercargill, 9810
New Zealand

Corresponding Author
Clint Rissmann
Email: clint@landwatersci.net

Document Information
Land and Water Science Report No: 20005
Report Date: 11.09.2020
Project Number: 20003

Reviewed By: Prof. Matthew Leybourne
Organisation: Queens University, Kingston, Canada
Position: Professor - Analytical Geochemist/Hydrochemist
Review Date: 02.04.2020

Reviewed By: Dr. Ton Snelder
Organisation: Land Water People
Position: Director LWP
Review Date: 01.06.2020

Document Status: Final

Citation Advice
Rissmann, C., and Pearson, L. (2020). Physiographic Controls over Water Quality State for the Northland Region. Land and Water Science Report 2020/05. p149.

Acknowledgements

We thank Northland Regional Council's Freshwater Scientist Manas Chakraborty, Science Team Manager Jean-Charles Perquin and the broader Science and Environmental Data teams for their technical support and data provision. We thank Dr Ton Sendler of LWP for review of the statistical modelling and Professor Matthew Leybourne, Queens University, Canada, for review of the landscape relationships to hydrochemistry and water quality.

Disclaimer: This report has been prepared by Land and Water Science Ltd. (Land and Water Science) exclusively for, and under contract to Northland Regional Council. Land and Water Science accepts no responsibility for any use of, or reliance on any contents of this report by any person or organisation other than Northland Regional Council, on any ground, for any loss, damage, or expense arising from such use or reliance. Information presented in this report is available to Northland Regional Council for use from March 2020.

Table of Contents

List of Figures

List of Tables

Report

Appendices

Executive Summary

Physiographic Approach to Water Quality – Integrating Land and Water

Water quality varies in rivers and streams due to land use and variation in landscape characteristics. For example, the colour is different in water flowing from a wetland due to the high quantity of organic matter compared to water draining from a high-altitude hill-country catchment. Some waters are 'hard' due to an abundance of minerals, such as calcium and magnesium, whereas others are 'soft' because they contain only minor concentrations of these ions. Some waters contain high concentrations of sediment others do not. The reason for this variation in water composition is often due to the different characteristics of the natural landscape in addition to land use pressures.

Other landscape characteristics, such as soil type and topography, also greatly influence water quality. For example, overland flow or runoff across the land surface to waterways is more common where soils are slowly permeable and imperfectly to poorly drained. Where fine-textured and poorly drained soils dominate a farm or a catchment, the risk of runoff and associated sediment, phosphorus, and microbial loss to waterways is elevated. Where soils are permeable and well-drained, the risk of runoff occurring is lower. Here, most contaminants are removed (attenuated) during the deep percolation of water down through the soil. Although areas of well-drained soils are great at filtering out sediment, phosphorus, and microbes from water they do tend to be leakier to nitrate. Whether or not the nitrate builds up in the aquifer underlying well-drained soils will depend on the characteristics of the underlying aquifer into which it drains. Specifically, if the aquifer is comprised of materials that favour the natural removal of nitrate (denitrification), then leached nitrate is likely to be removed before reaching the stream.

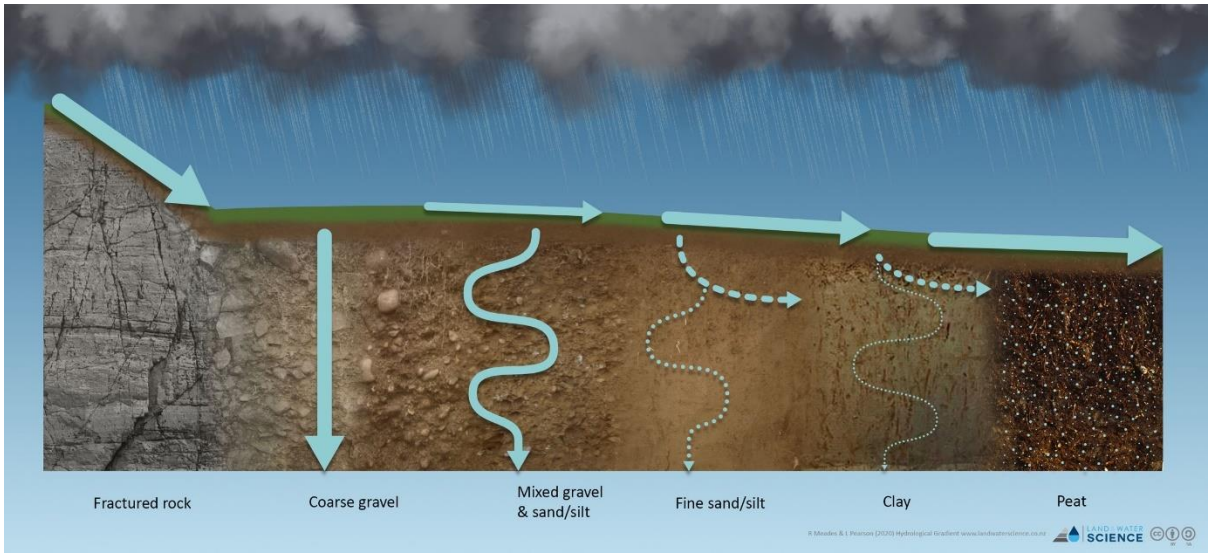

A simplified process-attribute gradient depicting the different hydrological pathway (response) water takes as slope, soil permeability, and drainage class vary.

The relationship between the processes controlling water quality (atmospheric, hydrological, redox, chemical and physical weathering) can be mapped using information about landscape characteristics (e.g. soil, geology, topography) and the chemistry of water. We name the maps of each of the dominant processes that influence water quality process-attribute gradients (PAG). Each of these maps attempts to replicate the natural gradients of the landscape that in conjunction with land use govern spatial variation in water quality. We also map the gradients of land use intensity to account for the variation in land use across the region. A total of 17 PAG (15 landscape and 2 land use) were

used for physiographic modelling of Northland's steady-state water quality. The following provides a summary of the main findings and a series of recommendations to improve further and enhance the value of the physiographic method for better understanding of the relationship between land and water.

Water Quality Drivers for Northland Rivers

The main foundation of the physiographic modelling is the 15 landscape PAG that were generated for the region (Rissmann et al., 2018a, Rissmann et al., 2018b; Rissmann et al., 2019a,b,c, McDonald et al., 2020). The PAG were developed to represent as accurately as possible the gradients in the four dominant processes that in combination with land use control water quality outcomes, specifically:

- Atmospheric
- Hydrological
- Redox (reduction-oxidation)
- Weathering processes – both physical and chemical

The development of each PAG is guided by measurement of water chemistry and quality in both ground and surface water. The chemical fingerprint of water is used to identify, extract, combine and classify landscape attributes from multiple different geospatial datasets (i.e., climatic, soil, geological). For example, groundwater hydrochemical measures are used to identify the types of rock and sediment that naturally favour the removal of nitrate within an aquifer. Surface water hydrochemistry is used to identify the likely water source by evaluating the chemical fingerprint of the water against the natural atmospheric gradients that determine rainfall volume but also its chemical composition. This is important, as specific chemicals dissolved in water can tell us about its origin and even the altitude at which the precipitation that now flows through a stream fell. For some PAG, soil geochemical and soil moisture fingerprints from next-generation radiometric and satellite datasets are used to guide the representation of the erodibility of the Northland landscape but also where and how much organic carbon (peat) is stored below the ground surface. Such information is critical for understanding why the quality of water changes from stream to stream or from place to place along a stream.

Testing PAG And Development of Water Quality Models

The main objective of the statistical modelling approach is to generate a transparent mathematical model of the 'best' relationship between PAG and/or land use and chemical fingerprint or water quality measure. There are two stages of modelling. The first uses the chemical fingerprints in water to test that the PAG do indeed represent the gradients in each dominant process. The second is dependent on the 1st stage and is when land use is incorporated to generate steady-state models of individual water quality measures.

Stage 1 utilises chemical fingerprints in the water, *not water quality measures*, to test if the PAG do indeed provide a reasonable representation of the actual atmospheric, hydrological, redox, and weathering processes gradients across the Northland Region. This is possible, as each process leaves a fingerprint within water that is measurable and interpretable. The use of chemical fingerprinting to understand the controls over water chemistry and quality forms the basis of the discipline of hydrochemistry. This testing phase is seen, as the most critical as it checks that the logic and understanding developed during the construction of each PAG is sound at a process level.

If the PAG do a reasonable job of estimating the fingerprints of each dominant process, only then is the second stage of modelling for water quality undertaken. Here, representations of land use

intensity are incorporated and combined with the 15 landscape PAG to generate models for each water quality measure using the regions 67 long term monitoring sites. Each model is comprised of an interpretable mathematical formula that links Northland's long-term State of Environment monitoring network to the landscape.

Both modelling stages employ the same machine learning or statistical modelling method that generates so-called "white box" models. These models differ from traditional "black box" models that are opaque and lack transparency about a model outcome – the model is not interpretable. The white box modelling employed is also smart enough to discard any PAG (or land use layer) that are not important predictors of a chemical fingerprint or water quality measure. It does this through billions of computations, that search for the best possible combination of PAG and/or land use that maximise accuracy and minimise the complexity of the resultant model. This type of modelling is also referred to as an 'evolutionary modelling approach' as it ultimately searches for the 'fittest' model for a given chemical fingerprint or water quality measure. During the evolution of a model, the PAG and/or land use layers that are are the most sensitive predictors are retained. Any PAG that do not both improve the accuracy and reduce the complexity of the model are discarded. The PAG retained are often predictable according to the chemical or water quality contaminant being modelled. Overly complicated, black-box models are considered by many to be a poor substitute for understanding and representing the important role of the landscape over water composition and quality.

The River Environment Classification (REC) version 2.4 was used to generate capture zones (watersheds) for each of the 67 long-term monitoring sites. The capture zones were then used to calculate mean scores for each of the 15 PAG and two land use PAG. These scores were then joined with median hydrochemical and water quality data to develop models of steady-state Total Nitrogen (TN), Ammoniacal Nitrogen (NH_4-N), Nitrate Nitrogen (NO_3-N), Dissolved Inorganic Nitrogen (DIN), Total Phosphorus (TP), Dissolved Reactive Phosphorus (DRP), microbial contamination as indicated by *E. coli,* Total Suspended Solids (TSS), clarity, and turbidity. The models developed use what is called 'cross-validation' to assess performance. Simply, the modelling approach withholds a large number of the sites, builds a model on the few sites and then tests to see if the model that has been built does a reasonable job of estimating the median values for all the withheld sites. The model switches the sites for model development in and out, after billions of calculations, seeking the best combination of sites, land use and PAGs that best estimate an individual water quality measure. The 95th percentile, and maximum values were also modelled for the regions State of Environment surface water monitoring network as per the National Objective Framework for assessing attribute state.

Modelling Results and Discussion

Assessment of measured and modelled concentrations was very good to reasonable for most water quality species. The final models for each water quality measure are a series of mathematical equations that combined different PAG, land use, and mathematical functions. The resulting equations (models) can then be used to estimate water quality across unmonitored stream reaches. To do this, capture zones (watersheds) for order 2 – 7 streams were used from REC1 (cumulative capture zones are currently unavailable for REC2.4). Mean land use and PAG scores were then calculated for each capture zone for each stream order. The relevant PAG scores were then 'plugged' into each model and an estimate of the likely steady-state water quality generated.

Model performance measures for Northland's river water quality (5-year median concentration).

	Nitrogen					Phosphorus		Sediment			Microbial
	TN	NO_3-N	DIN	TKN	TAM	TP	DRP	TSS	Turb.	Clarity	*E. coli*
Cross-validated R^2	0.86	0.80	0.84	0.75	0.76	0.67	0.69	0.70	0.79	0.65	0.61
Correlation Coefficient	0.93	0.90	0.92	0.87	0.87	0.82	0.83	0.84	0.89	0.81	0.79
Maximum Error	0.38	0.85	0.77	0.42	0.35	0.52	0.39	0.40	0.38	0.25	0.46
Mean Squared Error	0.02	0.08	0.05	0.01	0.01	0.02	0.02	0.01	0.01	0.01	0.02
Mean Absolute Error	0.10	0.20	0.17	0.06	0.08	0.09	0.10	0.08	0.07	0.05	0.11
Coefficients	8	5	8	8	7	6	6	7	6	7	7
Complexity	35	46	51	38	36	41	58	98	38	98	33

The models of steady-state water quality across the digital stream network are consistent with the underlying physiographic mapping of the region (Rissmann et al.,2018a,b; 2019b,c). Specifically, they indicate a robust spatial linkage between landscape attributes and hydrochemical signatures of the dominant processes and associated water quality outcomes. Some of the key findings of this work include:

- Nitrate nitrogen (NO_3-N), constitutes a relatively small fraction of the total TN concentration across Northland's monitoring sites (1/3rd of the TN concentration on average). Overall, Northland's NO_3-N levels are low by national standards, with reduced nitrogen species, i.e., ammoniacal and organic nitrogen, constituting the bulk of the load exported to streams. The addition of Total Kjeldahl Nitrogen to Northland's SOE test set would enable the organic nitrogen fraction to be determined and provide a better picture of the contribution of the relative N species (organic, ammoniacal, nitrate and nitrite) to regional waterways and receiving environments. The loading of organic and ammoniacal nitrogen to streams, lakes and harbours contributes to the store of potential mineralisable nitrogen in benthic sediments. Here it is important to note that organic and ammoniacal forms of nitrogen ultimately end up being mineralised to nitrate and nitrite.
- Dissolved Reactive Phosphorus exhibits a strong geological control with the highest concentrations associated with steep outcrops of Tangihua Volcanics. Basalt commonly contains higher elemental phosphorus concentrations than felsic sedimentary rock and weathers faster than felsic rock, supplying inorganic P to the river network. The spatial correlation between elevated DRP and Tangihua Volcanic Complex extends from Cape Reinga in the North to Tangihua Forest in the south, wherever the unit outcrops. However, it is also notable that there is a positive correlation between terrain ruggedness and DRP concentration derived from the Tangihua Volcanic Complex. Notably, the flat-lying Waipoua and Kerikeri flood basalts appear less implicated in DRP generation. Perhaps due to lower terrain ruggedness, mantling by siliceous materials and the development of a stable soil mantle. Other areas of moderately elevated DRP occur in association with peat and lacustrine sediments.
- Total Phosphorus (TP) also exhibits similar geological associations to DRP with respects to the Tangihua Volcanics and the peat and lacustrine rich portions of the Tauranga Formation and Karioitahi Group but not the Awhitu Group lignite. There is also evidence that land use and poorly drained soils play an important role in the distribution of the Particulate Phosphorus (PP) fraction of TP. This is consistent with overland flow and artificial drainage density being retained by the model, in addition to geological PAG. Further, PP is known to show a strong association with developed land with dissolved organic and inorganic forms

more commonly associated with natural state settings. Dune systems along Ninety Mile Beach also exhibit elevated TP but not DRP concentrations suggesting a larger particulate phosphorus export. Salt spray, redox cycling and microbial processes have been identified as key controls over PP export from dune front systems.

- There is a strong geological correlation between elevated sediment (i.e., turbidity, clarity and total suspended sediment) and soft and highly erodible lithologies as defined by the Erosion Susceptibility Classification (ESC) of Rissmann et al. (2018b). For example, the poorly lithified weak sedimentary rocks of the Northland Allochthon, including but not limited to the Punakitere Sandstone. Sediment is also elevated in relationship to depositional landforms, i.e., alluvium, peat, and lacustrine sediments of the Tauranga Group and Karioitahi Group, especially where the water table is shallow and soils poorly drained. Streams draining harder lithologies, such as the rocks of the Tangihua Volcanic Complex and Waipoua Basalt, show lower turbidity. Also notable, is that estimated sediment concentration is low across the areas of well-drained soils where surficial runoff and artificial drainage is less prevalent (e.g. across a significant area of the low relief Kerikeri flood basalts). Tributaries of the Wairoa River, including the Manganui, are identified as being particularly sediment rich.
- Highest median *E. coli* counts coincide with areas of erosion-prone land that has been developed for extensive or intensive land use. *E. coli* is also elevated across depositional landforms (floodplains etc.) where soils are poorly drained, and the local water table is shallow. For example, the majority of elevated *E. coli* counts coincide with developed sheep, beef and dairying land on highly erodible land not limited to the Punakitere Sandstone and other soft sedimentary rocks of the Northland Allochthon. The Karioitahi Group and Tauranga Group sediments are also implicated, especially where the water table is elevated, and soils are poorly drained. Questions surround the legitimacy of *E. coli* estimates for Ninety Mile Beach and from streams draining natural state catchments (i.e., Gum Fields Reserve). Otherwise, the model indicates low *E. coli* counts associated with streams draining natural state areas.
- Land use was also implicated in water quality, but overall, the influence of landscape factors was more important than land use on its own. However, due to the correlation between land use and landscape attributes, it is likely that some of the PAG are acting as surrogates for land use intensity (e.g. artificial drainage PAG). Issues of correlation can be addressed through the refinement of the land use layer and additional statistical treatment.

Water Quality State

The SoE monitoring sites were used to assess attribute state according to the National Objectives Framework (NOF) in the National Policy Statement for Freshwater Management (2017) for ecosystem health nitrate and ammonia toxicity, and human health for recreation as indicated by *E. coli*. Attribute state for ecosystem health attributes dissolved inorganic nitrogen and dissolved reactive phosphorus were also assessed according to the proposed NOF state in the draft NPSFM (2019). Attribute states for each ecosystem health and human health indicators were then assessed against the steady-state models for the digital stream network to predict state for unmonitored river reaches.

Northland steady-state results as evaluated against the National Objective Framework guidelines for freshwater management (NPSFM, 2017, 2019) indicate for nitrate toxicity all State of Environment monitoring sites are above national bottom lines (B band or better), for ammonia toxicity there is 1

site below national bottom lines (D band) during the annual maximum, and 4 sites below the ecological health national bottom line for Dissolved Inorganic Nitrogen. There are 23 sites below the national bottom line for DRP largely associated with annual medians. According to the NOF, *E.coli* is Northland's largest water quality issue with only 4 sites above the national bottom line. However, it is important to note that not all contaminants currently have NOF values to assess against. Sediment remains a pervasive and important water quality issue for the region with many of the processes controlling these issues being similar to *E.coli*.

Limitations

Limitations surrounding this work include the subset of 67 surface water monitoring sites that for pragmatic reasons are biased towards higher-order streams (≥3rd order) and larger drainage basin areas. This is relevant in terms of the use of modelling outputs to advise policy that seeks to target land use activities occurring at property scales. Specifically, most farms across the region range between 150 and 300 Ha whereas most geospatial data sets used to generate PAG were only as fine as 1:50,000 scale. However, it is important to note that the high-resolution Northland Wetness Gradient Layer (50 x 50 m and 20 x 20m data sets) and Erosion Susceptibility Classification PAG (50 x 50 m) were overall the most sensitive predictors of water quality across Northland. The retention of high-resolution datasets as the most important predictors of water quality is important, given that such layers can be used to improve the relevance of water quality modelling at property scales. Historically, the application of water quality modelling at property scales has not been possible due to the coarse nature of existing soil and geological data sets.

A limitation associated with the estimation of water quality across unmonitored areas relates to the use of REC1. Currently there is no cumulative stream order capture zones available for REC2.4 which is an essential requirement to applying physiographic models to a river network. Although the capture area difference between REC1 and 2.4 is relatively minor for SoE monitoring sites (≥3rd order), the REC 2.4 provides greater resolution over the digital stream network at lower stream orders. The greater resolution of REC 2.4 equates to a larger number of stream reaches. Therefore, when comparing between the two datasets many 1st order streams in REC1 are classified as 2nd order in REC2.4 and there are many more 1st order streams identified. As stream order and associated capture zones are assigned at points of confluence (figure below), or 'nodes' there are fewer node points in REC1.

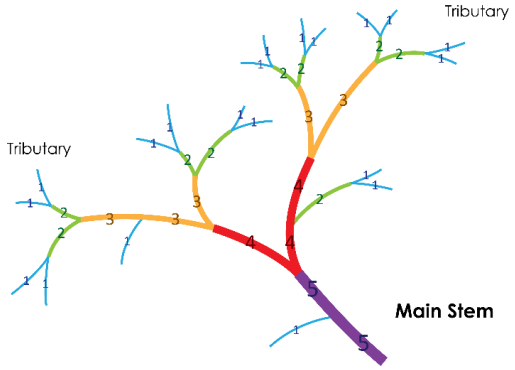

Example of a river network stream order classification. The point where two streams of the same order meet are called 'nodes'.

Therefore, the main limitation that arises when using REC1 to apply the predictive models is the smaller number of node points and hence capture zones. As the PAG models are applied to these node points, the resultant concentrations are applicable to these points but may be displayed over a longer river segment. Further work is required to generate a digital stream network that is more refined and flexible in terms of the number and accuracy of capture zones in order to maximise the value of PAG as predictors of regional water quality and providing measurement of water quality

analytes across a wider range of stream orders, and land uses (especially natural state). On its own, a higher resolution DEM will increase the certainty of capture zone delineation but will not remove the bias of applying a model calibrated on higher-order streams to low order streams. However, as an alternative, water quality models can be applied across the landscape, generating calibrated risk models for each water quality measures or for combined water quality risk. Such risk maps have the benefit of representing within capture zone variation in risk, and therefore the resolution of PAG is not limited by the architecture of REC, which was not developed with physiographic based landscape mapping in mind.

Summary

In terms of the relationship between land and water, physiographic science indicates that in addition to land use, Northland's landscape plays a critical role in determining the type and severity of water quality across the region. Physiographic modelling suggests that spatial variation in Northland's river water quality is governed primarily by the character of the landscape and to a lesser degree land use. However, these findings do not reduce the important role of land use over water quality. Instead, they indicate that the landscape attributes characteristic of a farm or catchment strongly influence the type and severity of water quality issues. The vital role of the landscape over water quality outcomes has long been recognised but often poorly characterised. As such, this work advances an overall framework that provides a better understanding of how the landscape influences water quality in addition to land use. Landscape knowledge is vital for guiding investment in mitigations that are appropriately targeted and least cost but also for generating robust policy that is relevant to land users and their communities.

Recommendations

Based on this and other work across the Northland Region, the following recommendations are made to enhance further the understanding and relevance of the region's natural resources. A key objective is to enhance the spatial and temporal resolution of datasets to underpin decision-making and ensure science outputs are more relevant at property scales. These recommendations will also likely improve the resolution and performance of the physiographic modelling undertaken to date. The main recommendations include:

Land Use

- Improving the representation of land use intensity (possibly based on livestock carrying rates, inputs or outputs) through integrating recent livestock census data released by Ministry for the Environment, Sentinel-2 based satellite (20 x 20 m) and NRC GIS consent and compliance data sets. This technical land use layer could be integrated with critical landscape attributes and pre-existing classifications of soil and geology to provide an integrated land use-water quality layer for the region.

Water Quality Monitoring

- The inclusion of monitoring across smaller order streams and natural state sites is recommended to improve the representativeness of the monitoring network for model calibration. This may include increasing the number of monitoring sites up-stream of long-term monitoring sites. However, a strategic assessment of the representativeness of monitoring relative to landscape factors and land use intensity is recommended before any investment in additional monitoring sites is made.

- In addition of Total Kjeldahl Nitrogen to Northland's SOE test set, we recommend the inclusion of chloride (Cl^-), dissolved iron (Fe^{II}), dissolved organic carbon (DOC), total alkalinity, dissolved silica ($SiO_{2(aq)}$) and potassium (K^+) to the regional monitoring test set for a period of 2 to 3 years. The main objective for including these chemical measures is to refine the understanding of the dominant processes better that in combination with land use, control water quality. Sampling of these chemical species across the flow range is critical, providing insight over the relative contribution from different geographical areas but also the compartments, i.e., surface runoff, soil, aquifer(s) that supply stream. It is worth collecting these additional measures monthly over the 2 – 3 year period. However, a seasonally targeted monitoring programme that is aligned with existing SOE monitoring runs may be sufficient if it adequately captures low, median, and high flow across the seasons.
- We strongly recommend an event sampling programme is put in place. The objective of which is to provide a more realistic picture of regional water quality. Such sampling is relevant to both steady-state and load-based measures of regional water quality. It is one of the most cost-effective ways to reduce uncertainty in water quality models attempting to estimate contaminant loads to the region's lakes, estuaries and harbours. Lower uncertainty equates to a more robust platform for decision-making. The importance of event sampling relates to the observation that the majority of a region's contaminant loads may occur in response to a handful of high flow or storm events – the majority of which are not sampled and as such not represented in regional monitoring data sets. Failing to sample such events is potentially one of the largest sources of uncertainty or error inherent in regional water quality data sets. Such a programme need not be exhaustive through focusing on the capture of 1 or 2 peak flow events per year as part of a long-term monitoring network commitment.

Landscape Attributes

- Ultimately, a finer scale digital river network and associated capture zones are required if the resolution provided by physiographic mapping is to be realised. Regional Li-DAR is the ideal platform for developing a new digital river network and associated capture zones for Northland. Such a layer would also improve regional understanding of surface water drainage at property scales, connecting farms to local drainage networks and streams. Alternatively (or in addition), water quality models can be applied to the land, generating calibrated risk maps for each individual water quality measure or one global risk model of the combined water quality risk. Such risk maps have the benefit of representing within capture zone variation in risk, and therefore the resolution of PAG is not limited by the architecture of the REC or other digital river network.

- The soil landscape is arguably the most important natural resource of any region - it forms the basis of most human endeavour. It is also a primary landscape control over water quality. Northland's regional soil survey could be significantly enhanced through the integration of radiometric survey, Li-DAR and Sentinel satellite data sets and existing soil survey. Such integration could provide more accurate maps of soil properties relevant to water quality but also primary production. This work would build on existing high-resolution classifications and data sets and enable property and in places paddock scale resolution over soil properties. Enhanced resolution over soil properties is also of benefit to water quality models making them more scalable and hence relevant to land users.

1 Introduction

In New Zealand, the physiographic method is being developed and applied nationally by Land and Water Science via several projects at local, catchment, regional, and national scales. The Our Land and Water National Science Challenge, Physiographic Environments of New Zealand (PENZ) programme has been developed to apply the physiographic method at the national scale (Rissmann et al., 2019). Under the PENZ programme, Northland Regional Council (NRC) supported the development of hydrological and redox Process-Attribute Gradient (PAG) layers for their region which required additional field sampling of surface water and groundwater hydrochemical measures to aid in the calibration process (Rissmann et al., 2018a). Northland also has two high-resolution PAG layers, erosion susceptibility classification (ESC; Rissmann et al., 2018b; McDonald et al., 2020) and wetness gradient layer (NGWL; Rissmann et al., 2019b,c) that are not available for the rest of the country.

The primary goals of the application of physiographic science at the regional scale is to attempt to provide: (i) greater understanding over 'how' and 'why' variation in water quality occurs, and (ii) to estimate steady-state water quality. Both objectives are designed to support regional council decision making as it pertains to extension, compliance, science, and policy development. For this work, the emphasis was placed on the provision of outputs for NRCs implementation of the National Policy Statement for Freshwater Management (NPSFM; Ministry for the Environment, 2014).

This report details the development of a steady-state water quality model for the Northland Region, which provides the following:

1. Current state water quality predictions for Total Nitrogen (TN), Ammoniacal Nitrogen (NH_4-N), Nitrate Nitrogen (NO_3-N), Dissolved Inorganic Nitrogen (DIN), Total Phosphorus (TP), Dissolved Reactive Phosphorus (DRP), microbial contamination as indicated by *E. coli,* Total Suspended Solids (TSS), clarity, and turbidity for each River Environment Classification (REC) reach, along with the associated percentiles (Q5, Q10, Q20, Q25, Q50, Q75, Q80, and Q95). Report *E. coli* by % exceedances >540/100mL and >260/100mL.
2. Evaluation of state against the NPS-FM at the catchment level,

Integration of flow to generate load for catchments with flow data will be presented in a separate report once flow data is available for the Northland Region.

This report builds upon earlier physiographic mapping of Northland (Rissmann et al., 2018a) and more recent, high-resolution mapping of Erosion Susceptibility (Rissmann et al., 2018b) and Wetness Gradients (Rissmann et al., 2019b,c) that include assessment of hydric soils, organic carbon stores and wetlands across the region. During the initial physiographic mapping of the region, hydrochemical evaluation of regional ground and surface water was undertaken. This included conceptualisation of the landscape controls over hydrochemical and water quality signatures. The following report builds upon the initial hydrochemical characterisation of Northland undertaken as part of the physiographic mapping of the region.

2 Physiographic Steady-State Water Quality Model

2.1 Physiographic Method for Water Quality Modelling Overview

It is widely recognised in hydrochemical and geochemical disciplines that four dominant process categories govern the composition of freshwater - atmospheric, hydrological, redox, and weathering (i.e., chemical and physical) (Moldan and Černý, 1994; Clark and Fritz, 1997; Güler and Thyne, 2004; Kendall and McDonnell, 1998; Leybourne and Goodfellow, 2010; Tratnyek et al., 2012; Rissmann et

al., 2015; Daughney et al., 2015). As such, the fundamental premise of the physiographic approach is that spatial variation in water composition (quality and hydrochemistry) can be understood by identifying and mapping the spatial coupling between *process* signals in water and the gradients in landscape *attributes* (Rissmann et al., 2016a; Rissmann et al., 2018c; Rissmann et al., 2019a). For example, spatial variation in the concentration of sodium (Na), chloride (Cl), and the stable isotopes of water (i.e., $\delta^{18}O$ and $\delta^{2}H$) in precipitation (atmospheric *process* signals) are known to be governed by altitude and distance from the coast (landscape *attributes*) (Clark and Fritz, 1997; Güler and Thyne, 2004; McMahon and Chapelle, 2008; Inamdar, 2011; Daughney et al., 2015); spatial variation in the Na, Cl, and the stable isotopes of surface and shallow groundwater (hydrological *process* signals) are known to vary according to water source and connectivity between recharge domains (landscape *attribute*) (Clark and Fritz, 1997; Kendall and McDonnell, 2008; Inamdar, 2011); spatial variation in groundwater pH, and hence alkalinity (weathering *process* signals), are governed by the acid neutralising capacity (ANC; landscape *attribute*) of soil and rock, as well as its degree of weathering (Wright, 1988; Moldan and Černý, 1994; Giller and Malmqvist, 2004; Lydersen et al., 2004; Leybourne and Goodfellow, 2010); aquifer reduction potential (redox process signals) varies according to the abundance of electron donors within an aquifer (attribute) (Krantz and Powars, 2002; McMahon and Chapelle, 2008; Rissmann, 2011; Beyer et al., 2016; Wilson et al., 2018), and; soft rock generates more sediment than hard rock (van Beek et al., 2008). Mapping the landscape attributes that govern gradients in each of these natural processes is central to the physiographic approach.

Expert knowledge and both hydrochemical and water quality signals are used to identify and test the spatial relationship between *process* signals (e.g. pH) in water and the gradients in landscape *attributes* (e.g. presence of calcareous sediments such as limestone) that govern each process. The use of measurement data is essential for:

(i) refining pre-existing maps of landscape attributes that have not been mapped with water in mind or do not contain the key attributes governing water quality outcomes

(ii) linking landscape compartments (i.e., land surface, soil, aquifer, surface waters), and

(iii) understanding the relative importance of each compartment in determining water composition and quality.

With this integrated perspective in mind, the ultimate aim of the physiographic method is to produce several process-attribute gradients (PAG) that depict the relationship between process signals in water and landscape attributes (Rissmann et al., 2018a). By mapping each dominant process known to influence water quality, it is possible to both estimate water quality but also explain, at a dominant process level, 'how' and 'why' water quality variation occurs. For example, why do water quality outcomes vary when land use intensity or type is similar? PAG can also be used to estimate the hydrochemical composition of water, including pH, alkalinity, major ions (calcium, chloride etc.) and many other measures (e.g. redox potential, water hardness). PAG can also be used to estimate hydrochemistry and water quality for natural state areas (conservation estate). The ability to explain why water quality varies differentiates the physiographic approach from other water quality models.

Figure 1 summarises the steps for physiographic mapping with a detailed description of the method provided in Rissmann et al. (2018c) and Rissmann et al., (2019a). First conceptual models of the drivers of variation in each dominant process are developed (Step 1) and used to generate process-attribute gradients (PAG) for each process (Steps 2 and 3, Table 1). The PAG are then tested against hydrochemical measures to assess whether they are spatially representative of each process category – atmospheric, hydrological, biogeochemical, chemical weathering and physical weathering (Step 4). If the PAG perform well, land-use intensity layer(s) are incorporated, and water quality measures are estimated.

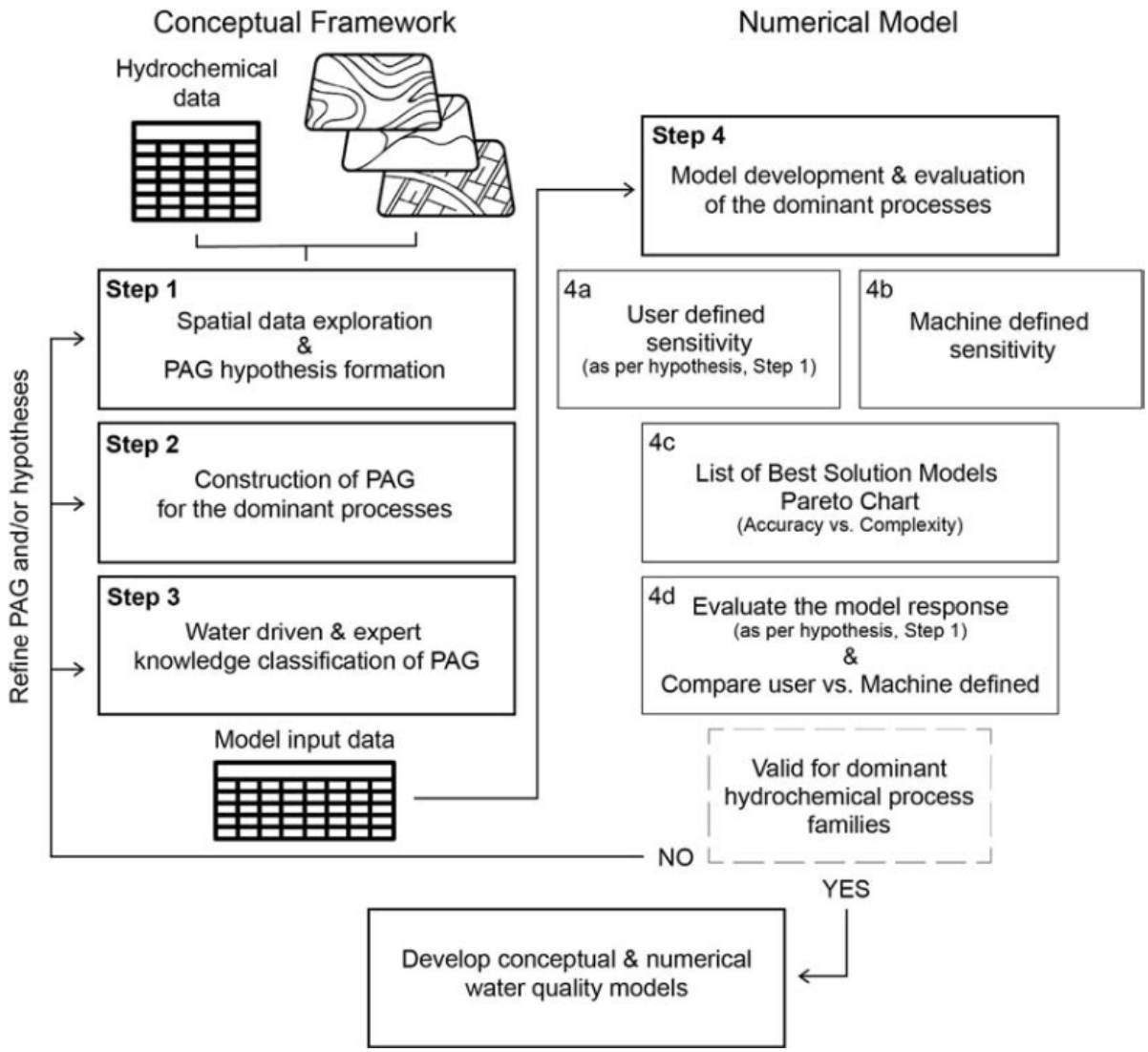

Figure 1. Key steps in the physiographic approach to water quality modelling from Rissmann et al. (2019a).

Table 1: Summary of Process Attribute Gradients represented in the Northland Water Quality Model.

Process	Role	Controlling Factor	Process Attribute Gradient	Scale	Data Scale
Atmospheric	The deposition of marine aerosols (wet and dry) and the stable isotopes of water under the local climatic setting, prior to redistribution by the hydrological network.	Topographic controls of elevation and distance from coast over δ^2H-H_2O and δ^2H-H_2O signatures and marine aerosol (Na^+, Cl^-, Br^-, B, Mg^{+2}, SO_4^{-2}) loading.	Precipitation (PPT), Stable isotope of oxygen (O18)	Macro (1,000 - 10,000 km^2)	Regional scale
Hydrological	The transport and mixing of solutes and particulates by water through the surface water and shallow groundwater network (where present).	Topographic domains (e.g. alpine, hill, lowland) and connectivity associated with distinct hydrological tracer signatures in surface waters and groundwaters.	Recharge domain (RCD)	Meso to Macro (1 - 1,000 km^2)	Regional scale higher order stream network and aquifers
		Soil series scale hydrological pathways occurring within recharge domains.	Overland flow (OLF), Deep drainage (DD), Lateral drainage (LAT), Natural soil bypass (NBP), Artificial drainage (ART)	Micro (0.01 - 10 km^2)	Soil polygon for 1:50,000 maps
		Catchment hydrological, organic carbon and seasonality of wetness classification, and depth to water table	Northland Wetness Gradient (NWGL), Equilibrium water table depth (EWT)	Sub-micro (10^{-6} - 10^{-5} km^2)	0.25 – 1 ha
		Property and paddock flow paths associated small scale drainage basins (<10 ha) and associated low order ephemeral, intermittent, and perennial streams.	Vector (riverlines)	Sub-micro (10^{-6} - 10^{-5} km^2)	Low order stream network
Redox	Low temperature (<35°C), microbially mediated succession of terminal electron species ('redox') in unsaturated zone (soil) and saturated zone (aquifer) materials.	Soil redox potential associated with soil drainage class, redox indicators (mottling and gleying) and carbon content.	Soil reduction potential (SRP), Northland Wetness Gradient (NWGL)	Micro (0.01 - 10 km^2)	Soil polygon for 1:50,000 maps
		Lithological-scale electron donor abundance of subsurface geology.	Geological reduction potential (GRP)	Meso to Macro (10 – 10,000 km^2)	Geological polygon for 1:50,000 - 1:250,000 maps
Weathering	Chemical: The Acid Neutralisation Capacity (ANC) of unsaturated zone and saturated zone materials (unconfined aquifers).	Lewis base concentration of soil.	Soil acid neutralisation capacity (SANC)	Micro (0.01 - 10 km^2)	Soil series polygon for 1:50,000 soil maps
		Lewis base concentration of geological materials that host aquifers.	Geological acid neutralisation capacity (GANC)	Meso to Macro (10 – 10,000 km^2)	1:50,000 - 1:250,000 geological maps
	Physical: Particulate transport to the stream network.	Inherent susceptibility of soil and geology to mass wasting and erosion susceptibility	Sediment Process Attribute Layer – erosion susceptibility class (ESC)	Sub-micro (10^{-6} - 10^{-5} km^2)	0.25 ha

2.2 Hydrochemical and Water Quality Data for Model Input

Northland Regional Council provided L&WS with all surface hydrochemistry and water quality data collected between 1986 and 2019 for 68 sites (n=11,673 samples). The sites have State of Environment (SOE) water quality monitoring and/or hydrochemical measures (PENZ) collected for physiographic application to the region (Rissmann et al., 2018a). Figure 3 shows the location of the sites and associated capture zone and site name, location, and available water quality measures in Table 2.

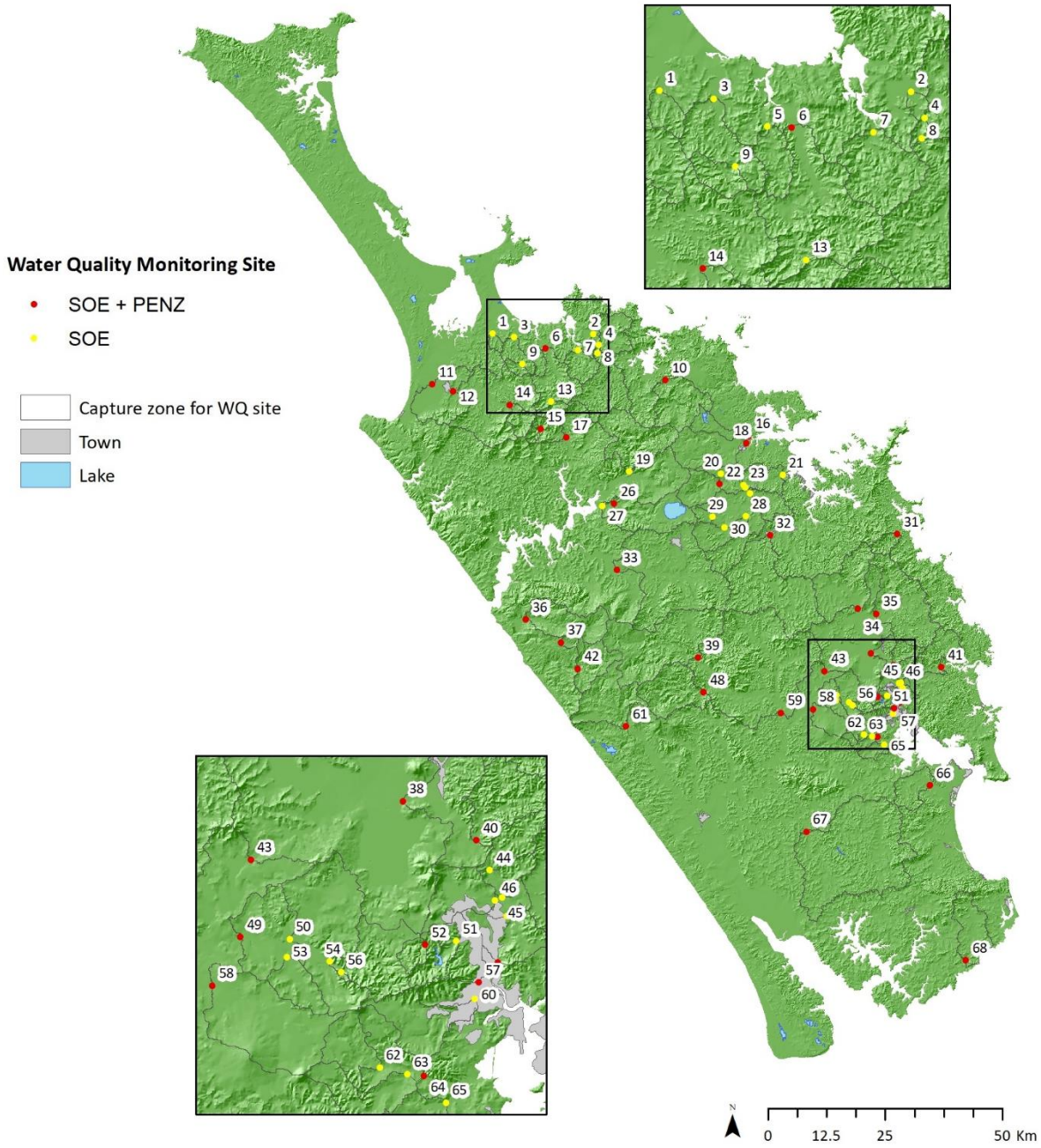

Figure 2: Northland surface water quality monitoring sites and associated capture zones. Sites with State of Environment (SOE) data and PENZ test set are shown in red and sites with SOE data only are shown in yellow (See Table 2 for site names). Capture zones for each monitoring point are also displayed as grey outlines.

Table 2: Surface water quality site reference. PENZ indicates where the extended suite of analytes for hydrologically conservative and redox sensitive species were measured, and SOE where standard water quality measures were available. No event samples were included in the steady-state model.

Site #	Site	Freshwater Management Unit	Easting	Northing	Hydrochemistry Data
1	Aurere at Pekerau Road	Doubtless Bay	1633459	6125735	SOE
2	Oruaiti at Windust Road	Doubtless Bay	1654906	6125632	SOE
3	Parapara at Taumata Road	Doubtless Bay	1638075	6125035	SOE
4	Stony at Sawyer Road	Doubtless Bay	1656071	6123396	SOE
5	Paranui at Paranui Road	Doubtless Bay	1642652	6122666	SOE
6	Oruru at Oruru Road	Doubtless Bay	1644740	6122563	PENZ and SOE
7	Kenana at Kenana Road	Doubtless Bay	1651704	6122183	SOE
8	Oruaiti at Sawyer Road	Doubtless Bay	1655830	6121640	SOE
9	Parapara at Parapara Toatoa Road	Doubtless Bay	1639905	6119265	SOE
10	Kaeo at Dip Road	Whangaroa	1670326	6115833	PENZ and SOE
11	Awanui at Waihue Channel	Awanui	1620713	6114952	PENZ and SOE
12	Awanui at FNDC take	Awanui	1625095	6113439	PENZ and SOE
13	Peria at Honeymoon Valley Road	Doubtless Bay	1645966	6111291	SOE
14	Victoria at Victoria Valley Road	Awanui	1637132	6110554	PENZ and SOE
15	Tapapa at SH1	Hokianga	1643752	6105453	PENZ and SOE
16	Waipapa at Landing	Bay of Islands	1688150	6103986	PENZ and SOE
17	Mangamuka at Iwitaua Road	Hokianga	1649247	6103622	PENZ and SOE
18	Kerikeri at Stone Store	Bay of Islands	1687631	6102447	PENZ and SOE
19	Waipapa at Forest Ranger	Hokianga	1662582	6096421	SOE
20	Waipapa at Waimate North Road	Bay of Islands	1682092	6095939	SOE
21	Waitangi at Wakelins	Hokianga	1695269	6095708	SOE
22	Waitangi at Waimate North Road	Bay of Islands	1681894	6093741	PENZ and SOE
23	Waitangi at SH10	Bay of Islands	1686946	6093563	SOE
24	Waiaruhe at Puketona	Bay of Islands	1687317	6093001	SOE
25	Mania at SH10	Bay of Islands	1688381	6091736	SOE
26	Utakura at Okaka Road	Hokianga	1659391	6089567	PENZ and SOE
27	Utakura at Horeke Road	Hokianga	1656910	6089081	SOE
28	Watercress at SH1	Bay of Islands	1687416	6086899	SOE
29	Pekepeka at Ohaeawai	Bay of Islands	1680346	6086802	SOE
30	Waiaruhe D/S Mangamutu Confluence	Bay of Islands	1682873	6084561	SOE
31	Punaruku at Russell Road	Whananaki Coast	1719724	6083074	PENZ and SOE
32	Waiharakeke at Stringers Road	Bay of Islands	1692604	6082806	PENZ and SOE
33	Punakitere at Taheke	Hokianga	1660001	6075453	PENZ and SOE
34	Waiotu at SH1	Northern Wairoa	1711381	6067240	PENZ and SOE
35	Whakapara at Cableway	Northern Wairoa	1715259	6066116	PENZ and SOE
36	Waimamaku at SH12	Waipoua	1640666	6064914	PENZ and SOE
37	Wairau at SH12	Waipoua	1648152	6060041	PENZ and SOE
38	Mangahahuru at Apotu Road Bridge	Northern Wairoa	1714117	6057720	PENZ and SOE
39	Mangakahia at Twin Bridges	Northern Wairoa	1677333	6056762	PENZ and SOE
40	Mangahahuru at Main Road	Northern Wairoa	1718886	6055192	PENZ and SOE
41	Ngunguru at Coalhill Lane	Whananaki Coast	1729072	6054775	PENZ and SOE
42	Waipoua at SH12	Waipoua	1651633	6054443	PENZ and SOE
43	Wairua at Purua	Northern Wairoa	1704273	6053948	PENZ and SOE

Site #	Site	Freshwater Management Unit	Easting	Northing	Hydrochemistry Data
44	Mangakino at Mangakino Lane	Whangarei	1719727	6053270	SOE
45	Mangakino U/S Waitaua Confluence	Whangarei	1720522	6051489	SOE
46	Waitaua at Vinegar Hill Road	Whangarei	1720066	6051317	SOE
47	Hatea at Whangarei Falls	Whangarei	1720857	6050300	SOE
48	Opouteke at Suspension Bridge	Northern Wairoa	1678503	6049460	PENZ and SOE
49	Mangere at Knight Road	Northern Wairoa	1703586	6048948	PENZ and SOE
50	Mangere at Kokopu Road	Northern Wairoa	1706785	6048813	SOE
51	Waiarohia at Whau Valley	Whangarei	1717568	6048671	SOE
52	Pukenui at Kanehiana Drive	Whangarei	1715558	6048441	PENZ and SOE
53	Mangapiu at Kokopu Road	Northern Wairoa	1706588	6047656	SOE
54	Mangere at Kara Road	Whangarei	1709388	6047363	SOE
55	Hatea at Mair Park	Northern Wairoa	1720284	6047290	PENZ and SOE
56	Mangere at Wood Road	Whangarei	1710121	6046658	SOE
57	Waiarohia at Second Avenue	Northern Wairoa	1719047	6046013	PENZ and SOE
58	Waipao at Draffin Road	Northern Wairoa	1701772	6045796	PENZ and SOE
59	Mangakahia at Titoki	Whangarei	1694999	6045028	PENZ and SOE
60	Raumanga at Bernard Street	Northern Wairoa	1718760	6044937	SOE
61	Kaihu at Gorge	Whangarei	1661946	6042161	PENZ and SOE
62	Otaika at Cemetery Road	Whangarei	1712613	6040509	SOE
63	Otakaranga at Otaika Valley Road	Whangarei	1714396	6040056	SOE
64	Otaika at Otaika Valley Raod	Whangarei	1715476	6039940	PENZ and SOE
65	Puwera at SH1	Bream Bay	1716892	6038226	SOE
66	Ruakaka at Flyger Road	Northern Wairoa	1726626	6029623	PENZ and SOE
67	Manganui at Mitaitai Road	Northern Wairoa	1700359	6019751	PENZ and SOE
68	Hakaru at Topuni	Doubtless Bay	1734330	5992416	PENZ and SOE

2.2.1 Data Quality Control and Quality Assurance

Data were inspected to identify a minimum of 5-years of sample collection across as many sites as possible. The interval between 2015 and 2019 was selected as the most representative steady-state dataset for the region. This dataset was augmented with data from 2014 for Raumanga at Bernard Street, Waiharakeke at Stringers Road, and Waipapa at Forest Ranger to achieve a 5-year record, and between 2011-2015 at Utakura at Horeke Rd.

We quantified the number of samples for each site and the total number of samples for the 5 years, 2015 – 2019[1], along with the number of censored values for each analyte (Appendix A). Overall, Total Ammoniacal Nitrogen (TAM), Nitrite Nitrogen (NO_2-N), Total Kjeldahl Nitrogen (TKN) and TN have ≥10% of censored values across all 68 sites. Notably, TAM is strongly influenced by censored values and rounding, a characteristic that is common for this analyte. By comparison, TKN is less affected by censored values and rounding and provides an integrated measure of organic and ammonaical nitrogen. For this reason, TKN is considered a better proxy for reduced forms of nitrogen. DIN also has limited values for some sites; therefore, a calculated DIN was used in this assessment by combining Nitrate Nitrite Nitrogen (NNN) and TAM measures.

Following an assessment of censored values, the raw data were inspected for outliers using cumulative probability plots (Reimann et al., 2005; Panno et al., 2006; Rissmann et al., 2018a).

[1] 6 Sites have different model period. *E. coil* measures only were augmented to achieve a minimum 60 samples across as close to a 5-year period as possible.

Cumulative probability plots of log_{10} transformed conductivity, major ions, and water quality measures identified Hatea at Mair Park and Kerikeri at Stone Store as having a significant number of samples influenced by seawater at 57 and 105 samples, respectively. Conductivity thresholds were identified at 25 mS/m at Hatea at Mari Park and 10 mS/m at Kerikeri at Stone Store above which seawater exerts a strong influence over water quality variables. Above these thresholds, TN, TKN, TP, DRP, Turbidity, and Clarity all exhibit strong inflexions associated with the mixing of ocean water. If not removed, these samples would result in misleading summary statistics (e.g., biased median, min., max., Q95 etc) and also an unrealistic estimate of load (Figure 3). The tide affects these sites predominantly over summer months when rivers are baseflow dominated. To ensure representativeness of water quality measures at baseflow, additional data was extracted from 2010-2014 for these sites that fell below each site-specific conductivity threshold (Appendix A). A check on water quality median values for a 6, 8, and 10-year intervals revealed no significant differences.

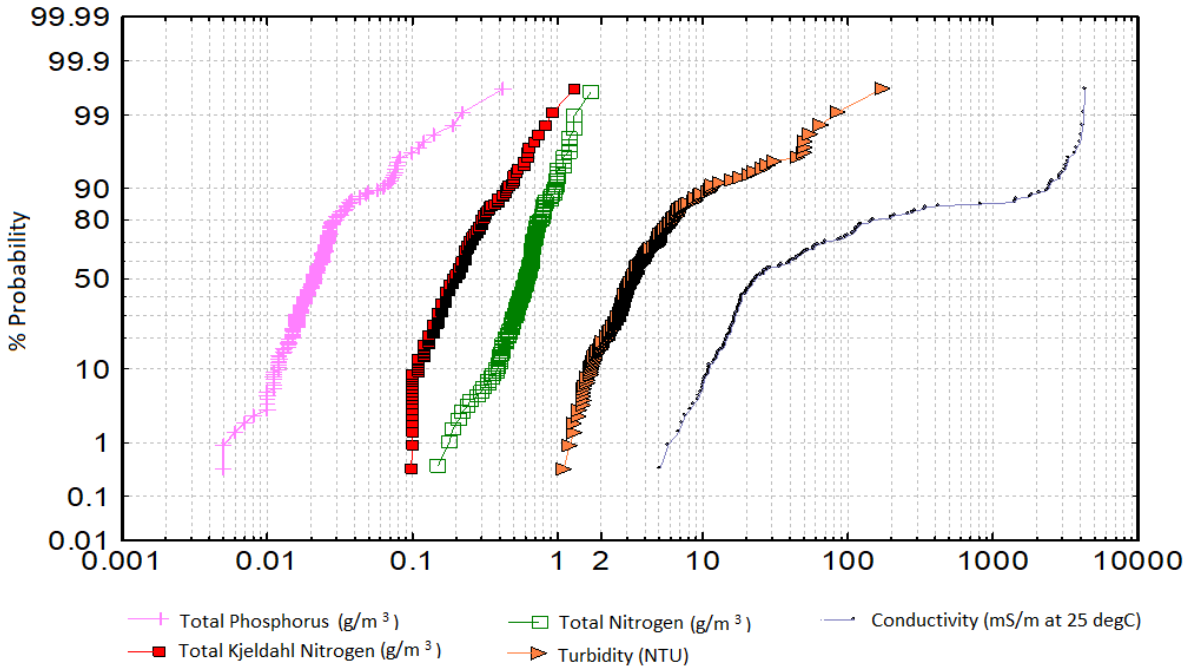

Figure 3: Cumulative probability plot of data from Hatea at Mair Park where TN, TKN, TP, and Turbidity all exhibit strong inflexions associated with the mixing of ocean water indicated by a conductivity of 25 mS/m.

The Mangapiu at Kokopu Road site was identified as an outlier based on its hydrochemical signatures (see Section 2.2.2). Specifically, strongly contrasting redox signatures that are commonly suggestive of a highly contaminated or non-representative site (i.e., the presence of elevated concentrations of both reduced and oxidised species). Discussion with Manas Chakraborty, NRC Freshwater Resource Scientist (February 2020) suggests the signatures observed at Mangapiu at Kokopu Road are due to in-stream stagnation associated with a lack of flow that appears to give rise to strong redox excursions (reducing conditions). Given the lack of flow and influence of stagnation over redox chemistry, this site is not considered representative of local conditions and as such was excluded from model development, reducing the dataset from 68 to 67 sites.

Cumulative probability plots of TSS, clarity, and turbidity also identified Otaika at Otaika Valley Road samples collected during event sampling as outliers. These 39 samples were removed from this site as not representative of routine State of Environment monitoring. Turbidity and clarity values from Punaruku at Russell Road and Waipapa at Forest Ranger were removed after personal communication with Manas Chakraborty (NRC Freshwater Resource Scientist, February 2020) due to

difficulties with sample collection at these sites likely influencing these water quality measures[2]. These outliers were excluded from model development resulting in a total of 65 sites for the turbidity and clarity models. As no other water quality measures appeared unusual, both sites were retained for modelling of other measures.

An anomalous median TAM value of 0.125 mg/L, c. 12 times higher than the overall network median, was also identified at the Waiaruhe D/S Mangamutu Confluence site. This outlier was excluded from modelling resulting in a total of 66 sites for the TAM models. No other measures appeared unusual at this site so were retained for modelling.

To assess the attribute state for *E. coli* the National Objectives Framework requires a minimum of 60 water samples over a maximum of 5-years (Ministry for the Environment, 2014). Where sites do not meet these criteria, attribute state may be determined using samples over a longer timeframe. Northland's dataset was augmented with additional samples to meet NOF criteria by including data most recent to January 2015 (i.e., December 2014 if 1 additional measure was required). Seven sites remain that do not meet the minimum sample number requirements and are to be taken as indicative only. These sites are Wairau at SH12, Punaruku at Russell Road, Tapapa at SH1, Puwera at SH1, Pukenui at Kanehiana Drive, Utakura at Okaka Bridge, and Raumanga at Bernard Street. Therefore, the data used in this analysis is different to that presented in Appendix 2.

2.2.2 Hydrochemistry and Water Quality Dataset

Following data quality control, mean, median, minimum, maximum, coefficient of variation (C.V.) and percentiles at 5, 10, 20, 25, 75, 80 and 95 were calculated for each site. Counts of repeat measures were also generated to inform the selection of analytes/measures for multivariate analysis.

Hydrochemical modelling of surface water data collected by NRC as part of the physiographic mapping of the region (see Rissmann et al. (2018a) was modelled using Geochemist Workbench software (GWB v. 14.0; Bethke, 2020) and the thermodynamic database "thermo.dat" (Delany and Lundeen, 1989). The modelling included assessment of water type (major ion facies), mineral saturation indices (e.g., 42 different mineral species), fugacity of dissolved gases (i.e., CO_2, O_2, H_2S and CH_4), redox potentials (pe or Eh), ionic strength, Total Dissolved Solids (TDS), water hardness and carbonate alkalinity. Redox category and Terminal Electron Accepting Process (TEAP) according to the Redox Assignment Workbook of Jürgen et al. (2009) had been previously calculated in Rissmann et al. (2018a) for sites with relevant data. Hydrochemical assessment is necessary for evaluating the performance of physiographic layers to replicate each dominant process known to govern water quality outcomes. Model data for each site is included in Appendix B.

2.2.3 Multivariate Analysis

Principal component analysis (PCA) was undertaken on median datasets using the recommendations of Güler et al. (2002) for hydrochemical and water quality data. This included $\log_{10}$ transformation, with the exception of pH, and z-scoring prior to analysis. PCA was applied to the following subsets of data:

- **Overall hydrochemical subset:** Total alkalinity, Carbonate alkalinity, TAM, Ca, Cl, Conductivity, DOC, DO, DRP, Mg, Mn^{II}, Fe^{II}, K, Si, Na, NNN, SO_4, TKN, TN, TP, pH, TDS, Ionic strength, Hardness; fugacities $fCH_{4(g)}$, $fCO_{2(g)}$, $fO_{2(g)}$; mineral saturation (log Q/K):

[2] Visual clarity measures at these reference sites were biased/constrained by methodology because of use of black disc equipment which was extendable up to 3 m max.

Amrph^silica, Aragonite, Calcite, Dolomite, Gypsum, Talc, Tridymite, $Fe(OH)_{3(ppd)}$, Goethite, Rhodochrosite, Siderite.

- **Redox subset:** DOC, DO, Mn^{II}, Fe^{II}, NNN, SO_4, DIN, NNN, TKN, TN, DRP, TP; pe[3] (redox potential); $fO_{2(g)}$, $fCO_{2(g)}$, $fCH_{4(g)}$ (fugacities); mineral saturation indices (log Q/K notation): $Fe(OH)_{3(ppd)}$, Rhodochrosite, Rhodonite, Siderite, Goethite, $Mn(OH)_{2(am)}$, $Mn(OH)_{3(c)}$, $MnHPO_{4(c)}$.
- **Sediment subset:** Clarity, Turbidity, *E. coli*, Turbidity Q95, Clarity Q95, and *E. coli* Q95. *E. coli* was included in this subset as it is often associated with sediment or at least is particle reactive, binding to organic and inorganic particles.

The PCA outputs for each subset were interpreted, and the scores for each significant Principal Component (e.g. PC1, PC2…) appended to the data for each respective site. An Eigenvalue of ≥1 is used as the threshold for determining significance.

2.2.4 Physiographic Process Attribute Gradient (PAG) Dataset

To define each PAG for Northland, attributes were selected from several national and regional GIS datasets. This included: topography and elevation from a 13m DEM[4] combined from four international and national scale DEM models (NASA SRTM3 DEM 28 m x 28 m or 0.08 Ha, Farr et al., 2007; MERIT DEM 79 x 79 m or 0.62 Ha, Yamazaki et al., 2019; JAXA AW3D DEM 28 x 28 m or 0.08 Ha, Tadono et al., 2014; NZ School of Surveying, Otago University NZSoSDEM v1.0, 15 m x 15 m or 0.02 Ha, Columbus et al., 2011); geological attributes from the 1:250 000 geological map series (QMAP) covering Northland (Isaac, 1996; Edbrooke and Brook, 2009), and the New Zealand Land Resource Inventory (NZLRI; 1:50 000; Newsome et al., 2008; Lynn et al. 2009); soil attributes from the Fundamental Soils Layer (1:50 000; Landcare Research, 2010), land cover from the Land Cover Database (LCDBv4.1; Landcare Research, 2015), and; land use from LUCAS (Ministry for the Environment, 2016). Hydrological input data, such as catchment area was generated from the River Environment Classification (RECv2.4; Snelder and Biggs, 2002); Equilibrium Water Table after (Westerhoff, 2018; GNS Science); riverlines from RECv2.4; climate input data such as precipitation volume from the National Climate Database (Chappell, 2013), and; $\delta^{18}O\text{-}H_2O$ of precipitation from the national isoscape model of Baisden et al. (2016). Rissmann et al. (2018a) provide detail over the development of hydrological and redox PAG for the Northland Region.

Notably, Northland has two additional PAG, Erosion Susceptibility Classification (ESC; Rissmann et al., 2018b; McDonald et al., 2020) and Northland Wetness Gradient Layer (NWGL; Rissmann et al., 2019b,c) that are not available for the rest of the country. These two layers are of a higher resolution than the Our Land and Water affiliated PAG, with property, and in places, paddock scale resolution over geology, mass wasting and erosion susceptibility, organic carbon content (electron donors) and hydrological gradients. These PAG utilise digital terrain models (8 x 8 m), radiometric survey (50 x 50 m) and/or Sentinel-2 satellite (20 x 20 m) datasets to produce a data-driven classification of the landscape.

Each of the physiographic PAG listed above are built upon a conceptual understanding of the controls over each key process. For example, expert knowledge suggests the pH of water should increase as the area of calcareous (e.g. limestone, shellbeds) sediments increases within the capture zone of a monitoring site. It is reasonable to expect higher pH in surface and groundwater across areas of limestone and lower pH in areas of felsic sedimentary rock or organic deposits (peat). Such hypotheses, based on expert knowledge, are then tested against regional ground and surface water

[3] The negative logarithm of electron concentration (−log[e^-]) in a solution in mV.
[4] This combined DEM has improved vertical resolution over the national 8m DEM.

data sets and relevant geospatial layers (e.g. geological map) with a GIS. The regional exploration of the relationship between hydrochemical signatures and landscape attributes was undertaken during physiographic mapping of the Northland Region (Rissmann et al., 2018a).

This exploration phase is fundamental to the physiographic method and assesses whether the assumed variation in hydrochemistry or water quality is consistent with expectations. Here it is important to recognise that waters inherit a hydrochemical fingerprint of the environment from which they were sampled from. For example, waters sampled from an area of peat wetland tend to have elevated organic carbon concentrations, low pH, and reducing redox signatures. Waters sampled from limestone terrain tend to have elevated alkalinity, calcium, pH and water hardness.

Using, the hydrochemical fingerprints provided by ground and surface water, it is possible to infer the conditions in which the water evolved. This is important given existing geospatial layers were seldom developed with water in mind and/or may lack information over the landscape attributes most important to hydrochemical and water quality signatures. For example, calcareous sediment may not be referenced in a geological map, and yet the hydrochemical signatures suggest a strong influence over water composition. This was the case across a significant area of Southland, where the hydrochemistry indicated a strong calcareous influence within what was an alluvial aquifer system despite no reference to the presence of calcareous sediments in QMAP. However, when bore logs were interrogated from across the area, the presence of thick shell bed deposits were observed (Rissmann et al., 2016). As such, the hydrochemistry helps identify where an existing geospatial classification fails to adequately account for the most important attributes of the landscape as they pertain to water composition and quality. Where it is not possible to corroborate hydrochemical signatures against observational data, we assume the hydrochemistry to be more representative of the environment than any existing geospatial framework.

Using this philosophy, conceptual models of the drivers of variation in each dominant process are developed (Step 1) and used to generate process-attribute gradients (PAG) for each dominant process (Steps 2 and 3, Table 1). For example, for Northland 2x PAG depicting precipitation and water source were developed; 5x PAG depicting hydrological gradients; 2x depicting redox; 3x depicting chemical weathering and 1x depicting physical weathering. When combined, the various layers provide an integrated geospatial platform that, along with land use intensity, enables spatial variation in the hydrochemistry and water quality. Tables 3 - 6 provide a summary of the provenance of the PAG layers used for modelling hydrochemical and water quality variation across Northland.

Prior to the use of PAG to model water quality, the ability of PAG to replicate each dominant process gradient is evaluated using a mathematical transparent modelling approach – so called ‘white-box’ modelling. The idea is to use the model to objectively test the ability of PAG to estimate spatial variation in the hydrochemical tracers of each dominant process. Importantly, the tracers used are not strongly influenced by land use. For example, pH and alkalinity are used to test the representativeness of the PAG developed to depict regional gradients in the acid neutralisation capacity of soil and geological materials. Similar tests are undertaken to test the PAG that depict regional hydrological, redox and physical weathering gradients. In each instance, hydrochemical tracers specific to each dominant process (e.g. redox) are used to test the suitability of the PAG prior to any assessment of water quality. This is done as a final test of the fitness of the PAG to replicate each of the dominant processes, that in addition to land use, influence water quality outcomes. If the PAG respond as expected only then are they considered fit to be used for evaluation of water quality measures.

Table 3: Hydrological Process Attribute Gradient Layers.

Process attribute gradient	PAG	Sample Types	Measures	GIS Dataset(s) and resolution	PAG Scale	Data Source
Precipitation	PPT	Precipitation	Volume	Average annual rainfall 1972-2016	Macro (1,000 - 10,000 km^2)	PENZ (NIWA, Macara, 2017)
$\delta^{18}O$-H_2O precipitation	O18	Precipitation	Stable isotopes of water: $\delta^{18}O$-H_2O (V-SMOW)	$\delta^{18}O$-H_2O precipitation isoscape (4 km^2 grid)	Macro (1,000 - 10,000 km^2)	PENZ (GNS Science, Baisden et al., 2016)
Northland Recharge Domain	NRCD	Soil waters, ground and surface waters	Dissolved major ions, electrical conductivity and stable isotopes of water: Na^+, Cl^-, Br^-, $\delta^{18}O$-H_2O, δ^2H-H_2O, $\delta^{13}C$-DIC, EC, NO_3^-	Fundamental Soil Layer (1:50,000), Aquifer type and extent (1:50,000)	Meso to macro (1 - 1,000 km^2)	PENZ (Rissmann et al. 2018a)
Overland flow	OLF	OLF runoff, surface waters	Clarity, TSS	Fundamental Soil Layer (1:50,000), 8 m DEM	Micro to meso (0.01 - 1 km^2)	PENZ (Rissmann et al. 2018a)
Deep drainage	DD	Ground and surface waters	Clarity, TSS	Fundamental Soil Layer (1:50,000)	Micro to meso (0.01 - 1 km^2)	PENZ (Rissmann et al. 2018a)
Lateral drainage	LAT	Soil water, ground and surface waters	Clarity, TSS	Fundamental Soil Layer, 8m DEM	Micro to meso (0.01 - 1 km^2)	PENZ (Rissmann et al. 2018a)
Artificial drainage	ART	Soil water	Clarity, TSS, DO, NO_3^-, Mn^{2+}, Fe^{2+}, SO_4^{2-}, DOC	Fundamental Soil Layer, 8m DEM, Land Cover Database version 4.1 (1 Ha)	Micro to meso (0.01 - 1 km^2)	PENZ (Rissmann et al. 2018a)
Natural soil zone bypass	NBP	Ground water, soil artificial drainage	DO, NO_3^-, Mn^{2+}, Fe^{2+}, SO_4^{2-}, DOC	NZLRI, Fundamental Soil Layer (1:50,000)	Micro to meso (0.01 - 1 km^2)	PENZ (Rissmann et al. 2019)
Equilibrium water table	EWT	Depth to water table	Depth to unconfined aquifer	National water table model (200m grid)	Micro (1 ha)	PENZ (GNS Science, Westerhoff et al., 2018)
Northland wetness gradient layer	NWGL	Airborne Radiometric, Sentinel satellite	Radiometrics: Total Count (attenuation layer); Sentinel-2 Satellite: Modified Normal Differential Wetness Index.	Airborne radiometrics (50 m grid), Sentinel-2 satellite (20 x 20 m), digital elevation models (13 x 13 m)	Micro (≤0.25 ha)	NRC (Rissmann et al., 2019a)

DD = deep drainage (vertical soil profile drainage); LAT = lateral drainage (horizon permeable drainage); ART = artificial drainage (subsurface mole-pipe and open ditch drainage); NBP = bypass (soil moisture deficit induced cracking of clay-rich soil and bypass of the soil matrix).

Table 4: Redox Process Attribute Gradient Layers.

Process attribute gradient	PAG	Sample Types	Measures	GIS Dataset(s) and resolution	PAG Scale	Data Source
Soil Reduction Potential	SRP	Soil water, ground and surface waters	DO, NO_3^-, Mn^{2+}, Fe^{2+}, SO_4^{2-}, DOC	Fundamental Soil Layer (1:50,000)	Micro to meso (0.01 - 1 km^2)	PENZ (Rissmann et al. 2018a)
Geological Reduction Potential	GRP	Ground and surface waters	DO, NO_3^-, Mn^{2+}, Fe^{2+}, SO_4^{2-}, DOC	QMAP (1:250,000), NZLRI (1:50,000)	Meso to macro (10 – 1,000 km^2)	PENZ (Rissmann et al. 2018a)

Table 5: Weathering Process Attribute Gradient Layers.

Process attribute gradient	PAG	Sample Types	Measures	GIS Dataset(s) and resolution	PAG Scale	Data Source
S-PAL physical weathering	ESC	Airborne Radiometric, terrain analysis (TRI)	Total count, K%, eTh, eU	Airborne Radiometric (50 m grid), terrain analysis (8 m DEM)	Micro (0.25 ha)	NRC (Rissmann et al. 2018b)
Soil Acid Neutralising Capacity	Soil_pH, CEC	Soil water, ground and surface waters	pH, Ca^{2+}, DIC, bicarbonate alkalinity, carbonate alkalinity, δ^{13}C-DIC	Fundamental Soil Layer (1:50,000)	Micro to meso (0.01 - 1 km^2)	PENZ (Rissmann et al. 2019)
Geological Acid Neutralising Capacity	GANC	Ground and surface waters	pH, Ca^{2+}, DIC, bicarbonate alkalinity, carbonate alkalinity, δ^{13}C-DIC	QMAP (1:250,000), NZLRI (1:50,000)	Meso to macro (10 – 1,000 km^2)	PENZ (Rissmann et al. 2019)

Table 6: Land Use Layers.

Process attribute gradient	PAG	Sample Types	Measures	GIS Dataset(s) and resolution	PAG Scale	Data Source
Land Use Intensity	LUI	Soil water, ground and surface waters	TN, NO_3^-, TAM, TP, DRP, TSS, Clarity Turbidity, *E.coli*	LUCAS (derived from 20 m satellite)	Micro (<1 ha)	Ministry for the Environment, 2016; PENZ (Rissmann et al. 2019)
Land Use - Microbial Input	LUM	Ground and surface waters	TN, NO_3^-, TAM, TP, DRP, TSS, Clarity Turbidity, *E.coli*	LUCAS (derived from 20 m satellite)	Micro (<1 ha)	Ministry for the Environment, 2016; PENZ (Rissmann et al. 2019)

2.3 Modelling of Water Quality

The modelling phase develops mathematically transparent ('white-box') models of a system, in this case, the hydrochemical and water quality systems, that minimises both model error and complexity[5]. The modelling data sets include the mean scores for each PAG, for each of the 67 water quality monitoring site capture zones (Figure 2). The mean scores are then spatially referenced to corresponding hydrochemical and water quality measures within a spreadsheet resulting in a total of 72 data columns. Once the data has been integrated, both the water quality and PAG scores are log10 transformed[6] prior to modelling. All predictors are included, and the model left to determine which PAG to retain. Importantly, during modelling, any PAG that do not improve the accuracy nor reduce the complexity of the model are discarded. This form of multi-objective modelling seeks to produce the simplest and most accurate models, avoiding issues of undue complexity typical of boosted regression trees and other statistical modelling approaches.

There are two phases to the modelling. The first assesses whether or not the PAG provide a reasonable proxy for the actual process gradients across the region (Step 4, Figure 1). For example, do the PAG provide a reasonable depiction of the actual redox gradients across the region? During this stage, we hypothesise which PAG are likely to be retained as the most sensitive predictors of a given process signal (e.g. redox signals) as well as the expected magnitude of response. For example, we might hypothesise that the soil and geological PAG representing Northland's regional acid neutralisation gradient will be: i. the most sensitive predictors of surface water pH, calcium and alkalinity concentration, and; ii. that pH, calcium and alkalinity will exhibit a positive magnitude (they increase) across the soil and geological acid neutralisation continuum. If the model responds as hypothesised for each dominant process, it is assumed that the PAG provide a reasonable proxy for the actual process gradients.

Importantly, during this initial testing phase, land use is not included as a predictor, given that the hydrochemical tracers used to test the representativeness of each PAG are largely independent of land use. For example, the conservative hydrological tracers chloride (Cl^-) and bromide (Br^-) used to test the representativeness of the hydrological PAG are dominantly derived from marine aerosols. Any land use contribution is minor and commonly subsumed by the much larger contribution from natural sources. The same applies to the tracers of redox and chemical weathering processes.

As such, phase 1 of the modelling process provides an independent means to test each PAG against hypothesis response. If our hypothesise surrounding the sensitivity and magnitude of response for each dominant process are valid only then do, we consider the PAG to be fit for water quality modelling. Following phase 1, land use layers are included as predictors, and water quality is modelled (phase 2).

2.3.1 Choice of Modelling Approach

Given the importance of the interpretation of each model, we place significant weight upon the use of transparent or so-called 'white-box' modelling approaches. Specifically, we favour the hybrid deterministic genetic programming (HDGP) approach of Schmidt and Lipson, (2009) that is specifically designed to identify the underlying drivers of variation in complex non-linear systems (Bongard and Lipson, 2005, 2007; Schmidt and Lipson, 2008, 2010, 2011, 2015). An important feature of HDGP is that it utilises symbolic equations to represent the system being modelled (Bongard and Lipson, 2005, 2007; Schmidt and Lipson, 2009a,b, 2010, 2011, 2015). The use of symbolism differs from numeric modelling approaches, e.g. the widely used Random Forests method, in that symbolic models have explanatory value (Schmidt and Lipson, 2009b, 2015; Lu et al.,

[5] This is a multi-objective modelling approach – least complex and most accurate models are retained. Others are discarded during the evolution of the model.
[6] As pH is already in a log form it is not transformed.

2016). Whilst traditional numeric modelling approaches may have observable input-output relationships, they commonly tend to lack clarity around the 'how' and 'why' variation occurs (i.e., they are 'black-box' models).

In addition to providing greater transparency, our preference for HDGP relates to the challenge of feature selection in high-dimensional data sets. Specifically, we note that Random Forests might overlook important variables (significantly related to the response) for various reasons. For example, the work of Stijven et al. (2011) notes that although Random Forests can efficiently find important variables, it may struggle to do so when many variables are equally important. Poor discrimination of variables with similar weightings results in the sensitivity of predictors varying randomly given such variables are not recognised as truly distinct. Also, Random Forests might value a variable considerably less than expected, with correlation with spurious variables amplifying this behaviour. Stijven et al. (2011) also note that variable importance is influenced by data distribution, which can result in misinterpretation. They conclude that caution is advised when using Random Forests to decide which variables to retain, even if the dataset is known not to exhibit strong correlations or unevenly balanced data. This is because data points in leaf nodes are similar, in a nearest neighbour sense, and the variables selected by Random Forests express proximity. In comparison, the HDGP is considered by some to identify important variables more consistently if models of sufficient quality are found (Stijven et al., 2011; Icke and Bongard, 2013; Arnaldo et al., 2014; Schmidt and Lipson, 2009, 2015) more consistently.

For the above reasons symbolic modelling approaches are increasingly being used to resolve better the underlying drivers of complex, non-linear natural systems both nationally and internationally (Whigham and Crapper, 2001; Khu et al., 2001; Bolshakov, 2013; Jagupilla et al., 2010,2015; Tinnoco et al., 2015; Duran et al., 2015; Wang et al., 2016; Atiquzzaman and Kandasamy, 2016; Creaco et al., 2016; Klotz et al., 2017; Dinu et al., 2017; Chadalawada et al., 2017; Praks and Brkic, 2018; Bright et al., 2019; Rissmann et al., 2019).

2.3.2 Model objective

The main objective of HDGP is to find a mathematically transparent model of a system, in this case, the hydrochemistry and water quality systems, that minimises both model error and complexity[7]. It does this via randomly combining different mathematical building blocks (i.e., basic arithmetic operators, trigonometric, and exponential functions) and assessing which combination provides the most straightforward model (i.e., most accurate and least complex). If a combination does not improve the accuracy of an estimate nor reduce the complexity of a model, it is discarded (Khu et al., 2001; Schmidt and Lipson, 2009, 2015; Figure 4).

[7] HDGP is a multi-objective modelling approach in so much as it seeks to minimise both complexity and error.

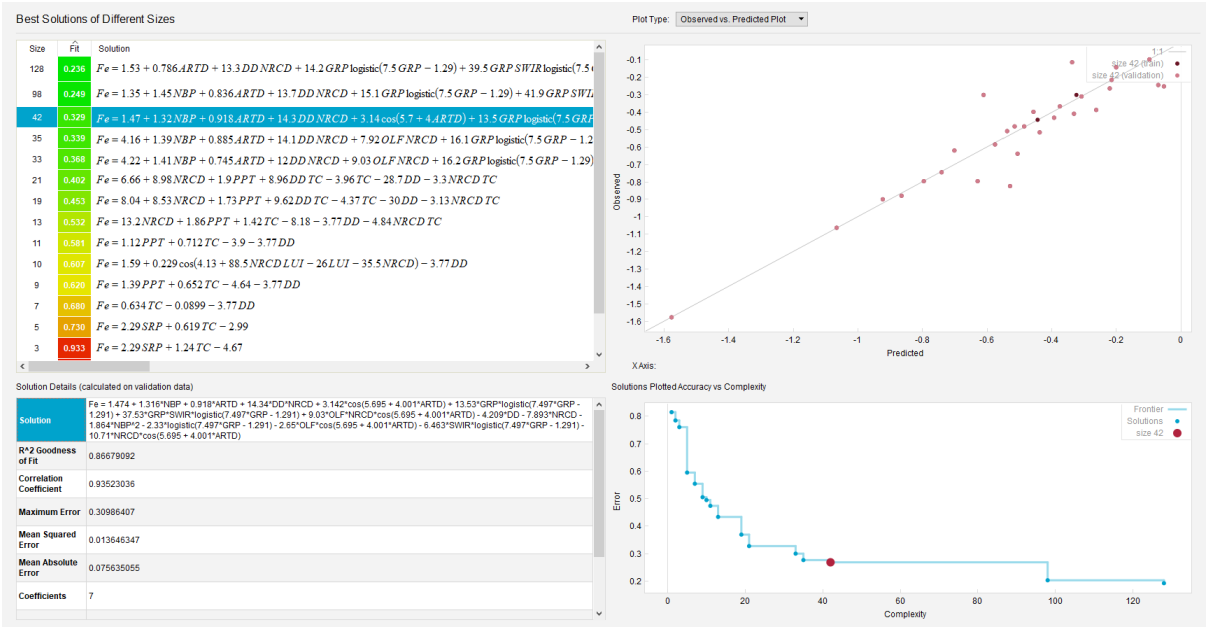

Figure 4. Example of HDGP outputs as applied to median dissolved iron (FeII) concentration across Northland's surface water SOE network. From top left to right and top to bottom are i. ensemble of best solution models ('fittest models'); ii. plot of observed versus predicted values, note training data and validation data are denoted by different shading; iii. solution details that are calculated on validation data (x-validated), and; iv. Pareto front of error versus complexity that forms the basis for model selection. The model at the 'knee' of the Prateo front is selected as the best compromise between error and complexity.

Through a process of elimination, the model converges upon the solution that 'best' defines the relationship between a set of predictors (i.e., PAG) and a target variable (e.g. a hydrochemical or water quality measure). For this reason, HDGP is described as an evolutionary algorithm where the modelling approach is conceptually like the 'survival of the fittest' theorem of evolutionary biology. The same evolutionary approach operates on the predictors, whereby any predictors that do not improve the accuracy and reduce the complexity of a model are discarded (Rissmann et al., 2019).

2.3.3 Overfitting, model selection and uncertainty

Despite the value of HDGP over conventional numerical modelling methods, the approach can be prone to overfitting. Here overfitting is avoided through the application of Pareto aware HDGP for the selection of models (see Kotanchek et al. 2007; 2010; Aho et al., 2014). Explicitly, the 'knee' of the Pareto front is used to identify the model that best represents the trade-off between complexity and accuracy. In addition to the use of Pareto front selection (Figure 4), model stability, maturity and percent convergence are used as indicators of model confidence. All models must achieve 100% convergence, with high stability and maturity scores. This sometimes requires running the models for several days or weeks, depending on the complexity and size of the data sets being modelled and the processing power of the computer being used.

In terms of model uncertainty, all performance metrics are generated via a disjunctive approach where the training and validation data sets are kept separate (e.g. 10% training: 90% validation; Schmidt and Lipson, 2009, 2015; Dubčáková, 2011). Accordingly, the performance of each model is evaluated against the measures that were withheld during model development - resulting in 'cross-validated' performance across 26 different error metrics not limited to the goodness of fit (R^2), mean absolute error (MAE), correlation coefficient (r) and model complexity.

2.3.4 Sensitivity and magnitude of response

Model outputs include measures of the sensitivity and magnitude of response of retained predictors. Here, sensitivity is defined as the relative impact within a model that a predictor variable has on the target variable. Where the model defines the numeric scores of the sensitivity of x on z for a model equation of the form z = f(x, y….), as follows:

Sensitivity = $\overline{\left|\frac{\partial z}{\partial x}\right|} \cdot \frac{\sigma(x)}{\sigma(z)}$, is evaluated at all input data points.

Positive magnitude = $\overline{\left|\frac{\partial z}{\partial x}\right|} \cdot \frac{\sigma(x)}{\sigma(z)}$, is evaluated where $\frac{\partial z}{\partial x} > 0$

Negative magnitude = $\overline{\left|\frac{\partial z}{\partial x}\right|} \cdot \frac{\sigma(x)}{\sigma(z)}$, is evaluated where $\frac{\partial z}{\partial x} < 0$

% Positive = the percent of data points where $\frac{\partial z}{\partial x} > 0$

% Negative = the number of data points where $\frac{\partial z}{\partial x} < 0$

Where:

$\frac{\partial z}{\partial x}$ is the partial derivative of z with respect to x,

$\sigma(x)$ is the standard deviation of x in the input data,

$\sigma(z)$ is the standard deviation of z,

$|x|$ denotes the absolute value of x and

$\bar{x}$ denotes the mean of x.

For the sake of clarity, Table 7 provides an example output of model sensitivity for median pH, 2015 – 2019, modelled for 789 surface water sites nationally using physiographic layers. The model has a cross-validated R^2 of 0.78. For this model, 5 of the 17 physiographic predictors were retained by the HDGP model as sensitive predictors of median pH nationally.

Table 7. Ranked sensitivity and magnitude of response, median pH.

Search	pH = f(PPT, O18, NRCD, SpH, GANC, CEC, ESC)					
Response	PAG	Sensitivity	% Positive	Positive Magnitude	% Negative	Negative Magnitude
	GANC	1.11	100%	1.11	0%	0
	ESC	0.63	100%	0.63	0%	0
	PPT	0.54	0%	0	100%	0.54
	O18	0.23	0%	0	100%	0.23
	SpH	0.04	100%	0.04	0%	0

Where GANC = Geological Acid Neutralisation Capacity; ESC = Erosion Susceptibility Classification; PPT = mean annual precipitation; O18 = precipitation source; SpH = Soil pH class.

The most sensitive predictor is Geological Acid Neutralisation Capacity (GANC) which exhibits a positive magnitude relative to pH. Specifically, median pH increases as the area of acid neutralising rock and sediment (e.g. limestone, shellbeds etc.) increase within the capture zone of a surface water monitoring site. A negative magnitude is when increases in a predictor (e.g. PPT = mean annual precipitation) lead to decreases in the target variable (e.g. pH). Where the larger the magnitude, the greater the impact the predictor has over the target variable.

Where: % positive indicates the likelihood that increasing this predictor (e.g. GANC) will increase the target variable (e.g. pH). If % positive = 70%, then 70% of the time increases in this variable lead to increases in the target variable (but the remaining 30% of the time it either decreases it or has no impact). If % positive = 0%, increases in this variable will not increase the target variable. Where the % negative indicates the likelihood that increasing this variable will decrease the target variable. If % negative = 60%, then 60% of the time increases in this variable lead to decreases in the target variable (but the remaining 40% of the time it either increases it or has no impact). If % negative = 0%, increases in this variable will not decrease the target variable.

2.3.5 Testing the Representativeness of PAGs

As per the physiographic method (Section 2.1.; Figure 1), the ability of each PAG to represent spatial variation in each dominant process is tested against tracers of each process (Rissmann et al., 2019). This step occurs prior to any assessment of the performance of PAG to estimate spatial variation in water quality indicators (N, P and *E. coli*). This step is important, as it uses hydrochemical tracers of each process to test if PAG provide a reasonable proxy for the actual process gradients. For example: the hydrological tracers Chloride (Cl), Bromide (Br) and Sodium (Na) are used to test the fitness of the atmospheric and hydrological PAG to estimate spatial variation in hydrological connectivity; redox tracers (i.e., Fe^{II}, Mn^{II}, DOC, redox-sensitive mineral saturation indices, redox potential (pe/Eh), dissolved gases) are used to test the fitness of redox and hydrological PAG to estimate spatial variation in redox; chemical weathering tracers (i.e., pH, alkalinity, major ions, mineral saturation indices, TDS, ionic strength), for chemical weathering PAG, and; physical weathering tracers (i.e., TSS, turbidity and clarity) for sediment PAG. Principal component scores for each subset and associated process are also estimated.

The rationale for excluding land-use during testing of the representativeness of PAG is that the tracers used are not dominated by a land use origin. For example, Cl, Br, and Na inputs to the environment are dominated by marine aerosolic and soil and rock weathering sources with negligible contribution from land use (Rissmann et al., 2016 and references therein). That is not to say that land use does not introduce these species to the environment, but that the magnitude of input from natural sources dwarfs any contribution from land use. The same applies to redox-sensitive species such as iron (Fe^{II}) and manganese (Mn^{II}) both of which are ubiquitous in soil and rock[8]. The same cannot be said for nitrogen, a key water quality measure, given it is tightly cycled in pristine environments. For example, national and international assessments of pre-industrial concentrations of NO_3-N in groundwater identify concentration ranges of 0.2 – 0.4 mg/L for oxidised aquifers (Rissmann, 2012 and references therein). As such, the current abundance of nitrate in the environment is strongly related to land use and requires the consideration of land use inputs for robust modelling. For this reason, nitrate nor phosphorus species are used to test the representativeness of PAG. There is a large body of research surrounding biogeochemical mass balance that provide useful context to discriminating the importance of land use over chemical species in the environment (Hem, 1984; Moldan and Černy, 1994; Evans et al., 2001; Baker et al., 2001)[9].

During testing of the representativeness of PAG, the actual sensitivity and magnitude of response of PAG over each process are evaluated against expert knowledge (Rissmann et al., 2019a). The idea is to test if the hypotheses of expected sensitivity and magnitude are consistent with the model response (Table 8). For example, does pH increase as the abundance of calcareous rock and sediment increase within the capture zone of a monitoring site?; do dissolved Fe^{II} and DOC increase

6 For example, iron is the 5th most abundant element in the earth's crust and is seldom limiting.

9 In terms of physical and chemical weathering there is a land use influence. However, we note that land use is a secondary or even tertiary control relative to variation in the inherent properties of the landscape (Rissmann et al., 2016 and references therein).

in concentration as the area of reducing soils and electron donor rich aquifers increase within a capture zone of a monitoring site?; does turbidity decrease as the area of hard rock geology increases and attendant erosion susceptibility decline? If the model responses are consistent with expert knowledge, then the PAG are considered a reasonable proxy of the actual process gradients and are subsequently regarded as fit to be used for the estimation of water quality.

Table 8. Ranked sensitivity and magnitude of response of predictors (PAG) retained for a model of median dissolved Fe (Fe^{II}) across Northland's SOE network.

Search	Fe^{II} = f(PPT, O18, NRCD, SpH, SRP, GRP, NWGL, GANC, CEC, ESC)					
Response	Variable	Sensitivity	% Positive	Positive Magnitude	% Negative	Negative Magnitude
	NGWL	0.78	100%	0.78	0%	0.00
	SRP	0.50	72%	0.59	28%	0.26
	EWT	0.13	100%	0.13	0%	0.00
	NRCD	0.11	100%	0.11	0%	0.00
	GRP	0.06	100%	0.06	0%	0.00

Where NWGL = Northland Wetness Gradient Layer; SRP = Soil Reduction Potential; EWT = Equilibrium Water Table; NRCD = Northland Recharge Domain; GRP = Geological Reduction Potential.

2.4 Principal Component Analysis

Principal Component Analysis (PCA), a common multivariate statistical tool was undertaken prior to modelling. Here it is used to provide additional context and understanding over the process signals in Northland's surface water data set. This builds on the assessment of Northland's regional hydrochemistry by Rissmann et al. (2018a) that was assessed as part of physiographic mapping of the region.

Principal component analysis (PCA) of the hydrochemical subset described in section 2.2.3 reveals six Eigenvalues that explain 93.5% of the variance in the dataset (Table 9). Of the six significant principal components (PC), PC1 and PC2 account for 73.2% of the variance in the dataset. PC1 shows positive weightings between major ions, conductivity, Ionic Strength (IS), TDS and saturation indices for common mineral species (Table 10). Specifically, IS, conductivity, and TDS are positively weighted with calcareous minerals (i.e., aragonite, calcite, dolomite and gypsum), silica minerals (i.e., amorphous silica, Chalcedony, Chrysotile, Cristobalite) and major ion concentrations. This association is consistent with the role of water-soil-rock interaction over water composition and dissolved solute load.

Table 9. Variance table for hydrochemical data subset.

Principal Component	Eigenvalue	Percent Variance (%)	Cumulative Variance (%)
1	23.9	45.9	45.9
2	14.2	27.3	73.2
3	4.2	8.1	81.3
4	2.7	5.2	86.5
5	2.1	4.1	90.7
6	1.4	2.8	93.5
7	0.8	1.6	95.1

Where cumulative variance is the proportion of the original variance explained by the components as a %.

Table 10. Eigenvectors of the hydrochemical subset, from median scores for Northland surface waters.

Analytes	PC1	PC2	PC3	PC4
Talk	0.19	0.06	0.03	-0.05
TAM	0.00	0.24	-0.04	0.01
Ca	0.17	0.12	-0.07	-0.05
Cl	0.08	0.12	0.13	0.18
Condy	0.17	0.12	0.08	0.05
DOC	-0.03	0.22	-0.15	0.08
DO	-0.01	-0.18	-0.08	0.39
DRP	0.11	0.14	0.12	0.05
Mg	0.19	0.00	0.04	-0.02
Mn^{II}	0.03	0.18	0.04	-0.23
Fe^{II}	-0.09	0.20	-0.05	0.05
K	0.01	0.23	0.04	0.09
Si	0.16	-0.06	0.25	0.08
Na	0.13	0.10	0.19	0.17
NNN	-0.01	0.14	-0.04	0.40
SO_4	0.03	0.21	-0.09	0.08
TKN	0.00	0.23	-0.11	0.09
TN	0.00	0.19	-0.04	0.33
TP	0.09	0.18	0.06	0.03
pH	0.17	-0.09	-0.20	0.01
Carbonate alkalinity	0.19	0.04	0.03	-0.08
TDS	0.18	0.08	0.10	0.02
Ionic strength	0.17	0.11	0.04	0.00
Hardness	0.18	0.10	0.01	-0.04
$fCH_{4(g)}$	0.03	0.14	-0.05	-0.06
$fCO_{2(g)}$	0.03	0.19	0.23	-0.02
$fO_{2(g)}$	0.01	-0.16	-0.14	0.41
Amrph^silica	0.15	-0.07	0.27	0.08
Aragonite	0.20	0.02	-0.11	-0.03
Calcite	0.20	0.02	-0.11	-0.03
Dolomite	0.20	0.00	-0.10	-0.02
$Fe(OH)_{3(ppd)}$	-0.07	0.21	-0.09	0.07
Goethite	-0.07	0.20	-0.08	0.07
Gypsum	0.12	0.18	-0.09	0.01
Rhodochrosite	0.18	0.06	-0.08	-0.12
Siderite	-0.04	0.24	0.06	0.01
Talc	0.19	-0.08	-0.07	0.02
Tridymite	0.15	-0.08	0.27	0.07

PC2 shows opposite weightings between DO and DOC, Mn^{II}, Fe^{II} and redox-sensitive minerals $Fe(OH)_{3(ppd)}$ and Goethite (see Figure 5). We also note a positive weighting between reduced forms of nitrogen TKN and TAM and DOC, Mn^{II} and Fe^{II}. Here it is important to note that two-thirds of Northland's nitrogen, by concentration, is organic and ammoniacal, with nitrate and nitrite making up the smaller fraction.

The role of water-soil-rock interaction over water composition (PC1) and dissolved solute and redox processes (PC2) as the dominant source of variation in hydrochemical data is well established internationally and nationally (Rissmann et al., 2015; Daughney et al., 2001, 2012, 2015). A similar pattern of redox control is observed for TP and DRP. These water quality species are indirectly influenced by the reduction of the oxides and oxyhydroxides of iron and aluminium, which are unstable under reducing conditions and release P into the environment. Colloidal forms of P, both inorganic and organic, are also important under reducing conditions and are small (nanometer), highly mobile colloidal species that are easily transported through porous media (see Rissmann et al., 2012). As documented in many hydrochemical studies, these patterns are consistent with redox controls over water composition (Rissmann, 2011; Rissmann et al., 2015; Daughney et al., 2001, 2012, 2015).

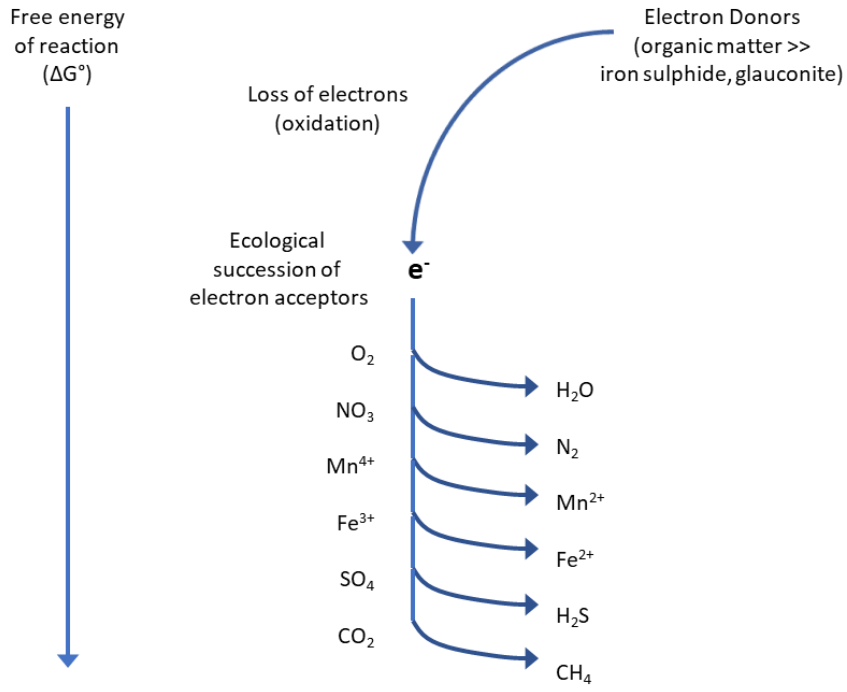

Figure 5. Ecological succession of electron-accepting processes and sequential production of final products. A decrease in free energy available to microbes occurs as each successive electron acceptor is consumed. Typically, organic matter (organic carbon) is by far the most common electron donor in groundwater but pyrite and glauconite may be locally significant (modified from McMahon and Chappelle, 2008).

The importance of water-soil-rock interaction (chemical weathering) and redox processes over hydrochemical evolution of waters is well established (Lasaga, 1984; Hem, 1985; Moldan and Černý, 1994; Fritz and Clark, 1997; Leybourne and Goodfellow, 2010; Tratnyek et al., 2012; Daughney et al., 2015). As such, it is not surprising that both of these dominant processes account for the majority (c. 73%) of variation in Northland's surface water data set. In fact, these two processes commonly account for the majority of variation in the chemical composition of waters both in New Zealand and globally (Hem, 1985; Moldan and Černý, 1994; Fritz and Clark, 1997; Tratnyek et al., 2012; Daughney et al., 2015; Rissmann et al., 2015; Rissmann and Pearson, 2018; Rissmann et al., 2016).

Focusing solely on redox, application of PCA to the redox subset described in section 2.2.3 reveals further insight. Specifically, five Eigenvalues that explain 91.8% of the variance in redox measures, with PC1 and PC2 explaining 67.1% of the total variation (Table 11).

Table 11. Variance table for redox data subset.

Principal Components	Eigenvalue	Variance (%)	Cumulative Variance (%)
1	9.5	39.4	39.4
2	6.6	27.6	67.1
3	3.1	12.9	80.0
4	1.7	6.9	86.9
5	1.2	4.9	91.8
6	0.8	3.5	95.3

Where cumulative variance is the proportion of the original variance explained by the components as a %.

The eigenvectors for the redox subset show a strong opposite weighting between DO/$fO_{2(g)}$ and DOC, Mn^{II}, Fe^{II}, fCO_2, reduced forms of nitrogen, phosphorus species and common redox-sensitive minerals (i.e., Siderite ($FeCO_3$), Goethite (α-FeO(OH)) and the poorly ordered hydroxides of iron (i.e, $Fe(OH)_{3(ppd)}$)) (Table 12). These patterns again reinforce the important role of redox processes over water composition and quality. However, it is notable that NNN is also oppositely weighted with DO. This particular relationship suggests that in addition to redox that hydrological pathway (e.g. tile drainage) and land use are also important drivers of NNN export across the region. This is consistent with land use being the major control over nitrate concentration in the environment, as discussed in section 2.3.5.

Table 12. Eigenvectors of redox subset, from median scores for Northland surface waters.

Analytes	PC1	PC2	PC3	PC4
DOC	0.2697	-0.0305	0.1189	0.1676
DO	-0.2382	-0.0462	0.3302	0.0642
DRP	0.1824	0.1918	0.0380	-0.3728
DIN	0.1974	-0.0340	0.4001	-0.1818
Mn	0.2247	0.1072	-0.2117	0.2239
Fe	0.2605	-0.1427	0.0452	0.3427
NNN	0.1840	-0.0453	0.4054	-0.1496
TKN	0.2833	0.0280	0.1440	-0.0227
TN	0.2329	-0.0404	0.3446	-0.1636
TP	0.2371	0.1638	0.0482	-0.2862
$fO_{2(g)}$	-0.2162	-0.0026	0.3784	0.1086
Eh	0.0992	-0.3490	-0.1257	-0.0566
pe	0.0731	-0.3508	-0.1398	-0.0800
$fCH_{4(g)}$	0.1428	0.0518	-0.0505	-0.0908
$fCO_{2(g)}$	0.2016	-0.0157	-0.1277	-0.3253
$fO_{2(g)}$	-0.2165	-0.0025	0.3781	0.1085
$Fe(OH)_{3(ppd)}$	0.2656	-0.0886	0.0778	0.3700
Goethite	0.2638	-0.0953	0.0725	0.3675
$Mn(OH)_{2(am)}$	0.0061	0.3768	0.0291	0.1684
$Mn(OH)_{3(c)}$	-0.0022	0.3776	0.0285	0.1645
$MnHPO_{4(c)}$	0.2246	0.2481	-0.0699	-0.0652
Rhodochrosite	0.0690	0.3666	-0.0449	0.0504
Rhodonite	-0.0108	0.3812	0.0189	0.0822
Siderite	0.3000	-0.0726	-0.0405	0.0914

Principal component 2 reveals a secondary driver of variation. Specifically, redox control between dissolved manganese (Mn^{II}), mineral forms of manganese (i.e., Rhodochrosite ($MnCO_3$), $Mn(OH)_{2(am)}$, $Mn(OH)_{3(c)}$, and $MnHPO_{4(c)}$), DRP and negative redox potentials (pe and Eh) (Table 12). These patterns revealed by PCA are consistent with expectations and are consistent with a strong redox control over the composition of Northland's surface waters.

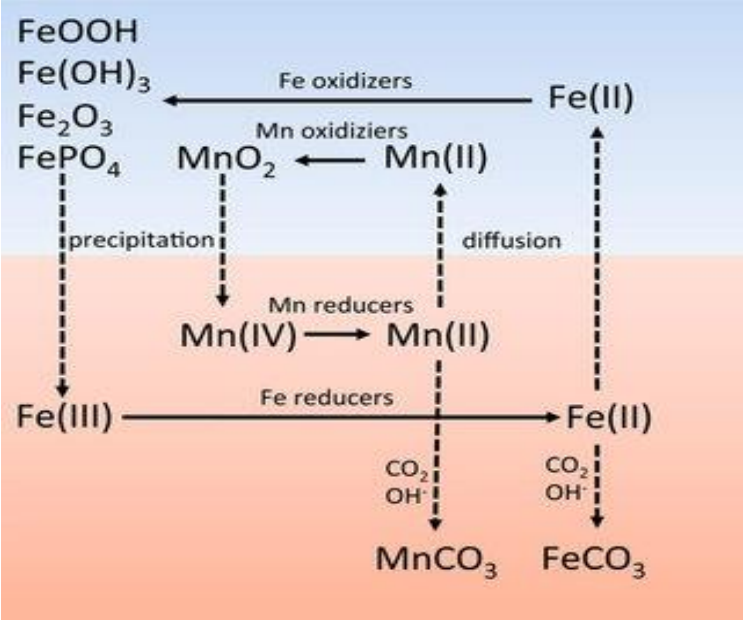

Figure 6. Manganese and iron minerals involved in redox cycling between oxic and anoxic systems (after Nealson and Saffarini 1994; modified). Reduced iron and manganese are oxidised by microorganisms under oxic conditions, precipitate as oxides and oxyhydroxides in the anoxic sediment, where they are re-mobilised by anaerobic iron and manganese reducers. Mobile Fe^{II} and Mn^{II} may then diffuse into the oxic zone or precipitate as, e.g. carbonates. Solid lines show (microbial) oxidation and reduction, dashed lines diffusion or precipitation. Besides carbonates, other poorly soluble, reduced compounds, may precipitate (not shown).

Finally, the application of PCA to the sediment subset identifies three significant eigenvalues that explain 90.6% of the variance in sediment proxies, with PC1 and PC2 explaining 74.4% of the total variance (Table 13).

Table 13. Variance table for sediment data subset.

Principal Components	Eigenvalue	Variance (%)	Cumulative Variance (%)
1	3.1	51.4	51.4
2	1.4	23.0	74.4
3	1.0	16.2	90.6
4	0.3	4.4	95.0

Where cumulative variance is the proportion of the original variance explained by the components as a %.

As expected PC1, accounting for 51.4% of the variance, shows opposite weightings for clarity and turbidity measures – high turbidity equates to low clarity (Table 14). *E. coli* is also positively weighted with turbidity and oppositely weighted with clarity. Again, this is expected with higher *E. coli* when waters are more turbid. PC2 reveals a subtler pattern of variation that includes stronger weightings

between Q95 measures and weaker weights for median measures. PC3 reveals an opposite weighting between Turbidity Q95 (most turbid) and median *E. coli*, perhaps reflecting source limitation of *E. coli* due to extended runoff Again, the underlying drivers of variance in Northland's surface water SOE data are consistent with our general understanding of the controls over water quality.

Table 14. Eigenvectors for sediment proxies.

Measure	PC1	PC2	PC3	PC4
Clarity	-0.48	0.34	0.04	-0.44
Turbidity	0.53	-0.15	-0.07	0.14
$Turbidity_{Q95}$	0.40	0.47	-0.33	0.30
$Clarity_{Q95}$	-0.45	0.39	-0.08	0.70
E. coli$_{Q95}$	0.30	0.67	-0.02	-0.41
E. coli	0.17	0.19	0.94	0.19

2.5 Dominant Process Hypotheses

From our earlier work assessing the relationships between landscape attributes and hydrochemical signatures regionally and application of PCA (section 2.4) to Northland's surface water data set we make the following hypotheses in Table 15 that are tested during phase 1 of modelling.

Table 15: High-level hypothesis over each dominant processes.

Dominant Process	Narrative	Sensitivity of PAG	Magnitude
Hydrological	Spatial variation in the indicators of water source and hydrological connectivity, i.e. the conservative hydrological tracers Cl^-, Br^- and Na^+ will be explained best by combination of the macro-scale atmospheric (O18, PPT) and recharge domain (NRCD) process-attribute gradients.	Mostly O^{18} > PPT> RCD	Cl^-, Br^- and Na^+ will exhibit a positive magnitude across the macro-scale hydrological PAG. This reflects the control of altitude and distance from the coast over marine aerosol deposition and subsequent routing of dissolved Na^+, Cl^- and Br^- by the hydrological network. Note O18 and PPT depict precipitation source and magnitude prior to redistribution by the hydrological network.
Redox	Spatial variation in redox indicators, i.e. DO, Mn^{2+}, Fe^{2+}, and DOC will be explained best by the combination of macro-scale hydrological (O18, PPT, NRCD), and meso- to microscale soil and geological redox potential (NRWGL, SRP, GRP) process-attribute gradients.	Hydrological > Redox	Mn^{2+}, Fe^{2+}, and DOC will show a positive magnitude, and DO a negative magnitude, across the macro-scale hydrological and meso-scale redox process-attribute gradients. This reflects the combined control of water source and routing (O^{18}, PPT, NRCD) and microbially mediated redox processes (NRWGL, SRP, GRP) over the speciation of redox sensitive species. Where soil drainage class and organic carbon content govern soil redox gradients and electron donor abundance and flushing govern groundwater redox gradients.
Chemical Weathering	Spatial variation in the indicators of chemical weathering, i.e., pH, Ca, Mg and total alkalinity will be explained best by combination of the macro-scale hydrological (O18, PPT, NRCD) and meso-scale weathering (SANC, GANC, ESC) process-attribute gradients.	Chemical Weathering ≥Hydrological	Total alkalinity, Ca, Mg and pH will show a positive magnitude across the meso-scale chemical weathering (SANC, GANC, ESC) and macro-scale hydrological process-attribute gradients (NRCD, O^{18}, PPT). This reflects the combined control of water routing (source and pathway) and acid neutralisation capacity of soil and geology over ANC and attendant chemical weathering. Note that the Erosion Susceptibility Classification is likely to be retained as a sensitive predictor given that some of the most erosion prone land is associated with calcareous sediments.
Physical Weathering	Spatial variation in the indicators of physical weathering, i.e. turbidity and clarity will be explained best by combination of the macro- and mesoscale hydrological (OLF, O18, PPT, RCD, ARTD, DD) and micro-scale Erosion Susceptibility (ESC) classification.	Physical Weathering ≥ Hydrological	Turbidity will exhibit a positive magnitude across the micro-scale ESC and macro-scale hydrological process-attribute gradients (O^{18}, OLF, ARTD, RCD); clarity will exhibit a negative magnitude across the macro-scale hydrological process-attribute gradients and ESC. This reflects the combined control of water source, hydrological flowpath, geological and soil susceptibility to mass wasting, erosion and sediment transport.

PAG = Process-attribute gradient; O^{18} = precipitation source prior to routing by the hydrological network; PPT = Mean Annual Precipitation; RCD = macroscale recharge domain (recharge source); OLF = % Effective Rainfall as Overland Flow; ARTD = Likely Artificial Drainage Density; DD = Deep Drainage (to aquifer); BP = bypass (soil moisture deficit induced cracking of clay-rich soil and bypass of the soil matrix); NRWGL = Northland Relative Wetness Gradient Layer; SRP = Soil Reduction Potential; GRP = geological reduction potential; SANC = Soil Acid Neutralisation Capacity; GANC = Geological Acid Neutralisation Capacity; ESC = Erosion Susceptibility.

3 Results and Discussion

This section assesses the ability of PAG to replicate the dominant process gradients that in addition to land use govern spatial variation in water quality across the region (see Figure 1 section 2.1). This forms an important component of the physiographic method and is designed to test if PAG provide a reasonable representation of the actual process gradients. Specifically, before any consideration of land use and/or water quality, we evaluate how well the PAG replicate signals of each dominant process. For example, does Cl, an excellent tracer of water source, decrease as the elevation and distance from the coast of a capture zone increases?; does dissolved iron (Fe^{II}) increase as the area of reducing soils and aquifers increase within the capture zone of a surface water monitoring point? If the PAG provide a reasonable estimate, then they are considered fit to be combined with a representation of land use and used to estimate water quality. This phase is considered amongst the most important in terms of assessing the validity of physiographic mapping as a basis for explaining 'how' and 'why' variation in water quality occurs.

3.1 Phase 1: Model Results of Spatial Representativeness of Regional PAG

The results exhibit strong performance in terms of measurement error and both the expected sensitivities and magnitude of response for the tracers of each dominant process (Tables 16 – 20). Models, model response, and performance measures for each measure or tracer are provided in Table 16 and Appendix C of this report. Below a summary of key responses is provided. As noted in the methodology, land-use intensity (LUI) is excluded from tests of representativeness.

Table 16. Assessment of the spatial representativeness of process-attribute gradients (PAG) for each dominant process against median concentrations of process-specific tracers.

	Hydrological Tracers			**Chemical Weathering Tracers**				**Redox Tracers**			**Sediment Tracers**	
Solution	Cl	Br	Na	pH	Talk.	Ca	Mg	DOC	Mn^{II}	Fe^{II}	Turbidity	Clarity
X-validated R^2	0.91	0.81	0.84	0.72	0.87	0.93	0.92	0.82	0.86	0.84	0.79	0.65
Correlation Coefficient	0.96	0.90	0.92	0.86	0.93	0.96	0.96	0.91	0.93	0.91	0.89	0.81
Maximum Error	0.09	0.16	0.15	1.62	0.22	0.19	0.19	0.25	0.35	0.34	0.38	0.25
Mean Squared Error	0.00	0.00	0.00	0.29	0.01	0.01	0.00	0.01	0.01	0.02	0.01	0.01
Mean Absolute Error	0.02	0.04	0.03	0.36	0.06	0.05	0.03	0.05	0.08	0.08	0.07	0.05
Coefficients	5	7	4	6	7	5	6	8	3	6	6	7
Complexity	31	36	55	37	37	74	54	35	45	38	38	98

The relative sensitivity and the magnitude of response of the models for the tracers of each dominant process identified for the Northland region are similar to that independently identified for Auckland, Bay of Plenty, Waikato, Manawatū, Canterbury, and Southland regions as part of the National Science Challenge, Our Land and Water, Physiographic Environments of New Zealand project (unpublished data). However, it is notable that Northland's higher resolution spatial datasets (i.e., radiometric and terrain-based erosion susceptibility classification and radiometric and sentinel satellite-based wetness gradient layers) were preferentially retained by the models at the cost of other lower resolution proxies (i.e., PAG based on 1:50,000 scale soil or geological survey data).

For example, Northland's wetness gradient layer ($NWGL_{MNDWI}$) was retained as the most sensitive predictor of dissolved iron (Fe^{II}) and the second most sensitive predictor of DOC concentrations in regional surface waters (Table 17). The HDGP modelling also identified a positive magnitude

between the $NWGL_{MNDWI}$ and both Fe^{II} and DOC concentrations, respectively across Northland's SOE network. This positive magnitude is consistent with expert knowledge that Fe^{II} and DOC concentrations increase as the abundance of organic carbon ($NGWL_{MNDWI}$) and the proportion of reducing soils (SRP) increase within the capture zone of a monitoring site (Rissmann et al., 2016; 2018a,d).

Table 17. Ranked sensitivity and magnitude of response for dissolved organic carbon (DOC)

Search	DOC = f(PPT, O18, NRCD, SpH, SRP, GRP, $NWGL_{TC}$, $NWGLM_{MNDWI}$, GANC, CEC, ESC)					
Response	Variable	Sensitivity	% Positive	Positive Magnitude	% Negative	Negative Magnitude
	SRP	1.15	81%	1.21	19%	0.87
	$NWGL_{MNDWI}$	0.67	100%	0.67	0%	0.00
	ARTD	0.51	50%	0.54	50%	0.48

Where SRP = Soil Reduction Potential; $NWGL_{MNDWI}$ = Northland Wetness Gradient Layer Modified Normalised Difference Wetness Index; ARTD = Estimated Artificial Drainage Density.

In another example, the HDGP modelling retained geological acid neutralising capacity (GANC) as the most sensitive predictor of median pH across Northland's SOE surface water network (Table 18), followed by the geologically and geochemically based ESC of Rissmann et al. (2018). The positive magnitude of the response of the model is also consistent with expectations. Namely, pH increases as the acid neutralisation capacity (ANC) of soil and geological materials increase within the capture zone of a monitoring site (Table 18). The same patterns of response were observed for Mg, Ca, alkalinity, and the saturation of carbonate minerals. This is consistent with process-level knowledge that the ANC of soil and rock materials dominate spatial variation in pH, alkalinity, dissolved calcium (Ca) and magnesium (Mg) concentrations (Rissmann et al., 2018d; Wright, 1988).

Table 18. Ranked sensitivity and magnitude of response for pH.

Search	pH = f(PPT, O18, NRCD, SpH, GANC, CEC, ESC)					
Response	PAG	Sensitivity	% Positive	Positive Magnitude	% Negative	Negative Magnitude
	GANC	1.11	100%	1.11	0%	0
	ESC	0.63	100%	0.63	0%	0
	PPT	0.54	0%	0	100%	0.54
	O18	0.23	0%	0	100%	0.23
	SpH	0.04	100%	0.04	0%	0

Where GANC = Geological Acid Neutralisation Capacity; ESC = Erosion Susceptibility Classification; PPT = mean annual precipitation; O18 = precipitation source; SpH = Soil pH class.

The Erosion Susceptibility Classification (ESC) of Rissmann et al. (2018b) was retained as a sensitive predictor of turbidity and clarity along with hydrological PAG (Table 19). Both the ESC and OLF PAG exhibit a dominantly positive magnitude, with turbidity increasing as the percent of annual precipitation occurring as OLF and ESC risk increase within a capture zone of a monitoring site. These observations are consistent with the expert understanding of the drivers of sediment generation. Well-drained soils (DD) were also retained as a sensitive predictor, with a negative magnitude of response consistent with lower levels of overland flow, a higher degree of matrix filtration and oxidising conditions. Similar behaviour was observed across Southland (Rissmann et al., 2019a).

Table 19. Ranked sensitivity and magnitude of response for turbidity (NTU)

Search	Turbidity = f(PPT, O18, NRCD, OLF, OLFDL, SRP, GRP, $NWGL_{TC}$, $NWGLM_{MNDWI}$, ARTD, DD, ESC)					
Response	Variable	Sensitivity	% Positive	Positive Magnitude	% Negative	Negative Magnitude
	OLF	4.12	97%	2.68	3%	46
	ESC	1.38	97%	1.23	3%	5.78
	$NWGL_{MNDWI}$	0.88	97%	0.53	3%	11
	O18	0.68	23%	0.23	77%	0.82
	DD	0.57	0%	0.00	100%	1

Where OLF = Overland Flow; ESC = Erosion Susceptibility Classification; $NWGL_{MNDWI}$ = Northland Wetness Gradient Layer Modified Normalised Difference Wetness Index; O18 = precipitation source; DD = Deep Drainage (soil profile drainage to an aquifer).

The most sensitive PAG retained as estimators of the hydrological tracers of water source and routing, (i.e., Cl, Br and Na), were mean annual precipitation volume (PPT), recharge domain (NRCD) (Table 20) and for bromide (Br) precipitation source (O18). The dominantly negative magnitude of response for PPT and NRCD is consistent with Cl, Br and Na concentrations decreasing as rainfall totals and recharge domain elevation (i.e., Range > Hill > Lowland) increases within a capture zone of a monitoring site.

Table 20. Ranked sensitivity and magnitude of response for chloride (Cl).

Search	Cl = f(PPT, O18, NRCD)					
Response	Variable	Sensitivity	% Positive	Positive Magnitude	% Negative	Negative Magnitude
	PPT	1.65	9%	3.80	91%	1.43
	NRCD	0.47	26%	0.51	74%	0.45

Where PPT = mean annual precipitation; NRCD = Northland Recharge Domain (i.e., rangeland, hill and lowland).

Model results are consistent with the hypothesised response of hydrochemical tracers to each PAG as outlined in Table 15.

3.2 Phase 1: Principal Components

In terms of principal components, PC1 of the hydrochemical subset defined in section 2.2.3 and discussed in section 2.4 is interpreted as reflecting water-soil-rock interaction processes. Using PC1 as the target variable, the model retained geological acid neutralisation capacity (GANC), mean annual precipitation volume (PPT), the geochemically and geologically based Erosion Susceptibility Classification (ESC) of Rissmann et al. (2018), total gamma-ray count (TC) and recharge domain (NRCD) as the most sensitive predictors (Table 21). Model performance included a cross-validated R^2 and Correlation Coefficient scores of 0.87 and a 0.93, respectively (Table 21). The retention of these PAG is consistent with the role of water-soil-rock interaction over dissolved solute load in regional rivers.

Table 21. Summary of x-validated model performance for Principal Components of the hydrochemical, redox and sediment subsets.

	$PC1_{hydrochem}$	$PC2_{redox}$	$PC1_{sediment}$	$PC2_{sediment}$
X-validated R^2	0.87	0.84	0.78	0.69
Correlation Coefficient	0.93	0.92	0.89	0.84
Maximum Error	2.52	5.10	2.35	1.80
Mean Squared Error	1.39	1.51	0.87	0.28
Mean Absolute Error	0.88	0.69	0.65	0.38
Coefficients	6	7	9	7
Complexity	26	53	44	96

The positive magnitude between both GANC and ESC and PC1 is also consistent with hypotheses (Table 22). Specifically, dissolved solute load increases as the area of calcareous and erodible sediments increase within the capture zone of a monitoring site. This is consistent with high rates of physical and chemical weathering of chemically reactive and erosion prone lithologies that also contain a significant calcareous mineral component. Here it is important to recognise that calcareous sediments weather c. six orders of magnitude faster than silicate minerals (Lasaga, 1984; Rissmann et al., 2016). As such, a relatively small proportion of calcareous sediment can have a disproportionate influence over alkalinity, pH, major ions and carbonate mineral saturation in waters (Leybourne and Goodfellow, 2010).

Also evident is that $NWGL_{TC}$ shows a negative magnitude of response (Table 22). Again, this is consistent with lower weathering rates (kinetic) for felsic rock characterised by poorly soluble minerals such as quartz and higher weathering rates for mafic lithologies (basalt etc.; see Lasaga, 1984). Precipitation volume exhibits a negative magnitude which is consistent with higher dilution rates, lower rates of water-soil-rock interaction associated with shorter water residence times that give rise to lower conductivity and TDS scores for upland stream reaches. The latter is again supported by the negative magnitude of response for Northland's recharge domains (NRCD), with more weathered and less reactive soil and sediment associated with lowland settings. The observed responses are consistent with expert knowledge and a shift from weathering to transport limited settings from upland and lowland.

Table 22. Ranked sensitivity and magnitude of response for $PC1_{wd}$ - water-soil-rock interaction, Northland surface water network.

Search: PC1wd = f(PPT, O18, NRCD, SRP, GRP, GANC, ESC, $NWGL_{TC}$, $NWGLM_{MNDWI}$)

Response	Variable	Sensitivity	% Positive	Positive Magnitude	% Negative	Negative Magnitude
	GANC	1.21	100%	1.21	0%	0
	PPT	0.82	0%	0	100%	0.82
	ESC	0.45	100%	0.45	0%	0
	$NWGL_{tc}$	0.28	0%	0	100%	0.28
	NRCD	0.19	0%	0	100%	0.19

Where GANC = Geological Acid Neutralisation Capacity; PPT = mean annual precipitation; ESC = Erosion Susceptibility Classification; $NWGL_{TC}$ = Northland Wetness Gradient Layer Total Gamma Ray Attenuation Layer; NRCD = Northland Recharge Domain.

PC2 is interpreted as reflecting microbially mediated redox processes (Table 23). The model performance included cross-validated R^2 and Correlation Coefficient scores of 0.84 and a 0.92, respectively (Table 21). Using PC2 (redox; sections 2.2.3 and 2.4) as the target variable, the model

retained $NWGL_{MNDWI}$, soil reduction potential (SRP), Equilibrium Water Table (EWT), geological reduction potential (GRP) and recharge domain (NRCD) as the most sensitive predictors (Table 23). This is consistent with expert knowledge with a positive magnitude of response for PC2 and each of the predictors. Specifically, reduced species increase as the area of organic carbon ($NWGL_{NDWI}$), reducing soils (SRP) and aquifers (GRP) increase within the capture zone of a monitoring site. Reducing signatures also increase as water table shallows. The latter is consistent with water table-driven variation in redox, longer water residence times for redox evolution and finer textured and imperfectly to poorly drained soils across lowland areas relative to upland areas.

Table 23. Ranked sensitivity and magnitude of response for PC2 - microbially mediated redox.

Search: PC2redox = f(PPT, O18, NRCD, SRP, GRP, GANC, ESC, $NWGL_{TC}$, $NWGLM_{MNDWI}$)

Response	Variable	Sensitivity	% Positive	Positive Magnitude	% Negative	Negative Magnitude
	$NWGL_{MNDWI}$	0.81626	90%	0.89549	10%	0.1032
	SRP	0.36409	100%	0.36409	0%	0
	EWT	0.28704	100%	0.28704	0%	0
	GRP	0.15438	100%	0.15438	0%	0
	NRCD	0.13314	100%	0.13314	0%	0

Where $NWGL_{MNDWI}$ = Northland Wetness Gradient Layer Modified Normalised Difference Wetness Index; SRP = Soil Reduction Potential; EWT = Equilibrium Water Table; GRP = Geological Reduction Potential; NRCD = Northland Recharge Domain.

Using PC1 as the target variable of the sediment subset, the model retained erosion susceptibility (ESC) and overland flow (OLF) as the most sensitive predictors (Table 24). The model performance included cross-validated R^2 and Correlation Coefficient scores of 0.78 and a 0.89, respectively (Table 21). The retention of ESC as by far the most sensitive predictor of PC1 is important, but we do note a split in the magnitude of response. This may relate to the inclusion of *E. coli*, whereby some of the most erodible land in Northland is associated with plantation forestry or native forest with relatively low rates of livestock and hence microbial loading. The retention of OLF and its positive magnitude is consistent with increased delivery of sediment to stream where the percent of mean annual rainfall occurring as OLF increases within a capture zone. However, it is important to note that OLF is of much lower sensitivity than ESC.

Table 24. Ranked sensitivity and magnitude of response of PC1 of the sediment subset, Northland surface water network.

$PC1_{sed}$ = f(PPT, O18, NRCD, ESC, TC, OLFDL, OLF, ARTD, NBP, $NWGL_{TC}$, $NWGL_{MNDWI}$)

Response	Variable	Sensitivity	% Positive	Positive Magnitude	% Negative	Negative Magnitude
	ESC	55.17	43%	105.14	57%	16.96
	OLF	0.18	100%	0.18	0%	0

Where ESC = Erosion Susceptibility Classification; OLF = Overland Flow.

Using PC2 as the target variable of the sediment subset, the model retained artificial drainage density (ARTD), total gamma-ray count ($NGWL_{TC}$), overland flow (OLF) and Northland recharge domain (NRCD) as the most sensitive predictors (Table 25 and Table 21). The retention of ARTD and OLF is consistent with localised soil hydrological controls over sediment generation across the

developed portions of the landscape. Bearing in mind the limitations of this model, PC2 appears to be associated with land use activities and soil drainage class.

Table 25. Ranked sensitivity and magnitude of response for PC2 sediment subset, Northland surface water monitoring network.

$PC2_{sed}$ = f(PPT, O18, NRCD, ESC, TC, OLFDL, OLF, ARTD, NBP, $NWGL_{TC}$, $NWGL_{MNDWI}$, LUI)

Response	Variable	Sensitivity	% Positive	Positive Magnitude	% Negative	Negative Magnitude
	ARTD	47.8	52%	10.5	48%	87.8
	$NWGL_{TC}$	19.6	57%	17.3	43%	22.7
	OLF	0.6	3%	0.4	97%	0.7
	NRCD	0.4	41%	0.5	59%	0.4

Where ARTD = Estimated Artificial Drainage Density; $NWGL_{TC}$ = Northland Wetness Gradient Layer Total Gamma Ray Attenuation Layer; OLF = Overland Flow; NRCD = Northland Recharge Domain.

Taking into account the limited data, the performance and response metrics of the HDGP models indicate that the PAG provide a useful approximation of the actual process gradients that, in addition to land use, govern spatial variation in water quality across the Northland Region.

3.3 Phase 2: Water Quality Model Performance

Based on the performance of PAG to estimate spatial variation in tracers of each dominant process land use was included, and steady-state water quality measures were estimated using HDGP. For each water quality model, all PAG were utilised along with two land-use layers (intensity - LUI, microbial - LUM) and the machine was left to determine the most sensitive predictors. The performance of the PAG and land-use layers to estimate spatial variation in median water quality across the 67 sites is summarised in Tables 26 and 27. The following section summarises the overall sensitivity of PAG and Appendix C provides ranked sensitivity of each water quality measure and water quality model algorithms.

Table 26. Model performance measures for median scores across Northland's water quality network.

Solution	TN	NO_3-N	DIN	TKN	TAM	TP	DRP	TSS	Turb.	Clarity	*E. coli*	DO
X-validated R^2	0.86	0.83	0.84	0.75	0.76	0.67	0.69	0.70	0.79	0.65	0.61	0.50
Correlation Coefficient	0.93	0.91	0.92	0.87	0.87	0.82	0.83	0.84	0.89	0.81	0.79	0.71
Maximum Error	0.38	0.68	0.77	0.42	0.35	0.52	0.39	0.40	0.38	0.25	0.46	0.11
Mean Squared Error	0.02	0.07	0.05	0.01	0.01	0.02	0.02	0.01	0.01	0.01	0.02	0.001
Mean Absolute Error	0.10	0.18	0.17	0.06	0.08	0.09	0.10	0.08	0.07	0.05	0.11	0.02
Coefficients	8	6	8	8	7	6	7	7	6	7	7	7
Complexity	35	46	51	38	36	41	108	98	38	98	33	37

Table 27. Model performance measures for Q95, Maximum for Total Ammoniacal Nitrogen (TAM) and Q5 for Dissolved Oxygen (DO) across Northland's water quality monitoring network.

Solution	TN_{Q95}	$NO_3\text{-}N_{Q95}$	DIN_{Q95}	TAM_{MAX}	TP_{Q95}	DRP_{Q95}	TSS_{Q95}	$Turb_{Q95}$	$Clarity_{Q5}$	$Ecoli_{Q95}$	DO_{Q5}
x-validated R^2	0.82	0.82	0.71	0.78	0.69	0.62	0.65	0.64	0.72	0.82	0.45
Correlation Coefficient	0.91	0.91	0.85	0.89	0.83	0.80	0.81	0.81	0.85	0.63	0.67
Maximum Error	0.38	0.46	0.65	0.88	0.58	0.64	0.88	0.66	0.36	0.06	0.14
Mean Squared Error	0.01	0.03	0.05	0.06	0.02	0.03	0.05	0.04	0.01	0.18	0.004
Mean Absolute Error	0.06	0.13	0.15	0.17	0.09	0.11	0.16	0.14	0.09	7	0.05
Coefficients	7	6	8	5	7	7	7	8	7	32	7
Complexity	35	45	58	37	41	33	45	40	45	0.82	37

Plots of the observed versus predicted values for median scores of each water quality measure are displayed below (Figures 7 - 16). Cross validation is shown by the training data represented by dark circles and validation by light circles on each figure.

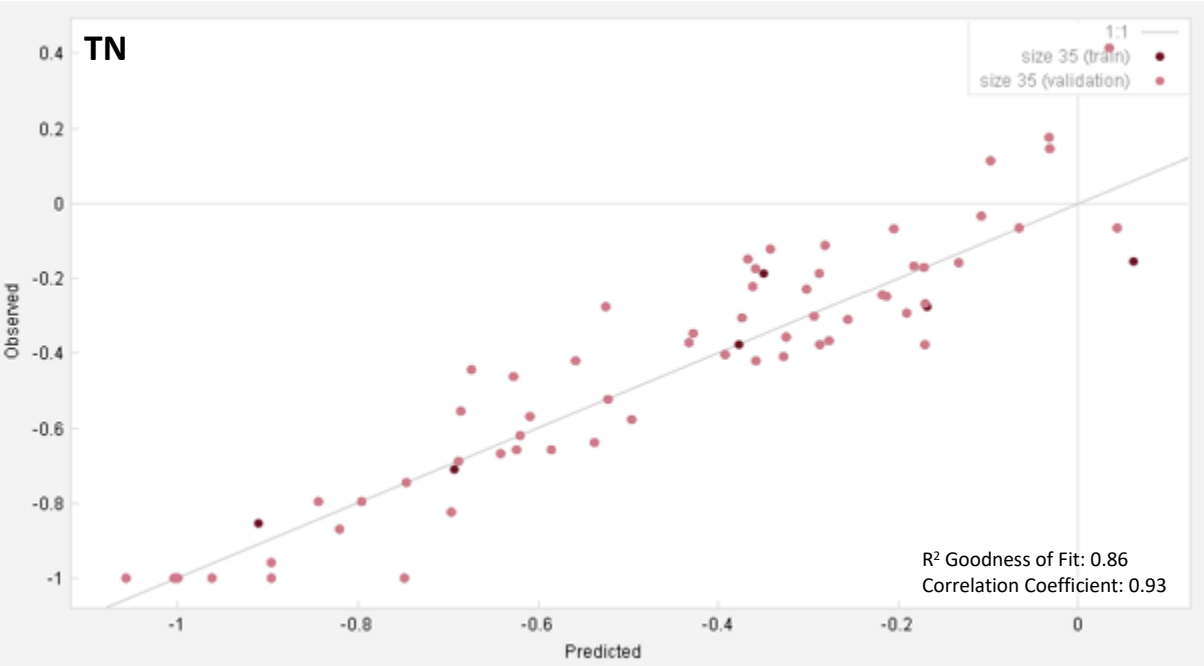

Figure 7. Log_{10} Total Nitrogen (TN, ppm) – Observed vs Predicted for 67 sites. Training data is represented by dark circles and validation by light circles.

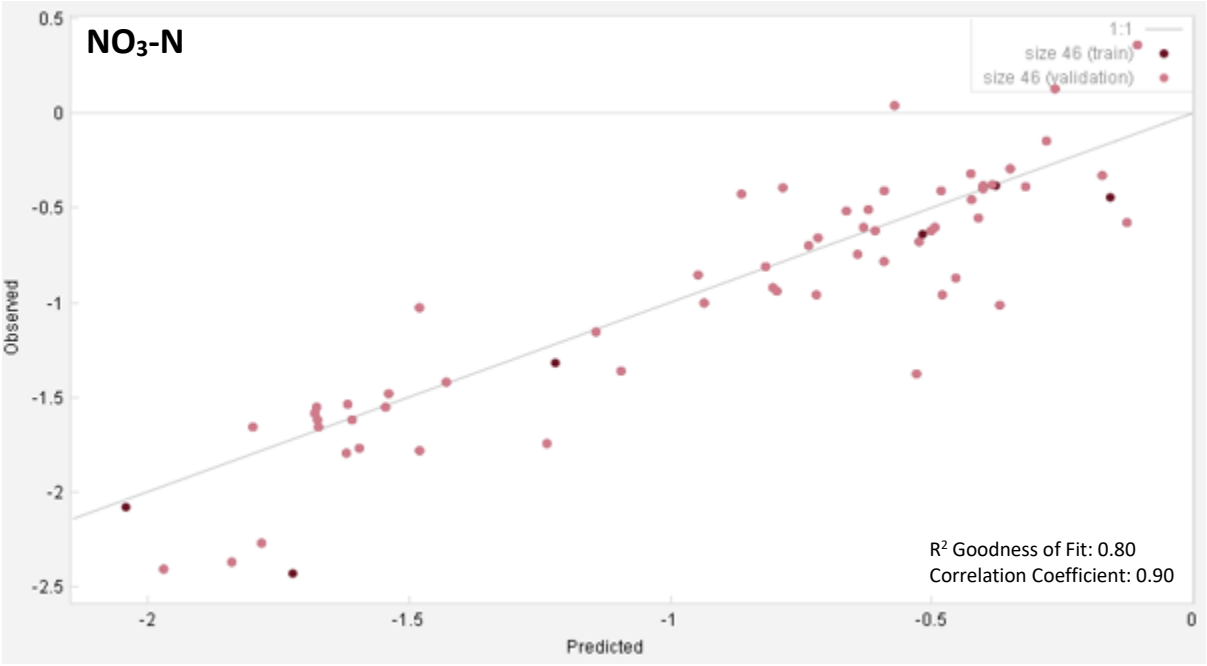

Figure 8. Log_{10} Nitrate Nitrogen (NO_3-N, ppm) – Observed vs Predicted for 67 sites.

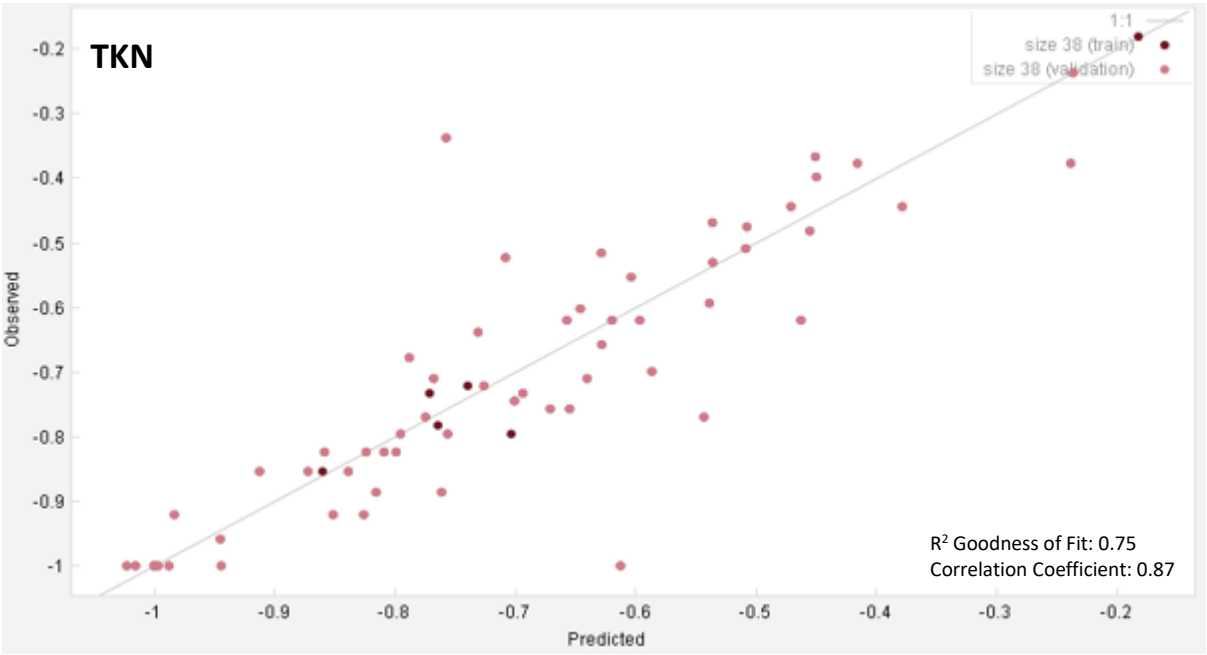

Figure 9. Log_{10} Total Kjeldahl Nitrogen (TKN, ppm) – Observed vs Predicted for 67 sites.

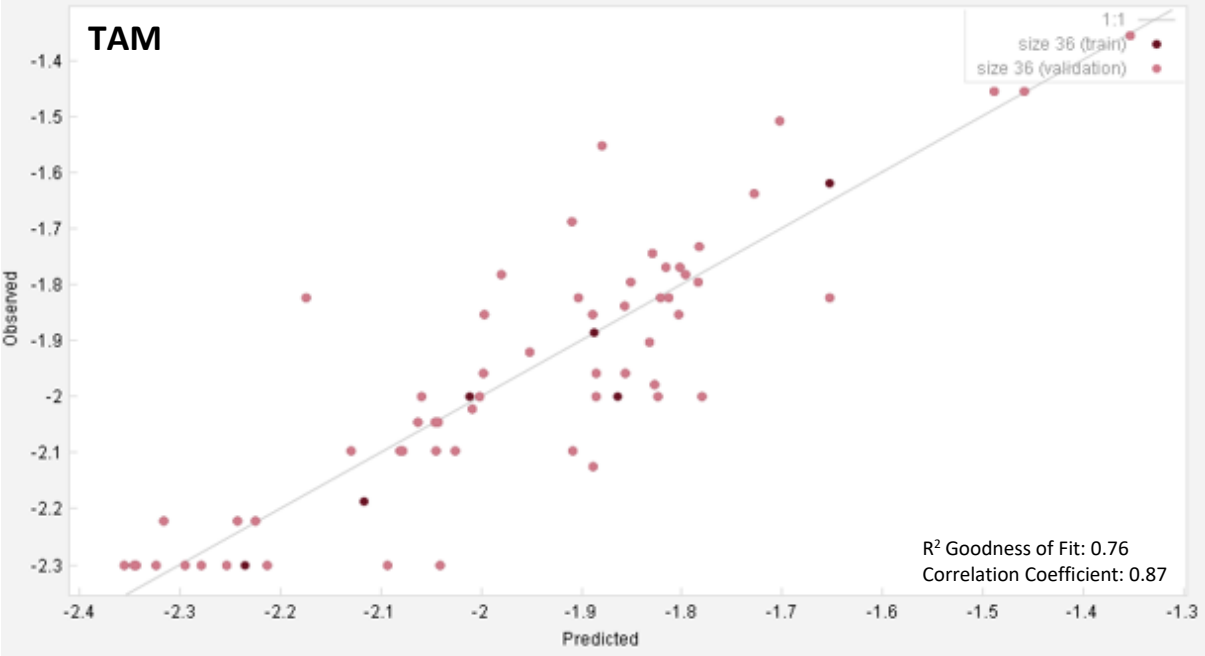

Figure 10. Log$_{10}$ Total Ammoniacal Nitrogen (TAM, ppm) – Observed vs Predicted for 66 sites. Note the influence of detection limit (censored) values at -2.3 (observed) over model performance.

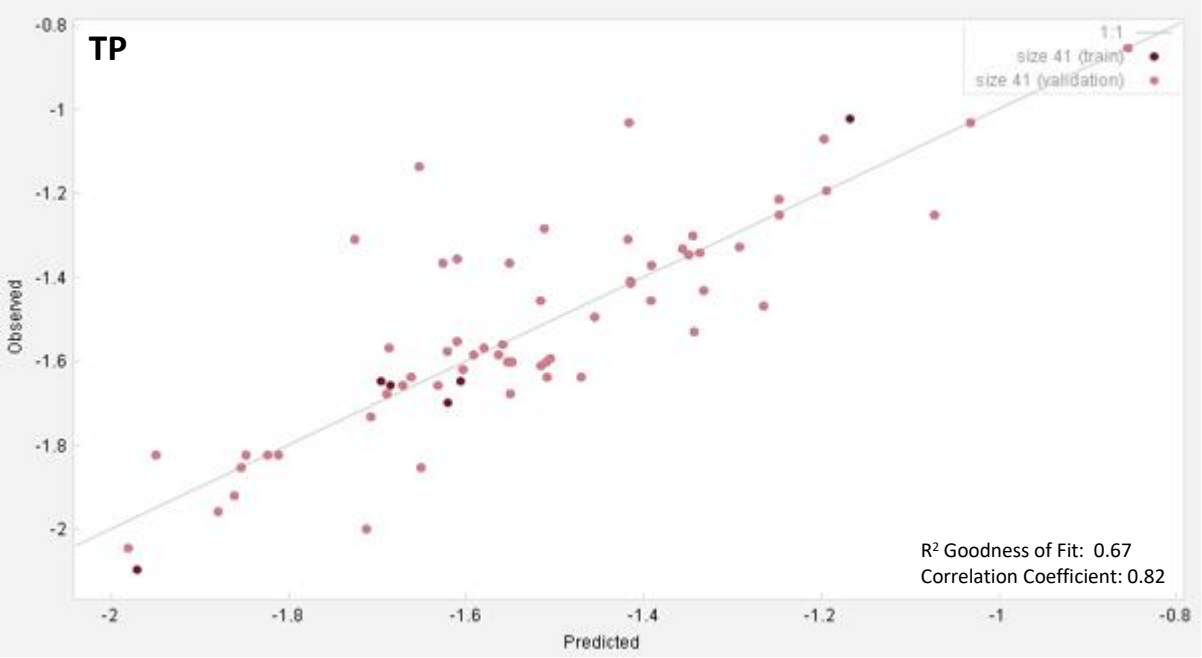

Figure 11. Log$_{10}$ Total Phosphorus (TP, ppm) – Observed vs Predicted for 67 sites.

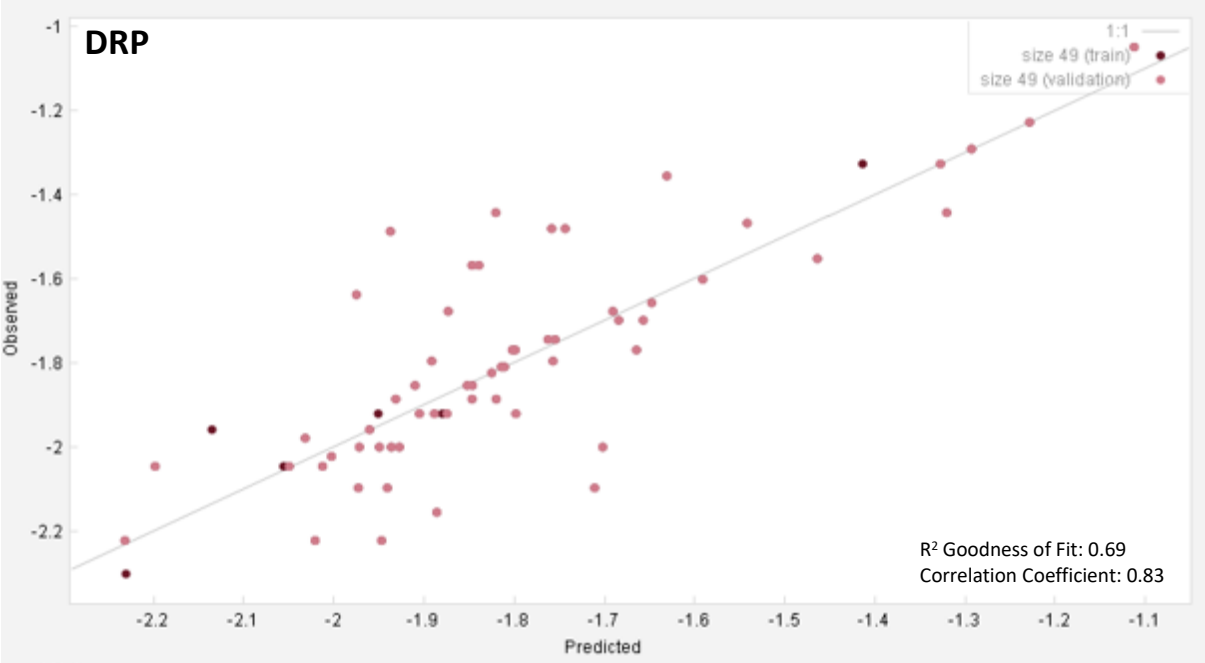

Figure 12. Log$_{10}$ Dissolved Reactive Phosphorus (DRP, ppm) – Observed vs Predicted for 67 sites.

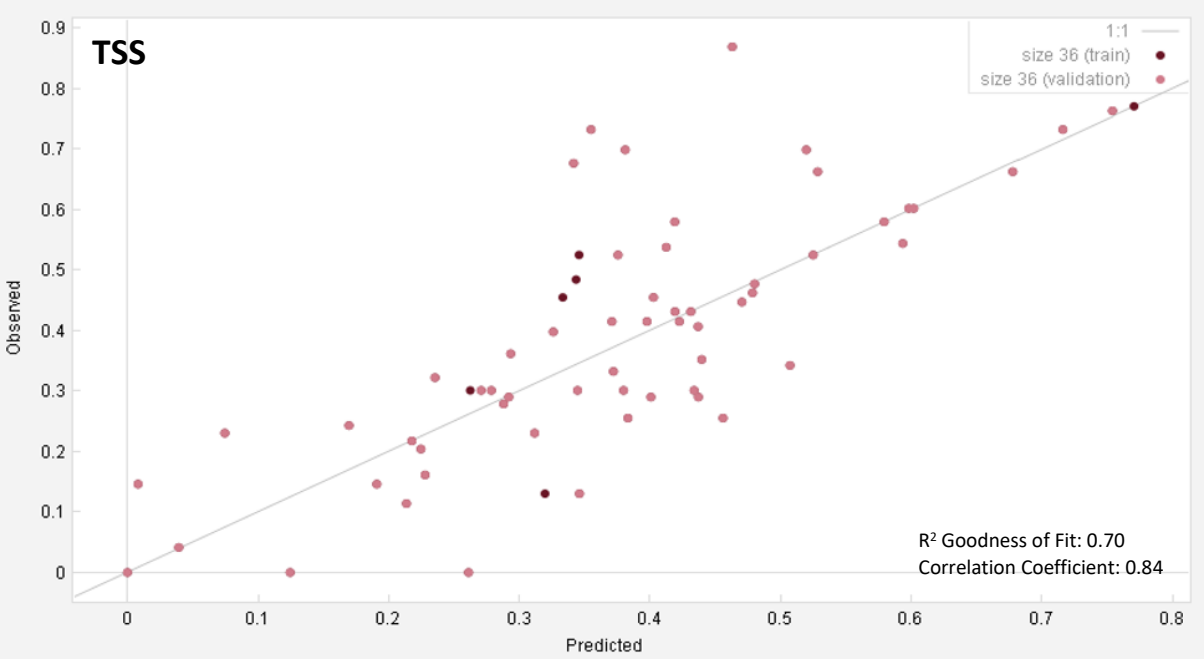

Figure 13. Log$_{10}$ Total Suspended Solids (TSS, ppm) – Observed vs Predicted for 67 sites.

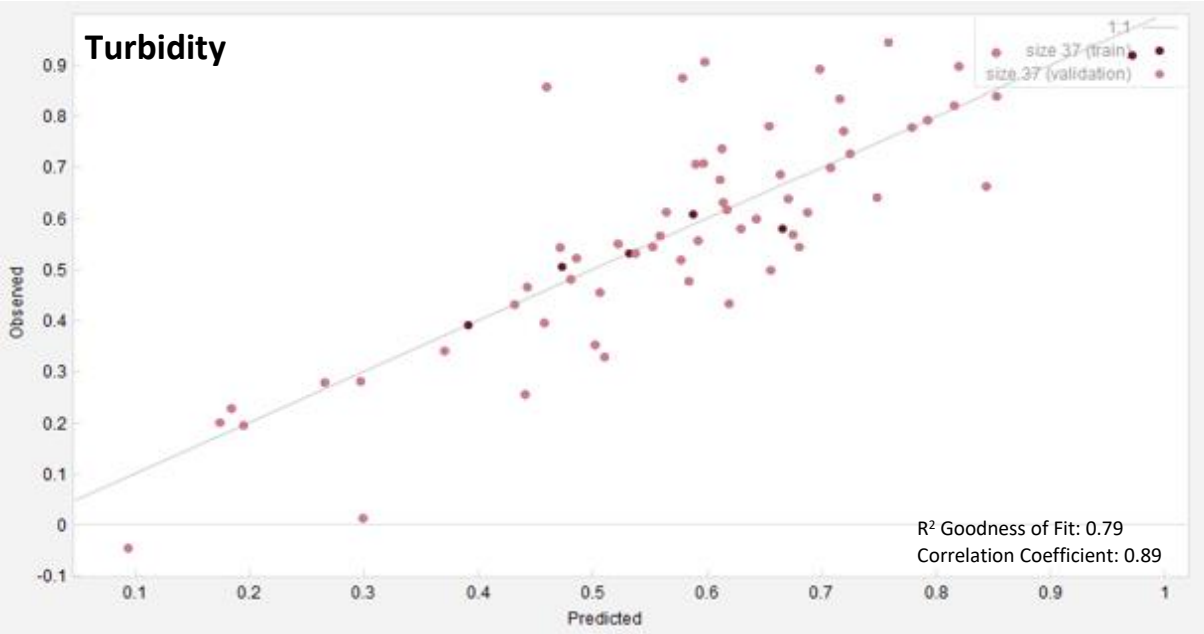

Figure 14. Log$_{10}$ Turbidity (NTU) – Observed vs Predicted for 65 sites.

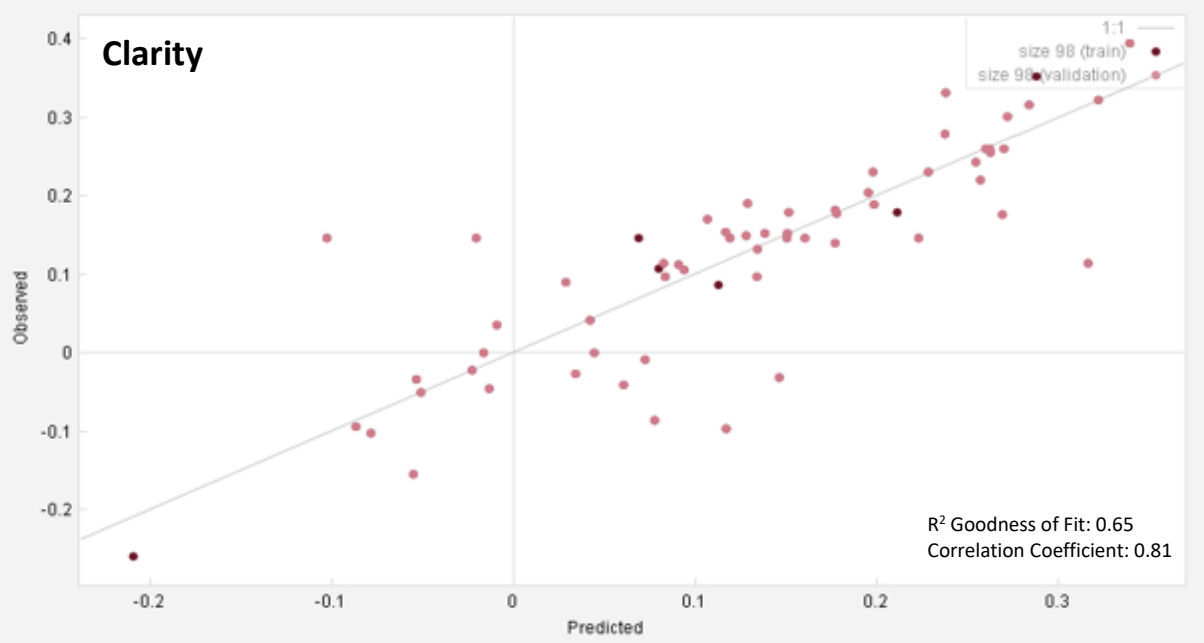

Figure 15. Log$_{10}$ Clarity (m) – Observed vs Predicted for 65 sites.

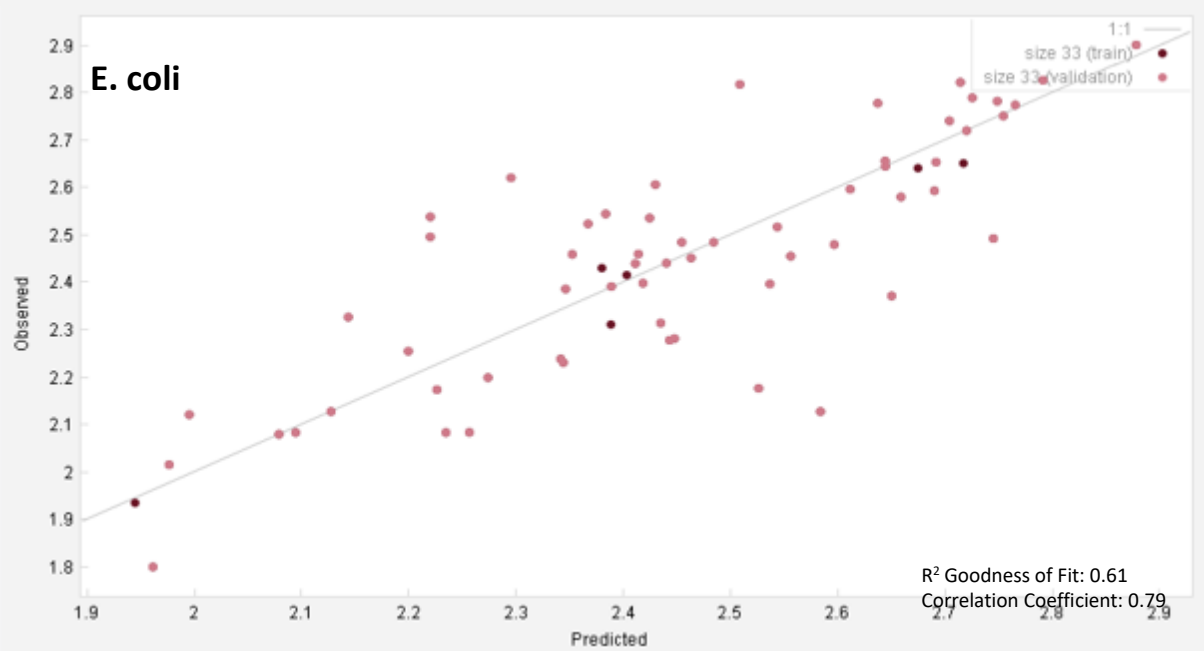

Figure 16. Log$_{10}$ E. coli (MPN) – Observed vs Predicted for 67 sites.

3.4 Sensitivity and Magnitude of Response by PAG

The sensitivity and magnitude of response of the PAG retained for individual water quality measures are provided in Appendix C. Below a more generalised ranking of the sensitivity of PAG by contaminant class (e.g. nitrogen species, phosphorus species) is provided (Tables 28 – 31). Each table summarises the relative rank of each PAG and related processes in order of importance for predicting spatial variation in overall N and P forms, *E. coli* and sediment. These ranks are generated by averaging the sensitivity scores for each individual water quality measure. For example, for 'N' overall sensitivity is based on the average scores for each PAG for TN, TKN, TAM and NNN. Please note that although land use was included in each model that it was not retained as a predictor in many instances.

Table 28. Ranked sensitivity of retained Process-Attribute-Gradients (PAG) for median Nitrogen (i.e., TN, TKN, TAM, NNN) species.

PAG	Sensitivity	Process
$NWGL_{MNDWI + TC}$	2.466	Hydrological/Redox
ESC	2.169	Physical Weathering/Geology
ARTD	1.46	Hydrological
LUI/LUM	0.811	Land Use
DD	0.758	Hydrological
PPT	0.441	Atmospheric
GRP	0.398	Redox
HYD	0.316	Hydrological
EWT	0.086	Hydrological
NBP	0.001	Hydrological
NRCD	0.001	Hydrological

Table 29. Ranked sensitivity of retained Process-Attribute-Gradients (PAG) for median Phosphorus (i.e., TP and DRP) species.

PAG	Sensitivity	Process
PPT	1.201	Atmospheric
ARTD	1.186	Hydrological
NBP	1.098	Hydrological
OLF	0.785	Hydrological
$NWGL_{MNDWI + TC}$	0.358	hydrological/Redox
GRP	0.314	Redox
DD	0.195	Hydrological
SRP	0.133	Redox
HYD	0.052	Hydrological

Table 30. Ranked sensitivity of retained Process-Attribute-Gradients (PAG) for median Sediment (i.e., Turbidity, Clarity and TSS) measures.

PAG	Sensitivity	Process
DD	2.049	Hydrological
NBP	1.132	Hydrological
ESC	0.644	Physical Weathering/Geology
$NWGL_{MNDWI + TC}$	0.514	Hydrological/Redox
GANC	0.350	Physical Weathering
HYD	0.250	Hydrological
LUI/LUM	0.224	Land use
OLF	0.112	Hydrological
SRP	0.100	Redox
GRP	0.080	Redox

Table 31. Ranked sensitivity of retained Process-Attribute-Gradients (PAG) for median E. coli.

PAG	Sensitivity	Process
DD	2.308	Hydrological
PPT	0.493	Atmospheric
$NWGL_{MNDWI + TC}$	0.460	Hydrological/Redox
LUI	0.011	Land use
HYD	0.003	Hydrological

Although there is significant complexity behind which PAG are retained for a given water quality contaminant, it is notable that hydrological and redox PAG, especially those derived from high resolution radiometric and satellite data, were typically retained as the most sensitive predictors of water quality variation across Northland (Tables 28 - 31). Land use is retained as a sensitive predictor of nitrogen, sediment, and *E. coli* but not for phosphorus species.

Table 32 provides a ranked summary of the sensitivity of PAG for predicting steady-state water quality across Northland. Once again, ranks are generated by averaging the sensitivity scores for each individual water quality measure for all contaminant classes (i.e., N, P, sediment and microbes). From Table 32 it is evident that the most sensitive predictors retained by the models are Deep Drainage, Northland's Wetness Gradient Layer (NWGL) and Erosion Susceptibility Classification (ESC)

(Rissmann et al., 2018 and 2019). The two latter of these layers are generated from high resolution radiometric (50 x 50 m or 0.25 Ha), terrain (12 m x 12 m) and satellite (20 x 20 m or 0.04 Ha) data sets and appear to provide greater constraint over spatial variation than PAG based on legacy data sets (e.g., LRI, QMap) that were generated at 1:50,000 scale or larger and were seldom developed with water quality in mind. Collectively, the DD, NWGL and ESC layers represent 52% of the sensitivity; the top 6 predictors 82.5% and land use 4.5%.

Table 32. Ranked overall sensitivity of retained PAG for all water quality measures across Northland's water quality monitoring network.

PAG	Sensitivity	Process
DD	5.31	Hydrological
$NWGL_{MNDWI + TC}$	3.798	Hydrological/Redox
ESC	2.813	Physical Weathering/Geology
ARTD	2.646	Hydrological
NBP	2.231	Hydrological
PPT	2.135	Atmospheric
LUI/LUM	1.046	Land Use
OLF	0.897	Hydrological
GRP	0.792	Redox
HYD	0.621	Hydrological
GANC	0.35	Physical Weathering
SRP	0.233	Redox
EWT	0.086	Hydrological
NRCD	0.001	Hydrological

With regards to land use, despite HDGP modelling each (possibly coupled) PAG separately in order to extract its less observable characteristics, it is likely that other PAG partially account for land-use gradients. A Pearson-Spearman-Kendall correlation matrix applied to the log_{10} transformed Northland data set reveals strong positive correlation between land use intensity (LUI) and both ARTD (artificial drainage density; r = 0.9) and Northland's Recharge Domain (NRCD; r = 0.60). Other PAG show weak (r <0.5 and most <0.3) correlations or none at all. Evidence for spatial correlation between land use and landscape attributes is important to acknowledge and raises the possibility that some PAG (e.g. ARTD) may partially represent land use intensity - this applies to the results of all water quality models[10].

Despite the spatial correlation between some PAG and land-use gradients, it is notable that the most sensitive predictors of spatial variation in water quality observed for Northland are consistent with a large number of biogeochemical and hydrochemical studies that note that atmospheric, hydrological (water source and pathway), redox and both chemical and physical weathering gradients play an important role over the spatial variation of water composition and quality (Table 33; Wright, 1988; Moldan and Černý, 1994; Clark and Fritz, 1997; Giller and Malmqvist, 1998; Kendall and McDonnell, 1998; Krantz and Powars, 2000; Lydersen et al., 2004; Doctor et al., 2008; McMahon and Chapelle, 2008; Gray et al., 2011; Inamdar, 2011; Rissmann, 2011; Rissmann et al., 2015; Daughney et al.,

[10] In recognition of the correlation between land use, hydrochemical tracers, those not strongly influenced by land use gradients, are used to evaluate the sensitivity of PAG to replicate process gradient (Section 3.1). As such, the process level controls indicated by hydrochemical tracers are considered to provide the most robust assessment of the process level controls over water quality. Rissmann et al. (in prep) have used this rationale to select PAG for the development of a national scale classification of water quality as part of the National Science Challenge, Our Land and Water.

2015). The observed sensitivity of landscape attributes over water quality is also consistent with the findings of section 3.2 and 3.3 for which hydrochemical tracers, those not strongly influenced by land use gradients, were used to evaluate the sensitivity of PAG to replicate process gradients.

Table 33. Ranked sensitivity by dominant process for all water quality measures.

Process	Sensitivity	Percentage
Hydrological	15.6	58.3
Redox	4.8	18.0
Physical Weathering	3.2	11.8
Atmospheric	2.1	8.0
Land Use	1.0	3.9

4 Estimating Water Quality Across the Digital River Network

The water quality models developed from log_{10} transformed data at 67 sites across the Northland region were applied to the River Environment Classification[11] (REC1) to estimate water quality at unmonitored sites. The model outputs were back-transformed by raising them to the power of 10 across the REC1 Order 2 and greater. Transformation bias was addressed following the method of Duan (1983). However, due to the high R^2 values and low residuals the change to the estimate values was small (c. <1 – 2%) and as such made little overall difference to the estimated values.

Application of water quality models utilises the REC capture zones at the node points where two stream orders of the same magnitude converge. This results in the model estimate accounting for lower-order contributions within a capture zone at the node point and not where the river lines join. Given the development of the models at stream orders greater than 2, it is expected that there will be some limitations at low order reaches.

Figures 17 to 28 show the predicted attribute values for median and Q95 for TP, NO_3-N, DIN, TKN, TP, DRP, TSS, turbidity and Clarity (Q5); median and maximum values for TAM, and baseflow (Q5) for DO and redox potential across the Northland Region river network.

[11] REC1 was used to apply the physiographic modelling as capture zones for each stream order are available for the region.

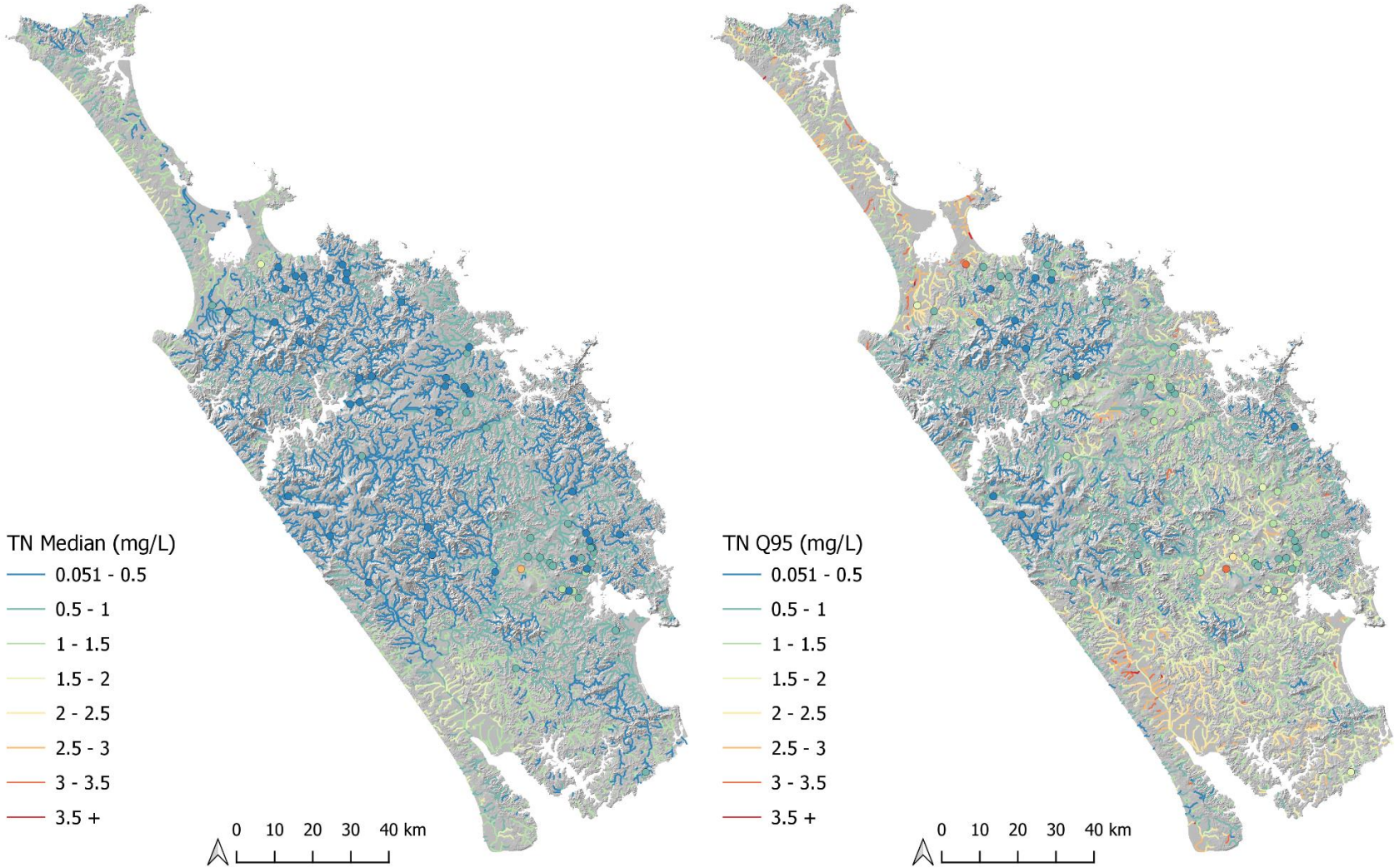

Figure 17. Predicted median Total Nitrogen (TN) (left) and 95th percentile TP (right) in Northland rivers. Circles denote the observed median and Q95 values for each of the monitoring sites. River reaches and observed measures (sites) are colour coded according to the same concentration gradient in mg/l.

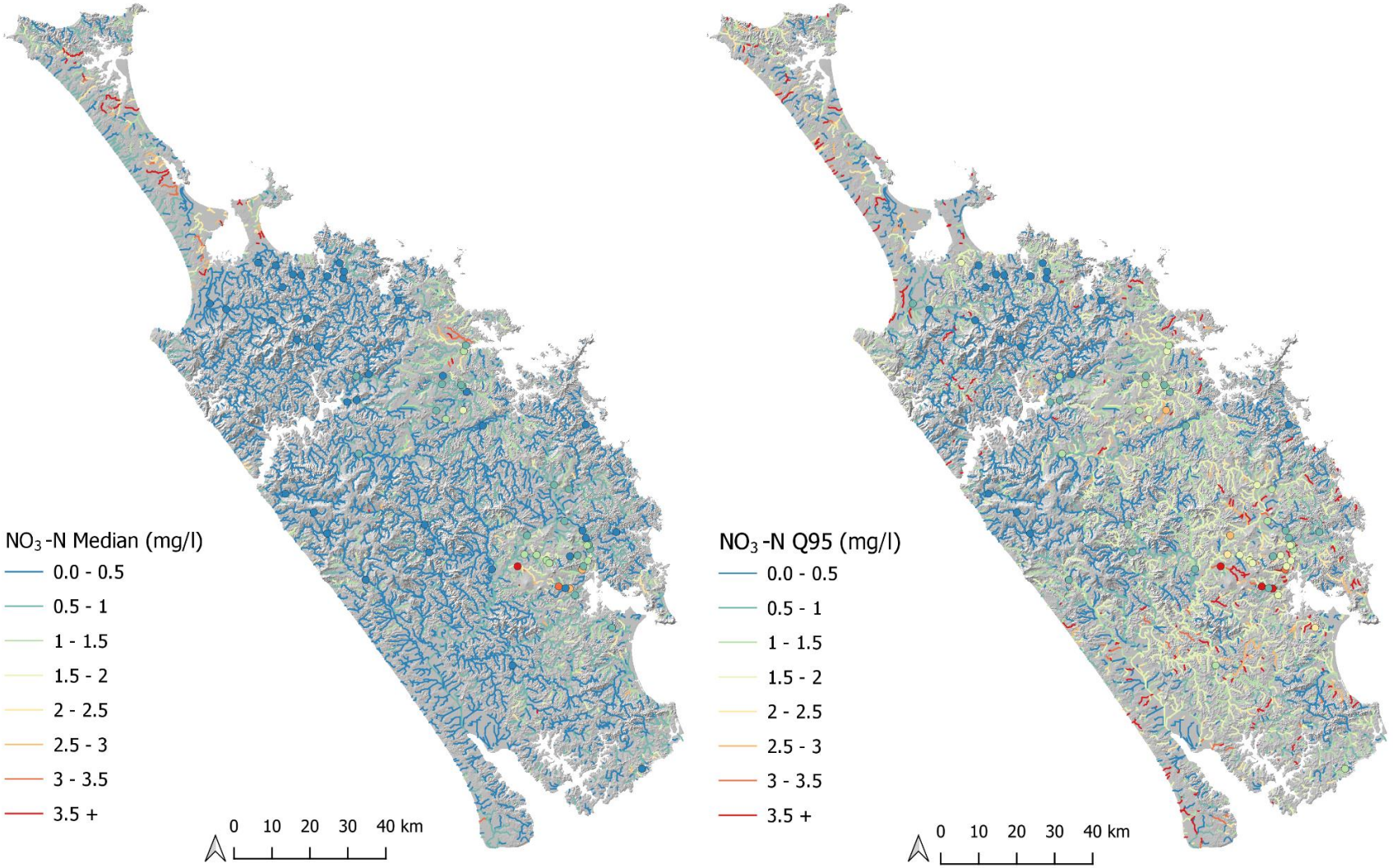

Figure 18. Predicted median Nitrate Nitrogen (NO_3-N) (left) and 95th percentile NO_3-N (right) in Northland rivers. Circles denote the observed median and Q95 values for each of the monitoring sites. River reaches and observed measures (sites) are colour coded according to the same concentration gradient in mg/l.

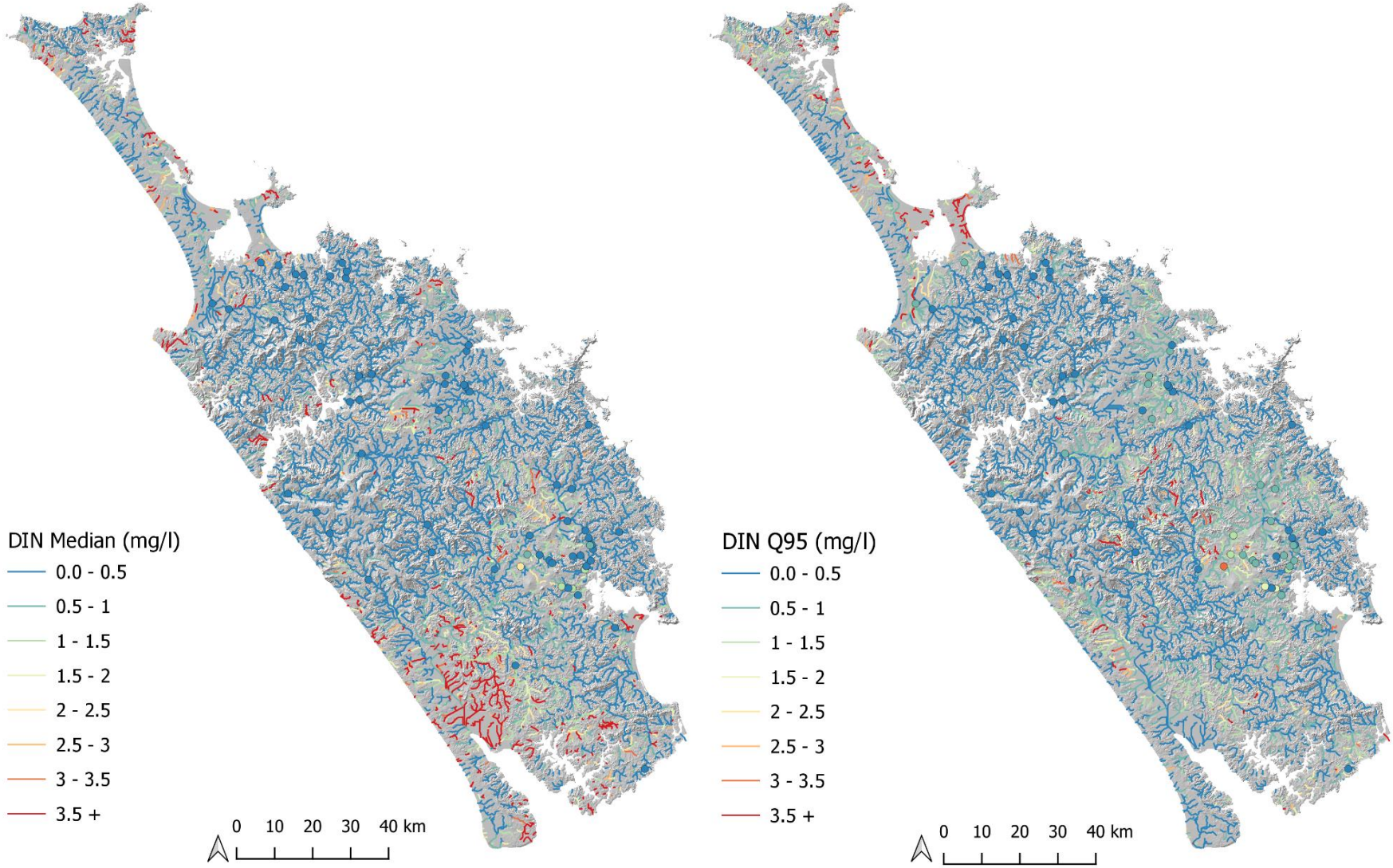

Figure 19. Predicted median Dissolved Inorganic Nitrogen (DIN) (left) and 95th percentile DIN (right) in Northland rivers. Circles denote the observed median and Q95 values for each of the monitoring sites. River reaches and observed measures (sites) are colour coded according to the same concentration gradient in mg/l.

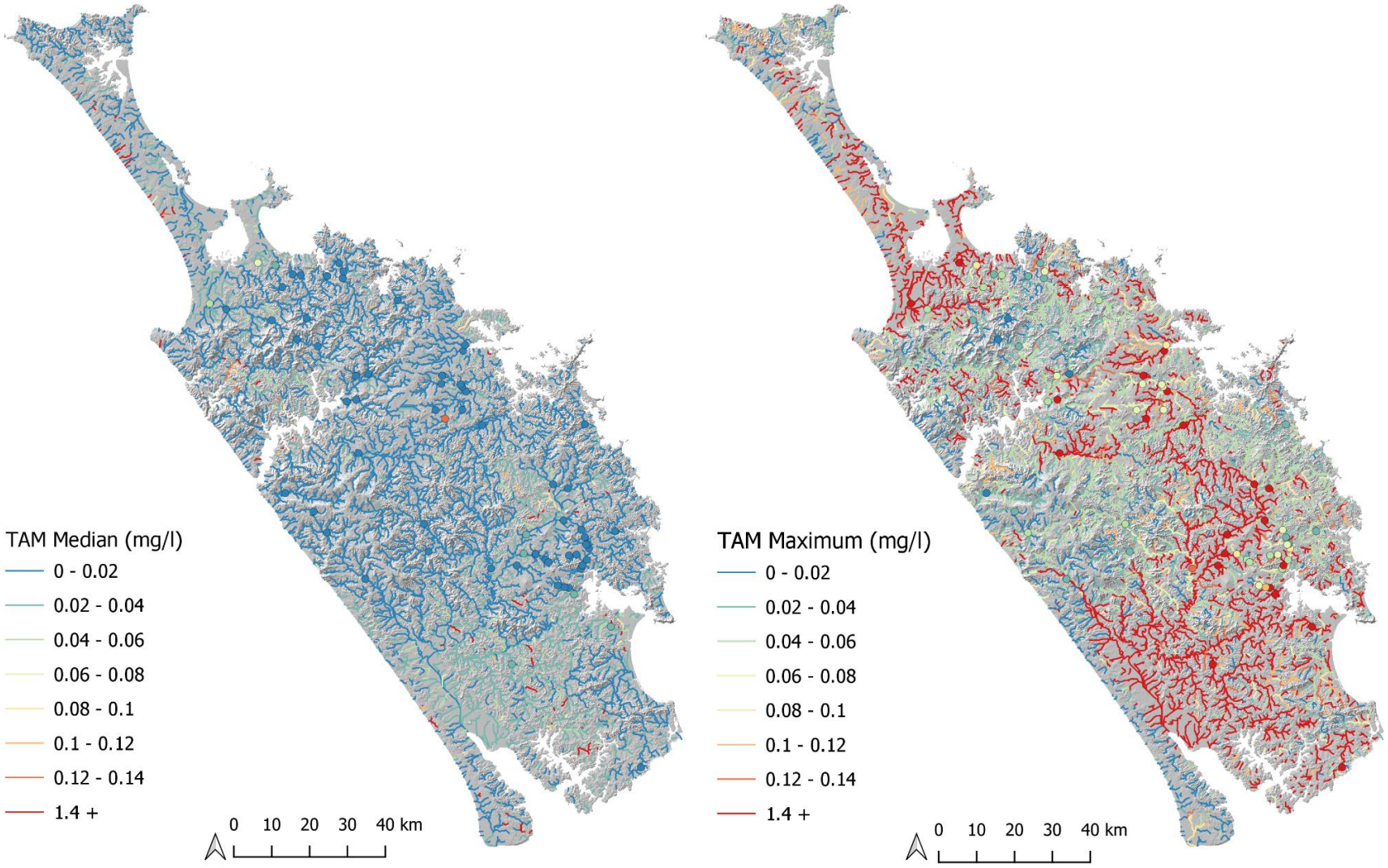

Figure 20. Predicted median Total Ammoniacal Nitrogen (TAM) (left) and 95th percentile TAM (right) in Northland rivers. Circles denote the observed median and Q95 values for each of the monitoring sites. River reaches and observed measures (sites) are colour coded according to the same concentration gradient in mg/l.

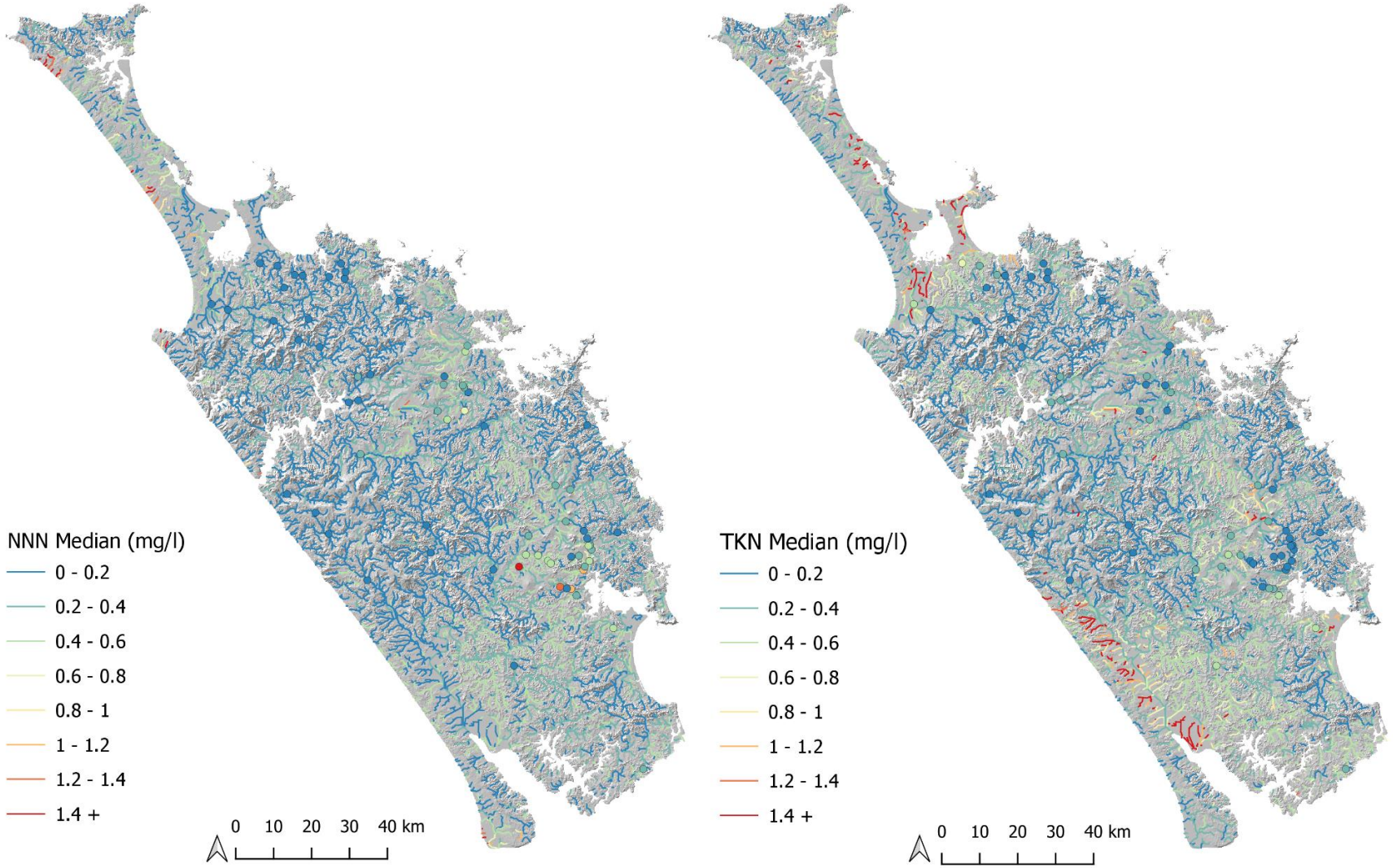

Figure 21. Predicted median Nitrate Nitrite Nitrogen (NNN) (left) and median Total Kjeldahl Nitrogen (TKN) (right) in Northland rivers. Circles denote the observed median and Q95 values for each of the monitoring sites. River reaches and observed measures (sites) are colour coded according to the same concentration gradient in mg/l.

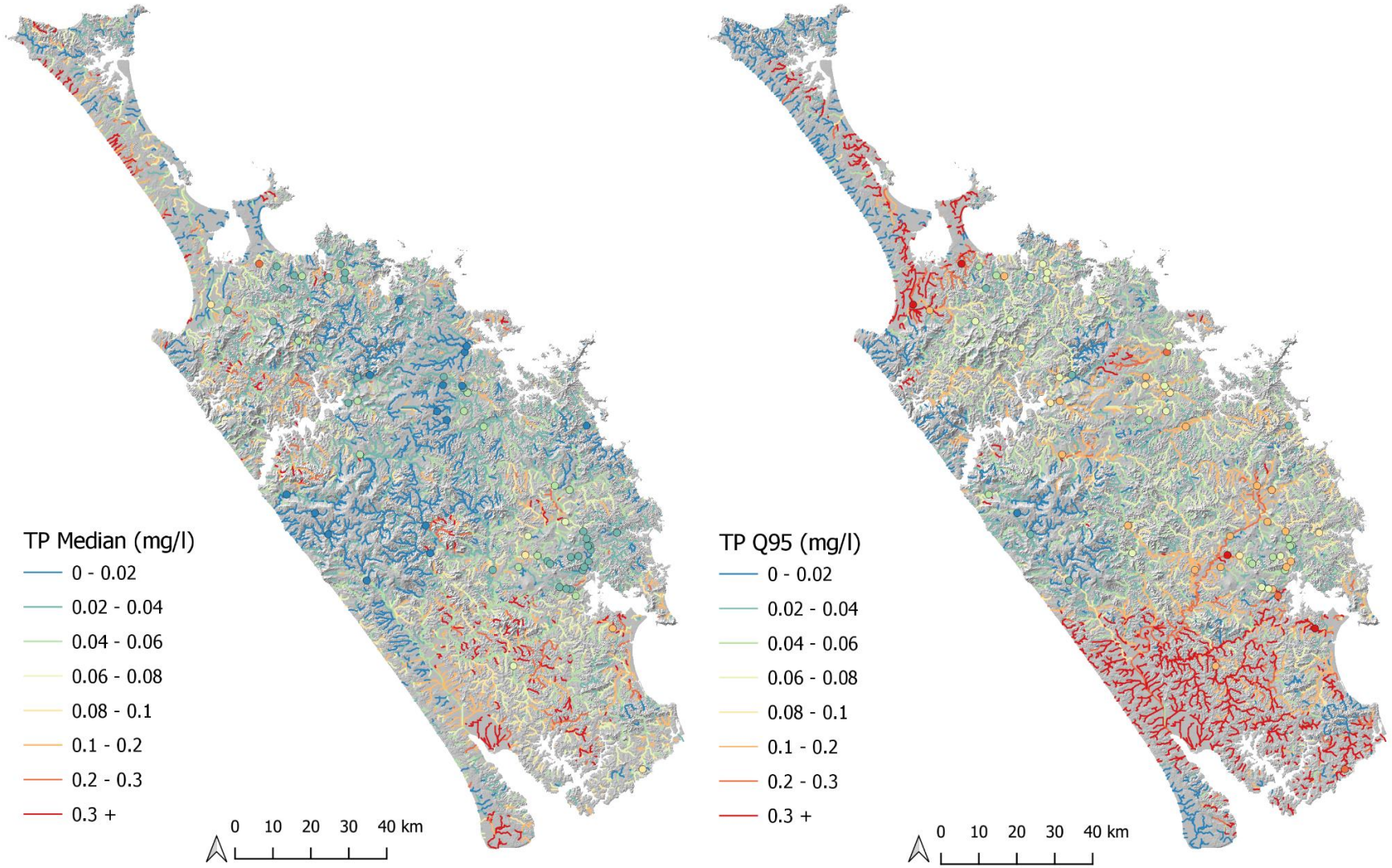

Figure 22. Predicted median Total Phosphorus (TP) (left) and 95th percentile TP (right) in Northland rivers. Circles denote the observed median and Q95 values for each of the monitoring sites. River reaches and observed measures (sites) are colour coded according to the same concentration gradient in mg/l.

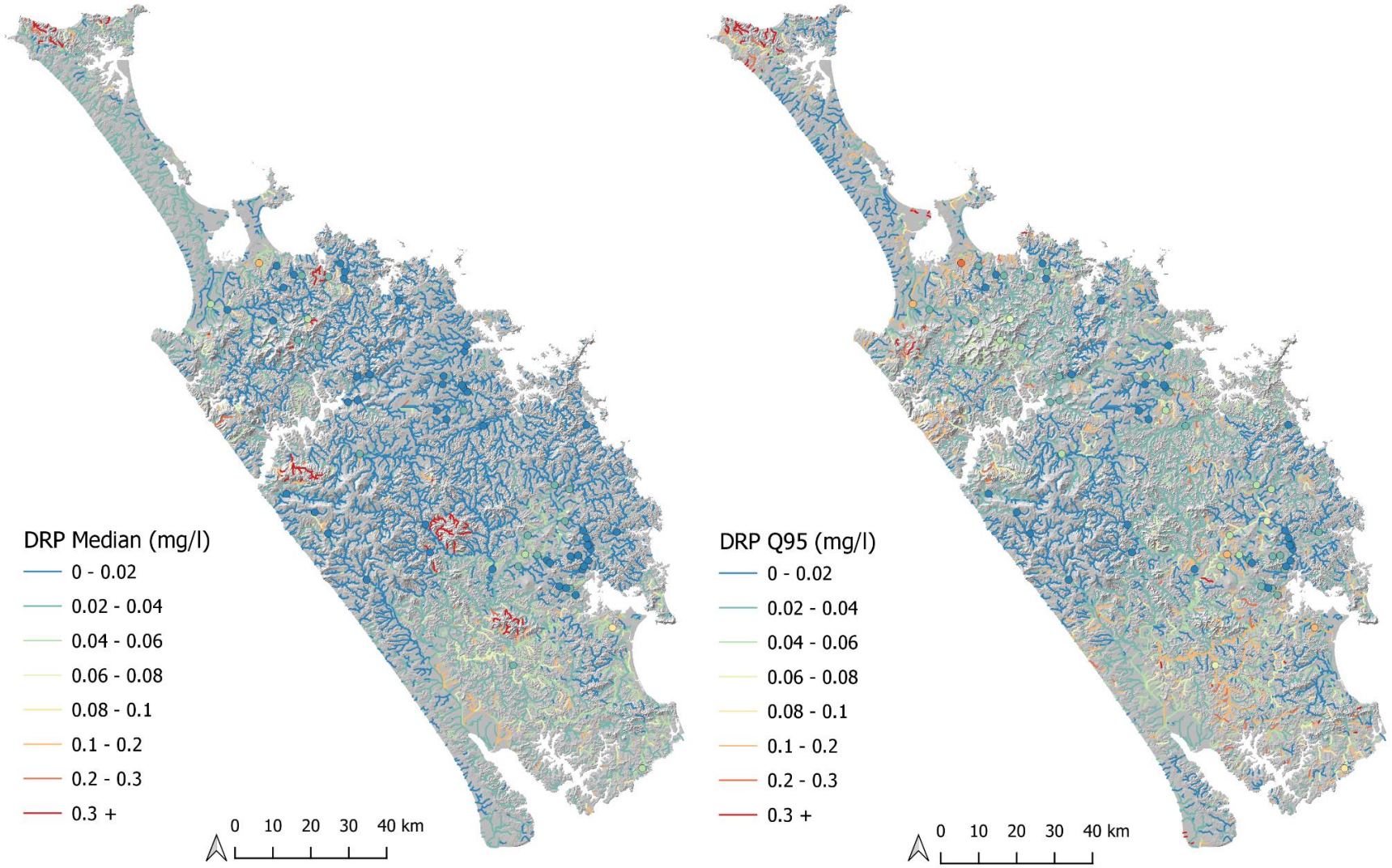

Figure 23: Predicted median Dissolved Reactive Phosphorus (DRP) (left) and 95th percentile DRP (right) in Northland rivers. Circles denote the observed median and Q95 values for each of the monitoring sites. River reaches and observed measures (sites) are colour coded according to the same concentration gradient in mg/l.

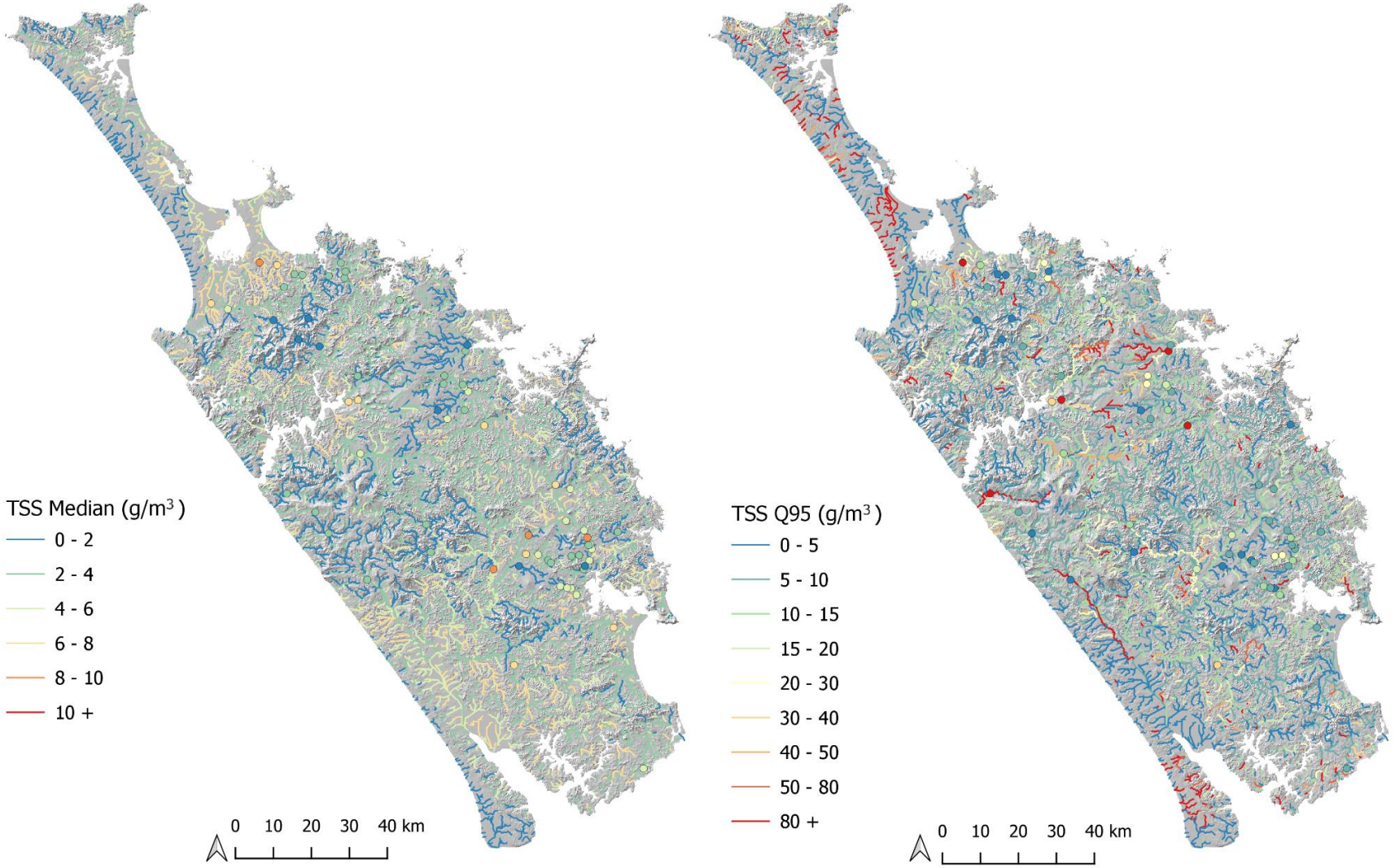

Figure 24. Predicted median Total Suspended Sediment (TSS) (left) and 95th percentile TSS (right) in Northland rivers. Circles denote the observed median and Q95 values for each of the monitoring sites. River reaches and observed measures (sites) are colour coded according to the same concentration gradient in g/m^3.

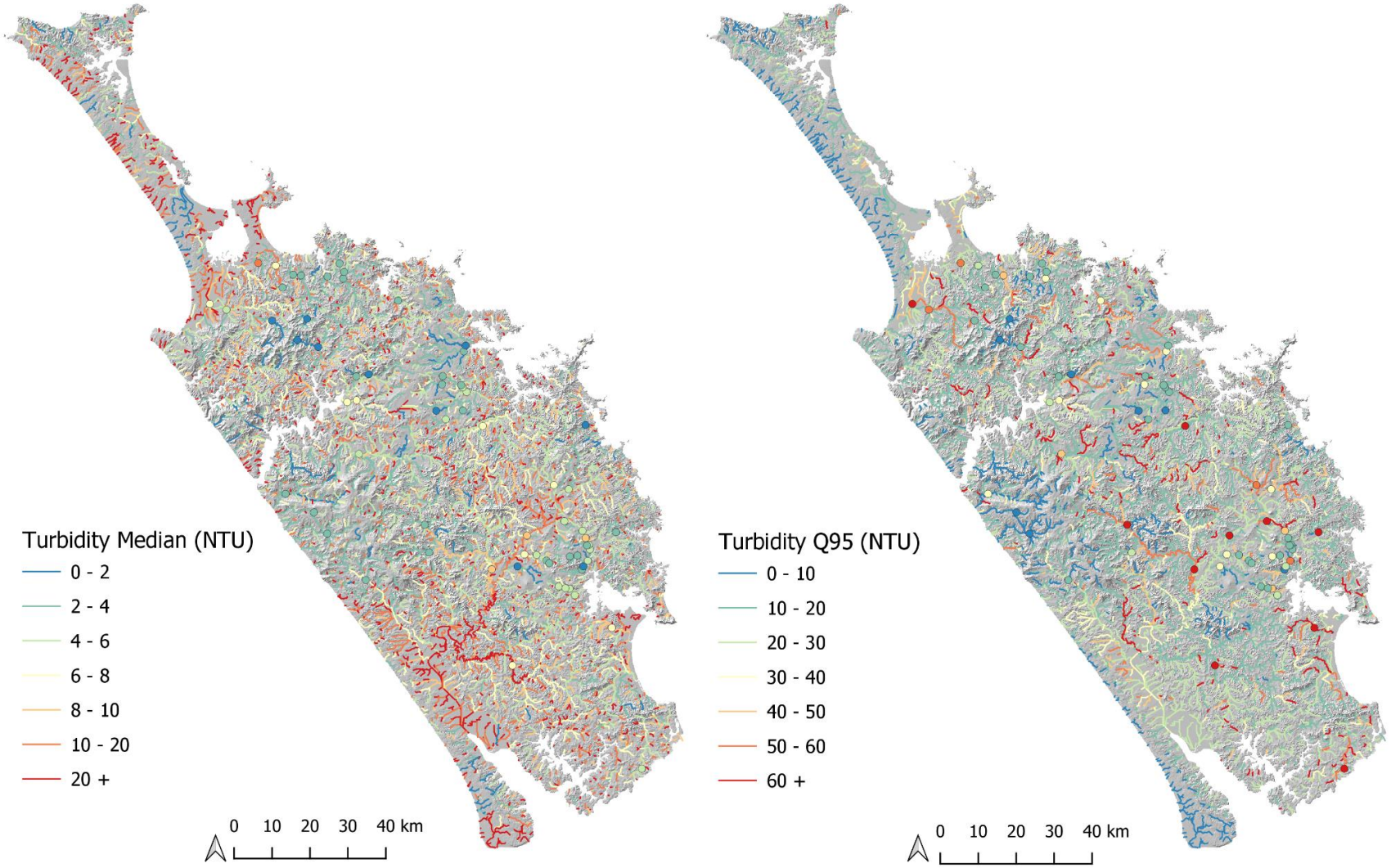

Figure 25. Predicted median Turbidity (left) and 95th percentile (right) in Northland rivers. Circles denote the observed median and Q95 values for each of the monitoring sites. River reaches and observed measures (sites) are colour coded according to the same concentration gradient in NTU.

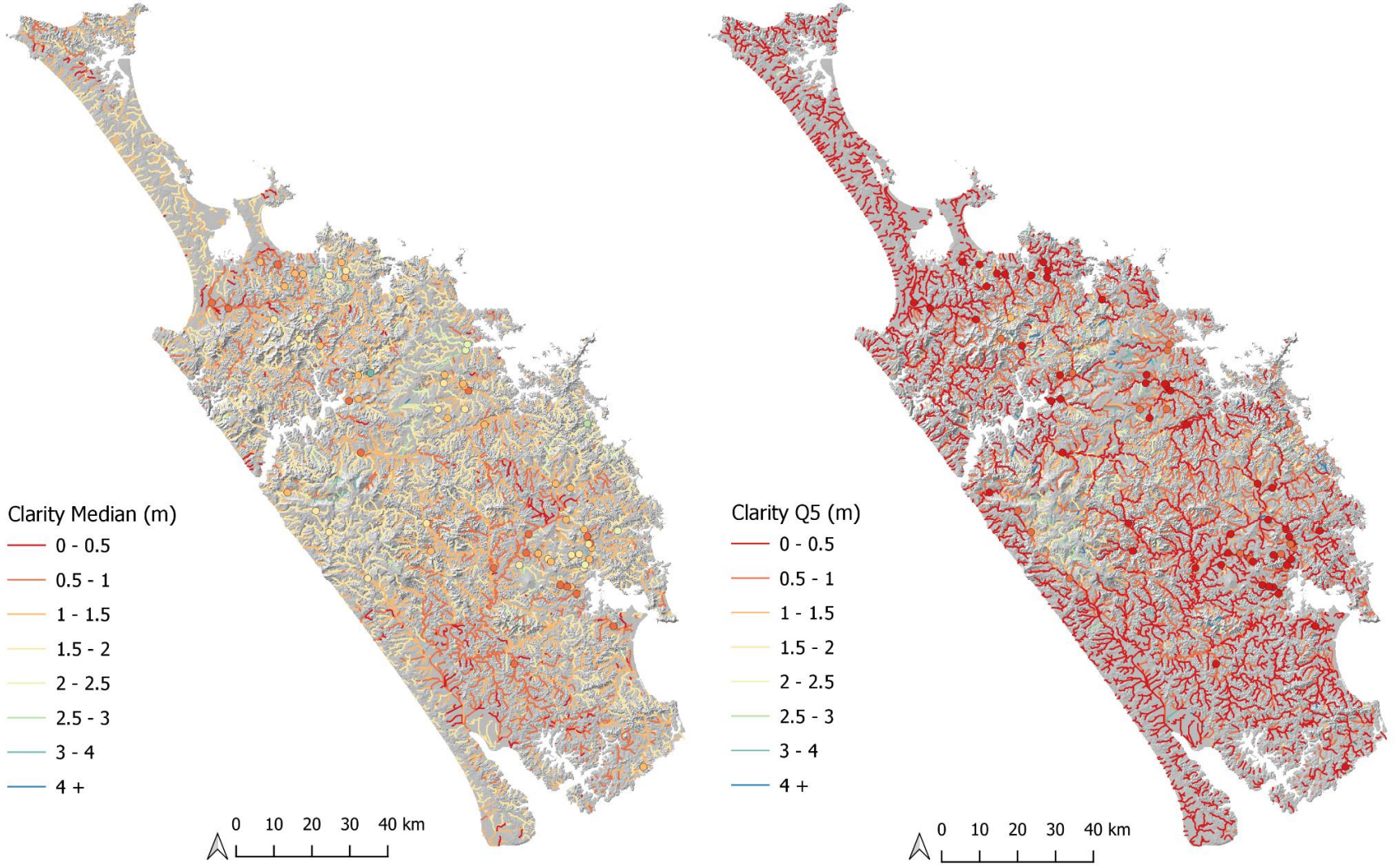

Figure 26. Predicted median Clarity (left) and Q5 (right) in Northland rivers. Note Q5 is occurring typically under high flow conditions. Circles denote the observed median and Q5 values for each of the monitoring sites. River reaches and observed measures (sites) are colour coded according to the same concentration gradient in meters.

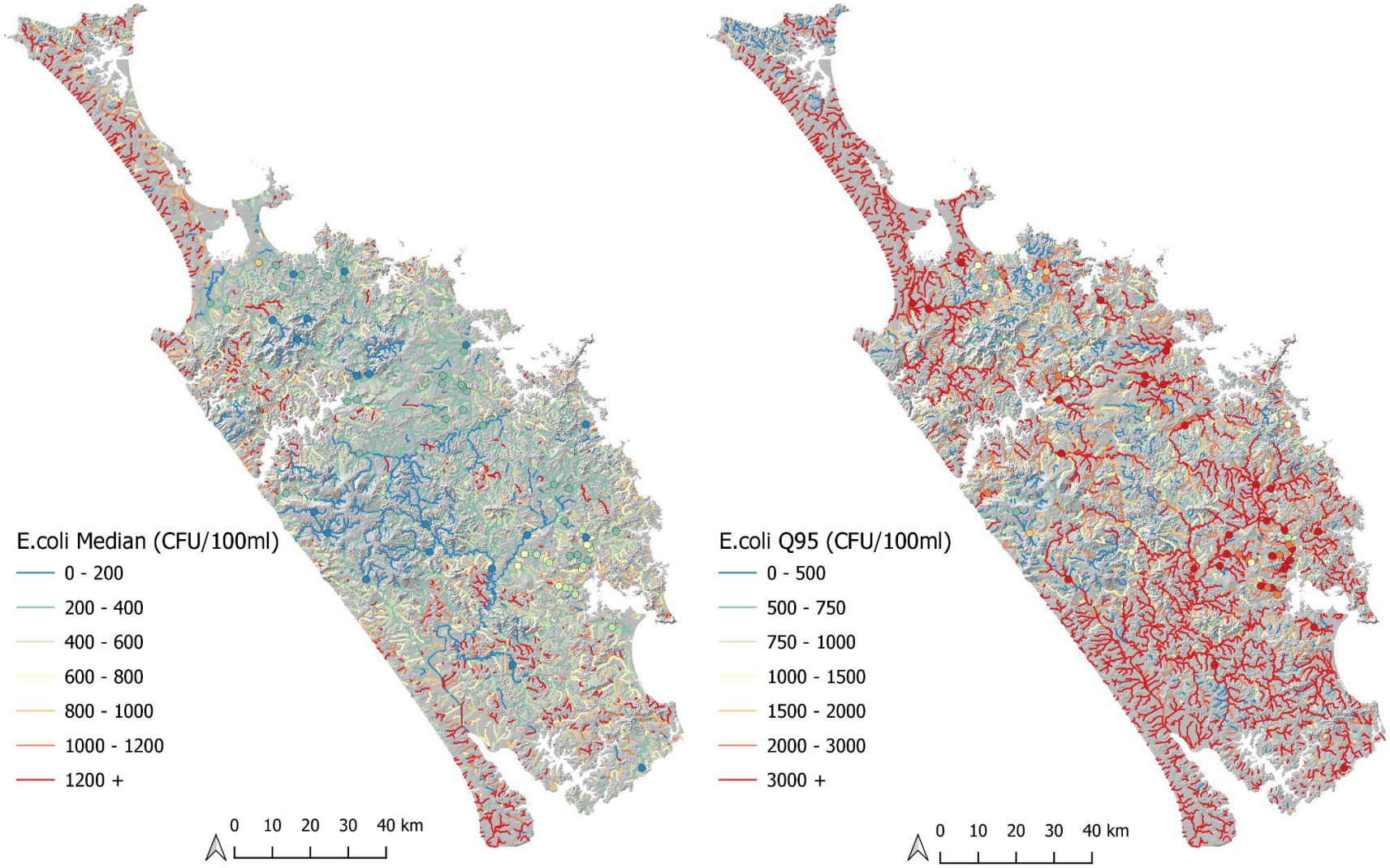

Figure 27. Predicted median E. coli (left) and 95th percentile (right) in Northland rivers. Circles denote the observed median and Q95 values for each of the monitoring sites. River reaches and observed measures (sites) are colour coded according to the same concentration gradient in CFU/100m

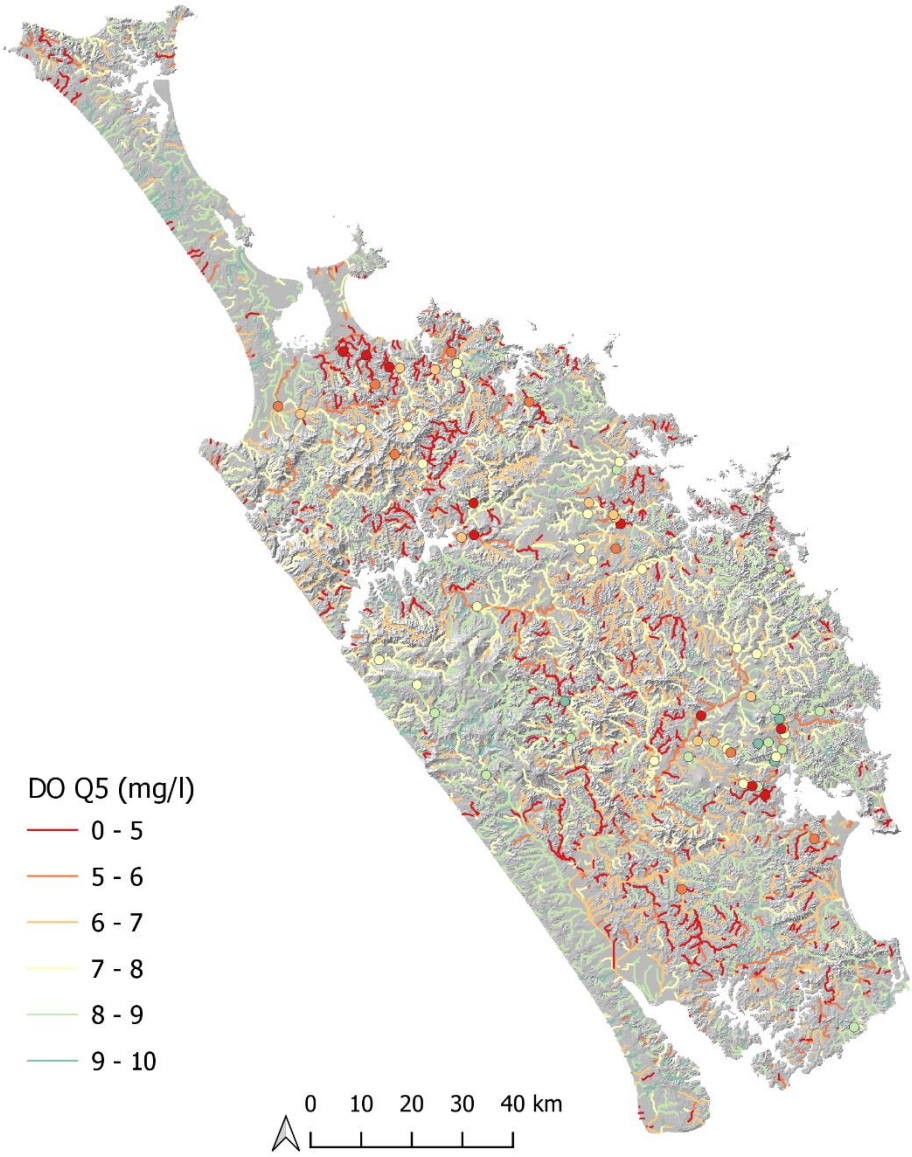

Figure 28. Predicted low flow (5th percentile) dissolved oxygen (right) in Northland rivers. Circles denote the observed Q5 values for each of the monitoring sites. River reaches and observed measures (sites) are colour coded according to the same concentration gradient in mg/l.

As DO is a poor proxy for redox potential in river systems, we have used PC2 of the hydrochemical subset (Section 2.2.3 and 2.4) to provide an integrated measure of redox potential across the region (Figure 29). This output indicates where streams are expected to be oxidising or reducing as a function of landscape characteristics. A spatial representation of redox potential provides critical context over the spatial pattern and speciation (forms) of N and P. Redox potential also influences stream clarity and absorbance and is recognised as a dominant control over the form (speciation), mobility and attenuation of phosphorus and nitrogen. The most sensitive predictors of redox potential were the NWGL (radiometric and Sentinel-2 satellite-based), Soil Reduction Potential (SRP), Equilibrium Water Table (Westerhoff et al., 2018), Geological Reduction Potential (GRP) and Northland Recharge Domain. Similar maps for each of the dominant processes governing water quality outcomes, i.e., hydrological, chemical and physical weathering, could be generated but was out of scope.

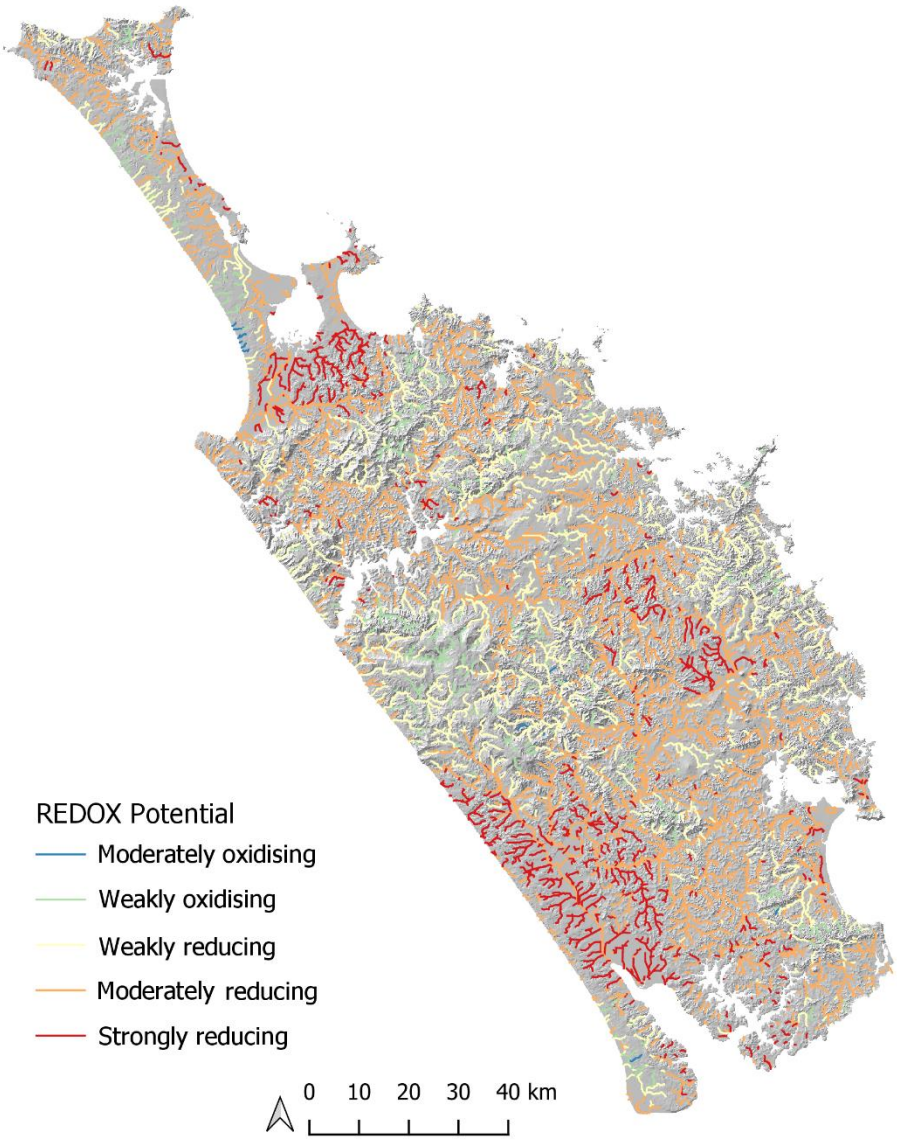

Figure 29: Redox potential of the reach is predicted according to PC2 (Section 3.1).There is a strong spatial correlation between estimated redox potential and reducing soils and lithologies.

4.1 Estimated Water Quality and Landscape Attributes

The resultant water quality estimates for unsampled stream reaches are suggestive of significant geological influence (Figure 30; Isaac, 1996; Edbrooke and Brook, 2009; Rissmann et al., 2018a,b; 2019b,c). For example, Total Kjeldahl Nitrogen (TKN), DRP, TAM and TP exhibit patterns of geological influence in addition to land use. Specifically, organic and ammoniacal nitrogen (TKN) shows a spatial relationship with reducing geological and aquifer materials such as lignite and peat (see also Figure 29, redox potential). Most notably, TKN is elevated where the Awhitu Group lignite and mudstones outcrop and or where peat and lacustrine deposits of the Tauranga Formation and Karioitahi Group sediments predominate (Figure 30). For example, TKN is elevated from Kaihu in the north to Te Kopuru in the south, adjacent to the Wairoa River. Here the Awhitu Group lignite outcrops with a number of small streams draining to the Wairoa River. Valley floor peat deposits and mixed sediment of alluvial and lacustrine origins also appear to influence TKN export with elevated concentrations observed across Ruawai. A similar pattern is seen in the north, west of Kaitaia, in the

vicinity of Kaimaumau and Karikari Peninsula in conjunction with peat and lacustrine sediments of the Karioitahi Group. North of Kaimaumau, the Awhitu Group lignite and mudstone also appear to influence organic and ammoniacal nitrogen export to the east from Pukenui to Te Hapua in the north. Northland groundwaters sampled from these geological formations exhibit some of the most reducing aquifer conditions and highest TKN concentrations (Rissmann et al., 2018a). Lignite and peat derived waters from across New Zealand exhibit similar patterns (Rissmann, 2011; Rissmann et al., 2012; 2016; unpublished data).

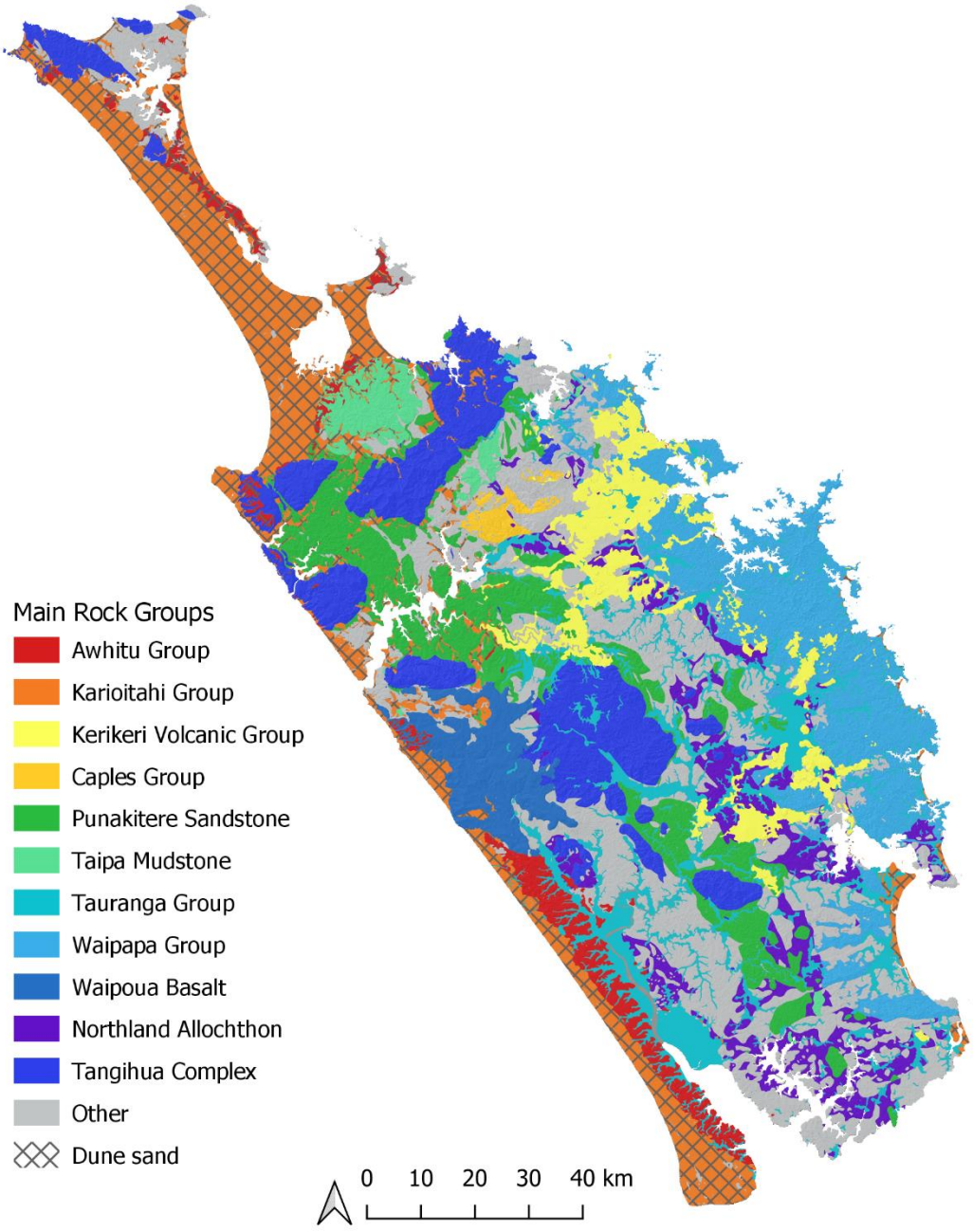

Figure 30. Main geological groups of the Northland Region. Data from QMap Stratalex (Isaac, 1996; Edbrooke and Brook, 2009).

Nitrate nitrogen, NO_3-N, constitutes a relatively small fraction of the total TN concentration across Northland's monitoring sites (1/3rd of the TN concentration on average, Figure 18). However, there are a small number of locations where it is the dominant species, most of which coincide with moderately to weakly oxidising redox potentials and agricultural land uses (Figures 29 and 30).

Modelled median NO_3-N is most uniformly elevated across the southern portion of the region from Whanageri in the south to Pokapu and Kawakawa in the north where land use and weakly oxidising to weakly reducing redox potentials coincide. Notably, the history of land development and land-use intensity is greatest across this area. There is a minor association between elevated NO_3-N in isolated streams draining greywacke basement rock along the east coast from Whanagaroa Bay to Kerikeri inlet and from Helena Bay to Whanageri Heads. The model also predicts elevated NO_3-N for isolated streams in conjunction with sand dunes along the west coast from Ninety Mile Beach in the north through to Pouto in the south. Small scale variation in estimated NO_3-N concentration draining dune front systems is spatially correlated with redox potential (e.g. streams with oxidising redox potentials are estimated as having higher NO_3-N concentrations). Overall, Northland's NO_3-N levels are low by national standards, with reduced nitrogen species, i.e., ammoniacal and organic nitrogen, constituting the bulk of the load exported to streams. This observation is consistent with the small extent of moderately or even weakly oxidising waters (Figure 28). As Total Nitrogen is the combination of ammonaical, organic nitrogen and oxidised forms of nitrogen (NO_3^- and NO_2^-) its distribution pattern reflects the controls over both reduced and oxidised forms (Figure 17).

Dissolved Reactive Phosphorus (Figure 23) also exhibits a strong geological control with the highest concentrations associated with steep outcrops of Tangihua Volcanics (Figure 30; Isaac, 1996; Edbrooke and Brook, 2009). Basalt commonly contains higher elemental phosphorus concentrations than felsic sedimentary rock (see the phosphorus concentration of common rocks—a potential driver of ecosystem P status; Porder and Ramachandran, 2013). It is also important to note that basalt, due to its high Lewis base concentration, weathers faster than siliceous rock, supplying inorganic P to the river network (Lasaga, 1984). The spatial correlation between elevated DRP and Tangihua Volcanic Complex extends from Cape Reinga in the North to Tangihua Forest in the south, wherever the unit outcrops (Figure 30). However, it is also notable that there is a positive correlation between terrain ruggedness and DRP concentration derived from the Tangihua Volcanic Complex. Notably, the flat-lying Waipoua and Kerikeri flood basalts do not appear to be implicated in DRP generation. Perhaps due to lower terrain ruggedness, mantling by siliceous materials and the development of a stable soil mantle (see Rissmann et al., 2018b).

Lower concentrations of DRP are spatially correlated with allochthonous rocks of felsic sedimentary and calcareous origins and with felsic basement rocks. These rock types are characterised by lower elemental phosphorus concentrations (Porder and Ramachandran, 2013). Other areas of moderately elevated DRP occur in association with peat and lacustrine sediments and reducing redox potentials. The association between elevated DRP and peat and lacustrine sediments is well established both nationally and globally (Zak and Gelbrecht, 2007; Niedermeier and Robertson, 2009; Rissmann et al., 2012, 2016; Van De Riet et al., 2013; Dimitrov et al., 2014; Wang et al., 2015; Rissmann et al., 2012, 2016; Tyre et al., 2016). Overall, there appears to be both a geological and redox control over DRP distribution. The use of phosphatic fertilisers and or animal dung over phosphate leaching is most problematic for wetland soils due to low anion exchange capacity and reducing conditions that favour phosphorus mobility (Rissmann et al., 2012).

Total Phosphorus (TP) also exhibits similar geological associations to DRP with respects to the Tangihua Volcanics and the peat and lacustrine rich portions of the Tauranga Formation and Karioitahi Group but not the Awhitu Group lignite (Figure 22; Isaac, 1996; Edbrooke and Brook, 2009). There is also evidence that land use and poorly drained soils play an important role in the distribution of the Particulate Phosphorus (PP) fraction of TP. This is consistent with overland flow and artificial drainage density being retained by the model in addition to geological PAG. Further, PP is known to show a strong association with developed land with dissolved organic and inorganic forms more commonly associated with natural state settings (Rissmann et al., 2018d). Sand dune systems along Ninety Mile Beach also exhibit elevated TP but not DRP concentrations suggesting a larger particulate phosphorus export. Salt spray, redox cycling and microbial processes have been identified as key controls over PP export from dune front systems (Figure 30; Beck et al., 2017).

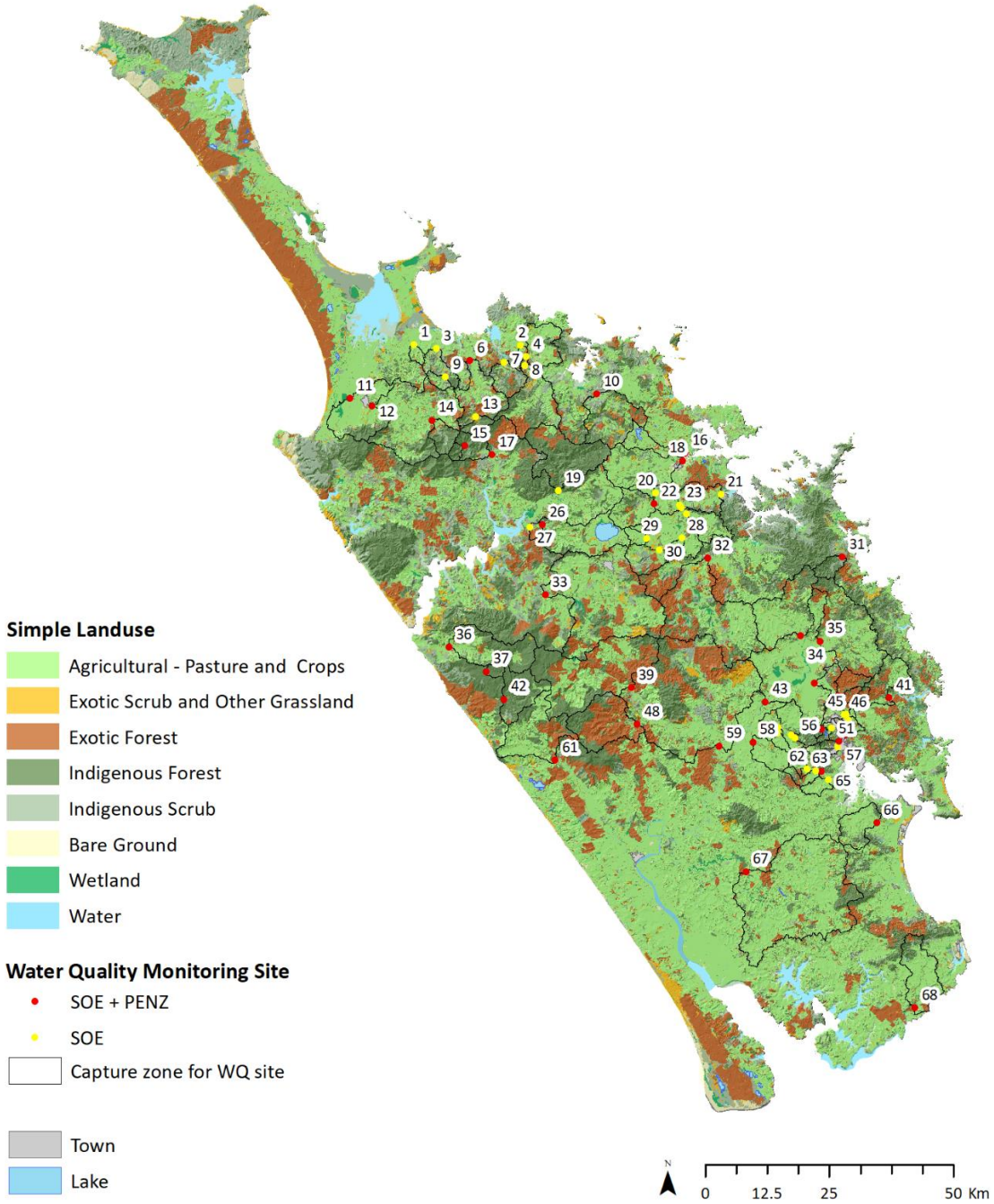

Figure 31: Land cover as a proxy for land use in the Northland region. Sites are identified in Table 2.

In terms of sediment, elevated median turbidity is mainly associated with highly erodible land (Figure 25 and Figure 31). Specifically, there is a strong geological correlation between turbidity and soft and highly erodible lithologies as defined by the ESC of Rissmann et al. (2018b). For example, the poorly lithified weak sedimentary rocks of the Northland Allochthon, including but not limited to the Punakitere Sandstone. Turbidity is also elevated in relationship to depositional landforms, i.e., alluvium, peat and lacustrine sediments of the Tauranga Group and Karioitahi Group, especially where the water table is shallow and soils poorly drained. Harder lithologies, such as the rocks of the Tangihua Volcanic Complex and Waipoua Basalt, show lower turbidity. Also notable, is that estimated turbidity is low across the areas of well-drained soils where surficial runoff and artificial

drainage is less prevalent (e.g. across a significant area of the low relief Kerikeri flood basalts). Tributaries of the Wairoa River, including the Manganui, are identified as being particularly turbid.

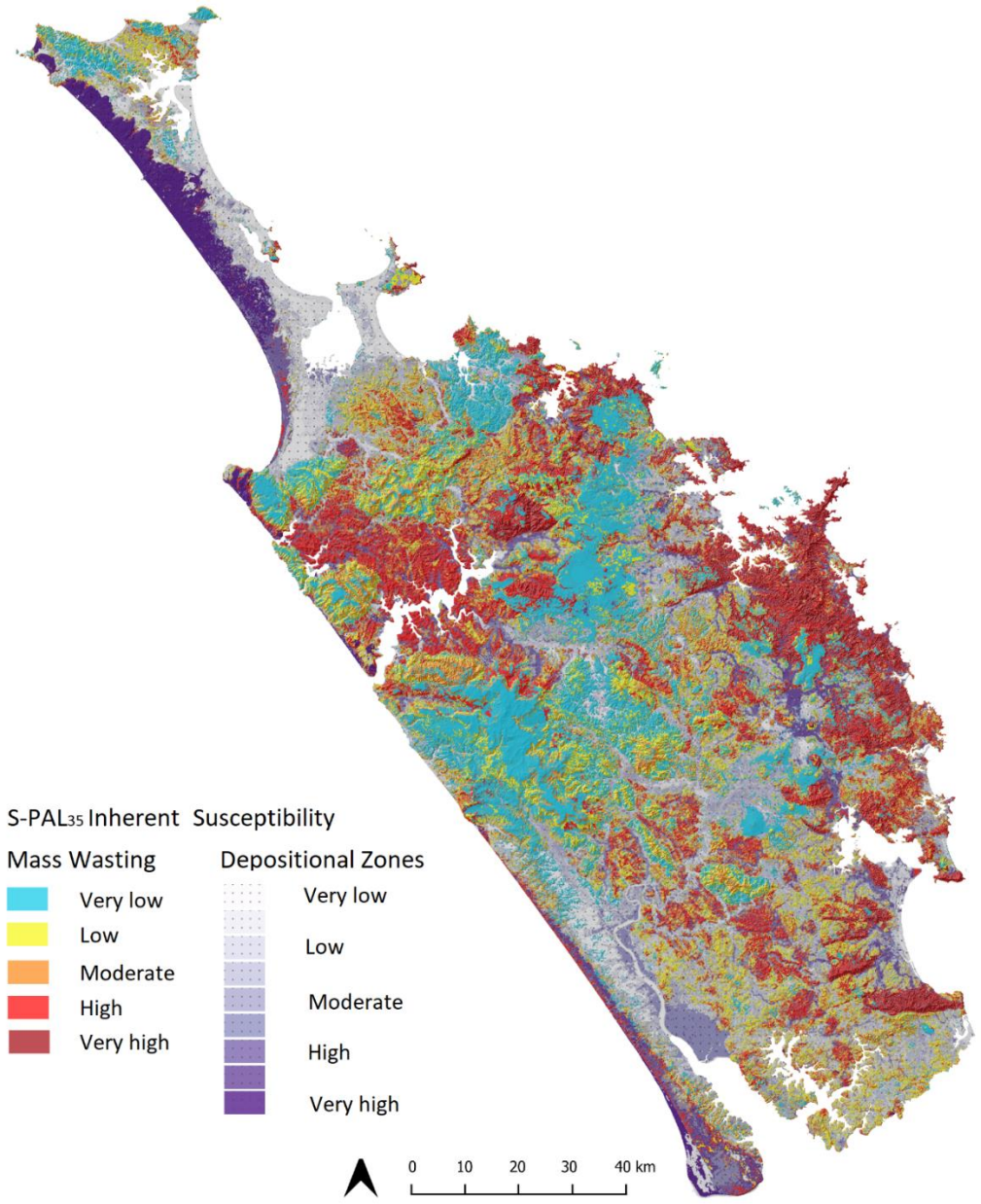

Figure 32. Erosion Susceptibility Class (Rissmann et al., 2018b; McDonald et al., 2020).

Estimated median clarity exhibits a broadly similar pattern to turbidity with the least clear streams associated with developed land and highly erodible lithologies, such as the weaker sedimentary rocks of the Northland allochthon (Figure 26 and 30). Floodplains are also implicated, especially where alluvium, peat and lacustrine sediments of the Tauranga Group and Karioitahi Group dominate, and the water table is shallow and soils poorly drained (Figure 30). The few streams with elevated median clarity issue from areas of hard rock, (e.g., Waipoua Basalts), and natural state conditions. Once again, the tributaries of the Wairoa River, including the Manganui, are identified as being of low median clarity as is the Awanui River in the north. Except for the developed areas, e.g. Brynderwyn hills, streams discharging from greywacke basement rocks along the eastern seaboard

are estimated as having moderate median clarity relative to other stream reaches. A similar pattern is noted for turbidity.

E. coli (Figure 27) shows both land use and geological patterns (Figure 30 and 31; Rissmann et al., 2018a,b). Specifically, the highest median *E. coli* counts coincide with areas of erosion-prone land that has been developed for extensive or intensive land use. *E. coli* is also elevated across depositional landforms (floodplains etc.) where soils are poorly drained, and the local water table is shallow. For example, the majority of elevated *E. coli* counts coincide with develop sheep, beef and dairying land on the highly erodible land not limited to the Punakitere Sandstone and other soft sedimentary rocks of the Northland Allochthon. The Karioitahi Group and Tauranga Group sediments are also implicated, especially where the water table is also elevated and soils a poorly drained. Questions surround the legitimacy of *E. coli* estimates for Ninety Mile Beach and from streams draining natural state catchments (i.e., Gum Fields Reserve). Otherwise, the model indicates low *E. coli* counts associated with streams draining natural state areas. An improved land use layer, especially one that provides a distributed representation of land use type and intensity, is likely required to improve or resolve *E. coli* estimates across these areas.

In summary, most of the water quality measures modelled show a relationship to landscape attributes, that in conjunction with land use, drive spatial variation in water quality outcomes. These relationships are consistent with the observations and understanding developed in collaboration with NRC staff over the last four years in response to:

(i) hydrochemical assessment of regional ground and surface waters as part of physiographic mapping of the region (Rissmann et al., 2018a).
(ii) high-resolution mapping and ground-truthing of Northland's Erosion Susceptibility Classification (Rissmann et al., 2018b; McDonald et al., 2020).
(iii) radiometric, satellite and terrain-based mapping of Northland's Wetness Gradient Layer (Rissmann et al., 2019b,c).

These works and the steady-state modelling provided here supports a significant landscape control over water quality outcomes that interact with land-use intensity to generate Northland's unique water quality outcomes.

4.2 Limitations

In terms of model performance, bias is associated with the subset of 67 surface water monitoring sites, that for pragmatic reasons, are related to higher-order streams (≥3) and larger drainage basin areas. Specifically, 50% of the 67 capture zones are >35 km^2, with only eight less than 10 km^2 (smallest is 500 ha). This is relevant as most farms across the region range between 150 and 300 Ha (pers. com. Duncan Kervell, NRC February 2020). As such, the ability of water quality models that utilise monitoring network data and coarse geospatial data sets to estimate water quality at property scales is likely limited. This is important given that error within water quality models tends to increase as drainage basin size decreases, reflecting increasing sensitivity to the resolution, and hence accuracy, of landscape attributes (Troy et al., 2008; Mattot et al., 2009; Moriasi et al., 2015).

The loss of accuracy at small scales is particularly relevant given most geospatial layers used in the development of PAG under the NSC-OLW PENZ project were only as fine as 1:50,000 scale. Finer scales are commonly considered more appropriate for assessing controls at property scales. However, the retention of the NWGL and ESC layers as the most sensitive predictors of spatial variation and the strong performance of the models supports the proposal of Rissmann et al. (2019). Specifically, that higher resolution (50 x 50 m or finer) and more accurate depiction of landscape attributes, based on actual measurement (e.g., radiometrics), can be used to improve the relevance of water quality modelling outputs at property scales. This statement is well supported by

contemporary studies that demonstrate that many of the same processes driving variation at large scales also govern variation across small scales (Moldan and Černý, 1994; Clark and Fritz, 1997; James and Roulet, 2006; Inamdar, 2011; Tratnyek et al., 2012).

A limitation associated with the estimation of water quality across unmonitored areas relates to the use of REC1. Currently there is no cumulative stream order capture zones available for REC2.4 which is an essential requirement to applying physiographic models to a river network. Although the capture area difference between REC1 and 2.4 is relatively minor for SoE monitoring sites (≥3rd order), the REC 2.4 provides greater resolution over the digital stream network at lower stream orders. The greater resolution of REC 2.4 equates to a larger number of stream reaches. Therefore, when comparing between the two datasets many 1st order streams in REC1 are classified as 2nd order in REC2.4 and there are many more 1st order streams identified. As stream order and associated capture zones are assigned at points of confluence or 'nodes' there are fewer node points in REC1. As such, the main limitation that arises when using REC1 to apply the predictive models is the smaller number of node points and hence capture zones. As the PAG models are applied to these node points, the resultant concentrations are applicable to these points but may be displayed over a longer river segment. Further work is required to generate a digital stream network that is more refined and flexible in terms of the number and accuracy of capture zones in order to maximise the value of PAG as predictors of regional water quality and providing measurement of water quality analytes across a wider range of stream orders, and land uses (especially natural state). On its own, a higher resolution DEM will increase the certainty of capture zone delineation but will not remove the bias of applying a model calibrated on higher-order streams to low order streams. However, as an alternative, water quality models can be applied across the landscape, generating calibrated risk models for each water quality measures or for combined water quality risk. Such risk maps have the benefit of representing within capture zone variation in risk, and therefore the resolution of PAG is not limited by the architecture of REC, which was not developed with physiographic based landscape mapping in mind.

Of the models, DRP, TSS, clarity, *E. coli* and DO were the worst-performing. However, the PAG that were retained, and their respective sensitivities and response magnitudes, were consistent with expectations. With regards to DO, the significant measurement error is likely due to re-equilibration of drainage waters with atmospheric oxygen within the stream, a factor not accounted for by physiographic mapping (Figure 28; Rissmann et al., 2019). Specifically, when low DO waters sourced from reducing soils and aquifers discharge to stream, they begin to re-equilibrate with atmospheric oxygen of higher partial pressure. Re-equilibration rate is correlated with the degree of turbulent flow, water temperature and instream metabolic processes. For this reason, we have used PC2 of the hydrochemical subset (Section 2.2.3 and 2.4) to provide an integrated measure of redox potential (Figure 29).

Due to the correlation between land use and landscape attributes, it is likely that some of the PAG are acting as surrogates for land use intensity (e.g. artificial drainage PAG). As such, a key recommendation is that future work considers removing the influence of land use over the models as undertaken for the Physiographics of Southland project (see Snelder, 2016). Removing the influence of land use reduces the influence of correlation which is beneficial when seeking to better evaluate the sensitivity of predictors over dominant processes and water quality measures. Removing the impact of land use is also important if physiographic modelling is to be used to evaluate different land use or climatic scenarios.

5 Evaluation of Water Quality State Against NPS-FM National Objectives Framework

To assess sites against the National Policy Statement for Freshwater Management National Objectives Framework (Ministry for the Environment, 2014, as amended 2017), the models developed for NO_3-N median and 95th percentile, TAM median and maximum, and *E. coli* median and 95th percentile were applied to Northland's 67 monitoring sites. State was assessed for both the measured and modelled values.

A draft National Policy Statement for Freshwater Management was released in September 2019 and is proposed as a full replacement of the current National Policy Statement for Freshwater Management 2014 (as amended 2017). This consultation draft introduced new national objectives for ecosystem health for DIN and DRP. State for Northland's 67 monitoring sites was assessed for these attributes for both the measured and modelled values against the draft NPSFM (2019).

5.1 Ecosystem Health – Nitrate toxicity

An assessment against the NOF state for nitrate toxicity at the 67 sites from the measured data identified 63 sites in the A band for median nitrate and 4 sites in the B band (Table 31). Modelled data showed an overall accuracy of 94% at predicting state across all 67 sites. However, the model underestimated high concentrations for four sites placing them within the A instead of the B band. For the 95th percentile, 64 sites were in the A band from measured data, with 3 sites in the B band with an overall accuracy of 97% (Table 31). The modelled state failed to predict the higher concentrations as accurately with 1 of 3 (measured) sites estimated to fall within the B band. Predicted state across Northland's river network for median and 95th percentile is shown in Figure 33.

Table 34. Assessment against the National Objectives Framework for nitrate toxicity for measured and modelled data.

Site Name	Measured NO_3-N (mg/l)	State	Model NO_3-N (mg/l)	Model State	Measured NO_3-N Q95 (mg/l)	State	Model NO_3-N Q95m (mg/l)	Model State
Wairau at SH12	0.004	A	0.019	A	0.006	A	0.008	A
Waimamaku at SH12	0.004	A	0.011	A	0.033	A	0.089	A
Victoria at Victoria Valley Road	0.004	A	0.014	A	0.073	A	0.074	A
Mangamuka at Iwitaua Road	0.005	A	0.016	A	0.061	A	0.054	A
Oruaiti at Sawyer Road	0.008	A	0.009	A	0.074	A	0.072	A
Waipoua at SH12	0.016	A	0.024	A	0.067	A	0.063	A
Awanui at FNDC	0.016	A	0.033	A	0.151	A	0.152	A
Punaruku at Russell Road	0.017	A	0.025	A	0.058	A	0.116	A
Kaeo at Dip Road	0.018	A	0.058	A	0.150	A	0.075	A
Oruru at Oruru Road	0.022	A	0.016	A	0.130	A	0.130	A
Parapara at Parapara Toatoa Road	0.022	A	0.021	A	0.049	A	0.087	A
Peria at Honeymoon Valley Road	0.024	A	0.021	A	0.049	A	0.067	A
Kenana at Kenana Road	0.024	A	0.025	A	0.101	A	0.276	A
Tapapa at SH1	0.026	A	0.021	A	0.066	A	0.047	A
Parapara at Taumata Road	0.028	A	0.021	A	0.081	A	0.093	A
Paranui at Paranui Road	0.028	A	0.028	A	0.151	A	0.127	A
Mangakahia at Twin Bridges	0.029	A	0.024	A	0.201	A	0.179	A
Waipapa at Forest Ranger	0.030	A	0.015	A	0.066	A	0.067	A
Oruaiti at Windust Road	0.033	A	0.029	A	0.145	A	0.225	A
Awanui at Waihue Channel	0.038	A	0.037	A	0.243	A	0.248	A
Stony Creek at Sawyer Road	0.042	A	0.296	A	0.160	A	0.160	A
Otakaranga at Otaika Valley Road	0.044	A	0.080	A	0.349	A	0.332	A
Aurere at Pekerau Road (C)	0.048	A	0.060	A	0.620	A	0.662	A
Opouteke at Suspension Bridge	0.070	A	0.072	A	0.395	A	0.339	A
Mangakahia at Titoki	0.094	A	0.033	A	0.386	A	0.436	A
Manganui at Mititai Road	0.097	A	0.427	A	0.441	A	0.648	A
Pukenui at Kanehiana Drive	0.100	A	0.116	A	0.255	A	0.319	A
Utakura at Horeke Rd	0.110	A	0.190	A	0.242	A	0.690	A
Waipapa at Waimate North Road	0.110	A	0.332	A	0.372	A	0.497	A
Ngunguru at Coalhill Lane	0.115	A	0.160	A	0.290	A	0.290	A
Waiharakeke at Stringers Road	0.120	A	0.157	A	0.358	A	0.504	A
Mania at SH10	0.135	A	0.352	A	0.360	A	0.613	A
Mangahahuru at Main Road	0.140	A	0.113	A	0.380	A	0.380	A
Utakura at Okaka Bridge	0.155	A	0.152	A	0.313	A	0.700	A
Mangakino at Mangakino Lane	0.165	A	0.256	A	0.394	A	0.524	A
Kaihu at Gorge	0.180	A	0.228	A	0.391	A	0.383	A
Hakaru at Topuni	0.200	A	0.184	A	0.431	A	0.491	A
Waitangi at Wakelins	0.210	A	0.299	A	0.446	A	0.675	A
Mangakino U/S Waitaua Confluence	0.220	A	0.192	A	0.432	A	0.225	A
Waitangi at SH10	0.230	A	0.304	A	0.400	A	0.675	A
Waiaruhe at Puketona	0.240	A	0.247	A	0.452	A	0.709	A
Whakapara at Cableway	0.240	A	0.316	A	0.595	A	0.462	A

Site Name	Measured NO_3-N (mg/l)	State	Model NO_3-N (mg/l)	Model State	Measured NO_3-N Q95 (mg/l)	State	Model NO_3-N Q95m (mg/l)	Model State
Waiotu at SH1	0.250	A	0.234	A	0.754	A	0.500	A
Puwera at SH1	0.250	A	0.321	A	0.688	A	0.668	A
Waipapa at Landing	0.265	A	0.749	A	0.441	A	0.617	A
Pekepeka at Ohaeawai	0.280	A	0.389	A	0.490	A	0.457	A
Mangahahuru at Apotu Road	0.305	A	0.217	A	0.490	A	0.353	A
Waitangi at Waimate North Road	0.310	A	0.239	A	0.490	A	0.466	A
Waiarohia at Second Avenue	0.350	A	0.377	A	0.615	A	0.614	A
Hatea at Whangarei Falls	0.360	A	0.696	A	0.550	A	0.709	A
Punakitere at Taheke	0.375	A	0.137	A	0.583	A	0.553	A
Wairua at Purua	0.390	A	0.257	A	1.060	A	0.635	A
Ruakaka at Flyger Road	0.390	A	0.330	A	0.834	A	0.922	A
Waiarohia at Whau Valley	0.400	A	0.397	A	0.741	A	0.652	A
Waiaruhe D/S Mangamutu Confluence	0.405	A	0.164	A	0.684	A	0.651	A
Mangere at Kokopu Road	0.410	A	0.479	A	0.731	A	0.682	A
Mangere at Wood Road	0.415	A	0.397	A	0.731	A	0.672	A
Kerikeri at Stone Store	0.415	A	0.420	A	0.635	A	0.506	A
Mangere at Kara Road	0.420	A	0.414	A	0.700	A	0.683	A
Hatea at Mair Park	0.470	A	0.671	A	0.695	A	0.731	A
Mangere at Knight Road	0.480	A	0.376	A	1.000	A	0.674	A
Waitaua at Vinegar Hill Road	0.510	A	0.447	A	0.701	A	0.725	A
Watercress at SH1	0.715	A	0.525	A	1.100	A	1.336	A
Otaika at Otaika Valley Road	1.100	B	0.269	A	1.600	B	0.611	A
Raumanga at Bernard Street	1.100	B	0.437	A	1.300	A	0.709	A
Otaika at Cemetery Road	1.350	B	0.545	A	1.800	B	0.783	A
Waipao at Draffin Road	2.300	B	0.784	A	3.320	B	1.481	B

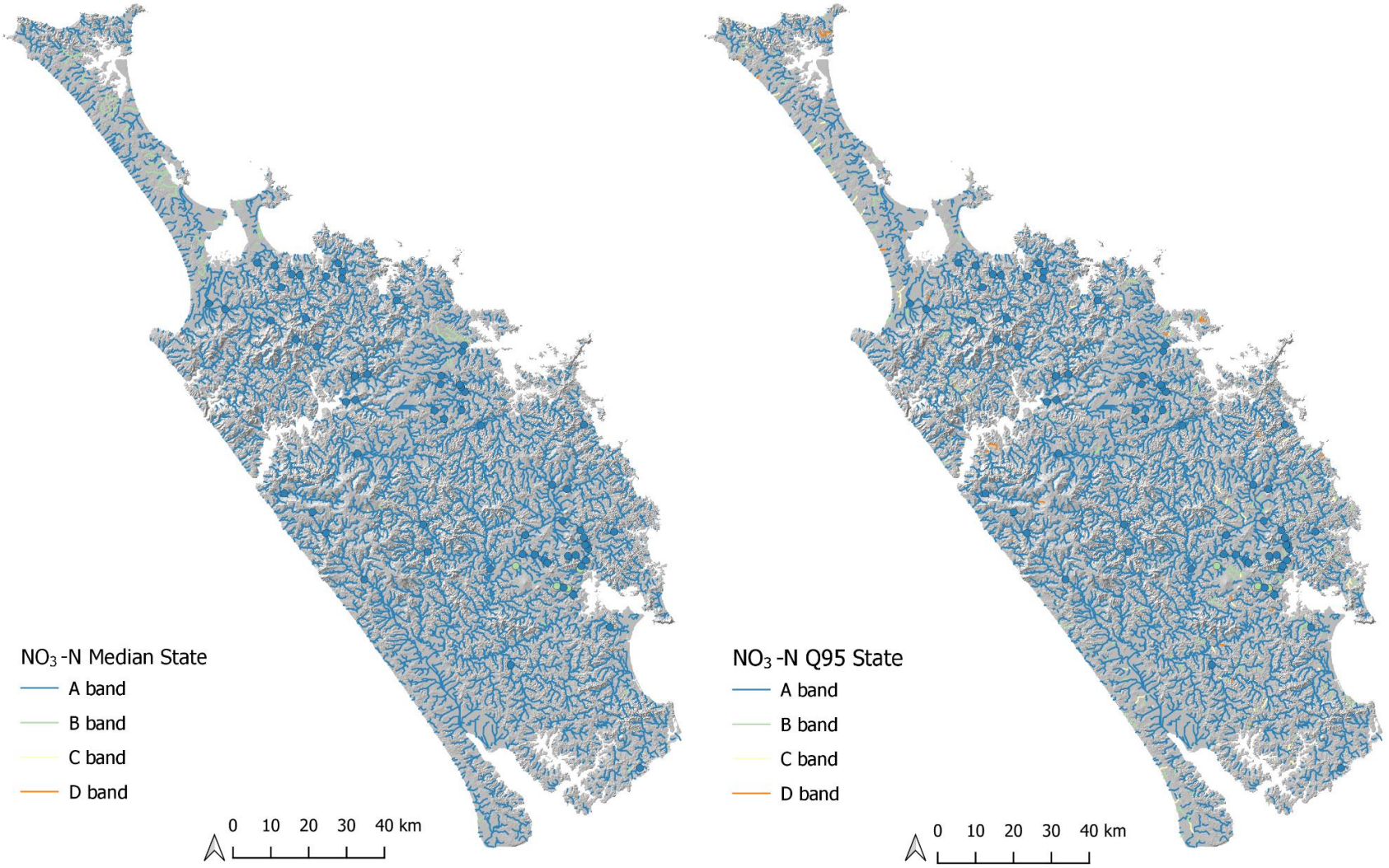

Figure 33. Predicted state of Northlands waterways for ecosystem health - nitrate toxicity. Attribute state is determined by median concentration (left) and Q95 (right). Circles denote the observed median and maximum values for each of the monitoring sites. River reaches and observed measures (sites) are colour coded according to the same concentration gradient.

5.2 Ecosystem Health – Ammonia toxicity

An assessment against the NOF state for ammonia toxicity at the 67 sites from the measured data identified 62 sites in the A band for median total ammoniacal nitrogen, 4 sites in the B band and 1 in the C band (Table 32). Modelled data was mostly comparable with all but 2 sites, Mangere at Knight Road and Waiaruhe D/S Mangamutu Confluence, identified correctly (97% accuracy). For measured TAM maximum state, there are 19 sites in the A band, 39 sites in the B band, 8 in the C band, and 1 in the D band (Table 32). Modelled TAM maximum state was generally good with 27 sites in the A band, 28 sites in the B band, 11 in the C band, and 1 in the D band, with an overall accuracy of 81%. Predicted state across Northland's river network for median and maximum values are shown in Figure 34.

Table 35. Assessment against the National Objectives Framework for ammonia toxicity measured and modelled data.

Site Name	Measured TAM (mg/l)	State	Model TAM (mg/l)	Model State	Measured TAM Max (mg/l)	State	Model TAM Max (mg/l)	Model State
Waipapa at Forest Ranger	0.004	A	0.005	A	0.008	A	0.026	A
Wairau at SH12	0.005	A	0.005	A	0.021	A	0.021	A
Waimamaku at SH12	0.005	A	0.005	A	0.017	A	0.040	A
Victoria at Victoria Valley Road	0.005	A	0.006	A	0.022	A	0.031	A
Mangamuka at Iwitaua Road	0.005	A	0.006	A	0.037	A	0.027	A
Waipoua at SH12	0.005	A	0.005	A	0.053	B	0.028	A
Punaruku at Russell Road	0.005	A	0.005	A	0.026	A	0.028	A
Peria at Honeymoon Valley Road	0.005	A	0.005	A	0.019	A	0.020	A
Tapapa at SH1	0.005	A	0.005	A	0.018	A	0.021	A
Mangakahia at Twin Bridges	0.005	A	0.008	A	0.045	A	0.045	A
Opouteke at Suspension Bridge	0.005	A	0.005	A	0.039	A	0.024	A
Kaihu at Gorge	0.005	A	0.010	A	0.035	A	0.035	A
Kenana at Kenana Road	0.006	A	0.006	A	0.025	A	0.025	A
Mangakino at Mangakino Lane	0.006	A	0.007	A	0.023	A	0.033	A
Pekepeka at Ohaeawai	0.006	A	0.006	A	0.073	B	0.072	B
Oruaiti at Sawyer Road	0.007	A	0.007	A	0.028	A	0.043	A
Awanui at FNDC	0.007	A	0.013	A	0.058	B	0.062	B
Kaeo at Dip Road	0.008	A	0.008	A	0.051	B	0.051	B
Oruru at Oruru Road	0.008	A	0.007	A	0.056	B	0.056	B
Oruaiti at Windust Road	0.008	A	0.009	A	0.024	A	0.031	A
Pukenui at Kanehiana Drive	0.008	A	0.007	A	0.042	A	0.037	A
Waipapa at Waimate North Road	0.008	A	0.016	A	0.290	B	0.224	B
Ngunguru at Coalhill Lane	0.008	A	0.007	A	0.034	A	0.052	B
Mangakahia at Titoki	0.009	A	0.009	A	0.139	B	0.139	B
Waiarohia at Whau Valley	0.009	A	0.009	A	0.078	B	0.040	A
Waipao at Draffin Road	0.009	A	0.009	A	0.320	B	0.097	B
Hatea at Mair Park	0.009	A	0.010	A	0.055	B	0.078	B
Paranui at Paranui Road	0.010	A	0.010	A	0.031	A	0.049	A
Stony Creek at Sawyer Road	0.010	A	0.015	A	0.080	B	0.077	B
Mangahahuru at Main Road	0.010	A	0.011	A	0.066	B	0.033	A
Waitangi at SH10	0.010	A	0.013	A	0.065	B	0.081	B

Site Name	Measured TAM (mg/l)	State	Model TAM (mg/l)	Model State	Measured TAM Max (mg/l)	State	Model TAM Max (mg/l)	Model State
Hatea at Whangarei Falls	0.010	A	0.010	A	0.084	B	0.089	B
Mangere at Kara Road	0.010	A	0.009	A	0.053	B	0.049	A
Watercress at SH1	0.010	A	0.017	A	0.080	B	0.133	B
Waitangi at Wakelins	0.010	A	0.014	A	0.067	B	0.101	B
Whakapara at Cableway	0.011	A	0.013	A	0.150	B	0.055	B
Waitangi at Waimate North Road	0.011	A	0.010	A	0.063	B	0.045	A
Waiarohia at Second Avenue	0.011	A	0.011	A	0.440	C	0.408	C
Punakitere at Taheke	0.012	A	0.011	A	0.180	B	0.427	C
Parapara at Parapara Toatoa Road	0.012	A	0.011	A	0.058	B	0.044	A
Kerikeri at Stone Store	0.013	A	0.013	A	0.150	B	0.109	B
Utakura at Horeke Rd	0.014	A	0.014	A	0.059	B	0.454	C
Mangere at Wood Road	0.014	A	0.009	A	0.060	B	0.050	A
Otaika at Otaika Valley Road	0.014	A	0.014	A	0.150	B	0.105	B
Waitaua at Vinegar Hill Road	0.014	A	0.016	A	0.061	B	0.047	A
Utakura at Okaka Bridge	0.015	A	0.016	A	0.430	C	0.461	C
Hakaru at Topuni	0.015	A	0.015	A	0.160	B	0.218	B
Mangakino U/S Waitaua Confluence	0.015	A	0.007	A	0.033	A	0.043	A
Waipapa at Landing	0.015	A	0.013	A	0.086	B	0.101	B
Raumanga at Bernard Street	0.015	A	0.015	A	0.053	B	0.070	B
Waiharakeke at Stringers Road	0.016	A	0.016	A	0.620	C	0.405	C
Mania at SH10	0.016	A	0.016	A	0.330	B	0.143	B
Mangahahuru at Apotu Road	0.016	A	0.011	A	0.170	B	0.070	B
Mangere at Kokopu Road	0.016	A	0.016	A	0.093	B	0.120	B
Otakaranga at Otaika Valley Road	0.017	A	0.013	A	0.120	B	0.101	B
Otaika at Cemetery Road	0.017	A	0.014	A	0.062	B	0.082	B
Waiaruhe at Puketona	0.018	A	0.015	A	0.095	B	0.104	B
Waiotu at SH1	0.018	A	0.016	A	0.320	B	0.130	B
Parapara at Taumata Road	0.020	A	0.009	A	0.081	B	0.045	A
Wairua at Purua	0.023	A	0.020	A	0.180	B	0.179	B
Aurere at Pekerau Road (C)	0.024	A	0.021	A	1.620	C	1.621	C
Manganui at Mititai Road	0.028	A	0.028	A	0.290	B	0.417	C
Mangere at Knight Road	0.031	B	0.019	A	1.600	C	1.601	C
Puwera at SH1	0.035	B	0.033	B	5.000	D	5.738	D
Ruakaka at Flyger Road	0.035	B	0.035	B	0.410	C	0.406	C
Awanui at Waihue Channel	0.044	B	0.044	B	1.300	C	1.018	C
Waiaruhe D/S Mangamutu Confluence	0.125	B	0.008	A	0.860	C	0.403	C

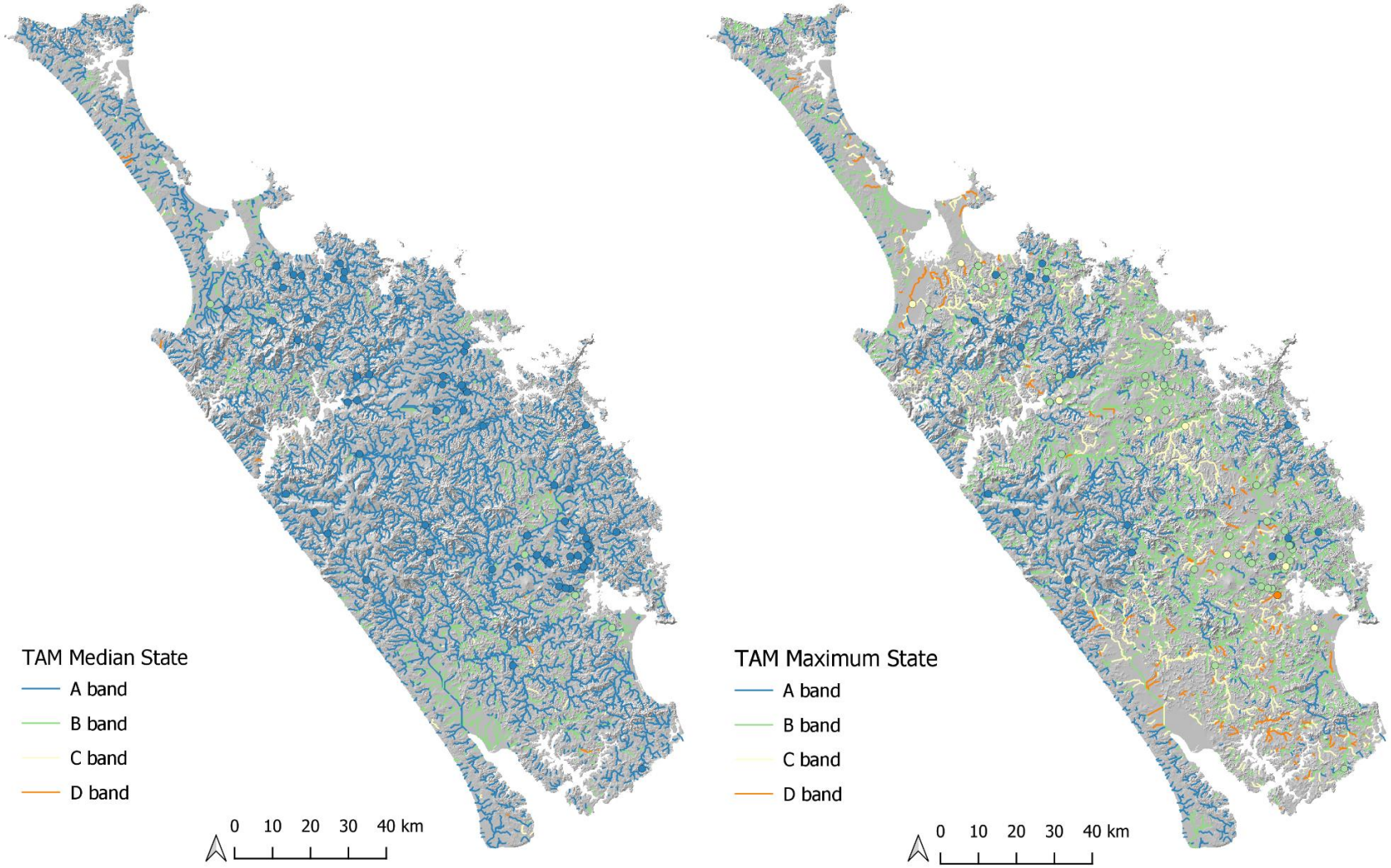

Figure 34. Predicted state of Northlands waterways for ecosystem health - ammonia toxicity. Attribute state is determined by median concentration (left) and maximum concentration (right). Circles denote the observed median and maximum values for each of the monitoring sites. River reaches and observed measures (sites) are colour coded according to the same concentration gradient.

5.3 Human Health for Recreation – *E. coli*

To assess the attribute state for *E. coli* the NOF requires a minimum of 60 water samples over a maximum of 5-years. Where sites do not meet this criterion, attribute state may be determined using samples over a longer timeframe. Northland's dataset was augmented with additional samples to meet NOF criteria by including data most recent to January 2015 (i.e., December 2014 if one additional measure was required). Seven sites remain that do not meet the minimum sample number requirements and are to be taken as indicative only. These sites are Wairau at SH12, Punaruku at Russell Road, Tapapa at SH1, Puwera at SH1, Pukenui at Kanehiana Drive, Utakura at Okaka Bridge, and Raumanga at Bernard Street.

Table 33 shows the assessment against the NOF state for the measured data by median, 95th percentile, % exceedances greater than 260 cfu/100 ml and 540 cfu/100 ml. The overall state was typically limited by the median concentration, with 2 sites in the B band, 2 in the C band, 25 in the D band, and 22 in the E band.

Modelled data was compared to the measured median and 95th percentile state in Table 34. The NOF assessment identified 8 sites in the A band, 12 sites in the B band, and 38 below the national bottom line in the E band. Modelled median data showed similar predictions with 7 in the A band, 22 in the D band and 38 in the E band, with an overall accuracy of 73%. For the 95th percentile, 1 site is in the A band, 7 sites in the B band, 6 sites in the C band, and 53 sites in the D band from measured data (Table 33). The modelled 95th percentile state had an overall accuracy of 84%, with 1 site in the A band, 7 sites in the B band, 1 site in the C band, and 58 sites in the D band. Predicted state across Northland's river network for median and 95th percentile is shown in Figure 35.

Table 36. E. coli (measured) assessment against the NPSFM for Human Health for Recreation. Sites with an overall state indicated with an asterisk (*) do not meet the minimum sample number requirements and are to be taken as indicative only.

Site Name	Number of samples	Median (cfu/100 ml)	Median State	95th percentile (cfu/100 ml)	Q95 State	*E. coli* >260 cfu/ 100 ml	% >260 cfu/ 100 ml	% >260 State	*E. coli* >540 cfu/ 100 ml	% >540 cfu/ 100 ml	% >540 State	Overall State
Tapapa at SH1	42	103.5	A	581.4	B	7	16.7	A	3	7.1	B	B*
Wairau at SH12	41	86.0	A	670.0	B	8	19.5	A	3	7.3	B	B*
Waipapa at Forest Ranger	60	81.1	A	1124.1	C	11	18.3	A	6	10.0	B	C
Punaruku at Russell Road	42	121.0	A	1057.6	C	9	21.4	B	4	9.5	B	C*
Hakaru at Topuni	60	134.0	D	17359.8	D	15	25.0	B	12	20.0	C	D
Kaihu at Gorge	60	181.5	D	3897.0	D	19	31.7	C	9	15.0	C	D
Kerikeri at Stone Store	89	228.0	D	12611.4	D	40	44.9	D	23	25.8	D	D
Mangakahia at Titoki	86	179.7	D	11690.0	D	34	39.5	D	21	24.4	D	D
Mangakahia at Twin Bridges	60	121.0	A	4489.4	D	22	36.7	D	11	18.3	C	D
Mangakino at Mangakino Lane	60	149.0	D	986.0	B	12	20.0	A	5	8.3	B	D
Manganui at Mititai Road	60	120.0	A	3638.2	D	17	28.3	B	13	21.7	D	D
Mania at SH10	60	235.0	D	1609.6	D	25	41.7	D	12	20.0	C	D
Opouteke at Suspension Bridge	60	145.0	D	1220.8	D	18	30.0	B	9	15.0	C	D
Oruaiti at Sawyer Road	60	194.0	D	2053.8	D	23	38.3	D	12	20.0	C	D
Paranui at Paranui Road	60	191.0	D	700.7	B	20	33.3	C	5	8.3	B	D
Pekepeka at Ohaeawai	60	212.0	D	628.6	B	21	35.0	D	4	6.7	B	D
Peria at Honeymoon Valley Road	60	132.0	D	500.7	A	13	21.7	B	3	5.0	A	D
Stony Creek at Sawyer Road	60	150.0	D	1520.9	D	17	28.3	B	8	13.3	C	D
Utakura at Horeke Rd	72	206.0	D	1509.9	D	28	38.9	D	8	11.1	C	D
Victoria at Victoria Valley Road	60	158.0	D	880.0	B	11	18.3	A	6	10.0	B	D
Waiaruhe at Puketona	60	243.5	D	790.4	B	27	45.0	D	11	18.3	C	D
Waiharakeke at Stringers Road	60	259.0	D	13123.7	D	30	50.0	D	16	26.7	D	D
Waipapa at Landing	60	189.5	D	3350.9	D	17	28.3	B	9	15.0	C	D
Waipapa at Waimate North Road	60	242.0	D	3676.6	D	26	43.3	D	11	18.3	C	D
Waipoua at SH12	60	64.0	A	2145.9	D	10	16.7	A	6	10.0	B	D

Site Name	Number of samples	Median (cfu/100 ml)	Median State	95th percentile (cfu/100 ml)	Q95 State	*E. coli* >260 cfu/ 100 ml	% >260 cfu/ 100 ml	% >260 State	*E. coli* >540 cfu/ 100 ml	% >540 cfu/ 100 ml	% >540 State	Overall State
Wairua at Purua	85	121.1	A	23326.0	D	26	30.6	C	19	22.4	D	D
Waitangi at SH10	60	259.5	D	4898.4	D	29	48.3	D	12	20.0	C	D
Waitangi at Wakelins	176	170.0	D	2419.2	D	57	32.4	C	31	17.6	C	D
Utakura at Okaka Bridge	47	250.0	D	4953.3	D	21	44.7	D	12	25.5	D	D*
Aurere at Pekerau Road (C)	63	437.0	E	1970.0	D	47	74.6	E	19	30.2	E	E
Awanui at FNDC	60	282.5	E	5620.2	D	32	53.3	E	19	31.7	E	E
Awanui at Waihue Channel	75	288.0	E	4885.7	D	40	53.3	E	22	29.3	D	E
Hatea at Mair Park	92	350.0	E	14798.4	D	57	62.0	E	31	33.7	E	E
Hatea at Whangarei Falls	132	447.5	E	4865.6	D	108	81.8	E	51	38.6	E	E
Kaeo at Dip Road	60	403.5	E	6571.8	D	38	63.3	E	22	36.7	E	E
Kenana at Kenana Road	60	333.5	E	1038.3	C	38	63.3	E	17	28.3	D	E
Mangahahuru at Apotu Road	60	310.0	E	7584.9	D	36	60.0	E	11	18.3	C	E
Mangahahuru at Main Road	60	452.5	E	3488.6	D	40	66.7	E	22	36.7	E	E
Mangakino U/S Waitaua Confluence	60	559.5	E	1720.3	D	55	91.7	E	32	53.3	E	E
Mangamuka at Iwitaua Road	60	345.0	E	2938.6	D	40	66.7	E	23	38.3	E	E
Mangapiu at Kokopu Road	60	1086.0	E	9915.5	D	54	90.0	E	46	76.7	E	E
Mangere at Kara Road	60	615.0	E	2433.8	D	53	88.3	E	33	55.0	E	E
Mangere at Knight Road	110	656.5	E	11288.4	D	101	91.8	E	75	68.2	E	E
Mangere at Kokopu Road	60	599.0	E	2206.6	D	54	90.0	E	38	63.3	E	E
Mangere at Wood Road	60	524.5	E	1436.4	D	50	83.3	E	29	48.3	E	E
Ngunguru at Coalhill Lane	60	310.5	E	7346.7	D	32	53.3	E	17	28.3	D	E
Oruaiti at Windust Road	60	275.0	E	2530.0	D	34	56.7	E	11	18.3	C	E
Oruru at Oruru Road	111	305.0	E	2778.5	D	66	59.5	E	25	22.5	D	E
Otaika at Cemetery Road	60	795.0	E	3873.0	D	46	76.7	E	35	58.3	E	E
Otaika at Otaika Valley Road	109	550.0	E	4507.4	D	93	85.3	E	56	51.4	E	E
Otakaranga at Otaika Valley Road	60	450.0	E	2417.8	D	44	73.3	E	28	46.7	E	E

Site Name	Number of samples	Median (cfu/100 ml)	Median State	95th percentile (cfu/100 ml)	Q95 State	*E. coli* >260 cfu/ 100 ml	% >260 cfu/ 100 ml	% >260 State	*E. coli* >540 cfu/ 100 ml	% >540 cfu/ 100 ml	% >540 State	Overall State
Parapara at Parapara Toatoa Road	60	301.5	E	1148.9	C	37	61.7	E	10	16.7	C	E
Parapara at Taumata Road	60	343.0	E	1107.3	C	42	70.0	E	14	23.3	D	E
Punakitere at Taheke	60	327.0	E	5863.4	D	36	60.0	E	24	40.0	E	E
Ruakaka at Flyger Road	60	464.5	E	8965.6	D	48	80.0	E	25	41.7	E	E
Waiarohia at Second Avenue	111	417.0	E	9232.0	D	74	66.7	E	38	34.2	E	E
Waiarohia at Whau Valley	60	380.0	E	2038.2	D	45	75.0	E	19	31.7	E	E
Waiaruhe D/S Mangamutu Confluence	60	280.0	E	1086.0	C	33	55.0	E	13	21.7	D	E
Waimamaku at SH12	60	286.5	E	2890.6	D	32	53.3	E	16	26.7	D	E
Waiotu at SH1	60	350.0	E	14620.2	D	39	65.0	E	14	23.3	D	E
Waipao at Draffin Road	60	676.5	E	9957.4	D	52	86.7	E	35	58.3	E	E
Waitangi at Waimate North Road	111	305.0	E	9635.0	D	63	56.8	E	30	27.0	D	E
Waitaua at Vinegar Hill Road	60	605.0	E	2082.7	D	54	90.0	E	34	56.7	E	E
Watercress at SH1	60	328.5	E	2018.9	D	42	70.0	E	20	33.3	E	E
Whakapara at Cableway	60	275.5	E	17455.7	D	32	53.3	E	13	21.7	D	E
Pukenui at Kanehiana Drive	46	394.5	E	6394.8	D	29	63.0	E	16	34.8	E	E*
Puwera at SH1	43	594.0	E	2253.8	D	36	83.7	E	23	53.5	E	E*
Raumanga at Bernard Street	55	670.0	E	3873.0	D	51	92.7	E	34	61.8	E	E*

Table 37. Assessment against the National Objectives Framework for E. coli measured and modelled data.

Site Name	Median (cfu/ 100 ml)	Median State	Model Median (cfu/ 100 ml)	Model State	Q95 (cfu/ 100 ml)	Q95 State	Model Q95 (cfu/ 100 ml)	Model State
Waipoua at SH12	64	A	91	A	2146	D	912	B
Waipapa at Forest Ranger	81	A	115	A	1124	C	1485	D
Wairau at SH12	86	A	88	A	670	B	688	B
Tapapa at SH1	104	A	95	A	581	B	379	A
Manganui at Mititai Road	120	A	120	A	3638	D	3652	D
Punaruku at Russell Road	121	A	172	D	1058	C	4581	D
Mangakahia at Twin Bridges	121	A	124	A	4489	D	1869	D
Wairua at Purua	121	A	181	D	23326	D	22461	D
Peria at Honeymoon Valley Road	132	D	99	A	501	A	655	B
Hakaru at Topuni	134	D	384	E	17360	D	16396	D
Opouteke at Suspension Bridge	145	D	134	D	1221	D	1503	D
Mangakino at Mangakino Lane	149	D	168	D	986	B	907	B
Stony Creek at Sawyer Road	150	D	336	E	1521	D	3393	D
Victoria at Victoria Valley Road	158	D	188	D	880	B	1544	D
Waitangi at Wakelins	170	D	221	D	2419	D	4633	D
Mangakahia at Titoki	180	D	158	D	11690	D	11726	D
Kaihu at Gorge	182	D	220	D	3897	D	2429	D
Waipapa at Landing	190	D	278	E	3351	D	3933	D
Paranui at Paranui Road	191	D	280	E	701	B	967	B
Oruaiti at Sawyer Road	194	D	245	D	2054	D	3212	D
Utakura at Horeke Rd	206	D	272	E	1510	D	4136	D
Pekepeka at Ohaeawai	212	D	139	D	629	B	2232	D
Kerikeri at Stone Store	228	D	240	D	12611	D	14249	D
Mania at SH10	235	D	447	E	1610	D	4942	D
Waipapa at Waimate North Road	242	D	222	D	3677	D	3620	D
Waiaruhe at Puketona	244	D	245	D	790	B	3624	D
Utakura at Okaka Bridge	250	D	262	E	4953	D	3915	D
Waiharakeke at Stringers Road	259	D	344	E	13124	D	12949	D
Waitangi at SH10	260	D	253	D	4898	D	8421	D
Oruaiti at Windust Road	275	E	258	D	2530	D	2673	D
Whakapara at Cableway	276	E	276	E	17456	D	9538	D
Waiaruhe D/S Mangamutu Confluence	280	E	225	D	1086	C	3018	D
Awanui at FNDC	283	E	291	E	5620	D	3508	D
Waimamaku at SH12	287	E	360	E	2891	D	3730	D
Awanui at Waihue Channel	288	E	259	D	4886	D	4990	D
Parapara at Parapara Toatoa Road	302	E	395	E	1149	C	1130	C
Oruru at Oruru Road	305	E	285	E	2779	D	2330	D
Waitangi at Waimate North Road	305	E	305	E	9635	D	10110	D
Mangahahuru at Apotu Road	310	E	556	E	7585	D	4896	D
Ngunguru at Coalhill Lane	311	E	556	E	7347	D	6749	D
Punakitere at Taheke	327	E	166	D	5863	D	3497	D

Site Name	Median (cfu/ 100 ml)	Median State	Model Median (cfu/ 100 ml)	Model State	Q95 (cfu/ 100 ml)	Q95 State	Model Q95 (cfu/ 100 ml)	Model State
Watercress at SH1	329	E	350	E	2019	D	1836	D
Kenana at Kenana Road	334	E	233	D	1038	C	1344	D
Parapara at Taumata Road	343	E	266	E	1107	C	965	B
Mangamuka at Iwitaua Road	345	E	166	D	2939	D	1772	D
Hatea at Mair Park	350	E	490	E	14798	D	4181	D
Waiotu at SH1	350	E	242	D	14620	D	10231	D
Waiarohia at Whau Valley	380	E	456	E	2038	D	1822	D
Pukenui at Kanehiana Drive	395	E	409	E	6395	D	822	B
Kaeo at Dip Road	404	E	269	E	6572	D	6736	D
Waiarohia at Second Avenue	417	E	197	D	9232	D	3808	D
Aurere at Pekerau Road (C)	437	E	473	E	1970	D	2948	D
Hatea at Whangarei Falls	448	E	522	E	4866	D	4208	D
Otakaranga at Otaika Valley Road	450	E	492	E	2418	D	2535	D
Mangahahuru at Main Road	453	E	441	E	3489	D	3490	D
Ruakaka at Flyger Road	465	E	441	E	8966	D	9779	D
Mangere at Wood Road	525	E	525	E	1436	D	2217	D
Otaika at Otaika Valley Road	550	E	506	E	4507	D	3941	D
Mangakino U/S Waitaua Confluence	560	E	568	E	1720	D	2020	D
Puwera at SH1	594	E	583	E	2254	D	4486	D
Mangere at Kokopu Road	599	E	434	E	2207	D	4343	D
Waitaua at Vinegar Hill Road	605	E	561	E	2083	D	2841	D
Mangere at Kara Road	615	E	532	E	2434	D	2439	D
Mangere at Knight Road	657	E	323	E	11288	D	4403	D
Raumanga at Bernard Street	670	E	619	E	3873	D	6388	D
Waipao at Draffin Road	677	E	518	E	9957	D	10680	D
Otaika at Cemetery Road	795	E	756	E	3873	D	3756	D

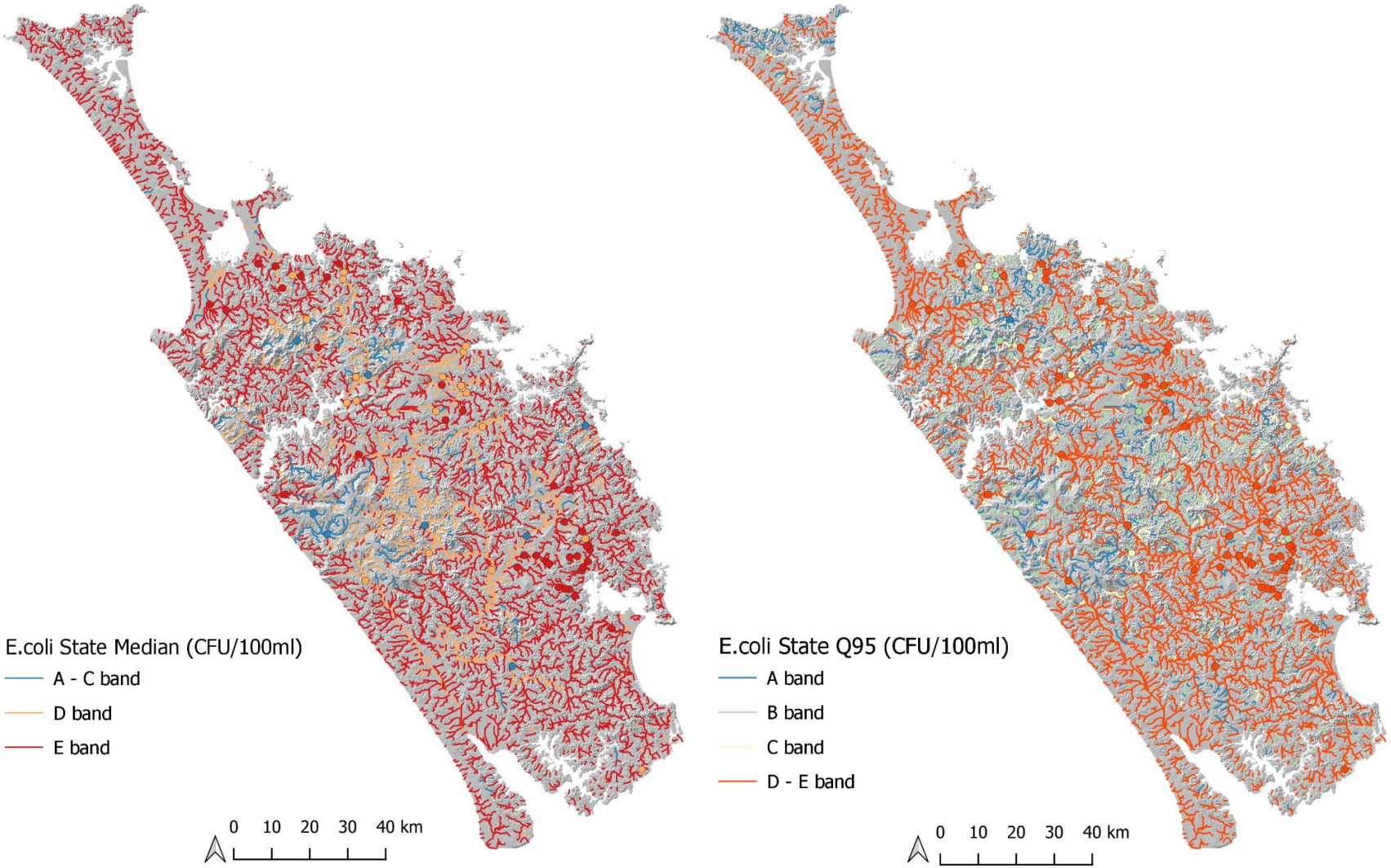

Figure 35. Predicted state of Northlands waterways for human health for recreation. E. coli state is determined by median concentration (left) and 95th percentile (right). Circles denote the observed median and Q95 values for each of the monitoring sites. River reaches and observed measures (sites) are colour coded according to the same concentration gradient.

5.4 Ecosystem Health – Dissolved Inorganic Nitrogen

An assessment of DIN against the proposed NOF state in the draft NPSFM (2019) at the 67 sites from the measured data identified 39 sites in the A band for median DIN, 20 sites in the B band, 4 sites in the C band, and 4 sites in the D band (Table 38). Modelled data showed an overall accuracy of 73% at predicting state across all 67 sites. However, it is important to note the data used for these models are calculated due to the lack of sufficient DIN measurements. For the 95th percentile, 42 sites were in the A band, 19 sites in the B band, 5 sites in the C band and 1 site in the D band from measured data. The modelled 95th percentile had an overall accuracy of 72% (Table 38). Both the median and 95th percentile models underestimated high concentrations. Predicted state across Northland's river network for median and 95th percentile is shown in Figure 36.

Table 38. Assessment against the proposed National Objectives Framework for dissolved inorganic nitrogen for measured and modelled data.

	Cal. DIN (mg/l)	State	Model DIN (mg/l)	Model State	Cal. DIN Q95 (mg/l)	State	Model DIN Q95m (mg/l)	Model State
Wairau at SH12	0.010	A	0.008	A	0.014	A	0.013	A
Victoria at Victoria Valley Road	0.011	A	0.011	A	0.098	A	0.077	A
Mangamuka at Iwitaua Road	0.012	A	0.011	A	0.067	A	0.067	A
Waimamaku at SH12	0.012	A	0.013	A	0.042	A	0.187	A
Waipapa at Forest Ranger	0.015	A	0.002	A	0.086	A	0.088	A
Oruaiti at Sawyer Road	0.016	A	0.004	A	0.089	A	0.093	A
Punaruku at Russell Road	0.024	A	0.067	A	0.066	A	0.067	A
Kaeo at Dip Road	0.028	A	0.018	A	0.166	A	0.111	A
Peria at Honeymoon Valley Road	0.029	A	0.020	A	0.056	A	0.064	A
Awanui at FNDC	0.029	A	0.029	A	0.171	A	0.181	A
Waipoua at SH12	0.030	A	0.024	A	0.072	A	0.033	A
Tapapa at SH1	0.031	A	0.038	A	0.072	A	0.089	A
Kenana at Kenana Road	0.031	A	0.018	A	0.111	A	0.111	A
Oruru at Oruru Road	0.032	A	0.010	A	0.162	A	0.200	A
Mangakahia at Twin Bridges	0.034	A	0.043	A	0.215	A	0.217	A
Parapara at Parapara Toatoa Road	0.035	A	0.023	A	0.070	A	0.077	A
Paranui at Paranui Road	0.036	A	0.014	A	0.158	A	0.245	A
Oruaiti at Windust Road	0.038	A	0.017	A	0.155	A	0.233	A
Parapara at Taumata Road	0.052	A	0.055	A	0.100	A	0.088	A
Stony Creek at Sawyer Road	0.058	A	0.025	A	0.175	A	0.762	B
Otakaranga at Otaika Valley Road	0.074	A	0.122	A	0.417	A	0.301	A
Opouteke at Suspension Bridge	0.075	A	0.044	A	0.404	A	0.263	A
Mangakahia at Titoki	0.088	A	0.020	A	0.433	A	0.437	A
Pukenui at Kanehiana Drive	0.108	A	0.082	A	0.261	A	0.261	A
Utakura at Horeke Rd	0.115	A	0.224	A	0.274	A	0.300	A
Awanui at Waihue Channel	0.127	A	0.066	A	0.792	B	0.273	A
Waipapa at Waimate North Road	0.128	A	0.128	A	0.502	A	0.489	A
Ngunguru at Coalhill Lane	0.130	A	0.109	A	0.318	A	0.315	A
Mania at SH10	0.144	A	0.301	B	0.404	A	0.420	A

	Cal. DIN (mg/l)	State	Model DIN (mg/l)	Model State	Cal. DIN Q95 (mg/l)	State	Model DIN Q95m (mg/l)	Model State
Mangahahuru at Main Road	0.146	A	0.183	A	0.388	A	0.233	A
Waiharakeke at Stringers Road	0.146	A	0.415	B	0.407	A	0.411	A
Utakura at Okaka Bridge	0.167	A	0.318	B	0.339	A	0.310	A
Mangakino at Mangakino Lane	0.172	A	0.185	A	0.402	A	0.662	B
Kaihu at Gorge	0.185	A	0.139	A	0.402	A	0.462	A
Manganui at Mititai Road	0.193	A	0.282	B	0.522	A	0.673	B
Waitangi at Wakelins	0.216	A	0.187	A	0.481	A	0.769	B
Aurere at Pekerau Road (C)	0.216	A	0.169	A	0.766	B	0.730	B
Hakaru at Topuni	0.220	A	0.172	A	0.499	A	0.583	B
Mangakino U/S Waitaua Confluence	0.236	A	0.148	A	0.463	A	0.463	A
Waitangi at SH10	0.252	B	0.165	A	0.413	A	0.983	B
Waiaruhe at Puketona	0.284	B	0.285	B	0.498	A	0.753	B
Pekepeka at Ohaeawai	0.285	B	0.180	A	0.497	A	0.509	A
Waipapa at Landing	0.289	B	0.196	A	0.470	A	0.630	B
Puwera at SH1	0.289	B	0.801	C	0.845	B	0.728	B
Waiotu at SH1	0.291	B	0.310	B	0.881	B	0.789	B
Whakapara at Cableway	0.292	B	0.104	A	0.646	B	0.580	B
Waitangi at Waimate North Road	0.320	B	0.137	A	0.504	A	0.715	B
Mangahahuru at Apotu Road	0.334	B	0.191	A	0.571	B	0.416	A
Waiarohia at Second Avenue	0.369	B	0.292	B	0.634	B	0.644	B
Hatea at Whangarei Falls	0.380	B	0.349	B	0.580	B	0.740	B
Punakitere at Taheke	0.398	B	0.176	A	0.616	B	0.616	B
Waiarohia at Whau Valley	0.411	B	0.274	B	0.750	B	0.433	A
Mangere at Kara Road	0.425	B	0.267	B	0.711	B	0.617	B
Mangere at Wood Road	0.433	B	0.282	B	0.747	B	0.639	B
Kerikeri at Stone Store	0.440	B	0.441	B	0.643	B	0.670	B
Mangere at Kokopu Road	0.443	B	0.666	C	0.748	B	1.035	B
Ruakaka at Flyger Road	0.444	B	0.300	B	0.937	B	0.343	A
Wairua at Purua	0.454	B	0.372	B	1.093	B	0.600	B
Hatea at Mair Park	0.480	B	0.337	B	0.723	B	0.678	B
Waiaruhe D/S Mangamutu Confluence	0.515	C	0.570	C	0.935	B	0.648	B
Waitaua at Vinegar Hill Road	0.519	C	0.707	C	0.730	B	0.843	B
Mangere at Knight Road	0.546	C	0.792	C	1.171	C	1.050	B
Watercress at SH1	0.725	C	0.200	A	1.116	C	0.905	B
Otaika at Otaika Valley Road	1.113	D	0.905	C	1.607	C	0.359	A
Raumanga at Bernard Street	1.117	D	0.493	B	1.352	C	0.410	A
Otaika at Cemetery Road	1.406	D	1.035	C	1.820	C	0.607	B
Waipao at Draffin Road	2.311	D	0.843	C	3.326	D	1.459	C

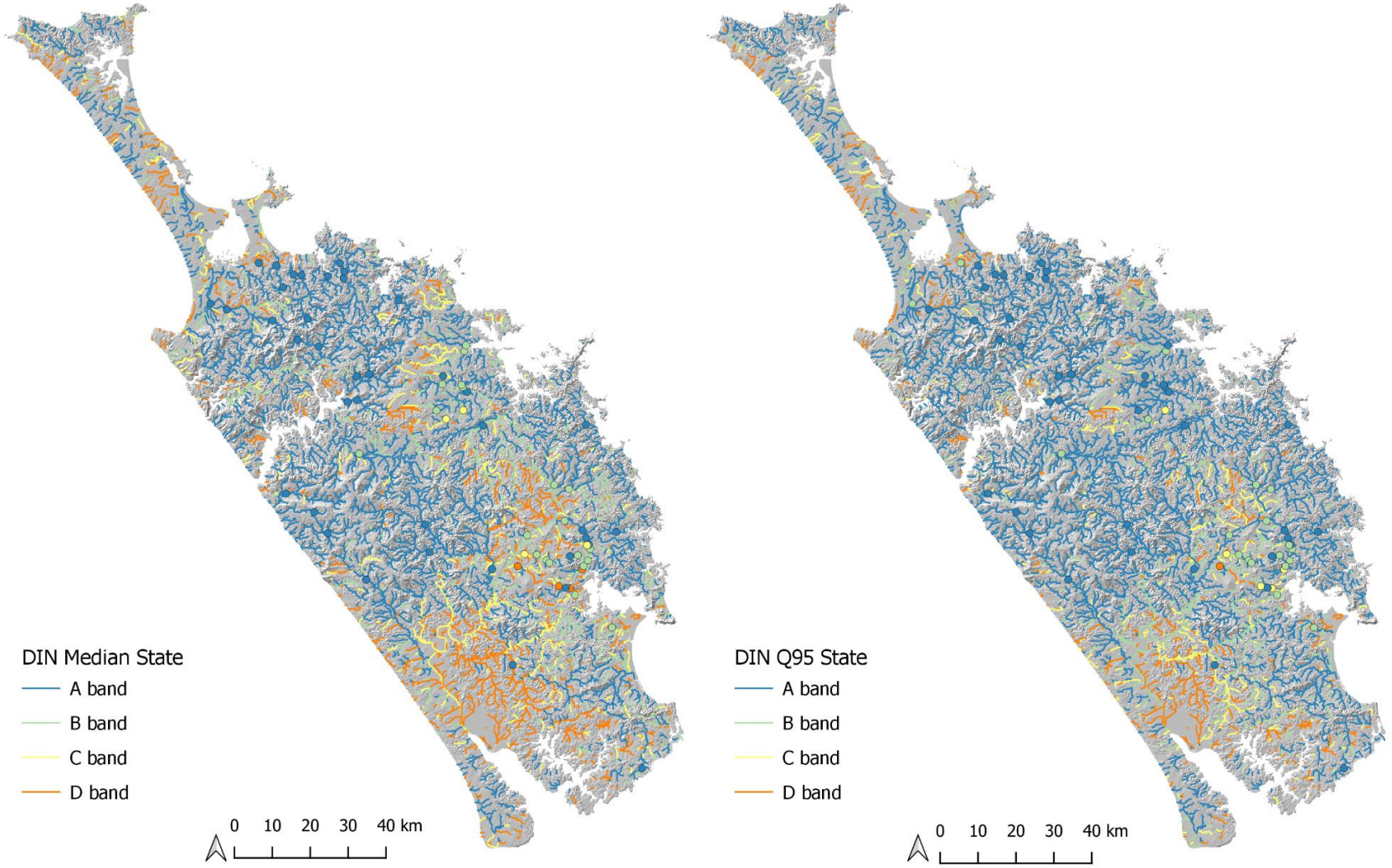

Figure 36. Predicted state of Northlands waterways for ecosystem health – dissolved inorganic nitrogen. Attribute state is determined by median concentration (left) and Q95 (right). Circles denote the observed median and maximum values for each of the monitoring sites. River reaches and observed measures (sites) are colour coded according to the same concentration gradient. State assessed using draft NPSFM (2019).

5.5 Ecosystem Health – Dissolved Reactive Phosphorus

An assessment of DRP against the proposed NOF state in the draft NPSFM (2019) at the 67 sites from the measured data identified 5 sites in the A band for median DRP, 15 in the B band, 25 sites in the C band, and 22 sites in the D band (Table 39). Modelled data showed an overall accuracy of 70% at predicting state across all 67 sites. The modelled 95th percentile had an accuracy of 61% (Table 39). Overall, it is inherently more difficult to predict ecological thresholds and subsequent state due to the narrow range of the NOF bands. Predicted state across Northland's river network for median and 95th percentile is shown in Figure 37.

Table 39. Assessment against the proposed National Objectives Framework for dissolved reactive phosphorus for measured and modelled data.

	Measured DRP (mg/l)	State	Model DRP (mg/l)	Model State	Measured DRP Q95 (mg/l)	State	Model DRP Q95m (mg/l)	Model State
Waipapa at Forest Ranger	0.005	A	0.004	A	0.007	A	0.015	A
Wairau at SH12	0.005	A	0.005	A	0.008	A	0.011	A
Waimamaku at SH12	0.006	A	0.012	C	0.009	A	0.022	B
Waipapa at Landing	0.006	A	0.010	B	0.011	A	0.014	A
Waitangi at Waimate North Road	0.006	A	0.006	A	0.012	A	0.016	A
Waipoua at SH12	0.007	B	0.012	C	0.010	A	0.010	A
Kaeo at Dip Road	0.008	B	0.010	B	0.017	A	0.025	B
Kaihu at Gorge	0.008	B	0.011	C	0.011	A	0.010	A
Paranui at Paranui Road	0.008	B	0.020	D	0.012	A	0.021	A
Mangakahia at Twin Bridges	0.009	B	0.006	A	0.013	A	0.016	A
Opouteke at Suspension Bridge	0.009	B	0.009	B	0.015	A	0.018	A
Waiaruhe D/S Mangamutu Confluence	0.009	B	0.009	B	0.016	A	0.023	B
Waitangi at SH10	0.009	B	0.009	B	0.015	A	0.016	A
Mangakahia at Titoki	0.010	B	0.010	B	0.020	A	0.021	A
Kerikeri at Stone Store	0.010	B	0.007	B	0.047	C	0.011	A
Otakaranga at Otaika Valley Road	0.010	B	0.018	C	0.018	A	0.036	C
Pekepeka at Ohaeawai	0.010	B	0.009	B	0.013	A	0.013	A
Punaruku at Russell Road	0.010	B	0.011	C	0.013	A	0.013	A
Utakura at Horeke Rd	0.010	B	0.011	C	0.025	B	0.020	A
Waitangi at Wakelins	0.010	B	0.011	C	0.022	B	0.022	B
Parapara at Parapara Toatoa Road	0.011	C	0.010	B	0.014	A	0.013	A
Hatea at Mair Park	0.011	C	0.013	C	0.015	A	0.016	A
Waitaua at Vinegar Hill Road	0.011	C	0.011	C	0.014	A	0.015	A
Hatea at Whangarei Falls	0.012	C	0.013	C	0.015	A	0.017	A
Mangakino at Mangakino Lane	0.012	C	0.012	C	0.016	A	0.015	A
Oruaiti at Sawyer Road	0.012	C	0.012	C	0.016	A	0.027	B
Oruaiti at Windust Road	0.012	C	0.014	C	0.016	A	0.021	A
Waiaruhe at Puketona	0.012	C	0.011	C	0.019	A	0.024	B
Mangahahuru at Main Road	0.013	C	0.012	C	0.018	A	0.015	A

	Measured DRP (mg/l)	State	Model DRP (mg/l)	Model State	Measured DRP Q95 (mg/l)	State	Model DRP Q95m (mg/l)	Model State
Stony Creek at Sawyer Road	0.013	C	0.014	C	0.022	B	0.017	A
Utakura at Okaka Bridge	0.013	C	0.011	C	0.031	C	0.020	A
Mangakino U/S Waitaua Confluence	0.014	C	0.016	C	0.019	A	0.017	A
Parapara at Taumata Road	0.014	C	0.012	C	0.023	B	0.020	A
Waiarohia at Second Avenue	0.014	C	0.014	C	0.020	A	0.021	A
Mangere at Knight Road	0.015	C	0.044	D	0.141	D	0.157	D
Mangere at Wood Road	0.015	C	0.014	C	0.020	A	0.019	A
Ngunguru at Coalhill Lane	0.016	C	0.016	C	0.024	B	0.015	A
Waiarohia at Whau Valley	0.016	C	0.016	C	0.023	B	0.025	B
Raumanga at Bernard Street	0.016	C	0.019	D	0.022	B	0.015	A
Waiharakeke at Stringers Road	0.016	C	0.014	C	0.032	C	0.026	B
Pukenui at Kanehiana Drive	0.017	C	0.015	C	0.024	B	0.025	B
Puwera at SH1	0.017	C	0.023	D	0.036	C	0.036	C
Waipapa at Waimate North Road	0.017	C	0.016	C	0.039	C	0.039	C
Awanui at FNDC	0.018	C	0.016	C	0.027	B	0.027	B
Otaika at Cemetery Road	0.018	C	0.018	C	0.028	B	0.028	B
Mania at SH10	0.020	D	0.024	D	0.028	B	0.042	C
Victoria at Victoria Valley Road	0.020	D	0.020	D	0.028	B	0.045	C
Otaika at Otaika Valley Road	0.021	D	0.020	D	0.033	C	0.030	B
Waiotu at SH1	0.021	D	0.014	C	0.051	C	0.033	C
Kenana at Kenana Road	0.022	D	0.022	D	0.033	C	0.033	C
Punakitere at Taheke	0.023	D	0.010	B	0.057	D	0.018	A
Wairua at Purua	0.025	D	0.027	D	0.055	D	0.054	C
Oruru at Oruru Road	0.027	D	0.016	C	0.039	C	0.028	B
Whakapara at Cableway	0.027	D	0.015	C	0.041	C	0.020	A
Watercress at SH1	0.033	D	0.024	D	0.046	C	0.049	C
Mangahahuru at Apotu Road	0.033	D	0.018	D	0.068	D	0.016	A
Waipao at Draffin Road	0.033	D	0.033	D	0.053	C	0.043	C
Mangamuka at Iwitaua Road	0.034	D	0.019	D	0.042	C	0.041	C
Manganui at Mititai Road	0.036	D	0.015	C	0.073	D	0.021	A
Tapapa at SH1	0.036	D	0.038	D	0.060	D	0.053	C
Awanui at Waihue Channel	0.044	D	0.025	D	0.110	D	0.110	D
Mangere at Kokopu Road	0.047	D	0.034	D	0.045	C	0.029	B
Peria at Honeymoon Valley Road	0.051	D	0.048	D	0.061	D	0.033	C
Hakaru at Topuni	0.059	D	0.032	D	0.093	D	0.115	D
Ruakaka at Flyger Road	0.089	D	0.097	D	0.161	D	0.161	D
Aurere at Pekerau Road (C)	0.104	D	0.047	D	0.201	D	0.290	D
Mangere at Kara Road	0.190	D	0.015	C	0.021	A	0.019	A

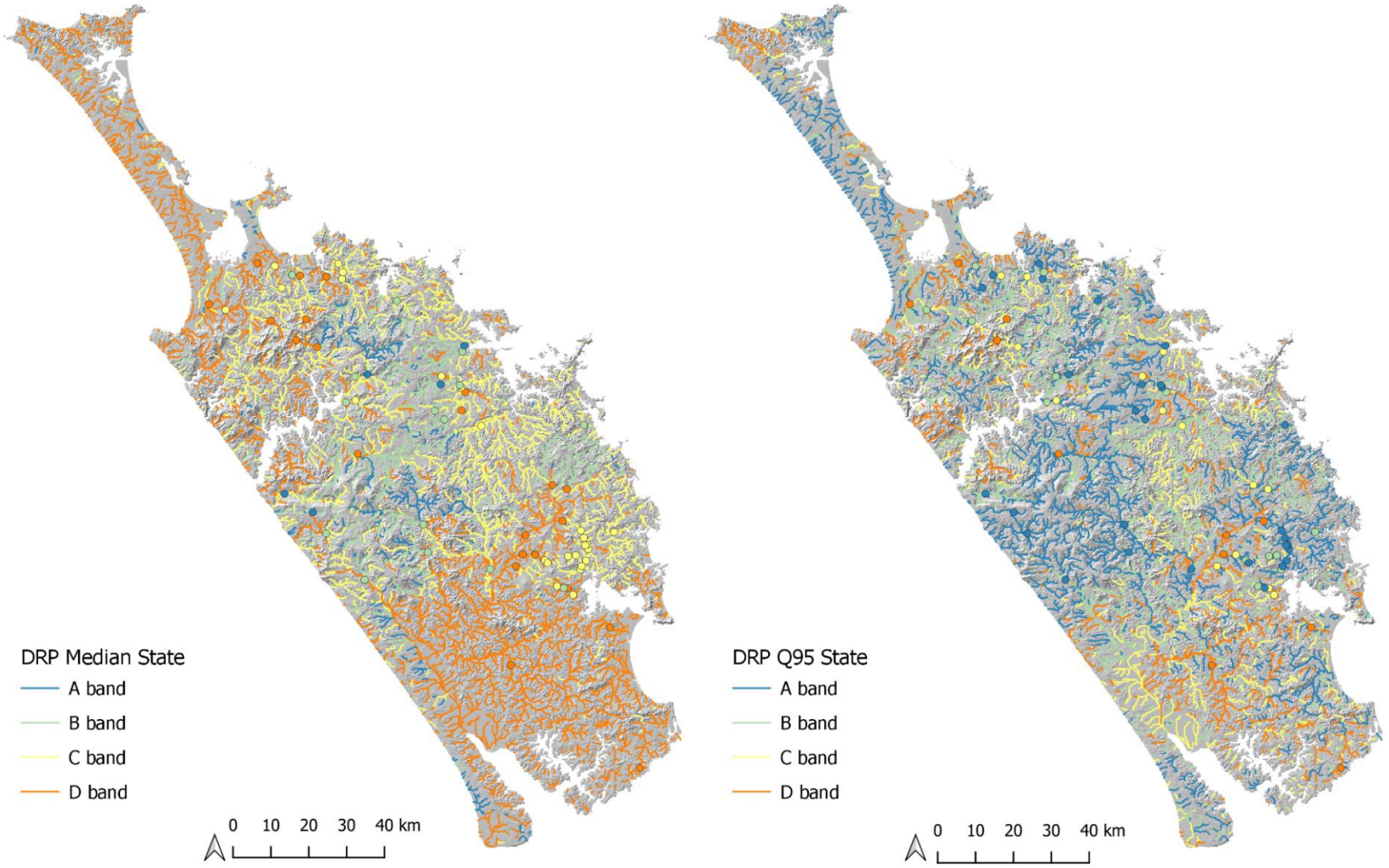

Figure 37. Predicted state of Northlands waterways for ecosystem health – dissolved reactive phosphorus. Attribute state is determined by median concentration (left) and Q95 (right). Circles denote the observed median and maximum values for each of the monitoring sites. River reaches and observed measures (sites) are colour coded according to the same concentration gradient. State assessed using draft NPSFM (2019).

6 Summary

Physiographic science was applied to the estimation of water quality across the Northland region according to the method of Rissmann et al. (2019). The physiographic water quality modelling framework utilises multiple geospatial layers (Section 2.1), NRC monitoring network data (Section 2.2), and a hybrid genetic programming approach (Section 2.3) to estimate water quality across the region. The method attempts to provide a deeper understanding of 'how' and 'why' variation in water quality occurs by building representations of the climatic, hydrological, redox, chemical and physical weathering gradients specific to the Northland region as a series of process-attribute gradients (PAG).

PAG are built to replicate the spatial coupling between each dominant process and landscape gradients (Section 2.0). For example, the Geological Reduction Potential (GRP) PAG describes gradients in natural aquifer redox potential that influence the composition (e.g. DO, Mn^{II}, Fe^{II}, TKN, TAM, DRP) and hence the quality of baseflow to streams across the region. The objective is to represent the underlying grain of the landscape that, in combination with land use, determines water quality outcomes. A total of 17 PAG, 2 land use layers and five years of monitoring data across 67 water quality monitoring sites were used to build mathematical models that explain variation in water quality as a function of 1 or more PAG and/or land use layers (Section 2.0).

The performance of the PAG to replicate each of the dominant processes was evaluated at a hydrochemical level prior to the estimation of water quality (Sections 2.0 and 3.0). This was done to test if PAG provide a reasonable representation of each dominant process known to influence water quality (Section 3.2). Based on the strong performance to estimate dominant processes (Section 3.2), land use layers were incorporated, and water quality models generated (Section 3.3). The resultant models were then applied to the digital stream network (REC1 ≥2nd order; Section 3.5) and the general relationships between estimated concentration and landscape attributes evaluated (Section 4.0). Of the models, TP (cross-validated R^2 = 0.67 and R = 0.82), DRP (0.69 and 0.83), Clarity (0.65 and 0.81), *E. coli* (0.61 and 0.79) and TSS (0.64 and 0.80) were the worst-performing.

The models of steady-state water quality across the digital stream network are consistent with the underlying physiographic mapping of the region (Rissmann et al.,2018a,b; 2019b,c). Specifically, they indicate a robust spatial linkage between landscape attributes and hydrochemical signatures of the dominant processes and associated water quality outcomes.

Some of the key findings of this work include:

- Nitrate nitrogen, NO_3-N, constitutes a relatively small fraction of the total TN concentration across Northland's monitoring sites (1/3rd of the TN concentration on average. Overall, Northland's NO_3-N levels are low by national standards, with reduced nitrogen species, i.e., ammoniacal and organic nitrogen, constituting the bulk of the load exported to streams. This observation is consistent with the small extent of moderately or even weakly oxidising waters. The loading of organic and ammoniacal nitrogen to streams, lakes, and harbours contributes to the store of potential mineralisable nitrogen in benthic sediments. Here it is important to note that organic and ammoniacal forms of nitrogen ultimately end up being mineralised to nitrate and nitrite.

- Dissolved Reactive Phosphorus exhibits a strong geological control with the highest concentrations associated with steep outcrops of Tangihua Volcanics. Basalt commonly contains higher elemental phosphorus concentrations than felsic sedimentary rock and weathers faster than siliceous rock, supplying inorganic P to the river network. The spatial correlation between elevated DRP and Tangihua Volcanic Complex extends from Cape Reinga in the North to Tangihua Forest in the south, wherever the unit outcrops. However, it

is also notable that there is a positive correlation between terrain ruggedness and DRP concentration derived from the Tangihua Volcanic Complex. Notably, the flat-lying Waipoua and Kerikeri flood basalts do not appear to be implicated in DRP generation. Perhaps due to lower terrain ruggedness, mantling by siliceous materials and the development of a stable soil mantle. Other areas of moderately elevated DRP occur in association with peat and lacustrine sediments and reducing redox potentials. The association between elevated DRP and peat and lacustrine sediments is well established both nationally and globally. Overall, there appears to be both a geological and redox control over DRP distribution. The use of phosphatic fertilisers and or animal dung over phosphate leaching is most problematic for wetland soils due to low anion exchange capacity and reducing conditions that favour phosphorus mobility.

- Total Phosphorus (TP) also exhibits similar geological associations to DRP with respects to the Tangihua Volcanics and the peat and lacustrine rich portions of the Tauranga Formation and Karioitahi Group but not the Awhitu Group lignite. There is also evidence that land use and poorly drained soils play an important role in the distribution of the Particulate Phosphorus (PP) fraction of TP. This is consistent with overland flow and artificial drainage density being retained by the model in addition to geological PAG. Further, PP is known to show a strong association with developed land with dissolved organic and inorganic forms more commonly associated with natural state settings. Sand dune systems along Ninety Mile Beach also exhibit elevated TP but not DRP concentrations suggesting a larger particulate phosphorus export. Salt spray, redox cycling and microbial processes have been identified as key controls over PP export from dune front systems.

- There is a strong geological correlation between elevated turbidity and soft and highly erodible lithologies as defined by the ESC of Rissmann et al. (2018b). For example, the poorly lithified weak sedimentary rocks of the Northland Allochthon, including but not limited to the Punakitere Sandstone. Turbidity is also elevated in relationship to depositional landforms, i.e., alluvium, peat and lacustrine sediments of the Tauranga Group and Karioitahi Group, especially where the water table is shallow and soils poorly drained. Harder lithologies, such as the rocks of the Tangihua Volcanic Complex and Waipoua Basalt, show lower turbidity. Also, is that estimated turbidity is low across the areas of well-drained soils where surficial runoff and artificial drainage is less prevalent (e.g. across a significant area of the low relief Kerikeri flood basalts). Tributaries of the Wairoa River, including the Manganui, are identified as being particularly sediment rich.

- Clarity exhibits a broadly similar pattern to turbidity with the least clear streams associated with developed land and highly erodible lithologies, such as the weaker sedimentary rocks of the Northland allochthon. Floodplains are also implicated, especially where alluvium, peat and lacustrine sediments of the Tauranga Group and Karioitahi Group dominate, and the water table is shallow and soils poorly drained. The few streams with elevated median clarity issue from areas of hard rock, (e.g., Waipoua Basalts), and natural state conditions. Once again, the tributaries of the Wairoa River, including the Manganui, are identified as being of low median clarity as is the Awanui River in the north. Except for the developed areas, e.g. Brynderwyn hills, streams discharging from greywacke basement rocks along the eastern seaboard are estimated as having moderate median clarity relative to other stream reaches. A similar pattern is noted for turbidity.

- Highest median *E. coli* counts coincide with areas of erosion-prone land that has been developed for extensive or intensive land use. *E. coli* is also elevated across depositional landforms (floodplains etc.) where soils are poorly drained, and the local water table is shallow. For example, the majority of elevated *E. coli* counts coincide with develop sheep, beef and dairying land on the highly erodible land not limited to the Punakitere Sandstone and other soft sedimentary rocks of the Northland Allochthon. The Karioitahi Group and Tauranga Group sediments are also implicated, especially where the water table is also elevated and soils a poorly drained. Questions surround the legitimacy of *E. coli* estimates for Ninety Mile Beach and from streams draining natural state catchments (i.e., Gum Fields Reserve). Otherwise, the model indicates low *E. coli* counts associated with streams draining natural state areas.

- Land use was also implicated in water quality, but overall, the influence of landscape factors was more important than land use on its own. However, due to the correlation between land use and landscape attributes, it is likely that some of the PAG are acting as surrogates for land use intensity (e.g. artificial drainage PAG).

- Northland steady-state results as evaluated against the National Objective Framework guidelines for freshwater management (NPSFM, 2017, 2019) indicate for nitrate toxicity all State of Environment monitoring sites are above national bottom lines (B band or better), for ammonia toxicity there is 1 site below national bottom lines (D band) during the annual maximum, and 4 sites below the ecological health national bottom line for Dissolved Inorganic Nitrogen. There are 23 sites below the national bottom line for DRP largely associated with annual medians. According to the NOF, *E.coli* is Northland's largest water quality issue with only 4 sites above the national bottom line. However, it is important to note that not all contaminants currently have NOF values to assess against. As such, sediment remains a pervasive and important water quality issue for the region with many of the processes controlling these issues being similar to *E.coli*.

Limitations surrounding this work include the subset of 67 surface water monitoring sites that for pragmatic reasons are biased towards higher-order streams (≥3rd order) and larger drainage basin areas. This is relevant in terms of the use of modelling outputs to advise policy that seeks to target land use activities occurring at property scales. Specifically, most farms across the region range between 150 and 300 Ha whereas most geospatial data sets used to generate PAG were only as fine as 1:50,000 scale. However, it is important to note that the high-resolution Northland Wetness Gradient Layer (50 x 50 m and 20 x 20m data sets) and Erosion Susceptibility Classification PAG (50 x 50 m) were overall the most sensitive predictors of water quality across Northland. The retention of high-resolution datasets as the most important predictors of water quality is important, given that such layers can be used to improve the relevance of water quality modelling at property scales. Historically, the application of water quality modelling at property scales has not been possible due to the coarse nature of existing soil and geological data sets.

A limitation associated with the estimation of water quality across unmonitored areas relates to the use of REC1. Currently there is no cumulative stream order capture zones available for REC2.4 which is an essential requirement to applying physiographic models to a river network. Although the capture area difference between REC1 and 2.4 is relatively minor for SoE monitoring sites (≥3rd order), the REC 2.4 provides greater resolution over the digital stream network at lower stream orders. The greater resolution of REC 2.4 equates to a larger number of stream reaches.

As such, the main limitation that arises when using REC1 to apply the predictive models is the smaller number of node points and hence capture zones. As the PAG models are applied to these node points, the resultant concentrations are applicable to these points but may be displayed over a

longer river segment. Further work is required to generate a digital stream network that is more refined and flexible in terms of the number and accuracy of capture zones in order to maximise the value of PAG as predictors of regional water quality and providing measurement of water quality analytes across a wider range of stream orders, and land uses (especially natural state). On its own, a higher resolution DEM will increase the certainty of capture zone delineation but will not remove the bias of applying a model calibrated on higher-order streams to low order streams. However, as an alternative, water quality models can be applied across the landscape, generating calibrated risk models for each water quality measures or for combined water quality risk. Such risk maps have the benefit of representing within capture zone variation in risk, and therefore the resolution of PAG is not limited by the architecture of REC, which was not developed with physiographic based landscape mapping in mind. In addition to the scale of PAG and the REC, the use of a land use intensity layer based on categorical scoring by enterprise type results in an averaged or homogenised representation of the actual pressure gradient within land uses.

7 Recommendations

Based on this and other work across the Northland Region, the following recommendations are made to enhance further the understanding and relevance of the region's natural resources. A key objective is to enhance the spatial and temporal resolution of datasets to underpin decision-making and ensure science outputs are more relevant at property scales. These recommendations will also likely improve the resolution and performance of the physiographic modelling undertaken to date. The main recommendations include:

Land Use

- Improving the representation of land use intensity (possibly based on livestock carrying rates, inputs or outputs) through integrating recent livestock census data released by Ministry for the Environment, Sentinel-2 based satellite (20 x 20 m) and NRC GIS consent and compliance data sets. This technical land use layer could be integrated with critical landscape attributes and pre-existing classifications of soil and geology to provide an integrated land use-water quality layer for the region.

Water Quality Monitoring

- The inclusion of monitoring across smaller order streams and natural state sites is recommended. This may include increasing the number of monitoring sites up-stream of long-term monitoring sites. However, a strategic assessment of the representativeness of monitoring relative to landscape factors and land use intensity is recommended before any investment in additional monitoring sites.
- In addition of Total Kjeldahl Nitrogen to Northland's SOE test set, we recommend the inclusion of chloride (Cl^-), dissolved iron (Fe^{II}), dissolved organic carbon (DOC), total alkalinity, dissolved silica ($SiO_{2(aq)}$) and potassium (K^+) to the regional monitoring test set for a period of 2 to 3 years. The main objective for including these chemical measures is to refine the understanding of the dominant processes better that in combination with land use, control water quality. Sampling of these chemical species across the flow range is critical, providing insight over the relative contribution from different geographical areas but also the compartments, i.e., surface runoff, soil, aquifer(s) that supply stream. It is worth collecting these additional measures monthly over the 2 – 3 year period. However, a seasonally targeted monitoring programme that is aligned with existing SOE monitoring runs may be sufficient if it adequately captures low, median, and high flow across the seasons.

- We strongly recommend an event sampling programme is put in place. The objective of which is to provide a more realistic picture of regional water quality. Such sampling is relevant to both steady-state and load-based measures of regional water quality. It is one of the most cost-effective ways to reduce uncertainty in water quality models attempting to estimate contaminant loads to the region's lakes, estuaries and harbours. Lower uncertainty equates to a more robust platform for decision-making. The importance of event sampling relates to the observation that the majority of a region's contaminant loads may occur in response to a handful of high flow or storm events – the majority of which are not sampled and as such not represented in regional monitoring data sets. Failing to sample such events is potentially one of the largest sources of uncertainty or error inherent in regional water quality data sets. Such a programme need not be exhaustive through focusing on the capture of 1 or 2 peak flow events per year as part of a long-term monitoring network commitment.

Landscape Attributes

- Ultimately, a finer scale digital river network and associated capture zones are required if the resolution provided by physiographic mapping is to be realised. Regional Li-DAR is the ideal platform for developing a new digital river network and associated capture zones for Northland. Such a layer would also improve regional understanding of surface water drainage at property scales, connecting farms to local drainage networks and streams. Alternatively (or in addition), water quality models can be applied to the land, generating calibrated risk maps for each individual water quality measure or one global risk model of the combined water quality risk. Such risk maps have the benefit of representing within capture zone variation in risk, and therefore the resolution of PAG is not limited by the architecture of the REC or other digital river network.
- The soil landscape is arguably the most important natural resource of any region - it forms the basis of most human endeavour. It is also a primary landscape control over water quality. Northland's regional soil survey could be significantly enhanced through the integration of radiometric survey, Li-DAR and Sentinel satellite data sets and existing soil survey. Such integration could provide more accurate maps of soil properties relevant to water quality but also primary production. This work would build on existing high-resolution classifications and data sets and enable property and in places paddock scale resolution over soil properties. Enhanced resolution over soil properties is also of benefit to water quality models making them more scalable and hence relevant to land users.

References

Aho, K., Derryberry, D., and Peterson, T. (2014). Model selection for ecologists: the worldviews of AIC and BIC, Ecology, 95: 631–636, doi:10.1890/13-1452.1.

Arnaldo, I., Krawiec, K., I., and Reilly, U. O. (2014). Multiple Regression Genetic Programming, (July). http://doi.org/10.1145/2576768.2598291

Atiquzzaman, M. and Kandasamy, J. (2016). Prediction of inflows from dam catchment using genetic programming. International Journal of Hydrology Science and Technology Volume 6, Issue 2; DOI: 10.1504/IJHST.2016.075560

Baisden, W.T., Keller, E.D., Van Hale, R., Frew, R.D., Wassenaar, L.I. (2016). Precipitation isoscapes for New Zealand: enhanced temporal detail using precipitation-weighted daily climatology. Isotopes in environmental and health studies, 52(4-5): 343-352

Baker, L. A., Hope, D., Xu, Y., and Edmonds, J. (2001). Multicompartment ecosystem mass balances as a tool for understanding and managing the biogeochemical cycles of human ecosystems. The Scientific World Journal, 1, 802-808.

Beck, M., Reckhardt, A., Amelsberg, J., Bartholomä, A., Brumsack, H. J., Cypionka, H., ... and Holtappels, M. (2017). The drivers of biogeochemistry in beach ecosystems: a cross-shore transect from the dunes to the low-water line. Marine Chemistry, 190, 35-50.

Becker, J. C., Rodibaugh, K. J., Labay, B. J., Bonner, T. H., Zhang, Y., and Nowlin, W. H. (2014). Physiographic gradients determine nutrient concentrations more than land use in a Gulf Slope (USA) river system. Freshwater Science, 33(3), 731–744. https://doi.org/10.1086/676635

Bethke, C.M., Farrell, B., and Sharifi, M. (2020). Software: The Geochemist's Workbench®, Release 14, GWB Essentials Guide. Aqueous Solutions, LLC. Champaign, Illinois.

Beyer, M., Rissmann, C., Rodway, E., Killick, M., and Pearson, L. (2016a). Technical Chapter 6: Influence of Soil and Geological Composition over Redox conditions for Southland groundwater and surface waters. Environment Southland. Technical Report. No: 2016/3. Invercargill, New Zealand

Bolshakov, V. (2013). Regression-based Daugava River Flood Forecasting and Monitoring. Information Technology and Management Science, Sciendo, 16(1):137-142.

Bongard, J.C. and Lipson, H. (2005). Nonlinear system identification using coevolution of models and tests. IEEE Transactions on Evolutionary Computation, 9(4)361-384.

Bongard, J., and Lipson, H. (2007). Automated reverse engineering of non-linear dynamical systems. PNAS June 12, 2007 104 (24) 9943-9948; https://doi.org/10.1073/pnas.0609476104

Bright, R. M. and O'Halloran, T. L. (2018). Developing a monthly radiative kernel for surface albedo change from satellite climatologies of Earth's shortwave radiation budget: CACK v1.0, Geosci. Model Dev., 12:3975–3990, https://doi.org/10.5194/gmd-12-3975-2019, 2019.

Chadalawada, J., Havlicek, V., and Babovic, V. (2017). A Genetic Programming Approach to System Identification of Rainfall-Runoff Models, (1), 3975-3992. http://doi.org/10.1007/s11269-017-1719-1

Chappell, P.R. (2013). The climate and weather of Northland. 3rd edition NIWA Science and Technology Series, 59 (3rd edition).

Clark, I. and Fritz, P. 1997. Environmental Isotopes in Hydrogeology (2nd edition). CRC Press ISBN: 1-56670-249-6.

Columbus, J., Sirguey, P., and Tenzer, R. (2011). A free fully assessed 15 metre digital elevation model for New Zealand. Survey Quarterly, 300(66), 16.

Creaco, E., L. Berardi, S. Sun, O. Giustolisi, and D. Savic (2016), Selection of relevant input variables in storm water quality modeling by multiobjective evolutionary polynomial regression paradigm, Water Resour. Res., 52, 2403–2419, doi:10.1002/2015WR017971

Daughney, C., Rissmann, C., Friedel, M., Morgenstern, U., Hodson, R., van der Raaij, R., Rodway, E., Martindale, H., Pearson, L., Townsend, D., Kees, L., Moreau, M., Millar, R., Horton, T., 2015. Hydrochemistry of the Southland Region, GNS Science Report 2015/24.

Delany, J.M. and Lundeen, S.R. (1989). The LLNL thermodynamic database Lawrence Livermore National Laboratory Report UCRL-21658 (1989).

Dimitrov, D. D., Bhatti, J. S., and Grant, R. F. (2014). The transition zones (ecotone) between boreal forests and peatlands: Ecological controls on ecosystem productivity along a transition zone between upland black spruce forest and a poor forested fen in central Saskatchewan. Ecological Modelling. https://doi.org/10.1016/j.ecolmodel.2014.07.020

Dinu, C., Drobot, R., Pricop, C., Blidaru, T.V., (2017). Genetic Programming Technique Applied for Flash-flood Modelling Usong Radar Rainfall Estimates. Mathematical Modelling in Civil Engineering Vol. 13-No. 4: 27-38 - 2017. Doi:10.1515/mmce-2017-0012

Doctor, D. H., Kendall, C., Sebestyen, S. D., Shanley, J. B., Ohte, N., and Boyer, E. W. (2008). Carbon isotope fractionation of dissolved inorganic carbon (DIC) due to outgassing of carbon dioxide from a headwater stream. Hydrological Processes. https://doi.org/10.1002/hyp.6833

Duan, N. (1983). Smearing estimate: a nonparametric retransformation method. Journal of the American Statistical Association, 78(383), 605-610.

Dubčáková, R. (2011). Eureqa: software review. Genetic programming and evolvable machines, 12(2): 173-178.

Duran, L., Fournier, M., Massei, N. and Dupont, J.P. (2015). Assessing the Nonlinearity of Karst Response Function under Variable Boundary Conditions. Groundwater 2015. doi: 10.1111/gwat.12337

Edbrooke, S.W., and Brook, F.J. (compilers) (2009). Geology of the Whangarei area. Institute of Geological and Nuclear Sciences 1:250 000 geological map 2. 1 sheet + 68 p. Lower Hutt, New Zealand. GNS Science. QMAP Whangarei.

Farr, T.G., Rosen, P.A., Caro, E., Crippen, R., Duren, R., Hensley, S., Kobrick, M., Paller, M., Rodriguez, E., Roth, l., Seal, D., Shaffer, S., Shimada, J., Umland, Werner, M. Oskin, M., Burbank, D., and Alsdorf, D. (2007). The shuttle radar topography mission. Reviews of geophysics, 45(2). https://doi.org/10.1029/2005RG000183

Giller, P. S., and Malmqvist, B. (1998). The Biology of Streams and Rivers. Biology of Habitats. https://doi.org/10.1145/2789211

Gray, D. P., Harding, J. S., Elberling, B., Horton, T., Clough, T. J., and Winterbourn, M. J. (2011). Carbon Cycling in Floodplain Ecosystems: Out-Gassing and Photosynthesis Transmit Soil δ13C Gradient Through Stream Food Webs. Ecosystems. https://doi.org/10.1007/s10021-011-9430-1

Güler, C., and Thyne, G. D. (2004). Delineation of hydrochemical facies distribution in a regional groundwater system by means of fuzzy c-means clustering. Water Resources Research, 40(12), 1–11. https://doi.org/10.1029/2004WR003299.

Güler, C., Thyne, G. D., McCray, J. E., and Turner, A. K. (2002). Evaluation of graphical and multivariate statistical methods for classification of water chemistry data. Hydrogeology Journal, 10(4), 455–474. https://doi.org/10.1007/s10040-002-0196-6

Hale, S. S., Paul, J. F., Heltshe, J. F., Hale, S. S., Paul, J. F., and Heltshe, J. F. (2017). Watershed landscape indicators of estuarine benthic condition. Estuaries, 27(2), 283-295. https://doi:10.1007/BF02803385

Hem, J. D. (1985). Study and interpretation of the chemical characteristics of natural water. US Geological Survey Water-Supply Paper.

Icke and Bongard. (2013). Improving Genetic Programming Based Symbolic Regression Using Deterministic Machine Learning, (June). http://doi.org/10.1109/CEC.2013.6557774.

Inamdar S. (2011). The use of geochemical mixing models to derive runoff sources and hydrologic flow paths. In: Levia D., Carlyle-Moses D., Tanaka T. (Eds). Forest Hydrology and Biogeochemistry. Ecological Studies (Analysis and Synthesis), v.216. Springer, Netherlands. doi:10.1007/978-94-007-1363-5_8

Isaac, M.J. (compiler) (1996). Geology of the Kaitaia area. Institute of Geological and Nuclear Sciences 1:250 000 geological map 1. 1 sheet + 43 p. Lower Hutt, New Zealand. GNS Science. QMAP Kaitaia.

Jagupilla, S.C., Vaccari, D.A., Miskewitz, R., Su, T.L., Hires, R.I. (2015). Symbolic regression of upstream, stormwater, and tributary *E. coli* concentrations using river flows. Water Environ Res. 2015 Jun;87(6):576.

James, A. L., and Roulet, N. T. (2006). Investigating the applicability of end-member mixing analysis (EMMA) across scale: A study of eight small, nested catchments in a temperate forested watershed. Water Resources Research, 42(8). https://doi.org/10.1029/2005WR004419

Johnson, L., Richards, C., Host, G., and Arthur, J. (1997). Landscape influences on water chemistry in Midwestern stream ecosystems. Freshwater Biology, 37(1), 193–208. https://doi.org/10.1046/j.1365-2427.1997.d01-539.x

Jürgen, B. C., McMahon, P. B., Chapelle, F. H., and Eberts, S. M. (2009). An Excel ® Workbook for Identifying Redox Processes in Ground Water An Excel ® Workbook for Identifying Redox Processes in Ground Water.

Kendall, C., and McDonnell, J.J., (eds.) (1998). Isotope Tracers in Catchment Hydrology. Amsterdam; New York: Elsevier, 1998

Khu, S. T., Liong, S. Y., Babovic, V., Madsen, H., and Muttil, N. (2001). Genetic programming and its application in real-time runoff forecasting. Journal of the American Water Resources Association. https://doi.org/10.1111/j.1752-1688.2001.tb00980.x

King, R. S., Baker, M. E., Whigham, D. F., Weller, D. E., Jordan, T. E., Kazyak, P. F., and Hurd, M. K. (2005). Spatial considerations for linking watershed land cover to ecological indicators in streams. Ecological Applications, 15(1), 137–153. https://doi.org/10.1890/04-0481

Klotz, D., Herrnegger, M., and Schulz, K. (2017). Symbolic Regression for the Estimation of Transfer Functions of Hydrological Models. Water Resources Research, 53(11), 9402-9423. https://doi.org/10.1002/2017WR021253

Kotanchek, M., Smits, G., and Vladislavleva, E. (2007). Trustable symbolic regression models: using ensembles, interval arithmetic and pareto fronts to develop robust and trust-aware models. In Genetic Programming Theory and Practice V. https://doi.org/10.1007/978-0-387-76308-8_12.

Kotanchek, M. E., Vladislavleva, E. Y., and Smits, G. F. (2010). Symbolic Regression Via Genetic Programming as a Discovery Engine: Insights on Outliers and Prototypes. https://doi.org/10.1007/978-1-4419-1626-6_4.

Krantz, D. E., and Powars, D. S. (2000). Hydrogeologic setting and potential for denitrification in ground water, Coastal Plain of Southern Maryland. U.S. Geological Survey Water-Resources Investigations Report. 00-4051, 19 p., retrieved from https://pubs.usgs.gov/wri/2000/4051/.

Land Information New Zealand. (2012). NZ 8m Digital Elevation Model. [raster]. https://data.linz.govt.nz/layer/51768-nz-8m-digital-elevation-model-2012/

Landcare Research. (2010). Fundamental Soil Layer New Zealand Soil Classification. [vector polygon]. https://lris.scinfo.org.nz/layer/48079-fsl-new-zealand-soil-classification/.

Landcare Research. (2015). Land Cover Database version 4.1 Mainland New Zealand. [vector polygon]. https://lris.scinfo.org.nz/layer/48423-lcdb-v41-land-cover-database-version-41-mainland-new-zealand/.

Lasaga, C. (1984). Chemical kinetics of water-rock interactions. Journal of Geophysical Research Solid Earth. https://doi.org/10.1029/JB089iB06p04009.

Leybourne, M. I., and Goodfellow, W. D. (2010). Geochemistry of surface waters associated with an undisturbed Zn–Pb massive sulfide deposit: water–rock reactions, solute sources and the role of trace carbonate. *Chemical Geology*, *279*(1-2), 40-54.

Lu, Q., Ren, J., and Wang, Z. (2016). Using Genetic Programming with Prior Formula Knowledge to Solve Symbolic Regression Problem, 2016. https://doi.org/10.1155/2016/1021378

Lydersen, E., Larssen, T., and Fjeld, E. (2004). The influence of total organic carbon (TOC) on the relationship between acid neutralizing capacity (ANC) and fish status in Norwegian lakes. Science of the Total Environment, 326(1–3), 63–69. https://doi.org/10.1016/j.scitotenv.2003.12.005

Lynn, I. H., Manderson, A. K., Page, M. J., Harmsworth, G. R., Eyles, G. O., Douglas, G. B., Mackay, A. D., Newsome, P. J. F. (2009). Land Use Capability Survey Handbook – a New Zealand handbook for the classification of land 3rd edition. Hamilton, AgResearch; Lincoln, Landcare Research; Lower Hutt, GNS Science. 163p.

Matott, L. S., Babendreier, J. E., and Purucker, S. T. (2009). Evaluating uncertainty in integrated environmental models: A review of concepts and tools. Water Resources Research. https://doi.org/10.1029/2008WR007301

McDonald, L., Pearson, L., and Rissmann, C. (2020). Validation of the Northland Sediment Process-Attribute Layer: Erosion Susceptibility Classification. Land and Water Science Report 2020/02. p26.

McMahon, P., and Chapelle, F. (2008). Redox processes and water quality of selected principal aquifer systems. Groundwater 46(2): 259-271.

Ministry for the Environment. (2014). National Policy Statement for Freshwater Management 2014. NZ Government, Revised August 2017.

Ministry for the Environment. (2016). LUCAS NZ Land Use Map. [vector polygon]. https://data.mfe.govt.nz/layer/52375-lucas-nz-land-use-map-1990-2008-2012-2016-v006/

Ministry for the Environment. (2019). Draft National Policy Statement for Freshwater Management 2019. Consultation draft. NZ Government.

Moldan, B., and Černý, J. V. (1994). Biogeochemistry of small catchments: a tool for environmental research. Chichester, England, UK: John Wiley and Sons Ltd

Moriasi, D.N., Gitau, M.W., Pai, N., and Daggupati, P. (2015). Hydrologic and water quality models: Performance measures and evaluation criteria. (2015). Transactions of the ASABE, 58(6), 1763-1785. https://doi:10.13031/trans.58.10715

Nealson, K. H., and Saffarini, D. (1994). Iron and Manganese in Anaerobic Respiration: Environmental Significance, Physiology, and Regulation. Annual Review of Microbiology. https://doi.org/10.1146/annurev.mi.48.100194.001523.

Newsome, P.F.J., Wilde, R.H., and Willoughby, E.J. (2008). Land Resource Information System Spatial Data Layers. Landcare Research, Palmerston North, New Zealand.

Niedermeier, A., and Robinson, J. S. (2009). Phosphorus dynamics in the ditch system of a restored peat wetland. Agriculture, Ecosystems and Environment. https://doi.org/10.1016/j.agee.2009.01.011

Panno, S. V., Kelly, W. R., Martinsek, A. T., and Hackley, K. C. (2006). Estimating background and threshold nitrate concentrations using probability graphs. Ground Water, 44(5), 697–709. https://doi.org/10.1111/j.1745-6584.2006.00240.x

Porder, S. and Ramachandran, S. (2012). The phosphorus concentration of common rocks – a potential driver of ecosystem P status. Plant Soil. DOI 10.1007/s11104-012-1490-2.

Praks, P. and Brkic, D. (2018). Symbolic Regression-Based Genetic Approximations of the Colebrook Equation for Flow Friction. Water 2018, 10(9), 1175

Reimann, C., Filzmoser, P., and Garrett, R. G. (2005). Background and threshold: critical comparison of methods of determination. The Science of the Total Environment, 346(1–3), 1–16. https://doi.org/10.1016/j.scitotenv.2004.11.023

Rissmann, C. (2012). The Extent of Nitrate in Southland Groundwaters. Environment Southland Technical Report, July 2012.

Rissmann, C., Wilson, K., and Hughes, B. (2012). Waituna Catchment Groundwater Resources. Environment Southland, Technical Report No. 2012-04. Invercargill, New Zealand.

Rissmann, C., Leybourne, M., Benn, C., and Christenson, B. (2015). The origin of solutes within the groundwaters of a high andean aquifer. Chemical Geology. https://doi.org/10.1016/j.chemgeo.2014.11.029

Rissmann, C., Rodway, E., Beyer, M., Hodgetts, J., Pearson, L., Killick, M., Marapara, T.R., Akbaripasand, A., Hodson, R., Dare, J., Millar, R., Ellis, T., Lawton, M., Ward, N., Hughes, B., Wilson, K., McMecking, J., Horton, T., May, D., and Kees, L. (2016). Physiographics of Southland Part 1: Delineation of key drivers of regional hydrochemistry and water quality. Environment Southland Technical Report No. 2016/3. Invercargill, New Zealand.

Rissmann, C. and Pearson, L. (2018). Identifying Pollutant Sources within the Waimea Catchment: Applying hydrochemical tracers to surface water time series data. Land and Water Science Report 2018/15. p54.

Rissmann, C., Pearson, L., Lindsay, J., Couldrey, M., and Lovett, A. (2018a). Application of Physiographic Science to the Northland Region: Preliminary Hydrological and Redox Process-Attribute Layers. Land and Water Science Report 2018/11. p88.

Rissmann, C., Pearson, L., Lindsay, J., and Couldrey, M. (2018b). Sediment Process-Attribute Layer for Northland. Land and Water Science Report 2018/35. p71

Rissmann, C., Pearson, L., Lindsay, J., Beyer, M., Marapara, T., Badenhop, A., and Martin, A. (2018c). Integrated landscape mapping of water quality controls for farm planning – applying a high resolution physiographic approach to the Waituna Catchment, Southland. In: Farm environmental planning – Science, policy and practice. (Eds. L. D. Currie and C.L. Christensen). http:flrc.massey.ac.nz/publications.html. Occasional Report No. 31. Fertilizer and Lime Research Centre, Massey University, Palmerston North, New Zealand. 19 pages.

Rissmann, C., Pearson, L., Lindsay, J. Marapara, M., and Badenhop, A. (2018d). Waituna Catchment: Technical Information and Physiographic Application. Land and Water Science Report 2018/01. Prepared for Living Water, 133p.

Rissmann, C.W.F., Pearson, L.K., Beyer, M., Couldrey, M.A., Lindsay, J.L., Martin, A.P., Baisden, W.T., Clough, T.J., Horton T.W., and Webster-Brown, J.G. (2019a). A hydrochemically guided landscape classification system for modelling spatial variation in multiple water quality indices: Process-attribute mapping. Science of the Total Environment 672: 815-833. https://doi.org/10.1016/j.scitotenv.2019.03.492.

Rissmann, C., Lindsay, J., Couldrey, M., and Pearson, L. (2019b). Mapping of Northland's hydric soils, wetlands, and water bodies. Land and Water Science Report 2019/28

Rissmann, C., Pearson, L., Lindsay, J., and Couldrey, M. (2019c). Mapping of Northland's Wetness Gradients utilising Radiometric and Satellite imagery – GIS Metadata. Land and Water Science Report 2019/38

Rissmann, C. (2011). Regional Mapping of Groundwater Denitrification Potential and Aquifer Sensitivity, 2011-12, 38p. https://doi.org/10.13140/2.1.3412.5606

Schmidt, M.D., and Lipson, H. (2008). Coevolution of Fitness Predictors. IEEE Transactions on Evolutionary Computation, 12(6):736-749.

Schmidt, M., and Lipson, H. (2009a). Symbolic regression of implicit equations. Genetic Programming Theory and Practice. https://doi.org/doi:10.1007/978-1-4419-1626-6_5

Schmidt, M., and Lipson, H. (2009b). Distilling Free-Form Natural Laws from Experimental Data. Science: 324(5923):81-85. DOI: 10.1126/science.1165893.

Schmidt M., Lipson H. (2010) Symbolic Regression of Implicit Equations. In: Riolo R., O'Reilly UM., McConaghy T. (eds) Genetic Programming Theory and Practice VII. Genetic and Evolutionary Computation. Springer, Boston, MA

Schmidt M., and Lipson H. (2011) Age-Fitness Pareto Optimization. In: Riolo R., McConaghy T., Vladislavleva E. (eds) Genetic Programming Theory and Practice VIII. Genetic and Evolutionary Computation, vol 8. Springer, New York, NY

Schmidt, M. and Lipson, H. (2015). Eureqa (Version 1.24. 0).

Snelder, T.H., and Biggs, B.J.F. (2002). Multiscale river environment classification for water resources management. Journal of the American Water Resources Association. https://doi.org/10.1111/j.1752-1688.2002.tb04344.x.

Stijven, S., Minnebo, W., and Vladislavleva, K. (2011). Separating the wheat from the chaff: On feature selection and feature importance in regression random forests and symbolic regression. In Genetic and Evolutionary Computation Conference, GECCO'11 - Companion Publication. https://doi.org/10.1145/2001858.2002059.

Stijven, S., Vladislavleva, E., Kordon, A., Willem, L., and Kotanchek, M. E. (2016). Prime-Time: Symbolic Regression Takes Its Place in the Real World. https://doi.org/10.1007/978-3-319-34223-8_14.

Tadono, T., Ishida, H., Oda, F., Naito, S., Minakawa, K., and Iwamoto, H. (2014). Precise global DEM generation by ALOS PRISM. ISPRS Annals of the Photogrammetry, Remote Sensing and Spatial Information Sciences, 2(4), 71.

Thomas, A. L., Dambrine, E., King, D., Party, J. P., and Probst, A. (1999). A spatial study of the relationships between streamwater acidity and geology, soils and relief (Vosges, northeastern France). Journal of Hydrology, 217(1–2), 35–45. https://doi.org/10.1016/S0022-1694(99)00014-1

Tinoco, R.O., Goldstein, E.B., and Coco, G. (2015). A data-driven approach to develop physically sound predictors: Application to depth-averaged velocities on flows through submerged arrays of rigid cylinders. American Geophysical Union 2015; DOI: 10.1002/2014WR016380

Tratnyek, P. G., Grundl, T. J., and Haderlein, S.B. (Eds) (2012). Aquatic Redox Chemistry. American Chemical Society symposium series 1071; Oxford University Press, 20

Troy, T.J., Wood, E. F., and Sheffiels, J. (2008). An efficient calibration method for continental-scale land surface modelling. Water Resources Investigation. https://doi.org/10.1029/2007WR006513.

Tye, A. M., Rawlins, B. G., Rushton, J. C., and Price, R. (2016). Understanding the controls on sediment-P interactions and dynamics along a non-tidal river system in a rural–urban catchment: the River Nene. Applied geochemistry, 66, 219-233.

van Beek, R., Cammeraat, E., Andreu, V., Mickovski, S. B., and Dorren, L. (2008). Hillslope Processes: Mass Wasting, Slope Stability and Erosion. Ecotechnological Solutions, 2008:17–64.

Van De Riet, B. P., Hefting, M. M., and Verhoeven, J. T. A. (2013). Rewetting drained peat meadows: Risks and benefits in terms of nutrient release and greenhouse gas exchange. Water, Air, and Soil Pollution. https://doi.org/10.1007/s11270-013-1440-5

Wang, G., Yu, X., Bao, K., Xing, W., Gao, C., Lin, Q., and Lu, X. (2015). Effect of fire on phosphorus forms in Sphagnum moss and peat soils of ombrotrophic bogs. Chemosphere. https://doi.org/10.1016/j.chemosphere.2014.01.084

Wang, Y.F., Huai, W.X., and Wang, W.J. (2016). Physically sound formula for longitudinal dispersion coefficients of natural rivers. Journal of Hydrology; http://dx.doi.org/10.1016/j.jhydrol.2016.11.058

Westerhoff, R., White, P., and Miguez-Macho, G. (2018). Application of an improved global-scale groundwater model for water table estimation across New Zealand. *Hydrology and Earth System Sciences*, *22*(12), 6449-6472.

Whigham, P.A., and Crapper, P.F. (2001). Modelling Rainfall-Runoff using Genetic Programming. Mathematical and Computer Modelling 33 (2001) 707-721.

Wilson, S. R., Close, M. E., and Abraham, P. (2018). Applying linear discriminant analysis to predict groundwater redox conditions conducive to denitrification. Christchurch, New Zealand. Journal of Hydrology, 556: 611-624. https://doi:10.1016/j.jhydrol.2017.11.045

Wright, R. F. (1988). Influence of Acid Rain on Weathering Rates. In: A. Lerman, and M. Meybeck, Physical and Chemical Weathering in Geochemical Cycles p.181-196. Oslo, Norway: Kluwer Academic Publishers.

Yamazaki D., Ikeshima, D., Tawatari, R., Yamaguchi, T., O'Loughlin, F., Neal, J.C., Sampson, C.C., Kanae, S., and Bates, P.D. (2017). A high accuracy map of global terrain elevations. Geophysical Research Letters, vol.44, pp.5844-5853, 2017 doi: 10.1002/2017GL072874.

Zak, D., and Gelbrecht, J. (2007). The mobilisation of phosphorus, organic carbon and ammonium in the initial stage of fen rewetting (a case study from NE Germany). Biogeochemistry. https://doi.org/10.1007/s10533-007-9122-2

Appendix A: Hydrochemical and Water quality Dataset QA/QC

Table A.1. Date of samples for steady-state water quality model.

	2010	2011	2012	2013	2014	2015	2016	2017	2018	2019	Sample total	QC	Comment
Aurere at Pekerau Road							9	12	12	12	45	B	Combined Aurere site (2015-2019)
Aurere at Pekerau Road_OLD						12	6				18	B	Combined Aurere site (2015-2019)
Awanui at FNDC						12	12	12	12	12	60	A	
Awanui at Waihue Channel						16	15	15	16	14	76	A+	
Hakaru at Topuni						12	12	12	13	12	61	A	
Hatea at Mair Park	3	6	8	5	14	9	12	10	17	8	92	B	Tidal influence removed (2010-2019)
Hatea at Whangarei Falls						28	26	24	27	28	133	A+	
Kaeo at Dip Road						12	12	12	12	13	61	A	
Kaihu at Gorge						12	12	12	13	11	60	A	
Kenana at Kenana Road						12	12	12	12	12	60	A	
Kerikeri at Stone Store	6	10	10	9	8	6	9	8	10	5	81	B	Tidal influence removed (2010-2019)
Mangahahuru at Apotu Road						12	12	12	15	12	63	A	
Mangahahuru at Main Road						12	12	12	15	12	63	A	
Mangakahia at Titoki						12	18	24	22	12	88	A+	
Mangakahia at Twin Bridges						12	11	12	13	12	60	A	
Mangakino at Mangakino Lane						12	12	12	12	12	60	A	
Mangakino U/S Waitaua Confluence						12	12	12	12	12	60	A	
Mangamuka at Iwitaua Road						12	12	12	12	12	60	A	
Manganui at Mititai Road						12	12	12	13	12	61	A	
Mangapiu at Kokopu Road						12	12	12	12	12	60	A	
Mangere at Kara Road						12	12	12	12	12	60	A	
Mangere at Knight Road						24	24	24	25	15	112	A+	
Mangere at Kokopu Road						12	12	12	12	12	60	A	
Mangere at Wood Road						12	12	12	12	12	60	A	

	2010	2011	2012	2013	2014	2015	2016	2017	2018	2019	Sample total	QC	Comment
Mania at SH10						12	12	12	12	12	60	A	
Ngunguru at Coalhill Lane						12	12	12	13	12	61	A	
Opouteke at Suspension Bridge						12	12	12	13	11	60	A	
Oruaiti at Sawyer Road						12	12	12	12	12	60	A	
Oruaiti at Windust Road						12	12	12	12	11	59	A	
Oruru at Oruru Road						24	24	24	24	15	111	A+	
Otaika at Cemetery Road						12	12	12	12	12	60	A	
Otaika at Otaika Valley Road						24	24	24	25	14	111	A+	
Otakaranga at Otaika Valley Road						12	12	12	12	12	60	A	
Paranui at Paranui Road						12	12	12	12	12	60	A	
Parapara at Parapara Toatoa Road						12	12	12	12	12	60	A	
Parapara at Taumata Road						12	12	12	12	12	60	A	
Pekepeka at Ohaeawai						12	12	12	12	12	60	A	
Peria at Honeymoon Valley Road						11	12	12	12	11	58	A	
Pukenui at Kanehiana Drive							10	12	13	12	47	C	< 5 years data
Punakitere at Taheke						11	12	11	13	12	59	A	
Punaruku at Russell Road							6	12	13	12	43	C	< 5 years data
Puwera at SH1							9	11	12	12	44	C	< 5 years data
Raumanga at Bernard Street					9	12	12	12	10		55	B	5-years of data 2014-2018
Ruakaka at Flyger Road						12	12	12	13	12	61	A	
Stony Creek at Sawyer Road						12	12	12	12	11	59	A	
Tapapa at SH1							6	12	12	12	42	C	< 5 years data
Utakura at Horeke Rd		12	12	12	12	24					72	B	5-years of data 2011-2015
Utakura at Okaka Bridge							12	12	15	12	51	C	< 5 years data
Victoria at Victoria Valley Road						12	12	12	12	12	60	A	
Waiarohia at Second Avenue						24	24	24	26	15	113	A+	
Waiarohia at Whau Valley						13	13	13	13	13	65	A	
Waiaruhe at Puketona						12	12	11	12	12	59	A	

	2010	2011	2012	2013	2014	2015	2016	2017	2018	2019	Sample total	QC	Comment
Waiaruhe D/S Mangamutu Confluence						12	11	11	12	15	61	A	
Waiharakeke at Stringers Road					12	12	12	12	8		56	B	5-years of data 2014-2018
Waimamaku at SH12						12	12	12	12	12	60	A	
Waiotu at SH1						12	12	12	14	12	62	A	
Waipao at Draffin Road						12	12	12	13	12	61	A	
Waipapa at Forest Ranger					12	12	12	12	9		57	B	5-years of data 2014-2018
Waipapa at Landing						12	12	12	13	12	61	A	
Waipapa at Waimate North Road						12	12	11	12	12	59	A	
Waipoua at SH12						12	12	12	12	12	60	A	
Wairau at SH12							6	12	13	12	43	C	< 5 years data
Wairua at Purua						12	18	24	22	11	87	A+	
Waitangi at SH10						12	12	11	12	12	59	A	
Waitangi at Waimate North Road						24	24	24	25	15	112	A+	
Waitangi at Wakelins						35	39	36	39	29	178	A+	
Waitaua at Vinegar Hill Road						13	13	13	13	13	65	A	
Watercress at SH1						12	12	12	12	12	60	A	
Whakapara at Cableway						12	12	12	14	12	62	A	
Total samples	9	28	30	26	67	850	897	917	957	806	4587		

Table A.2. Summary of blanks and censored values in dataset.

Analytes	Total samples	Blanks	% blanks	Censored values	% censored
Talk	105	4592	98	0	0
TAM	4348	349	7	793	17
B	98	4599	98	21	0
Br	105	4592	98	0	0
Ca	98	4599	98	0	0
Cl	105	4592	98	0	0
Conductivity	4311	386	8	0	0
DOC	96	4601	98	0	0
DO%	4327	370	8	0	0
DO	4303	394	8	0	0
DRP	4333	364	8	5	0
DIN	606	4091	87	43	1
E. coli	4574	123	3	21	0
Mg	98	4599	98	0	0
Mn	98	4599	98	0	0
NO_3	4182	515	11	242	5
NO_2	4146	551	12	2230	47
NNN	4331	366	8	237	5
K	98	4599	98	0	0
Clarity	4217	480	10	251	5
Si	105	4592	98	0	0
Na	98	4599	98	0	0
SO_4	105	4592	98	0	0
SS	37	4660	99	0	0
Temp	4540	157	3	0	0
TKN	4152	545	12	765	16
TN	4326	371	8	459	10
TP	4332	365	8	5	0
TSS	826	3871	82	109	2
Turb	4363	334	7	2	0
VSS	637	4060	86	114	2
pH	4295	402	9	0	0
Total samples	4,697				

Appendix B: Statistics for Northland Water Quality Sites

Table B.1. Summary statistics for all Northland sites. This data was used as input for water quality modelling for all analytes except E.coli. Modelling and NOF State assessment for E.coli was undertaken on an augmented dataset to achieve the minimum 60 sample requirement.

	TN	TAM	NNN	NO_3-N	DIN	DIN (cal.)	TP	DRP	TSS	Turbidity	Clarity	DO	*E. coli*
Aurere at Pekerau Road (C)													
Count	63	63	63	63	10	63	63	63	10	63	62	62	63
Mean	1.816	0.126	0.098	0.225	0.074	0.359	0.269	0.117	21.08	24.43	1.24	9.29	1382.34
Minimum	1.110	0.026	0.002	0.004	0.014	0.036	0.112	0.043	1.00	2.72	0.30	1.60	306.00
Maximum	4.500	1.620	0.580	0.990	0.160	2.280	0.740	0.330	140.00	118.10	3.17	18.90	5976.00
Q5	1.159	0.029	0.002	0.006	0.024	0.072	0.138	0.057	1.54	5.06	0.32	3.14	405.20
Q10	1.258	0.032	0.006	0.010	0.035	0.083	0.143	0.063	2.08	7.34	0.47	4.34	457.20
Q20	1.388	0.039	0.016	0.032	0.037	0.111	0.164	0.072	2.36	11.18	0.50	5.80	546.60
Q25	1.410	0.042	0.021	0.045	0.043	0.131	0.174	0.078	2.50	12.67	0.58	7.10	620.75
Q50 Median	1.590	0.062	0.048	0.139	0.069	0.216	0.241	0.104	5.90	16.15	1.13	9.30	985.00
Q75	1.910	0.102	0.115	0.358	0.093	0.476	0.320	0.136	9.65	29.53	1.74	12.10	1437.75
Q80	2.096	0.135	0.130	0.404	0.098	0.529	0.338	0.143	14.40	34.00	1.90	12.58	1821.60
Q95	3.120	0.327	0.392	0.620	0.138	0.766	0.501	0.201	91.40	56.19	2.52	14.90	3610.65
Awanui at FNDC													
Count	60	60	60	60	10	60	60	60	16	60	60	59	60
Mean	0.302	0.012	0.045	0.044	0.066	0.058	0.051	0.019	3.72	17.2	1.09	8.46	1537.5
Minimum	0.100	0.005	0.002	0.002	0.005	0.007	0.010	0.008	0.80	0.8	0.10	5.80	57.0
Maximum	1.700	0.058	0.200	0.200	0.220	0.216	0.420	0.057	22.00	350.0	2.60	10.40	24196.0
Q5	0.100	0.005	0.002	0.002	0.005	0.007	0.020	0.011	0.85	1.0	0.10	6.78	95.9
Q10	0.100	0.005	0.002	0.002	0.005	0.007	0.022	0.014	0.93	1.2	0.20	6.98	109.0
Q20	0.140	0.005	0.002	0.002	0.005	0.008	0.025	0.016	1.00	1.7	0.40	7.50	157.6
Q25	0.170	0.005	0.002	0.002	0.005	0.009	0.027	0.016	1.00	2.2	0.40	7.65	179.8
Q50 Median	0.220	0.008	0.017	0.017	0.019	0.029	0.032	0.018	2.25	4.4	1.00	8.50	282.5
Q75	0.345	0.015	0.086	0.082	0.118	0.100	0.049	0.020	3.30	10.8	1.63	9.35	647.5
Q80	0.384	0.017	0.092	0.091	0.126	0.111	0.059	0.021	4.20	11.6	1.80	9.48	810.8
Q95	0.701	0.033	0.151	0.151	0.189	0.171	0.121	0.027	11.80	59.1	2.33	10.00	5620.2

	TN	TAM	NNN	NO_3-N	DIN	DIN (cal.)	TP	DRP	TSS	Turbidity	Clarity	DO	*E. coli*
Awanui at Waihue Channel													
Count	59	75	59	59	11	75	59	61	9	59	59	61	75
Mean	0.741	0.116	0.099	0.082	0.311	0.194	0.137	0.060	6.82	20.8	0.78	7.86	1374.1
Minimum	0.100	0.005	0.002	0.002	0.076	0.010	0.025	0.014	2.60	1.6	0.10	2.50	20.0
Maximum	4.400	1.300	0.730	0.720	0.830	1.780	0.790	0.440	21.00	390.0	2.00	10.90	22470.0
Q5	0.243	0.009	0.002	0.002	0.098	0.015	0.043	0.019	2.92	3.1	0.19	5.30	99.7
Q10	0.278	0.018	0.004	0.004	0.120	0.021	0.049	0.022	3.24	3.3	0.20	5.70	113.0
Q20	0.366	0.024	0.011	0.008	0.140	0.036	0.064	0.031	3.64	4.8	0.30	6.40	154.8
Q25	0.380	0.027	0.014	0.011	0.145	0.042	0.078	0.032	3.80	5.3	0.30	6.70	160.5
Q50 Median	0.530	0.044	0.052	0.038	0.220	0.127	0.093	0.044	4.60	7.8	0.79	8.20	288.0
Q75	0.860	0.120	0.130	0.115	0.370	0.232	0.130	0.060	8.40	12.5	1.20	9.00	574.0
Q80	0.926	0.142	0.164	0.134	0.380	0.242	0.134	0.066	8.48	17.4	1.25	9.30	678.0
Q95	1.710	0.457	0.282	0.243	0.800	0.792	0.483	0.110	16.04	71.0	1.60	9.80	4885.7
Hakaru at Topuni													
Count	59	59	59	59	9	59	59	59	15	59	60	60	60
Mean	0.705	0.027	0.208	0.204	0.247	0.235	0.117	0.060	3.13	15.5	1.33	10.12	3720.8
Minimum	0.120	0.005	0.002	0.002	0.020	0.007	0.047	0.028	1.00	1.1	0.10	6.90	20.0
Maximum	3.000	0.160	0.480	0.470	0.450	0.600	0.630	0.110	10.00	230.0	2.42	13.40	92080.0
Q5	0.279	0.005	0.002	0.002	0.072	0.011	0.059	0.034	1.00	1.9	0.20	8.60	31.0
Q10	0.290	0.006	0.004	0.004	0.124	0.018	0.062	0.040	1.28	2.1	0.50	8.89	52.0
Q20	0.360	0.009	0.064	0.061	0.162	0.075	0.075	0.046	1.94	2.9	0.70	9.28	74.6
Q25	0.390	0.010	0.079	0.076	0.170	0.094	0.080	0.048	2.00	2.9	0.87	9.30	91.0
Q50 Median	0.600	0.015	0.210	0.200	0.200	0.220	0.093	0.059	2.20	4.6	1.43	10.20	134.0
Q75	0.790	0.032	0.325	0.325	0.350	0.363	0.115	0.068	3.30	7.5	1.77	11.00	240.0
Q80	0.864	0.037	0.340	0.330	0.358	0.392	0.120	0.073	3.52	10.0	1.80	11.10	468.0
Q95	1.530	0.088	0.441	0.431	0.418	0.499	0.268	0.093	7.69	110.0	2.31	11.61	17719.6

Hatea at Mair Park

	TN	TAM	NNN	NO_3-N	DIN	DIN (cal.)	TP	DRP	TSS	Turbidity	Clarity	DO	*E. coli*
Count	85	92	92	86	6	92	92	92	6	92	91	92	92
Mean	0.718	0.014	0.466	0.450	0.492	0.480	0.032	0.011	3.92	9.8	1.53	10.15	2335.5
Minimum	0.180	0.005	0.016	0.016	0.170	0.027	0.005	0.003	1.00	1.3	0.12	7.00	62.0
Maximum	1.700	0.055	1.250	0.810	0.830	1.265	0.220	0.032	17.00	85.0	3.35	12.30	44000.0
Q5	0.364	0.005	0.206	0.203	0.215	0.212	0.010	0.005	1.05	2.0	0.31	8.11	108.6
Q10	0.456	0.005	0.271	0.260	0.260	0.295	0.011	0.005	1.10	2.4	0.52	8.91	135.0
Q20	0.550	0.005	0.342	0.330	0.350	0.357	0.015	0.007	1.20	2.9	1.00	9.32	185.0
Q25	0.580	0.006	0.370	0.360	0.353	0.377	0.016	0.008	1.20	3.1	1.05	9.58	200.8
Q50 Median	0.680	0.010	0.470	0.460	0.420	0.480	0.021	0.011	1.35	4.5	1.41	10.40	350.0
Q75	0.800	0.017	0.563	0.550	0.690	0.577	0.027	0.013	1.58	6.8	2.05	10.80	800.5
Q80	0.902	0.020	0.580	0.570	0.760	0.597	0.030	0.013	1.60	8.5	2.18	10.90	1335.0
Q95	1.200	0.033	0.709	0.695	0.813	0.723	0.104	0.015	13.15	50.2	2.90	11.50	14798.4
Hatea at Whangarei Falls													
Count	60	60	60	60	10	60	60	60	10	60	58	61	132
Mean	0.534	0.013	0.347	0.345	0.336	0.360	0.024	0.012	3.95	5.6	1.39	9.03	951.6
Minimum	0.100	0.005	0.042	0.042	0.042	0.047	0.011	0.005	0.80	0.9	0.18	5.60	108.0
Maximum	1.400	0.084	0.850	0.850	0.870	0.867	0.094	0.017	10.00	55.0	2.80	12.00	9804.0
Q5	0.190	0.005	0.056	0.054	0.052	0.069	0.014	0.006	1.25	2.4	0.73	7.10	181.6
Q10	0.278	0.005	0.119	0.119	0.062	0.127	0.015	0.008	1.70	2.8	0.87	7.10	213.3
Q20	0.384	0.006	0.178	0.168	0.117	0.200	0.018	0.009	1.88	3.3	0.99	7.70	265.8
Q25	0.398	0.007	0.200	0.200	0.143	0.219	0.019	0.010	2.00	3.4	1.02	8.00	307.0
Q50 Median	0.530	0.010	0.360	0.360	0.245	0.380	0.023	0.012	3.35	4.1	1.22	9.30	447.5
Q75	0.623	0.016	0.483	0.473	0.495	0.492	0.025	0.013	5.10	5.1	1.62	9.90	717.8
Q80	0.652	0.016	0.500	0.500	0.544	0.506	0.027	0.014	5.36	5.6	1.81	10.10	794.0
Q95	0.884	0.027	0.560	0.551	0.767	0.580	0.038	0.015	8.20	10.0	2.55	11.10	4865.6
Kaeo at Dip Road													
Count	60	60	60	60	10	60	60	60	16	60	59	59	60

	TN	TAM	NNN	NO_3-N	DIN	DIN (cal.)	TP	DRP	TSS	Turbidity	Clarity	DO	*E. coli*
Mean	0.218	0.011	0.043	0.043	0.039	0.054	0.025	0.009	4.16	11.6	1.38	8.98	1267.5
Minimum	0.100	0.005	0.002	0.002	0.005	0.007	0.005	0.004	0.80	0.5	0.20	2.30	43.0
Maximum	1.100	0.051	0.210	0.210	0.120	0.229	0.200	0.038	20.00	270.0	2.90	11.50	12033.0
Q5	0.100	0.005	0.002	0.002	0.005	0.007	0.009	0.004	0.85	1.1	0.30	5.69	96.5
Q10	0.100	0.005	0.002	0.002	0.005	0.009	0.009	0.005	0.93	1.4	0.38	6.68	128.0
Q20	0.100	0.005	0.003	0.003	0.012	0.011	0.011	0.006	1.00	1.8	0.63	7.80	185.6
Q25	0.100	0.005	0.004	0.004	0.015	0.011	0.012	0.006	1.00	1.9	0.85	8.20	221.0
Q50 Median	0.160	0.008	0.019	0.018	0.019	0.028	0.015	0.008	2.30	2.9	1.38	9.50	403.5
Q75	0.240	0.012	0.072	0.071	0.044	0.094	0.022	0.009	4.05	6.1	1.88	10.20	715.8
Q80	0.270	0.015	0.091	0.091	0.056	0.103	0.025	0.009	4.20	8.7	2.00	10.40	909.6
Q95	0.650	0.025	0.150	0.150	0.111	0.166	0.076	0.017	16.25	38.4	2.60	10.90	6571.8
Kaihu at Gorge													
Count	59	59	59	59	9	59	59	59	14	59	58	59	60
Mean	0.391	0.008	0.197	0.196	0.198	0.205	0.020	0.008	2.23	5.4	1.67	10.07	715.3
Minimum	0.100	0.005	0.002	0.002	0.012	0.007	0.006	0.003	1.00	0.8	0.10	7.60	60.0
Maximum	1.400	0.035	0.470	0.470	0.490	0.485	0.190	0.014	5.10	75.0	3.07	11.40	11000.0
Q5	0.100	0.005	0.004	0.004	0.016	0.009	0.008	0.004	1.00	1.0	0.52	8.48	74.0
Q10	0.100	0.005	0.012	0.012	0.021	0.019	0.009	0.005	1.06	1.1	0.66	9.08	85.8
Q20	0.182	0.005	0.058	0.058	0.056	0.067	0.011	0.006	1.32	1.3	0.96	9.30	109.6
Q25	0.220	0.005	0.082	0.080	0.078	0.087	0.011	0.007	1.43	1.8	1.15	9.35	125.5
Q50 Median	0.360	0.005	0.180	0.180	0.150	0.185	0.014	0.008	1.95	3.0	1.66	10.20	173.0
Q75	0.515	0.009	0.330	0.330	0.310	0.336	0.021	0.009	2.08	4.6	2.10	10.80	347.5
Q80	0.544	0.010	0.360	0.360	0.342	0.365	0.023	0.009	2.62	5.4	2.31	10.90	470.8
Q95	0.777	0.019	0.391	0.391	0.450	0.402	0.038	0.011	4.91	13.0	3.00	11.20	3364.7
Kenana at Kenana Road													
Count	60	60	60	60	10	60	60	60	10	60	59	58	60
Mean	0.150	0.008	0.037	0.037	0.029	0.045	0.036	0.023	2.51	8.1	1.65	8.46	436.5

	TN	TAM	NNN	NO_3-N	DIN	DIN (cal.)	TP	DRP	TSS	Turbidity	Clarity	DO	*E. coli*
Minimum	0.100	0.005	0.002	0.002	0.005	0.007	0.019	0.012	0.80	1.2	0.20	4.00	75.0
Maximum	0.800	0.025	0.130	0.130	0.130	0.155	0.090	0.037	7.80	160.0	4.90	13.50	2187.0
Q5	0.100	0.005	0.002	0.002	0.005	0.008	0.023	0.016	0.89	1.3	0.49	6.07	130.9
Q10	0.100	0.005	0.004	0.004	0.005	0.009	0.026	0.016	0.98	1.4	0.61	6.37	158.8
Q20	0.100	0.005	0.008	0.008	0.007	0.015	0.028	0.018	1.32	2.0	0.96	7.04	188.2
Q25	0.100	0.005	0.010	0.010	0.009	0.017	0.029	0.019	1.40	2.2	1.05	7.48	210.5
Q50 Median	0.100	0.006	0.024	0.024	0.015	0.031	0.034	0.022	1.75	3.3	1.70	8.40	333.5
Q75	0.150	0.010	0.062	0.061	0.024	0.071	0.039	0.027	2.75	6.9	2.10	9.60	555.8
Q80	0.162	0.011	0.068	0.068	0.033	0.079	0.040	0.028	3.00	8.5	2.10	9.70	614.2
Q95	0.323	0.015	0.101	0.101	0.099	0.111	0.059	0.033	6.00	17.1	2.76	11.06	1038.3
Kerikeri at Stone Store													
Count	70	90	90	71	5	90	90	89	21	89	88	90	89
Mean	0.669	0.022	0.404	0.402	0.448	0.425	0.052	0.015	11.93	7.9	2.04	10.23	2720.8
Minimum	0.240	0.005	0.105	0.120	0.180	0.118	0.006	0.004	0.90	0.9	0.12	5.90	10.0
Maximum	1.900	0.150	0.890	0.890	0.650	0.927	0.600	0.110	111.00	106.2	3.51	18.70	65000.0
Q5	0.330	0.006	0.145	0.145	0.228	0.158	0.009	0.006	1.00	1.1	0.59	8.44	52.0
Q10	0.359	0.007	0.189	0.180	0.276	0.216	0.010	0.007	1.00	1.3	0.84	8.80	81.4
Q20	0.420	0.009	0.268	0.280	0.372	0.287	0.013	0.008	1.00	1.7	1.27	9.10	104.6
Q25	0.440	0.010	0.291	0.305	0.420	0.302	0.014	0.008	1.00	1.9	1.42	9.40	131.0
Q50 Median	0.645	0.012	0.410	0.410	0.440	0.440	0.019	0.010	1.00	2.5	2.19	10.30	228.0
Q75	0.778	0.020	0.510	0.510	0.550	0.526	0.040	0.015	2.00	4.3	2.68	11.00	545.0
Q80	0.826	0.024	0.530	0.520	0.570	0.543	0.061	0.016	3.00	6.1	2.80	11.00	807.8
Q95	1.310	0.065	0.626	0.635	0.630	0.643	0.231	0.047	104.00	38.2	3.05	11.70	12611.4
Mangahahuru at Apotu Road													
Count	60	60	60	60	10	60	60	60	10	60	60	59	60
Mean	0.594	0.034	0.284	0.280	0.372	0.317	0.079	0.036	2.97	13.3	1.24	8.84	1843.0
Minimum	0.210	0.005	0.032	0.032	0.190	0.044	0.028	0.012	1.30	1.6	0.03	3.30	86.0

	TN	TAM	NNN	NO_3-N	DIN	DIN (cal.)	TP	DRP	TSS	Turbidity	Clarity	DO	*E. coli*
Maximum	2.000	0.170	0.540	0.540	0.630	0.630	0.380	0.100	7.20	170.0	2.80	11.50	54750.0
Q5	0.260	0.008	0.067	0.067	0.199	0.077	0.032	0.016	1.53	2.6	0.16	6.07	138.5
Q10	0.269	0.008	0.079	0.077	0.208	0.089	0.034	0.017	1.75	2.8	0.62	6.60	171.7
Q20	0.366	0.009	0.152	0.150	0.218	0.186	0.045	0.020	1.80	3.3	0.91	7.56	190.0
Q25	0.388	0.010	0.195	0.193	0.225	0.209	0.050	0.022	2.00	3.8	0.95	8.00	199.8
Q50 Median	0.540	0.017	0.310	0.305	0.335	0.334	0.064	0.033	2.85	5.5	1.25	9.10	310.0
Q75	0.663	0.042	0.390	0.383	0.518	0.435	0.088	0.045	3.08	8.0	1.57	10.10	439.5
Q80	0.720	0.055	0.402	0.400	0.546	0.448	0.092	0.048	3.12	8.9	1.61	10.20	487.4
Q95	1.225	0.102	0.491	0.490	0.603	0.571	0.153	0.068	5.40	61.3	2.00	11.11	7584.9
Mangahahuru at Main Road													
Count	60	60	60	60	10	60	60	60	14	60	60	58	60
Mean	0.318	0.011	0.144	0.143	0.107	0.155	0.038	0.013	3.56	10.9	1.31	9.78	1006.2
Minimum	0.100	0.005	0.022	0.022	0.047	0.034	0.008	0.005	1.20	3.0	0.07	7.90	75.0
Maximum	1.900	0.066	0.440	0.430	0.180	0.452	0.250	0.019	14.00	120.0	2.27	11.80	12997.0
Q5	0.100	0.005	0.034	0.031	0.049	0.047	0.017	0.009	1.46	3.6	0.29	8.10	119.5
Q10	0.109	0.005	0.039	0.039	0.051	0.052	0.018	0.009	1.72	3.8	0.83	8.50	169.9
Q20	0.170	0.007	0.060	0.060	0.065	0.070	0.019	0.011	2.00	4.3	0.95	8.84	226.0
Q25	0.170	0.007	0.070	0.068	0.069	0.086	0.021	0.011	2.10	4.6	1.12	9.03	240.0
Q50 Median	0.265	0.010	0.140	0.140	0.112	0.146	0.025	0.013	3.00	5.3	1.36	9.75	452.5
Q75	0.343	0.013	0.180	0.180	0.130	0.188	0.032	0.014	3.30	6.6	1.58	10.40	693.3
Q80	0.380	0.014	0.190	0.190	0.138	0.195	0.034	0.014	3.34	7.5	1.64	10.56	833.0
Q95	0.905	0.019	0.380	0.380	0.176	0.388	0.123	0.018	8.15	45.3	2.15	11.42	3488.6
Mangakahia at Titoki													
Count	86	86	86	50	9	86	86	86	9	86	87	42	86
Mean	0.395	0.017	0.138	0.152	0.133	0.155	0.045	0.011	7.39	19.7	1.07	9.05	1696.5
Minimum	0.110	0.001	0.001	0.002	0.005	0.002	0.009	0.001	2.40	1.0	0.02	7.00	18.5
Maximum	1.700	0.139	0.437	0.437	0.280	0.576	0.390	0.072	19.00	280.0	2.80	10.50	32550.0

	TN	TAM	NNN	NO_3-N	DIN	DIN (cal.)	TP	DRP	TSS	Turbidity	Clarity	DO	*E. coli*
Q5	0.131	0.003	0.001	0.002	0.005	0.005	0.014	0.002	2.68	1.5	0.10	7.71	42.1
Q10	0.144	0.004	0.002	0.003	0.005	0.007	0.014	0.003	2.96	1.8	0.24	8.00	59.2
Q20	0.171	0.005	0.005	0.011	0.010	0.011	0.017	0.004	3.28	2.8	0.41	8.20	84.2
Q25	0.186	0.005	0.010	0.021	0.013	0.016	0.018	0.005	3.40	3.2	0.46	8.25	91.5
Q50 Median	0.279	0.009	0.075	0.094	0.071	0.088	0.027	0.010	5.80	8.1	0.82	9.10	179.7
Q75	0.479	0.017	0.258	0.260	0.260	0.276	0.038	0.013	6.80	13.8	1.56	9.88	499.8
Q80	0.528	0.020	0.260	0.278	0.264	0.294	0.045	0.014	10.48	18.0	1.79	9.98	882.0
Q95	1.116	0.055	0.378	0.386	0.276	0.433	0.153	0.020	17.80	100.8	2.55	10.29	11690.0
Mangakahia at Twin Bridges													
Count	59	59	59	59	10	59	59	59	16	59	58	59	60
Mean	0.256	0.007	0.070	0.069	0.059	0.077	0.031	0.009	4.41	13.0	1.62	10.61	1159.7
Minimum	0.100	0.005	0.002	0.002	0.005	0.007	0.006	0.004	0.90	0.4	0.10	6.00	8.6
Maximum	2.000	0.045	0.360	0.360	0.160	0.381	0.580	0.021	32.00	170.0	3.07	12.00	43520.0
Q5	0.100	0.005	0.002	0.002	0.005	0.007	0.008	0.005	0.98	0.7	0.29	9.40	19.0
Q10	0.100	0.005	0.002	0.002	0.005	0.007	0.009	0.006	1.05	1.0	0.39	9.60	26.8
Q20	0.100	0.005	0.002	0.002	0.005	0.008	0.011	0.007	1.10	1.2	0.78	9.86	47.6
Q25	0.100	0.005	0.003	0.003	0.005	0.008	0.012	0.007	1.25	1.3	0.95	10.15	62.0
Q50 Median	0.160	0.005	0.029	0.029	0.029	0.034	0.015	0.009	2.50	3.5	1.55	10.80	121.0
Q75	0.265	0.006	0.130	0.125	0.106	0.138	0.020	0.011	3.15	5.9	2.48	11.30	336.5
Q80	0.300	0.007	0.148	0.148	0.118	0.160	0.022	0.011	3.60	7.2	2.66	11.40	458.2
Q95	0.767	0.016	0.210	0.201	0.156	0.215	0.100	0.013	13.55	61.5	3.00	11.82	1695.2
Mangakino at Mangakino Lane													
Count	60	60	60	60	10	60	60	60	10	60	55	59	60
Mean	0.375	0.007	0.203	0.203	0.364	0.210	0.029	0.012	6.60	10.4	0.73	10.25	236.4
Minimum	0.100	0.005	0.077	0.075	0.084	0.084	0.013	0.006	2.60	4.8	0.10	8.70	29.0
Maximum	2.200	0.023	1.400	1.400	1.400	1.405	0.110	0.019	14.00	75.0	1.92	13.20	1600.0
Q5	0.148	0.005	0.096	0.096	0.088	0.106	0.016	0.008	2.69	5.4	0.36	9.09	58.7

	TN	TAM	NNN	NO_3-N	DIN	DIN (cal.)	TP	DRP	TSS	Turbidity	Clarity	DO	*E. coli*
Q10	0.190	0.005	0.100	0.100	0.091	0.109	0.017	0.009	2.78	5.7	0.40	9.18	63.0
Q20	0.216	0.005	0.110	0.110	0.106	0.120	0.020	0.010	2.96	6.6	0.50	9.60	82.2
Q25	0.230	0.005	0.128	0.120	0.110	0.134	0.021	0.010	3.15	6.9	0.52	9.60	94.3
Q50 Median	0.300	0.006	0.165	0.165	0.185	0.172	0.026	0.012	4.00	8.4	0.70	10.20	149.0
Q75	0.385	0.008	0.200	0.200	0.370	0.206	0.031	0.014	9.10	10.5	0.89	10.85	231.0
Q80	0.410	0.008	0.210	0.210	0.478	0.215	0.035	0.014	10.16	11.0	0.95	10.90	238.8
Q95	0.929	0.011	0.394	0.394	1.126	0.402	0.054	0.016	14.00	17.2	1.37	11.52	986.0
Mangakino U/S Waitaua Confluence													
Count	57	57	57	57	10	57	57	57	10	57	55	56	57
Mean	0.420	0.016	0.249	0.248	0.377	0.265	0.028	0.014	4.48	7.3	1.01	8.68	715.2
Minimum	0.100	0.005	0.076	0.076	0.150	0.084	0.011	0.006	1.50	3.7	0.35	6.00	189.0
Maximum	2.000	0.033	1.200	1.200	1.200	1.221	0.074	0.026	12.00	30.0	1.90	12.10	2382.0
Q5	0.170	0.007	0.128	0.128	0.159	0.144	0.018	0.009	1.64	4.4	0.49	6.38	216.0
Q10	0.196	0.008	0.150	0.150	0.168	0.166	0.019	0.010	1.77	4.7	0.58	6.45	331.4
Q20	0.292	0.011	0.170	0.170	0.170	0.181	0.021	0.011	1.80	5.0	0.72	7.20	401.2
Q25	0.310	0.012	0.170	0.170	0.173	0.192	0.023	0.011	1.80	5.2	0.73	7.73	450.0
Q50 Median	0.380	0.015	0.220	0.220	0.225	0.236	0.025	0.014	2.55	5.9	0.95	9.10	563.0
Q75	0.430	0.021	0.270	0.270	0.410	0.283	0.030	0.016	6.40	7.4	1.23	9.65	860.0
Q80	0.448	0.021	0.280	0.280	0.502	0.296	0.032	0.016	7.44	8.0	1.26	9.90	881.2
Q95	0.846	0.027	0.440	0.432	0.980	0.463	0.052	0.019	10.74	12.6	1.63	10.45	1721.0
Mangamuka at Iwitaua Road													
Count	60	60	60	60	10	60	60	60	10	60	60	59	60
Mean	0.138	0.007	0.016	0.016	0.016	0.023	0.046	0.032	2.68	4.3	1.61	9.32	869.8
Minimum	0.100	0.005	0.002	0.002	0.005	0.007	0.006	0.003	0.71	0.3	0.20	5.30	51.0
Maximum	0.600	0.037	0.190	0.190	0.047	0.203	0.110	0.044	7.30	60.0	4.91	11.30	11199.0
Q5	0.100	0.005	0.002	0.002	0.005	0.007	0.032	0.015	0.73	0.5	0.47	7.11	72.5
Q10	0.100	0.005	0.002	0.002	0.005	0.007	0.035	0.025	0.75	0.6	0.74	8.20	120.8

	TN	TAM	NNN	NO_3-N	DIN	DIN (cal.)	TP	DRP	TSS	Turbidity	Clarity	DO	*E. coli*
Q20	0.100	0.005	0.002	0.002	0.005	0.008	0.036	0.028	0.95	0.7	1.10	8.70	173.0
Q25	0.100	0.005	0.003	0.003	0.005	0.009	0.037	0.029	1.03	0.8	1.18	8.80	204.8
Q50 Median	0.100	0.005	0.006	0.005	0.011	0.012	0.043	0.034	1.70	1.6	1.50	9.40	345.0
Q75	0.130	0.006	0.013	0.013	0.019	0.025	0.046	0.037	2.95	3.3	1.90	10.15	815.0
Q80	0.150	0.008	0.020	0.020	0.023	0.035	0.047	0.038	3.98	3.7	2.00	10.34	872.0
Q95	0.295	0.013	0.061	0.061	0.043	0.067	0.077	0.042	7.21	14.0	3.00	10.80	2938.6
Manganui at Mititai Road													
Count	59	59	59	59	9	59	59	59	9	59	58	60	60
Mean	0.679	0.043	0.162	0.158	0.223	0.205	0.087	0.039	9.71	13.4	0.88	8.16	990.9
Minimum	0.270	0.005	0.002	0.002	0.005	0.007	0.016	0.010	2.80	1.5	0.10	1.60	20.0
Maximum	1.400	0.290	0.580	0.560	0.600	0.602	0.230	0.130	44.00	100.0	2.00	11.50	19863.0
Q5	0.289	0.005	0.002	0.002	0.005	0.009	0.027	0.016	2.96	2.4	0.29	5.69	29.9
Q10	0.340	0.007	0.002	0.002	0.005	0.011	0.034	0.020	3.12	3.4	0.30	6.81	30.0
Q20	0.386	0.011	0.003	0.003	0.015	0.014	0.052	0.027	3.56	4.4	0.51	7.38	41.0
Q25	0.415	0.012	0.004	0.003	0.021	0.018	0.054	0.030	3.80	4.6	0.56	7.70	52.0
Q50 Median	0.650	0.028	0.097	0.097	0.100	0.193	0.073	0.036	5.00	7.2	0.80	8.30	120.0
Q75	0.840	0.047	0.285	0.285	0.420	0.308	0.110	0.045	6.00	13.0	1.18	9.13	381.0
Q80	0.924	0.052	0.330	0.320	0.464	0.369	0.120	0.051	8.80	15.0	1.32	9.30	556.0
Q95	1.310	0.143	0.451	0.441	0.572	0.522	0.182	0.073	31.60	60.5	1.63	10.11	3876.4
Mangapiu at Kokopu Road													
Count	58	58	58	58	8	58	58	58	8	57	53	58	58
Mean	2.047	0.180	0.666	0.643	1.035	0.846	0.397	0.201	7.34	12.6	0.70	6.47	2827.9
Minimum	1.000	0.011	0.002	0.002	0.190	0.018	0.120	0.041	2.40	2.1	0.27	0.60	31.0
Maximum	7.500	1.000	2.000	1.900	2.100	2.540	0.840	0.540	12.00	75.0	1.60	9.60	37000.0
Q5	1.200	0.034	0.106	0.096	0.414	0.244	0.169	0.053	3.21	3.7	0.33	2.96	146.8
Q10	1.300	0.052	0.204	0.201	0.638	0.299	0.187	0.089	4.01	4.8	0.45	3.60	268.3
Q20	1.500	0.065	0.314	0.294	0.834	0.458	0.254	0.110	4.82	7.0	0.54	5.24	437.0

	TN	TAM	NNN	NO_3-N	DIN	DIN (cal.)	TP	DRP	TSS	Turbidity	Clarity	DO	*E. coli*
Q25	1.500	0.072	0.393	0.343	0.838	0.542	0.273	0.123	4.93	7.8	0.55	5.50	565.0
Q50 Median	1.800	0.130	0.605	0.585	0.960	0.776	0.370	0.190	7.20	9.2	0.67	6.65	1086.0
Q75	2.100	0.208	0.905	0.883	1.150	1.075	0.468	0.238	9.15	13.2	0.77	7.98	2236.0
Q80	2.200	0.228	0.982	0.956	1.220	1.112	0.518	0.266	10.48	15.7	0.86	8.20	3683.8
Q95	3.560	0.551	1.600	1.515	1.820	1.882	0.720	0.453	12.00	27.6	1.10	9.00	10138.4
Mangere at Kara Road													
Count	60	60	60	60	10	60	60	60	10	59	60	60	60
Mean	0.550	0.012	0.376	0.374	0.367	0.388	0.028	0.015	2.09	5.4	1.57	9.29	841.0
Minimum	0.180	0.005	0.058	0.058	0.081	0.068	0.013	0.002	0.70	1.2	0.26	7.20	98.0
Maximum	1.200	0.053	0.800	0.790	0.660	0.806	0.100	0.035	3.90	60.0	2.80	11.10	4300.0
Q5	0.229	0.005	0.066	0.066	0.103	0.081	0.016	0.010	0.84	1.8	0.77	7.60	215.2
Q10	0.259	0.005	0.109	0.108	0.125	0.118	0.017	0.011	0.97	2.1	0.93	8.14	257.7
Q20	0.308	0.006	0.148	0.140	0.170	0.158	0.020	0.012	1.08	2.3	1.17	8.40	316.4
Q25	0.360	0.007	0.180	0.178	0.188	0.189	0.022	0.013	1.20	2.5	1.22	8.40	355.5
Q50 Median	0.570	0.010	0.420	0.420	0.420	0.425	0.026	0.015	2.10	3.5	1.51	9.40	615.0
Q75	0.710	0.013	0.548	0.548	0.503	0.577	0.030	0.016	2.85	5.1	1.88	10.13	981.8
Q80	0.750	0.013	0.582	0.582	0.524	0.587	0.032	0.017	2.90	5.6	1.98	10.22	1153.4
Q95	0.871	0.027	0.701	0.700	0.624	0.711	0.049	0.021	3.45	13.0	2.48	10.70	2433.8
Mangere at Knight Road													
Count	110	110	110	110	10	110	110	110	16	109	109	111	110
Mean	1.070	0.071	0.511	0.505	0.528	0.583	0.118	0.061	3.26	11.1	1.01	8.41	4137.2
Minimum	0.180	0.005	0.002	0.002	0.025	0.012	0.027	0.016	1.80	2.4	0.10	5.00	121.0
Maximum	7.000	1.600	1.200	1.200	1.100	2.400	1.100	0.490	7.40	140.0	2.50	13.10	141360.0
Q5	0.300	0.010	0.036	0.036	0.068	0.048	0.040	0.023	1.95	2.7	0.30	6.15	200.5
Q10	0.349	0.012	0.085	0.085	0.111	0.105	0.049	0.028	2.00	3.0	0.64	6.60	289.8
Q20	0.458	0.018	0.180	0.180	0.128	0.199	0.058	0.034	2.00	3.7	0.75	7.40	385.8
Q25	0.543	0.019	0.223	0.223	0.150	0.255	0.063	0.035	2.00	3.9	0.80	7.60	461.0

	TN	TAM	NNN	NO_3-N	DIN	DIN (cal.)	TP	DRP	TSS	Turbidity	Clarity	DO	*E. coli*
Q50 Median	0.925	0.031	0.480	0.480	0.535	0.546	0.085	0.047	2.90	6.0	0.98	8.70	656.5
Q75	1.300	0.055	0.768	0.760	0.830	0.811	0.110	0.060	4.25	9.0	1.22	9.30	987.8
Q80	1.400	0.064	0.800	0.780	0.856	0.848	0.120	0.065	4.40	9.8	1.30	9.50	1212.6
Q95	2.100	0.216	1.055	1.000	1.037	1.171	0.342	0.141	5.68	39.2	1.66	9.85	11288.4
Mangere at Kokopu Road													
Count	60	60	60	60	10	60	60	60	10	59	49	60	60
Mean	0.726	0.021	0.399	0.397	0.354	0.420	0.057	0.030	3.43	7.1	1.30	8.87	1635.5
Minimum	0.260	0.005	0.002	0.002	0.077	0.013	0.025	0.014	1.70	2.1	0.27	6.30	120.0
Maximum	1.800	0.093	0.810	0.810	0.690	0.825	0.260	0.110	5.40	90.0	2.50	10.60	27000.0
Q5	0.280	0.010	0.070	0.070	0.101	0.084	0.032	0.020	1.93	2.5	0.54	7.00	239.6
Q10	0.310	0.011	0.108	0.107	0.125	0.122	0.038	0.021	2.15	2.8	0.75	7.30	307.7
Q20	0.388	0.013	0.148	0.140	0.130	0.170	0.042	0.022	2.84	3.4	0.92	7.90	374.2
Q25	0.428	0.014	0.200	0.200	0.140	0.223	0.042	0.023	3.08	3.7	1.01	8.00	390.0
Q50 Median	0.695	0.017	0.415	0.410	0.360	0.443	0.049	0.028	3.35	4.7	1.30	8.95	599.0
Q75	0.960	0.023	0.575	0.573	0.525	0.593	0.058	0.032	3.88	6.3	1.52	9.73	1141.0
Q80	0.982	0.023	0.634	0.632	0.540	0.647	0.062	0.033	4.10	6.8	1.55	9.90	1175.2
Q95	1.300	0.045	0.732	0.732	0.641	0.748	0.092	0.045	5.00	18.2	2.12	10.40	2206.6
Mangere at Wood Road													
Count	60	60	60	60	10	60	60	60	10	59	59	60	60
Mean	0.568	0.015	0.410	0.408	0.394	0.425	0.029	0.015	2.75	6.0	1.44	8.30	982.7
Minimum	0.100	0.005	0.029	0.029	0.120	0.046	0.013	0.008	1.00	1.9	0.26	5.00	97.0
Maximum	1.300	0.060	0.830	0.820	0.600	0.844	0.130	0.022	9.10	75.0	2.95	10.60	16000.0
Q5	0.190	0.007	0.100	0.100	0.152	0.118	0.018	0.010	1.05	2.2	0.46	5.78	159.5
Q10	0.270	0.008	0.149	0.139	0.183	0.169	0.019	0.011	1.09	2.5	0.68	6.47	215.4
Q20	0.360	0.010	0.180	0.180	0.230	0.193	0.021	0.013	1.26	2.9	0.89	7.00	297.2
Q25	0.405	0.011	0.245	0.245	0.248	0.254	0.022	0.014	1.33	3.0	0.93	7.20	323.8
Q50 Median	0.565	0.014	0.420	0.415	0.410	0.433	0.028	0.015	1.45	3.7	1.40	8.45	524.5

	TN	TAM	NNN	NO_3-N	DIN	DIN (cal.)	TP	DRP	TSS	Turbidity	Clarity	DO	*E. coli*
Q75	0.723	0.017	0.580	0.573	0.565	0.593	0.032	0.017	2.68	5.4	1.84	9.43	890.0
Q80	0.742	0.019	0.592	0.592	0.572	0.603	0.033	0.018	3.48	5.8	1.95	9.62	922.4
Q95	0.931	0.025	0.731	0.731	0.591	0.747	0.041	0.020	7.62	13.1	2.40	10.21	1436.4
Mania at SH10													
Count	60	60	60	60	8	60	60	60	8	60	60	59	60
Mean	0.458	0.026	0.149	0.148	0.158	0.175	0.050	0.021	3.09	6.4	0.99	6.76	380.6
Minimum	0.100	0.005	0.002	0.002	0.016	0.010	0.024	0.006	1.20	2.0	0.20	2.10	52.0
Maximum	1.100	0.330	0.420	0.410	0.400	0.610	0.120	0.059	9.80	29.0	2.70	9.40	2143.0
Q5	0.139	0.008	0.002	0.002	0.021	0.016	0.028	0.014	1.20	2.1	0.30	3.68	84.0
Q10	0.226	0.008	0.006	0.005	0.027	0.019	0.029	0.016	1.20	2.4	0.30	4.00	98.9
Q20	0.268	0.010	0.012	0.012	0.051	0.030	0.033	0.017	1.28	3.0	0.50	5.36	120.8
Q25	0.308	0.013	0.025	0.025	0.068	0.043	0.035	0.017	1.35	3.3	0.50	5.55	134.8
Q50 Median	0.420	0.016	0.135	0.135	0.122	0.144	0.047	0.020	1.95	4.4	1.00	7.00	235.0
Q75	0.573	0.024	0.240	0.240	0.243	0.266	0.058	0.024	3.50	7.4	1.38	8.35	370.8
Q80	0.620	0.029	0.252	0.252	0.246	0.287	0.060	0.025	3.64	8.3	1.42	8.54	525.6
Q95	0.852	0.046	0.361	0.360	0.348	0.404	0.085	0.028	7.70	17.1	1.79	9.20	1609.6
Ngunguru at Coalhill Lane													
Count	60	60	60	60	10	60	60	60	14	60	60	58	60
Mean	0.332	0.010	0.132	0.131	0.159	0.142	0.036	0.015	2.92	10.2	2.00	10.10	1270.4
Minimum	0.100	0.005	0.002	0.002	0.040	0.007	0.011	0.002	1.00	0.9	0.10	7.80	31.0
Maximum	1.400	0.034	0.370	0.370	0.370	0.375	0.190	0.031	15.00	140.0	3.03	12.60	19863.0
Q5	0.100	0.005	0.006	0.006	0.045	0.014	0.018	0.009	1.00	1.2	0.29	8.46	75.0
Q10	0.100	0.005	0.009	0.009	0.049	0.016	0.019	0.010	1.06	1.3	0.61	8.84	99.9
Q20	0.150	0.005	0.023	0.023	0.057	0.036	0.020	0.012	1.32	1.8	1.39	9.14	156.0
Q25	0.170	0.005	0.042	0.042	0.061	0.053	0.022	0.012	1.40	1.8	1.51	9.33	170.0
Q50 Median	0.240	0.008	0.120	0.115	0.085	0.130	0.026	0.016	1.90	3.2	2.15	10.10	310.5
Q75	0.400	0.012	0.205	0.205	0.250	0.218	0.034	0.018	2.15	5.5	2.75	10.70	568.0

	TN	TAM	NNN	NO_3-N	DIN	DIN (cal.)	TP	DRP	TSS	Turbidity	Clarity	DO	*E. coli*
Q80	0.454	0.014	0.232	0.230	0.266	0.240	0.037	0.019	2.52	6.5	2.80	10.90	705.8
Q95	0.848	0.024	0.291	0.290	0.352	0.318	0.090	0.024	8.76	65.3	3.00	11.73	7346.7
Opouteke at Suspension Bridge													
Count	59	59	59	59	9	59	59	59	15	59	58	58	60
Mean	0.311	0.007	0.140	0.139	0.122	0.147	0.025	0.009	1.79	8.6	1.58	10.23	500.5
Minimum	0.100	0.005	0.002	0.002	0.005	0.007	0.004	0.004	0.50	0.0	0.10	6.30	10.0
Maximum	2.100	0.039	0.960	0.950	0.330	0.969	0.340	0.024	4.00	160.0	3.00	12.30	14136.0
Q5	0.100	0.005	0.002	0.002	0.005	0.007	0.009	0.005	0.50	0.7	0.32	8.17	29.0
Q10	0.100	0.005	0.002	0.002	0.005	0.008	0.010	0.006	0.65	0.9	0.49	8.87	45.0
Q20	0.100	0.005	0.003	0.003	0.005	0.009	0.011	0.007	0.98	1.1	0.88	9.60	55.4
Q25	0.125	0.005	0.005	0.005	0.005	0.012	0.012	0.008	1.00	1.3	0.91	9.70	60.0
Q50 Median	0.180	0.005	0.070	0.070	0.052	0.075	0.014	0.009	1.30	2.7	1.42	10.35	134.0
Q75	0.355	0.007	0.225	0.225	0.180	0.234	0.019	0.011	2.45	5.0	2.32	10.98	315.5
Q80	0.440	0.008	0.270	0.270	0.232	0.279	0.020	0.011	2.92	6.7	2.63	11.10	376.4
Q95	0.784	0.014	0.395	0.395	0.322	0.404	0.061	0.015	3.86	26.9	2.85	11.72	1157.7
Oruaiti at Sawyer Road													
Count	58	58	58	58	8	58	58	58	8	58	57	56	58
Mean	0.218	0.008	0.028	0.028	0.042	0.036	0.026	0.012	8.31	7.3	1.27	9.80	539.1
Minimum	0.100	0.005	0.002	0.002	0.005	0.007	0.008	0.006	0.80	0.8	0.20	4.00	41.0
Maximum	0.720	0.028	0.230	0.230	0.220	0.235	0.076	0.021	34.00	55.0	3.46	13.10	5000.0
Q5	0.100	0.005	0.002	0.002	0.005	0.007	0.013	0.008	0.87	1.1	0.29	7.30	62.4
Q10	0.100	0.005	0.002	0.002	0.005	0.008	0.014	0.009	0.94	1.3	0.30	8.20	94.4
Q20	0.110	0.005	0.003	0.003	0.005	0.008	0.017	0.011	1.16	1.9	0.41	8.80	120.0
Q25	0.120	0.005	0.003	0.003	0.006	0.010	0.018	0.011	1.30	2.0	0.50	9.08	124.0
Q50 Median	0.195	0.007	0.008	0.008	0.010	0.016	0.023	0.012	2.85	3.4	1.40	9.90	204.5
Q75	0.250	0.009	0.038	0.038	0.027	0.050	0.030	0.014	8.20	5.9	1.70	10.75	480.3
Q80	0.260	0.009	0.053	0.051	0.045	0.067	0.032	0.015	13.24	8.1	1.79	11.00	570.2

	TN	TAM	NNN	NO_3-N	DIN	DIN (cal.)	TP	DRP	TSS	Turbidity	Clarity	DO	*E. coli*
Q95	0.475	0.018	0.074	0.074	0.166	0.089	0.062	0.016	28.75	32.8	2.96	12.33	2161.4
Oruaiti at Windust Road													
Count	59	59	59	59	9	59	59	59	9	59	57	57	60
Mean	0.262	0.010	0.059	0.058	0.022	0.069	0.028	0.012	5.38	6.9	1.34	8.76	684.6
Minimum	0.100	0.005	0.002	0.002	0.005	0.008	0.007	0.005	0.80	1.3	0.20	3.80	74.0
Maximum	0.920	0.024	0.590	0.580	0.073	0.599	0.087	0.026	36.00	60.0	3.40	12.60	8164.0
Q5	0.100	0.005	0.002	0.002	0.005	0.010	0.010	0.008	0.88	1.5	0.30	5.26	133.4
Q10	0.100	0.005	0.004	0.004	0.005	0.010	0.013	0.009	0.96	1.6	0.30	6.50	159.5
Q20	0.126	0.005	0.006	0.006	0.005	0.015	0.017	0.010	1.00	2.0	0.50	7.70	184.6
Q25	0.150	0.005	0.008	0.008	0.005	0.016	0.019	0.010	1.00	2.3	0.70	7.90	225.0
Q50 Median	0.220	0.008	0.033	0.033	0.015	0.038	0.024	0.012	1.80	3.8	1.40	9.00	275.0
Q75	0.305	0.012	0.071	0.071	0.033	0.088	0.034	0.014	2.30	6.5	1.80	9.80	467.0
Q80	0.344	0.013	0.081	0.080	0.036	0.095	0.035	0.014	2.30	8.2	1.90	10.20	509.0
Q95	0.660	0.024	0.145	0.145	0.060	0.155	0.065	0.016	22.52	17.7	2.57	11.22	2530.0
Oruru at Oruru Road													
Count	111	111	111	111	11	111	111	111	16	111	110	108	111
Mean	0.237	0.013	0.043	0.042	0.028	0.057	0.053	0.029	2.36	11.7	1.21	8.17	1080.9
Minimum	0.100	0.005	0.002	0.002	0.005	0.007	0.021	0.006	1.00	0.1	0.10	4.50	40.0
Maximum	2.100	0.056	0.210	0.210	0.082	0.262	0.420	0.056	6.20	310.0	3.17	12.40	17329.0
Q5	0.100	0.005	0.002	0.002	0.005	0.007	0.034	0.021	1.00	1.2	0.30	6.07	98.0
Q10	0.100	0.005	0.002	0.002	0.005	0.007	0.037	0.022	1.00	1.5	0.30	6.40	140.0
Q20	0.100	0.005	0.003	0.003	0.005	0.009	0.039	0.024	1.00	2.0	0.58	6.84	170.0
Q25	0.100	0.005	0.004	0.004	0.005	0.011	0.040	0.025	1.00	2.2	0.73	7.20	192.0
Q50 Median	0.150	0.008	0.022	0.022	0.010	0.032	0.044	0.027	1.65	3.6	1.28	8.10	305.0
Q75	0.250	0.017	0.072	0.072	0.048	0.087	0.051	0.033	3.28	6.3	1.70	9.30	507.5
Q80	0.280	0.020	0.088	0.084	0.050	0.110	0.052	0.034	4.10	7.6	1.80	9.40	610.0
Q95	0.725	0.039	0.140	0.130	0.075	0.162	0.107	0.039	4.85	50.0	2.07	10.37	2778.5

	TN	TAM	NNN	NO_3-N	DIN	DIN (cal.)	TP	DRP	TSS	Turbidity	Clarity	DO	*E. coli*
Otaika at Cemetery Road													
Count	60	60	60	60	8	60	60	60	8	60	56	60	60
Mean	1.524	0.020	1.308	1.304	1.253	1.328	0.040	0.019	7.50	6.7	0.92	9.03	1164.3
Minimum	0.330	0.005	0.130	0.130	0.920	0.147	0.014	0.006	2.80	2.0	0.18	6.60	51.0
Maximum	2.100	0.062	2.000	2.000	1.600	2.016	0.210	0.044	16.00	28.0	1.91	11.30	5794.0
Q5	1.100	0.007	0.870	0.860	0.983	0.898	0.023	0.012	3.12	2.4	0.38	7.10	129.0
Q10	1.200	0.009	0.965	0.956	1.046	0.986	0.025	0.014	3.43	2.7	0.51	7.48	159.4
Q20	1.300	0.013	1.100	1.100	1.140	1.117	0.029	0.015	3.94	3.3	0.58	8.24	237.2
Q25	1.400	0.014	1.100	1.100	1.175	1.154	0.031	0.016	4.15	3.8	0.68	8.50	319.3
Q50 Median	1.500	0.017	1.400	1.350	1.250	1.406	0.035	0.018	5.40	5.1	0.93	9.10	795.0
Q75	1.725	0.024	1.500	1.500	1.325	1.519	0.042	0.022	10.30	7.7	1.13	9.60	1659.5
Q80	1.800	0.027	1.600	1.600	1.360	1.620	0.043	0.023	11.56	9.1	1.16	9.74	1921.4
Q95	1.905	0.037	1.800	1.800	1.530	1.820	0.063	0.028	14.95	19.4	1.57	10.91	3873.0
Otaika at Otaika Valley Road													
Count	109	109	109	109	8	109	109	109	14	109	107	110	109
Mean	1.414	0.020	1.091	1.085	0.968	1.112	0.051	0.022	2.16	10.2	1.26	9.72	1596.5
Minimum	0.790	0.005	0.210	0.210	0.610	0.282	0.016	0.013	0.80	1.0	0.10	6.90	64.0
Maximum	4.000	0.150	1.800	1.800	1.400	1.809	0.600	0.051	5.20	190.0	3.00	12.20	24196.0
Q5	1.000	0.005	0.592	0.588	0.663	0.631	0.024	0.015	0.93	2.0	0.18	8.25	187.0
Q10	1.100	0.007	0.698	0.696	0.715	0.720	0.026	0.016	1.00	2.4	0.50	8.60	211.0
Q20	1.200	0.009	0.796	0.796	0.776	0.845	0.031	0.018	1.00	2.7	0.68	9.00	293.0
Q25	1.200	0.010	0.860	0.860	0.790	0.875	0.031	0.019	1.20	2.9	0.75	9.20	313.0
Q50 Median	1.400	0.014	1.100	1.100	0.935	1.113	0.037	0.021	2.00	4.1	1.23	9.80	550.0
Q75	1.600	0.024	1.300	1.300	1.075	1.320	0.049	0.024	2.58	6.6	1.70	10.40	1000.0
Q80	1.600	0.026	1.400	1.400	1.180	1.409	0.055	0.025	2.76	7.9	1.84	10.40	1200.0
Q95	1.860	0.059	1.600	1.600	1.365	1.607	0.112	0.033	4.03	45.2	2.37	11.00	4507.4
Otakaranga at Otaika Valley Road													

	TN	TAM	NNN	NO_3-N	DIN	DIN (cal.)	TP	DRP	TSS	Turbidity	Clarity	DO	*E. coli*
Count	58	58	58	58	8	58	58	58	8	58	51	58	58
Mean	0.478	0.024	0.127	0.126	0.097	0.151	0.034	0.011	3.70	6.6	1.02	7.36	919.7
Minimum	0.150	0.005	0.002	0.002	0.014	0.008	0.010	0.006	2.50	1.5	0.12	2.90	73.0
Maximum	1.700	0.120	1.500	1.500	0.280	1.509	0.170	0.030	5.30	60.0	2.17	11.60	9800.0
Q5	0.210	0.006	0.002	0.002	0.024	0.010	0.014	0.006	2.50	2.8	0.30	4.64	121.7
Q10	0.250	0.007	0.003	0.003	0.034	0.012	0.017	0.007	2.50	3.1	0.50	5.21	149.4
Q20	0.320	0.010	0.008	0.008	0.043	0.023	0.019	0.008	2.70	3.7	0.64	5.54	231.8
Q25	0.343	0.012	0.011	0.010	0.044	0.025	0.020	0.008	2.88	3.8	0.70	5.90	247.8
Q50 Median	0.425	0.017	0.045	0.044	0.085	0.074	0.030	0.010	3.45	5.0	1.00	7.20	450.0
Q75	0.538	0.027	0.158	0.150	0.108	0.193	0.039	0.013	4.45	6.8	1.24	9.05	1101.5
Q80	0.570	0.031	0.186	0.182	0.118	0.226	0.042	0.014	4.80	7.3	1.32	9.30	1460.0
Q95	0.905	0.066	0.358	0.350	0.228	0.417	0.073	0.018	5.27	13.4	1.84	10.03	2453.3
Paranui at Paranui Road													
Count	60	60	60	60	10	60	60	60	9	60	60	58	60
Mean	0.330	0.011	0.043	0.042	0.033	0.054	0.028	0.008	2.18	6.2	1.39	6.24	286.0
Minimum	0.100	0.005	0.002	0.002	0.007	0.012	0.009	0.004	1.10	1.5	0.30	3.30	41.0
Maximum	1.200	0.031	0.300	0.300	0.120	0.310	0.170	0.018	3.40	95.0	2.75	9.40	2200.0
Q5	0.160	0.005	0.007	0.007	0.008	0.014	0.012	0.005	1.14	1.9	0.40	3.79	83.9
Q10	0.170	0.005	0.009	0.009	0.009	0.015	0.013	0.006	1.18	2.1	0.86	4.10	86.0
Q20	0.208	0.005	0.011	0.010	0.010	0.021	0.016	0.007	1.44	2.5	1.08	4.62	110.0
Q25	0.228	0.006	0.011	0.011	0.011	0.024	0.017	0.007	1.60	2.6	1.10	4.83	120.0
Q50 Median	0.270	0.010	0.028	0.028	0.024	0.036	0.021	0.008	2.00	3.5	1.40	6.15	191.0
Q75	0.385	0.013	0.044	0.044	0.040	0.055	0.028	0.009	2.80	5.6	1.70	7.60	350.0
Q80	0.414	0.013	0.049	0.049	0.045	0.062	0.032	0.010	2.92	6.4	1.72	8.04	392.8
Q95	0.546	0.020	0.151	0.151	0.090	0.158	0.053	0.012	3.28	14.1	2.49	8.92	700.7
Parapara at Parapara Toatoa Road													
Count	60	60	60	60	10	60	60	60	10	60	60	58	60

	TN	TAM	NNN	NO_3-N	DIN	DIN (cal.)	TP	DRP	TSS	Turbidity	Clarity	DO	*E. coli*
Mean	0.232	0.012	0.022	0.021	0.026	0.034	0.024	0.011	3.16	5.4	1.30	8.42	532.6
Minimum	0.100	0.005	0.002	0.002	0.005	0.007	0.010	0.005	1.20	1.6	0.20	4.90	63.0
Maximum	0.750	0.058	0.068	0.065	0.076	0.082	0.037	0.030	6.60	19.0	2.50	13.40	6900.0
Q5	0.120	0.005	0.002	0.002	0.005	0.009	0.015	0.008	1.65	1.7	0.40	5.29	132.8
Q10	0.129	0.005	0.002	0.002	0.005	0.010	0.016	0.008	2.10	2.0	0.50	6.57	159.6
Q20	0.148	0.005	0.004	0.004	0.006	0.014	0.017	0.009	2.36	2.9	0.94	6.94	190.0
Q25	0.160	0.006	0.005	0.004	0.008	0.016	0.019	0.009	2.45	3.1	1.05	7.15	207.8
Q50 Median	0.215	0.013	0.022	0.022	0.021	0.035	0.023	0.011	2.80	4.0	1.40	8.55	301.5
Q75	0.273	0.015	0.032	0.032	0.034	0.048	0.028	0.012	3.50	5.3	1.63	9.40	421.5
Q80	0.304	0.015	0.037	0.036	0.039	0.053	0.028	0.012	3.72	6.1	1.80	9.66	467.2
Q95	0.382	0.022	0.049	0.049	0.064	0.070	0.033	0.014	5.52	15.0	2.10	10.42	1148.9
Parapara at Taumata Road													
Count	60	60	60	60	10	60	60	60	10	60	60	57	60
Mean	0.348	0.024	0.035	0.037	0.062	0.058	0.038	0.017	7.22	10.1	0.83	6.61	949.3
Minimum	0.140	0.005	0.002	0.002	0.021	0.015	0.020	0.009	3.20	2.3	0.20	0.60	86.0
Maximum	0.690	0.081	0.089	0.280	0.170	0.169	0.180	0.120	14.00	60.0	1.90	12.90	28000.0
Q5	0.198	0.009	0.004	0.004	0.029	0.024	0.023	0.010	3.47	3.1	0.20	0.70	158.1
Q10	0.229	0.012	0.011	0.011	0.036	0.030	0.027	0.010	3.74	4.1	0.30	1.66	182.0
Q20	0.240	0.013	0.016	0.016	0.044	0.038	0.029	0.012	4.76	5.6	0.40	2.58	214.8
Q25	0.258	0.015	0.019	0.017	0.046	0.041	0.030	0.012	5.35	6.2	0.50	4.20	242.5
Q50 Median	0.345	0.021	0.029	0.028	0.052	0.052	0.035	0.014	7.40	7.5	0.81	7.90	343.0
Q75	0.415	0.029	0.046	0.044	0.061	0.075	0.040	0.016	8.05	10.0	1.10	8.90	500.0
Q80	0.442	0.031	0.054	0.052	0.064	0.080	0.043	0.017	8.40	12.2	1.10	9.00	594.8
Q95	0.530	0.051	0.076	0.081	0.125	0.100	0.053	0.023	11.84	24.1	1.41	10.12	1107.3
Pekepeka at Ohaeawai													
Count	60	60	60	60	10	60	60	60	10	60	60	59	60
Mean	0.386	0.009	0.272	0.270	0.188	0.280	0.020	0.010	1.24	2.4	2.03	9.31	291.3

	TN	TAM	NNN	NO_3-N	DIN	DIN (cal.)	TP	DRP	TSS	Turbidity	Clarity	DO	*E. coli*
Minimum	0.100	0.005	0.003	0.003	0.049	0.011	0.008	0.005	0.38	0.1	0.20	3.70	31.0
Maximum	0.780	0.073	0.510	0.510	0.410	0.522	0.100	0.014	2.90	22.0	7.52	11.90	1725.0
Q5	0.148	0.005	0.057	0.057	0.057	0.066	0.009	0.006	0.52	0.7	1.00	7.54	57.7
Q10	0.199	0.005	0.064	0.064	0.064	0.079	0.010	0.007	0.67	1.0	1.10	7.98	81.9
Q20	0.230	0.005	0.138	0.138	0.074	0.144	0.012	0.008	0.78	1.3	1.26	8.80	117.6
Q25	0.240	0.005	0.158	0.155	0.092	0.164	0.013	0.008	0.85	1.4	1.40	8.90	131.0
Q50 Median	0.395	0.006	0.280	0.280	0.180	0.285	0.015	0.010	1.00	1.9	1.82	9.40	212.0
Q75	0.503	0.008	0.393	0.390	0.230	0.401	0.019	0.011	1.50	3.0	2.10	10.15	301.3
Q80	0.526	0.010	0.410	0.402	0.248	0.415	0.020	0.011	1.64	3.1	2.52	10.40	340.0
Q95	0.624	0.016	0.491	0.490	0.370	0.497	0.064	0.013	2.41	4.1	3.13	10.80	628.6
Peria at Honeymoon Valley Road													
Count	58	58	58	58	9	58	58	58	9	58	57	56	60
Mean	0.128	0.006	0.025	0.025	0.022	0.031	0.057	0.050	1.43	2.3	2.08	9.71	235.3
Minimum	0.100	0.005	0.002	0.002	0.010	0.007	0.038	0.025	0.71	0.5	1.00	6.60	10.0
Maximum	0.640	0.019	0.087	0.087	0.045	0.092	0.100	0.062	3.20	14.4	3.72	13.50	3076.0
Q5	0.100	0.005	0.002	0.002	0.010	0.007	0.044	0.038	0.75	0.7	1.26	7.98	40.2
Q10	0.100	0.005	0.002	0.002	0.011	0.010	0.045	0.039	0.78	0.8	1.50	8.30	52.0
Q20	0.100	0.005	0.010	0.010	0.013	0.015	0.048	0.044	0.92	1.0	1.80	8.70	74.8
Q25	0.100	0.005	0.012	0.012	0.014	0.018	0.052	0.045	1.00	1.1	1.80	8.90	75.0
Q50 Median	0.100	0.005	0.024	0.024	0.020	0.029	0.056	0.051	1.40	1.7	2.10	9.65	132.0
Q75	0.100	0.005	0.038	0.038	0.026	0.044	0.063	0.057	1.60	2.2	2.30	10.63	248.5
Q80	0.106	0.006	0.041	0.041	0.030	0.047	0.065	0.057	1.68	2.5	2.38	10.80	323.4
Q95	0.283	0.009	0.051	0.049	0.041	0.056	0.071	0.061	2.64	6.6	3.04	11.53	500.7
Pukenui at Kanehiana Drive													
Count	46	46	46	46	10	46	46	46	10	46	46	46	46
Mean	0.254	0.010	0.115	0.114	0.133	0.125	0.031	0.017	6.31	7.2	1.88	10.33	1141.7
Minimum	0.100	0.005	0.054	0.054	0.069	0.059	0.016	0.008	0.80	2.4	0.18	8.60	31.0

	TN	TAM	NNN	NO_3-N	DIN	DIN (cal.)	TP	DRP	TSS	Turbidity	Clarity	DO	*E. coli*
Maximum	0.910	0.042	0.280	0.280	0.210	0.322	0.093	0.027	30.00	34.0	3.00	12.50	9804.0
Q5	0.100	0.005	0.066	0.066	0.080	0.073	0.017	0.010	0.94	2.6	0.33	9.33	65.8
Q10	0.100	0.005	0.070	0.070	0.091	0.080	0.019	0.012	1.07	2.6	0.94	9.55	85.5
Q20	0.100	0.005	0.077	0.076	0.099	0.087	0.021	0.014	1.34	2.7	1.37	9.70	173.0
Q25	0.100	0.005	0.078	0.078	0.100	0.090	0.022	0.014	1.45	2.8	1.42	9.83	178.0
Q50 Median	0.205	0.008	0.100	0.100	0.115	0.108	0.025	0.017	3.50	3.4	1.82	10.30	394.5
Q75	0.290	0.011	0.120	0.120	0.178	0.127	0.034	0.018	6.25	5.1	2.45	10.90	690.0
Q80	0.320	0.012	0.120	0.120	0.192	0.135	0.036	0.019	7.40	5.8	2.80	10.90	820.0
Q95	0.743	0.017	0.255	0.255	0.206	0.261	0.057	0.024	20.91	32.8	3.00	11.50	6394.8
Punakitere at Taheke													
Count	58	58	58	58	10	58	58	58	14	58	55	58	60
Mean	0.729	0.020	0.350	0.346	0.421	0.370	0.070	0.028	4.17	16.6	1.17	9.66	1774.6
Minimum	0.170	0.005	0.002	0.002	0.006	0.011	0.016	0.008	1.00	0.9	0.10	5.50	41.0
Maximum	2.100	0.180	0.770	0.760	0.770	0.778	0.620	0.170	16.00	340.0	2.80	11.40	24196.0
Q5	0.271	0.005	0.005	0.003	0.138	0.012	0.019	0.009	1.00	1.1	0.21	7.87	107.5
Q10	0.324	0.006	0.053	0.053	0.271	0.061	0.021	0.011	1.00	1.5	0.31	8.27	120.8
Q20	0.484	0.007	0.202	0.202	0.316	0.215	0.031	0.015	1.06	2.0	0.64	8.84	177.8
Q25	0.548	0.008	0.253	0.250	0.323	0.266	0.033	0.017	1.15	2.2	0.70	9.03	188.5
Q50 Median	0.710	0.012	0.380	0.375	0.390	0.398	0.049	0.023	1.95	5.1	0.91	9.80	313.0
Q75	0.853	0.025	0.488	0.488	0.543	0.513	0.066	0.031	4.60	9.9	1.60	10.48	930.0
Q80	0.908	0.028	0.510	0.500	0.566	0.518	0.071	0.033	6.32	11.0	1.72	10.50	1098.4
Q95	1.190	0.051	0.585	0.583	0.707	0.616	0.174	0.057	13.40	48.8	2.63	11.00	6554.8
Punaruku at Russell Road													
Count	42	42	42	42	10	42	42	42	10	42	42	42	42
Mean	0.175	0.006	0.025	0.025	0.030	0.031	0.016	0.010	1.59	3.1	2.80	9.67	512.8
Minimum	0.100	0.005	0.002	0.002	0.015	0.007	0.008	0.007	0.40	0.2	0.14	7.80	15.0
Maximum	1.500	0.026	0.200	0.200	0.055	0.205	0.078	0.015	3.00	33.0	5.00	11.40	12997.0

	TN	TAM	NNN	NO_3-N	DIN	DIN (cal.)	TP	DRP	TSS	Turbidity	Clarity	DO	*E. coli*
Q5	0.100	0.005	0.002	0.002	0.015	0.007	0.009	0.007	0.40	0.5	0.64	8.12	26.2
Q10	0.100	0.005	0.006	0.006	0.016	0.011	0.010	0.008	0.40	0.5	1.09	8.51	32.0
Q20	0.100	0.005	0.008	0.008	0.017	0.014	0.011	0.009	0.48	0.6	2.77	8.82	52.0
Q25	0.100	0.005	0.010	0.010	0.018	0.018	0.011	0.009	0.63	0.7	2.85	8.90	57.0
Q50 Median	0.100	0.005	0.017	0.017	0.027	0.024	0.012	0.010	1.70	1.1	3.00	9.85	121.0
Q75	0.170	0.005	0.028	0.028	0.039	0.034	0.015	0.012	2.20	2.0	3.00	10.25	229.0
Q80	0.190	0.005	0.032	0.032	0.042	0.041	0.016	0.012	2.32	2.5	3.00	10.48	261.4
Q95	0.289	0.010	0.058	0.058	0.050	0.066	0.034	0.013	2.91	16.9	4.65	10.90	1057.6
Puwera at SH1													
Count	43	43	43	43	8	43	43	43	8	43	36	43	43
Mean	1.155	0.184	0.295	0.282	0.522	0.479	0.079	0.019	6.34	9.2	0.96	7.00	1295.7
Minimum	0.420	0.005	0.002	0.002	0.008	0.007	0.027	0.006	2.50	1.3	0.10	0.40	100.0
Maximum	9.700	5.000	1.600	1.500	2.200	6.400	0.410	0.046	18.00	75.0	2.20	11.20	16000.0
Q5	0.542	0.008	0.002	0.002	0.023	0.010	0.027	0.009	2.54	2.8	0.39	0.71	142.1
Q10	0.572	0.011	0.002	0.002	0.037	0.025	0.034	0.010	2.57	3.1	0.47	2.02	213.6
Q20	0.610	0.017	0.030	0.029	0.106	0.056	0.039	0.011	3.36	3.6	0.63	3.50	334.4
Q25	0.640	0.019	0.046	0.038	0.155	0.085	0.041	0.012	4.03	3.8	0.67	4.65	383.5
Q50 Median	0.860	0.035	0.250	0.250	0.295	0.289	0.056	0.017	5.40	6.0	0.89	8.20	594.0
Q75	1.100	0.065	0.390	0.380	0.530	0.490	0.076	0.022	6.08	8.6	1.30	9.30	815.0
Q80	1.200	0.083	0.406	0.390	0.586	0.501	0.087	0.026	6.18	10.8	1.31	9.68	950.0
Q95	1.980	0.457	0.716	0.688	1.658	0.845	0.217	0.036	13.91	20.9	1.55	10.57	2253.8
Raumanga at Bernard Street													
Count	54	54	54	54	0	54	54	54	0	54	49	51	55
Mean	1.261	0.016	1.059	1.052		1.076	0.029	0.017		3.7	1.56	10.50	1006.7
Minimum	0.730	0.005	0.560	0.560		0.577	0.011	0.009		0.8	0.64	8.60	180.0
Maximum	1.800	0.053	1.600	1.600		1.609	0.110	0.063		32.0	2.73	13.00	4611.0
Q5	0.987	0.008	0.707	0.707		0.735	0.016	0.010		1.2	0.73	9.05	227.9

	TN	TAM	NNN	NO_3-N	DIN	DIN (cal.)	TP	DRP	TSS	Turbidity	Clarity	DO	*E. coli*
Q10	1.100	0.009	0.810	0.803		0.823	0.018	0.012		1.4	0.87	9.30	297.0
Q20	1.100	0.011	0.880	0.876		0.904	0.021	0.013		1.6	1.12	9.60	387.0
Q25	1.125	0.011	0.903	0.900		0.917	0.022	0.013		1.6	1.21	10.00	438.5
Q50 Median	1.300	0.015	1.100	1.100		1.117	0.027	0.016		2.5	1.55	10.50	670.0
Q75	1.300	0.019	1.200	1.200		1.214	0.031	0.018		3.6	1.90	11.00	1075.0
Q80	1.400	0.019	1.200	1.200		1.217	0.031	0.019		4.2	1.94	11.10	1225.2
Q95	1.570	0.030	1.335	1.300		1.352	0.044	0.022		9.5	2.57	11.95	3873.0
Ruakaka at Flyger Road													
Count	59	59	59	59	9	59	59	59	15	59	60	60	60
Mean	1.001	0.063	0.441	0.430	0.606	0.505	0.169	0.098	4.58	18.5	0.87	8.28	4063.8
Minimum	0.360	0.006	0.035	0.035	0.320	0.050	0.054	0.035	2.50	3.1	0.10	4.90	98.0
Maximum	3.700	0.410	1.500	1.400	0.900	1.880	0.670	0.290	15.00	310.0	1.68	10.50	98040.0
Q5	0.439	0.016	0.085	0.081	0.352	0.110	0.083	0.051	2.85	4.6	0.20	5.78	165.5
Q10	0.476	0.020	0.136	0.134	0.384	0.168	0.087	0.053	3.00	5.2	0.45	6.56	216.0
Q20	0.600	0.024	0.242	0.236	0.400	0.268	0.110	0.065	3.00	5.9	0.63	7.18	271.0
Q25	0.610	0.025	0.270	0.265	0.400	0.296	0.115	0.068	3.25	6.3	0.73	7.38	293.0
Q50 Median	0.860	0.035	0.390	0.390	0.640	0.444	0.140	0.089	3.80	7.9	0.93	8.30	441.0
Q75	1.150	0.049	0.575	0.565	0.720	0.650	0.175	0.120	4.65	9.7	1.03	9.43	696.5
Q80	1.240	0.056	0.624	0.610	0.744	0.686	0.180	0.130	4.84	10.4	1.10	9.62	797.4
Q95	2.000	0.331	0.844	0.834	0.852	0.937	0.355	0.161	8.14	60.5	1.40	10.11	9767.2
Stony Creek at Sawyer Road													
Count	59	59	59	59	9	59	59	59	9	59	57	57	60
Mean	0.271	0.013	0.066	0.066	0.040	0.079	0.028	0.014	2.01	5.2	1.58	9.73	503.1
Minimum	0.100	0.005	0.002	0.002	0.005	0.008	0.009	0.005	1.00	1.0	0.20	2.60	10.0
Maximum	1.000	0.080	0.480	0.480	0.110	0.488	0.130	0.052	2.90	36.0	3.00	14.40	12033.0
Q5	0.100	0.005	0.003	0.003	0.006	0.010	0.012	0.008	1.08	1.3	0.40	7.68	34.3
Q10	0.100	0.005	0.005	0.005	0.007	0.012	0.013	0.009	1.16	1.6	0.62	8.48	41.0

	TN	TAM	NNN	NO_3-N	DIN	DIN (cal.)	TP	DRP	TSS	Turbidity	Clarity	DO	*E. coli*
Q20	0.126	0.005	0.011	0.011	0.007	0.018	0.017	0.011	1.44	2.2	1.02	9.12	84.0
Q25	0.145	0.006	0.013	0.013	0.008	0.026	0.018	0.011	1.60	2.6	1.20	9.20	94.3
Q50 Median	0.230	0.010	0.044	0.042	0.020	0.058	0.021	0.013	2.00	3.6	1.60	9.70	150.0
Q75	0.355	0.013	0.100	0.100	0.080	0.118	0.032	0.015	2.40	5.7	1.90	10.40	282.0
Q80	0.400	0.014	0.120	0.120	0.083	0.135	0.034	0.016	2.56	6.6	2.02	10.78	336.6
Q95	0.511	0.027	0.160	0.160	0.101	0.175	0.068	0.022	2.86	13.1	2.80	11.92	1520.9
Tapapa at SH1													
Count	42	42	42	42	10	42	42	42	10	42	42	42	42
Mean	0.141	0.006	0.032	0.031	0.037	0.038	0.049	0.039	1.17	3.1	1.93	9.75	219.9
Minimum	0.100	0.005	0.002	0.002	0.014	0.007	0.027	0.022	0.57	0.4	0.10	5.10	16.0
Maximum	0.720	0.018	0.160	0.160	0.060	0.178	0.110	0.068	2.20	45.0	3.79	11.80	3448.0
Q5	0.100	0.005	0.002	0.002	0.020	0.007	0.033	0.027	0.57	0.4	0.90	5.40	20.1
Q10	0.100	0.005	0.003	0.003	0.027	0.008	0.034	0.030	0.57	0.4	1.00	7.88	30.0
Q20	0.100	0.005	0.009	0.009	0.030	0.014	0.037	0.032	0.71	0.6	1.40	8.84	42.6
Q25	0.100	0.005	0.011	0.011	0.032	0.018	0.038	0.033	0.76	0.6	1.53	9.50	52.0
Q50 Median	0.100	0.005	0.026	0.026	0.038	0.031	0.047	0.036	1.10	0.9	1.90	10.35	103.5
Q75	0.148	0.005	0.039	0.039	0.039	0.044	0.053	0.043	1.55	2.7	2.29	10.70	175.0
Q80	0.166	0.006	0.042	0.040	0.041	0.047	0.058	0.045	1.60	2.7	2.60	10.78	198.0
Q95	0.240	0.010	0.067	0.066	0.056	0.072	0.073	0.060	1.93	6.5	3.10	11.40	581.4
Utakura at Horeke Rd													
Count	67	72	72	67	0	72	72	72	59	72	69	72	72
Mean	0.461	0.017	0.106	0.108		0.123	0.046	0.012	15.47	13.0	1.04	8.46	790.3
Minimum	0.210	0.005	0.002	0.002		0.007	0.018	0.006	0.00	1.8	0.10	4.60	20.0
Maximum	1.320	0.059	0.350	0.340		0.391	0.232	0.054	260.00	160.0	2.70	11.60	19863.0
Q5	0.250	0.006	0.002	0.002		0.012	0.022	0.006	1.00	1.9	0.29	6.31	63.0
Q10	0.270	0.008	0.010	0.010		0.020	0.024	0.007	1.80	2.4	0.45	6.91	75.0
Q20	0.310	0.010	0.026	0.033		0.036	0.027	0.007	2.00	3.5	0.55	7.30	109.2

	TN	TAM	NNN	NO_3-N	DIN	DIN (cal.)	TP	DRP	TSS	Turbidity	Clarity	DO	*E. coli*
Q25	0.310	0.010	0.035	0.038		0.050	0.028	0.007	3.00	4.4	0.62	7.30	120.3
Q50 Median	0.380	0.014	0.098	0.110		0.115	0.039	0.010	5.00	6.6	0.94	8.35	206.0
Q75	0.550	0.018	0.155	0.160		0.185	0.050	0.013	16.00	12.5	1.33	9.80	355.0
Q80	0.592	0.021	0.180	0.180		0.205	0.058	0.015	17.40	14.3	1.46	9.90	414.0
Q95	1.025	0.040	0.250	0.242		0.274	0.085	0.025	37.70	29.0	2.24	10.50	1509.9
Utakura at Okaka Bridge													
Count	48	48	48	48	10	48	48	48	10	47	40	47	47
Mean	0.550	0.027	0.151	0.150	0.145	0.178	0.052	0.015	17.89	11.5	1.14	7.92	1134.1
Minimum	0.190	0.005	0.002	0.002	0.005	0.007	0.019	0.006	1.20	1.1	0.30	2.90	97.0
Maximum	1.800	0.430	0.690	0.690	0.340	1.120	0.180	0.042	140.00	110.0	2.18	10.50	17000.0
Q5	0.228	0.005	0.002	0.002	0.006	0.009	0.026	0.007	1.29	2.2	0.40	4.10	110.0
Q10	0.307	0.005	0.006	0.004	0.007	0.012	0.030	0.009	1.38	2.6	0.48	4.86	126.8
Q20	0.344	0.008	0.019	0.018	0.010	0.030	0.032	0.009	2.20	3.1	0.69	5.70	158.4
Q25	0.365	0.009	0.031	0.030	0.019	0.042	0.033	0.010	2.43	3.6	0.72	6.20	186.0
Q50 Median	0.495	0.015	0.155	0.155	0.152	0.167	0.043	0.013	3.35	6.9	1.10	8.60	250.0
Q75	0.655	0.021	0.223	0.223	0.245	0.238	0.053	0.017	7.68	9.4	1.58	9.70	553.0
Q80	0.682	0.023	0.240	0.240	0.252	0.255	0.055	0.018	8.28	10.8	1.75	9.80	702.8
Q95	1.065	0.041	0.313	0.313	0.304	0.339	0.110	0.031	81.41	35.9	2.01	10.27	4953.3
Victoria at Victoria Valley Road													
Count	60	60	60	60	10	60	60	60	15	59	60	59	60
Mean	0.147	0.007	0.018	0.017	0.013	0.025	0.031	0.021	1.29	4.3	1.80	9.41	302.2
Minimum	0.100	0.005	0.002	0.002	0.005	0.007	0.013	0.012	0.71	0.2	0.10	4.30	13.0
Maximum	0.530	0.022	0.200	0.160	0.028	0.205	0.140	0.029	3.20	65.0	4.93	11.30	3200.0
Q5	0.100	0.005	0.002	0.002	0.005	0.007	0.016	0.014	0.71	0.4	0.30	7.77	68.7
Q10	0.100	0.005	0.002	0.002	0.005	0.007	0.018	0.015	0.73	0.4	0.78	8.08	74.9
Q20	0.100	0.005	0.002	0.002	0.005	0.008	0.021	0.017	0.79	0.6	1.16	8.30	91.4
Q25	0.100	0.005	0.002	0.002	0.005	0.008	0.023	0.017	0.80	0.7	1.30	8.50	96.8

	TN	TAM	NNN	NO_3-N	DIN	DIN (cal.)	TP	DRP	TSS	Turbidity	Clarity	DO	*E. coli*
Q50 Median	0.100	0.005	0.004	0.004	0.010	0.011	0.027	0.020	1.00	1.0	1.80	9.50	158.0
Q75	0.170	0.006	0.015	0.015	0.019	0.022	0.031	0.024	1.50	3.2	2.03	10.35	246.0
Q80	0.192	0.007	0.020	0.020	0.021	0.027	0.033	0.025	1.84	3.8	2.40	10.64	256.6
Q95	0.312	0.015	0.078	0.073	0.027	0.098	0.063	0.028	2.71	17.2	3.11	11.01	880.0
Waiarohia at Second Avenue													
Count	111	111	111	111	9	111	111	111	15	111	104	111	111
Mean	0.491	0.019	0.330	0.328	0.345	0.349	0.034	0.014	2.87	5.7	2.05	10.07	2525.8
Minimum	0.100	0.005	0.002	0.002	0.016	0.010	0.011	0.006	0.80	0.6	0.10	6.90	19.0
Maximum	1.800	0.440	1.100	1.000	0.700	1.108	0.430	0.059	13.00	80.0	3.57	13.80	130000.0
Q5	0.105	0.005	0.015	0.015	0.026	0.027	0.014	0.007	0.94	0.8	0.30	7.80	97.5
Q10	0.130	0.005	0.032	0.031	0.036	0.039	0.016	0.009	1.00	0.9	0.68	8.10	146.0
Q20	0.250	0.006	0.110	0.110	0.044	0.138	0.017	0.010	1.00	1.2	1.16	9.00	187.0
Q25	0.290	0.007	0.160	0.160	0.046	0.187	0.018	0.011	1.00	1.3	1.30	9.30	224.5
Q50 Median	0.500	0.011	0.350	0.350	0.350	0.369	0.022	0.014	2.00	1.8	2.07	10.00	417.0
Q75	0.605	0.016	0.475	0.470	0.550	0.495	0.029	0.016	3.40	3.2	3.00	10.80	702.0
Q80	0.630	0.018	0.510	0.510	0.574	0.532	0.031	0.017	3.52	4.5	3.00	10.90	988.0
Q95	0.950	0.041	0.615	0.615	0.664	0.634	0.101	0.020	6.70	28.0	3.39	12.45	9232.0
Waiarohia at Whau Valley													
Count	60	60	60	60	8	60	60	60	8	60	55	60	60
Mean	0.591	0.011	0.426	0.425	0.306	0.437	0.031	0.016	6.50	3.3	1.89	9.50	726.4
Minimum	0.100	0.005	0.035	0.035	0.097	0.049	0.011	0.009	0.80	0.9	0.35	7.70	52.0
Maximum	1.000	0.078	0.790	0.790	0.450	0.799	0.130	0.031	36.00	17.2	4.10	13.00	9804.0
Q5	0.238	0.005	0.138	0.138	0.116	0.145	0.017	0.010	0.80	1.0	0.76	8.10	81.1
Q10	0.307	0.005	0.196	0.196	0.134	0.201	0.018	0.010	0.80	1.2	0.90	8.29	118.8
Q20	0.428	0.005	0.280	0.280	0.194	0.291	0.020	0.013	0.96	1.4	1.24	8.60	218.6
Q25	0.470	0.005	0.308	0.308	0.233	0.313	0.022	0.013	1.10	1.5	1.35	8.78	259.0
Q50 Median	0.590	0.009	0.400	0.400	0.315	0.411	0.028	0.016	2.15	2.3	1.82	9.55	380.0

	TN	TAM	NNN	NO_3-N	DIN	DIN (cal.)	TP	DRP	TSS	Turbidity	Clarity	DO	*E. coli*
Q75	0.720	0.012	0.570	0.570	0.425	0.579	0.034	0.017	3.68	3.0	2.39	10.10	758.0
Q80	0.756	0.013	0.600	0.600	0.432	0.610	0.035	0.018	4.76	3.4	2.76	10.30	871.8
Q95	0.990	0.021	0.741	0.741	0.447	0.750	0.065	0.023	25.50	11.2	3.02	10.91	2038.2
Waiaruhe at Puketona													
Count	59	59	59	59	8	59	59	59	8	59	59	58	60
Mean	0.472	0.022	0.237	0.235	0.260	0.259	0.031	0.012	4.11	5.3	1.37	8.69	365.3
Minimum	0.100	0.005	0.002	0.002	0.023	0.008	0.010	0.003	0.80	1.0	0.20	6.40	93.0
Maximum	0.820	0.095	0.530	0.520	0.510	0.562	0.094	0.028	12.00	19.0	3.00	10.70	2282.0
Q5	0.130	0.005	0.004	0.004	0.045	0.014	0.013	0.007	0.80	1.2	0.39	6.74	108.5
Q10	0.156	0.006	0.019	0.017	0.068	0.024	0.015	0.008	0.80	1.7	0.50	7.27	133.6
Q20	0.276	0.007	0.075	0.072	0.104	0.081	0.018	0.010	0.88	2.1	0.78	7.90	174.6
Q25	0.310	0.009	0.097	0.097	0.119	0.105	0.018	0.010	0.95	2.5	0.80	8.00	182.3
Q50 Median	0.490	0.018	0.250	0.240	0.280	0.284	0.025	0.012	2.60	4.1	1.40	8.70	243.5
Q75	0.630	0.030	0.365	0.360	0.383	0.393	0.038	0.014	4.93	7.1	1.75	9.70	403.3
Q80	0.650	0.030	0.384	0.380	0.386	0.434	0.041	0.014	7.20	8.0	1.86	9.80	520.0
Q95	0.771	0.052	0.452	0.452	0.468	0.498	0.074	0.019	11.23	13.1	2.79	10.32	790.4
Waiaruhe D/S Mangamutu Confluence													
Count	54	54	54	54	12	54	54	54	12	54	53	53	54
Mean	0.859	0.130	0.427	0.423	0.721	0.557	0.023	0.010	4.13	6.1	1.49	9.20	922.3
Minimum	0.480	0.006	0.240	0.240	0.420	0.302	0.008	0.003	1.40	0.8	0.20	3.50	19.0
Maximum	3.000	0.860	0.810	0.800	1.600	1.550	0.130	0.028	9.80	70.0	3.00	11.90	24810.0
Q5	0.607	0.009	0.276	0.276	0.431	0.371	0.010	0.005	1.51	1.8	0.50	7.26	68.2
Q10	0.623	0.010	0.303	0.303	0.443	0.421	0.011	0.006	1.60	2.0	0.82	8.02	116.0
Q20	0.676	0.019	0.340	0.340	0.476	0.450	0.013	0.007	1.68	2.4	1.04	8.54	165.8
Q25	0.693	0.048	0.353	0.350	0.493	0.459	0.015	0.007	1.90	3.2	1.10	8.70	187.8
Q50 Median	0.755	0.125	0.410	0.405	0.565	0.515	0.019	0.009	2.60	4.3	1.42	9.20	287.5
Q75	0.858	0.170	0.480	0.470	0.918	0.582	0.025	0.012	5.43	6.4	1.80	10.00	492.3

	TN	TAM	NNN	NO_3-N	DIN	DIN (cal.)	TP	DRP	TSS	Turbidity	Clarity	DO	*E. coli*
Q80	0.920	0.170	0.484	0.484	0.978	0.586	0.026	0.012	6.80	6.9	1.90	10.26	584.8
Q95	1.475	0.264	0.690	0.684	1.325	0.935	0.044	0.016	9.80	11.0	2.52	10.84	1488.0
Waiharakeke at Stringers Road													
Count	53	53	53	53	0	53	53	53	15	53	50	53	57
Mean	0.638	0.039	0.130	0.128		0.169	0.061	0.018	28.53	20.8	1.10	9.39	2113.5
Minimum	0.260	0.005	0.002	0.002		0.007	0.013	0.005	1.00	0.9	0.21	5.60	13.0
Maximum	2.600	0.620	0.460	0.460		0.890	0.300	0.057	191.00	200.0	2.60	11.70	32550.0
Q5	0.316	0.009	0.003	0.003		0.013	0.018	0.007	1.00	1.6	0.30	7.06	86.0
Q10	0.352	0.009	0.006	0.006		0.018	0.018	0.007	1.40	2.2	0.42	7.92	121.0
Q20	0.404	0.011	0.026	0.026		0.043	0.026	0.009	2.00	2.9	0.52	8.30	137.6
Q25	0.420	0.012	0.052	0.052		0.069	0.032	0.011	2.00	3.3	0.61	8.60	148.0
Q50 Median	0.510	0.016	0.130	0.120		0.146	0.043	0.016	4.00	6.8	1.09	9.70	265.0
Q75	0.730	0.033	0.170	0.160		0.197	0.071	0.023	20.50	14.2	1.57	10.40	554.0
Q80	0.822	0.043	0.186	0.180		0.237	0.077	0.025	28.00	17.3	1.65	10.50	646.4
Q95	1.200	0.092	0.362	0.358		0.407	0.162	0.032	132.90	90.9	2.09	11.10	13503.8
Waimamaku at SH12													
Count	58	59	58	58	9	59	59	58	9	58	57	59	60
Mean	0.182	0.006	0.011	0.011	0.020	0.017	0.018	0.006	19.76	7.3	1.53	9.91	997.6
Minimum	0.100	0.005	0.002	0.002	0.005	0.007	0.004	0.003	0.90	0.6	0.10	6.00	74.0
Maximum	1.200	0.017	0.064	0.061	0.076	0.076	0.140	0.013	160.00	80.0	3.72	11.70	17000.0
Q5	0.100	0.005	0.002	0.002	0.005	0.007	0.005	0.003	0.90	0.8	0.24	7.35	100.0
Q10	0.100	0.005	0.002	0.002	0.005	0.007	0.006	0.004	0.90	1.0	0.46	8.48	120.0
Q20	0.100	0.005	0.002	0.002	0.005	0.007	0.008	0.004	1.32	1.3	0.79	9.06	137.6
Q25	0.100	0.005	0.002	0.002	0.005	0.007	0.008	0.005	1.60	1.4	0.83	9.45	152.5
Q50 Median	0.135	0.005	0.004	0.004	0.012	0.012	0.010	0.006	2.70	3.0	1.40	10.20	285.0
Q75	0.190	0.007	0.020	0.020	0.021	0.026	0.013	0.007	3.40	4.9	2.10	10.90	522.0
Q80	0.216	0.008	0.021	0.021	0.027	0.028	0.014	0.008	3.48	6.0	2.40	11.00	637.6

	TN	TAM	NNN	NO_3-N	DIN	DIN (cal.)	TP	DRP	TSS	Turbidity	Clarity	DO	*E. coli*
Q95	0.370	0.012	0.034	0.033	0.060	0.042	0.060	0.009	97.44	36.0	3.00	11.32	2422.9
Waiotu at SH1													
Count	60	60	60	60	10	60	60	60	14	60	59	61	60
Mean	0.674	0.033	0.311	0.308	0.296	0.343	0.067	0.025	3.88	13.3	1.26	8.96	2297.3
Minimum	0.100	0.005	0.005	0.003	0.014	0.014	0.022	0.008	1.60	2.5	0.10	6.60	86.0
Maximum	2.700	0.320	0.980	0.980	0.770	1.054	0.570	0.160	7.80	160.0	2.80	10.90	32550.0
Q5	0.200	0.008	0.007	0.007	0.031	0.018	0.025	0.014	1.86	3.3	0.38	7.20	118.9
Q10	0.210	0.009	0.020	0.020	0.047	0.034	0.030	0.015	2.12	3.7	0.62	7.50	139.4
Q20	0.258	0.010	0.056	0.054	0.077	0.071	0.035	0.016	2.64	4.2	0.87	7.90	178.6
Q25	0.310	0.012	0.091	0.090	0.091	0.105	0.037	0.016	2.98	4.4	0.96	8.00	217.5
Q50 Median	0.670	0.019	0.250	0.250	0.185	0.291	0.046	0.021	3.80	6.2	1.25	9.00	350.0
Q75	0.863	0.026	0.503	0.500	0.505	0.536	0.059	0.026	4.00	8.4	1.50	9.90	522.3
Q80	0.924	0.041	0.512	0.512	0.520	0.581	0.068	0.028	4.00	9.6	1.61	10.00	684.2
Q95	1.605	0.111	0.754	0.754	0.676	0.881	0.183	0.051	7.28	56.5	2.03	10.40	14620.2
Waipao at Draffin Road													
Count	59	59	59	59	9	59	59	59	15	59	59	60	60
Mean	2.653	0.021	2.346	2.339	1.844	2.367	0.064	0.037	1.61	7.6	1.95	10.45	3736.4
Minimum	1.700	0.005	1.200	1.200	1.400	1.225	0.026	0.018	1.00	0.9	0.10	7.80	131.0
Maximum	3.600	0.320	3.600	3.600	2.800	3.605	0.590	0.250	2.20	170.0	3.24	13.30	104620.0
Q5	1.880	0.005	1.380	1.380	1.400	1.410	0.030	0.021	1.00	1.0	0.29	8.09	158.6
Q10	2.000	0.005	1.480	1.480	1.400	1.507	0.034	0.023	1.00	1.1	0.90	9.08	238.2
Q20	2.200	0.006	1.660	1.660	1.460	1.696	0.038	0.026	1.00	1.3	1.38	9.50	300.6
Q25	2.300	0.007	1.750	1.750	1.500	1.771	0.040	0.028	1.20	1.4	1.53	9.85	331.0
Q50 Median	2.600	0.009	2.300	2.300	1.500	2.311	0.045	0.033	1.60	1.9	2.00	10.60	663.0
Q75	3.100	0.016	2.800	2.800	2.200	2.810	0.056	0.038	2.00	3.2	2.65	11.10	1242.5
Q80	3.140	0.024	2.840	2.840	2.360	2.859	0.059	0.039	2.00	3.8	2.80	11.20	1764.0
Q95	3.500	0.080	3.320	3.320	2.720	3.326	0.162	0.053	2.13	37.3	3.00	12.02	10706.8

	TN	TAM	NNN	NO_3-N	DIN	DIN (cal.)	TP	DRP	TSS	Turbidity	Clarity	DO	*E. coli*
Waipapa at Forest Ranger													
Count	57	57	57	9	0	57	57	57	0	57	57	0	60
Mean	0.120	0.004	0.023	0.030		0.027	0.013	0.005		3.6	3.07		238.3
Minimum	0.041	0.001	0.001	0.004		0.002	0.005	0.002		0.4	0.26		15.6
Maximum	0.643	0.008	0.141	0.083		0.149	0.102	0.008		41.2	6.50		2909.0
Q5	0.054	0.002	0.002	0.005		0.004	0.006	0.003		0.5	0.68		23.1
Q10	0.058	0.002	0.002	0.006		0.004	0.007	0.003		0.7	0.84		28.5
Q20	0.061	0.002	0.003	0.009		0.005	0.008	0.004		0.9	1.42		33.8
Q25	0.065	0.002	0.003	0.011		0.006	0.008	0.004		1.0	1.68		42.0
Q50 Median	0.093	0.004	0.011	0.030		0.015	0.009	0.005		2.0	3.23		81.1
Q75	0.128	0.004	0.033	0.039		0.038	0.011	0.006		3.8	4.55		193.5
Q80	0.143	0.005	0.038	0.040		0.043	0.013	0.006		4.8	4.77		212.2
Q95	0.268	0.006	0.082	0.066		0.086	0.022	0.007		9.4	5.57		1124.1
Waipapa at Landing													
Count	60	60	60	60	10	60	60	60	14	60	60	60	60
Mean	0.467	0.017	0.237	0.236	0.236	0.254	0.018	0.006	2.02	4.4	2.21	9.15	1208.5
Minimum	0.100	0.005	0.024	0.023	0.040	0.034	0.004	0.002	0.60	0.3	0.18	7.00	37.0
Maximum	1.300	0.086	0.490	0.480	0.470	0.512	0.130	0.015	5.10	45.0	3.25	11.10	28000.0
Q5	0.179	0.005	0.028	0.028	0.055	0.048	0.004	0.003	0.73	0.8	0.61	7.30	75.0
Q10	0.199	0.007	0.035	0.035	0.071	0.054	0.006	0.003	0.80	0.8	0.80	7.49	85.9
Q20	0.278	0.009	0.070	0.070	0.143	0.087	0.008	0.004	0.80	0.9	1.47	7.88	133.2
Q25	0.298	0.010	0.075	0.075	0.160	0.103	0.008	0.004	0.83	1.1	1.75	7.98	134.0
Q50 Median	0.420	0.015	0.270	0.265	0.185	0.289	0.011	0.006	1.00	1.6	2.48	9.10	189.5
Q75	0.573	0.020	0.363	0.363	0.358	0.377	0.015	0.007	2.30	3.1	2.85	10.25	353.5
Q80	0.614	0.021	0.370	0.370	0.364	0.389	0.017	0.008	3.40	4.3	2.89	10.40	428.8
Q95	0.981	0.040	0.451	0.441	0.430	0.470	0.064	0.011	5.04	17.7	3.00	10.90	3350.9

	TN	TAM	NNN	NO_3-N	DIN	DIN (cal.)	TP	DRP	TSS	Turbidity	Clarity	DO	*E. coli*
Waipapa at Waimate North Road													
Count	59	59	59	59	8	59	59	59	8	59	59	58	60
Mean	0.590	0.024	0.266	0.147	0.201	0.290	0.060	0.020	9.16	8.2	1.35	8.71	2056.0
Minimum	0.100	0.005	0.002	0.002	0.005	0.007	0.008	0.003	1.00	0.9	0.20	4.30	20.0
Maximum	7.200	0.290	7.000	0.900	0.450	7.015	0.380	0.079	37.00	130.0	2.90	11.20	77010.0
Q5	0.149	0.005	0.002	0.002	0.005	0.008	0.017	0.005	1.53	1.4	0.39	6.73	40.5
Q10	0.196	0.005	0.002	0.002	0.005	0.010	0.018	0.007	2.05	1.6	0.51	7.00	72.9
Q20	0.242	0.006	0.006	0.003	0.009	0.015	0.026	0.011	2.54	1.9	0.80	7.70	98.0
Q25	0.265	0.007	0.010	0.007	0.012	0.024	0.029	0.013	2.58	1.9	0.95	8.13	121.8
Q50 Median	0.390	0.008	0.110	0.110	0.215	0.128	0.039	0.017	4.75	2.7	1.30	8.95	242.0
Q75	0.540	0.016	0.250	0.240	0.330	0.286	0.060	0.026	10.03	5.1	1.65	9.58	420.3
Q80	0.584	0.018	0.270	0.264	0.358	0.310	0.066	0.028	10.48	7.2	1.81	9.76	507.2
Q95	1.130	0.101	0.406	0.372	0.429	0.502	0.158	0.039	27.90	18.4	2.62	10.20	3676.6
Waipoua at SH12													
Count	59	59	59	59	10	59	59	59	16	59	58	59	60
Mean	0.143	0.008	0.025	0.025	0.027	0.033	0.011	0.007	1.66	2.9	1.76	10.30	250.6
Minimum	0.100	0.005	0.002	0.002	0.008	0.007	0.004	0.002	1.00	1.4	0.45	7.70	10.0
Maximum	0.410	0.053	0.150	0.150	0.066	0.155	0.032	0.011	3.20	16.0	3.06	11.90	2400.0
Q5	0.100	0.005	0.003	0.003	0.009	0.010	0.006	0.003	1.00	1.5	0.67	8.89	10.0
Q10	0.100	0.005	0.005	0.005	0.009	0.012	0.007	0.004	1.00	1.6	1.03	9.38	20.0
Q20	0.100	0.005	0.008	0.007	0.011	0.014	0.007	0.005	1.00	1.7	1.35	9.70	30.6
Q25	0.100	0.005	0.009	0.008	0.013	0.015	0.008	0.005	1.00	1.7	1.42	9.80	39.5
Q50 Median	0.110	0.005	0.016	0.016	0.022	0.030	0.009	0.007	1.40	2.2	1.75	10.40	63.0
Q75	0.165	0.007	0.036	0.036	0.032	0.045	0.012	0.008	1.98	2.7	2.04	10.95	139.5
Q80	0.170	0.007	0.040	0.039	0.036	0.047	0.012	0.008	2.50	3.7	2.12	11.00	156.8
Q95	0.287	0.030	0.067	0.067	0.058	0.072	0.023	0.010	3.05	6.8	2.80	11.20	1632.7

	TN	TAM	NNN	NO_3-N	DIN	DIN (cal.)	TP	DRP	TSS	Turbidity	Clarity	DO	*E. coli*
Wairau at SH12													
Count	41	41	41	41	10	41	41	41	10	41	40	41	41
Mean	0.162	0.006	0.004	0.004	0.009	0.010	0.010	0.005	2.73	3.8	1.43	9.22	211.5
Minimum	0.100	0.005	0.002	0.002	0.005	0.007	0.004	0.002	1.00	0.1	0.40	7.30	10.0
Maximum	0.410	0.021	0.008	0.008	0.024	0.024	0.025	0.008	12.00	11.0	2.83	10.50	2400.0
Q5	0.100	0.005	0.002	0.002	0.005	0.007	0.004	0.002	1.05	1.6	0.66	7.60	10.0
Q10	0.100	0.005	0.002	0.002	0.005	0.008	0.005	0.003	1.09	2.1	0.75	8.00	10.0
Q20	0.100	0.005	0.003	0.002	0.005	0.008	0.005	0.004	1.10	2.2	0.86	8.20	20.0
Q25	0.100	0.005	0.003	0.003	0.005	0.009	0.006	0.004	1.15	2.3	1.02	8.40	28.0
Q50 Median	0.140	0.005	0.004	0.004	0.007	0.010	0.008	0.005	1.35	3.2	1.51	9.60	86.0
Q75	0.170	0.005	0.005	0.005	0.011	0.011	0.012	0.006	2.58	4.3	1.83	9.90	210.0
Q80	0.200	0.007	0.005	0.005	0.012	0.011	0.014	0.007	2.68	4.4	1.90	10.20	247.0
Q95	0.350	0.009	0.008	0.006	0.020	0.014	0.018	0.008	7.95	9.2	2.08	10.20	670.0
Wairua at Purua													
Count	85	85	85	49	8	85	85	85	8	85	85	41	85
Mean	0.818	0.045	0.373	0.397	0.456	0.417	0.088	0.028	5.89	18.4	0.85	8.38	2837.8
Minimum	0.160	0.003	0.001	0.002	0.011	0.005	0.016	0.007	1.40	2.1	0.07	3.80	20.0
Maximum	2.500	0.180	1.380	1.110	1.200	1.484	0.472	0.089	21.00	204.0	2.80	10.50	52000.0
Q5	0.213	0.005	0.001	0.004	0.013	0.007	0.037	0.010	1.61	3.4	0.10	5.00	35.4
Q10	0.230	0.005	0.004	0.005	0.016	0.010	0.041	0.012	1.82	3.6	0.22	6.60	45.0
Q20	0.285	0.007	0.014	0.035	0.059	0.031	0.048	0.015	2.40	5.2	0.40	7.40	56.0
Q25	0.330	0.008	0.077	0.110	0.095	0.082	0.048	0.016	2.75	5.8	0.51	7.60	74.0
Q50 Median	0.773	0.023	0.389	0.390	0.420	0.454	0.061	0.025	4.60	8.8	0.90	8.80	121.1
Q75	1.100	0.058	0.570	0.570	0.715	0.620	0.089	0.036	5.23	12.3	1.15	9.20	460.0
Q80	1.284	0.075	0.605	0.640	0.736	0.693	0.100	0.039	5.26	19.2	1.20	9.40	826.4
Q95	1.764	0.152	0.966	1.060	1.046	1.093	0.198	0.055	15.51	88.5	1.66	10.30	23326.0

	TN	TAM	NNN	NO_3-N	DIN	DIN (cal.)	TP	DRP	TSS	Turbidity	Clarity	DO	*E. coli*
Waitangi at SH10													
Count	59	59	59	59	8	59	59	59	8	59	59	58	60
Mean	0.400	0.014	0.210	0.210	0.250	0.225	0.027	0.009	5.91	5.7	1.35	8.76	1008.7
Minimum	0.100	0.005	0.002	0.002	0.005	0.007	0.005	0.002	0.80	0.7	0.20	5.40	51.0
Maximum	0.790	0.065	0.440	0.440	0.410	0.453	0.150	0.021	22.00	25.3	3.15	11.30	24196.0
Q5	0.100	0.005	0.003	0.003	0.035	0.010	0.009	0.005	0.80	1.1	0.29	6.86	74.9
Q10	0.148	0.005	0.006	0.006	0.065	0.019	0.010	0.006	0.80	1.2	0.40	7.24	129.1
Q20	0.242	0.006	0.055	0.053	0.131	0.064	0.014	0.007	0.88	1.9	0.60	7.78	159.6
Q25	0.260	0.008	0.074	0.073	0.165	0.082	0.015	0.007	0.95	2.3	0.70	8.10	185.5
Q50 Median	0.420	0.010	0.240	0.230	0.285	0.252	0.020	0.009	3.05	3.8	1.28	8.85	259.5
Q75	0.510	0.015	0.330	0.330	0.348	0.349	0.030	0.011	5.95	6.9	1.85	9.50	477.3
Q80	0.538	0.016	0.340	0.340	0.372	0.358	0.032	0.011	9.24	8.4	1.92	9.86	539.2
Q95	0.681	0.041	0.400	0.400	0.407	0.413	0.061	0.015	18.85	17.2	2.81	10.50	4898.4
Waitangi at Waimate North Road													
Count	111	111	111	111	11	111	111	111	15	111	110	110	111
Mean	0.498	0.013	0.298	0.297	0.248	0.311	0.027	0.007	6.06	11.6	1.55	9.48	1599.8
Minimum	0.100	0.005	0.026	0.024	0.051	0.032	0.005	0.002	0.80	1.0	0.19	4.60	23.0
Maximum	2.200	0.063	0.710	0.700	0.470	0.750	0.280	0.023	29.00	230.0	3.11	11.70	34480.0
Q5	0.195	0.005	0.081	0.081	0.052	0.090	0.008	0.004	0.94	1.3	0.36	7.69	73.0
Q10	0.250	0.005	0.100	0.100	0.052	0.113	0.010	0.005	1.00	1.5	0.50	8.10	110.0
Q20	0.300	0.007	0.170	0.160	0.140	0.181	0.011	0.005	1.00	1.8	0.80	8.80	161.0
Q25	0.325	0.008	0.185	0.185	0.165	0.196	0.012	0.006	1.00	2.0	0.97	9.00	177.5
Q50 Median	0.450	0.011	0.310	0.310	0.240	0.320	0.015	0.006	2.00	3.3	1.51	9.60	305.0
Q75	0.570	0.015	0.390	0.390	0.350	0.407	0.022	0.008	6.25	7.9	2.06	10.28	554.0
Q80	0.610	0.016	0.410	0.410	0.380	0.421	0.026	0.008	10.16	10.0	2.21	10.40	631.0
Q95	0.970	0.030	0.490	0.490	0.435	0.504	0.097	0.012	22.00	36.0	2.80	10.86	9635.0

Waitangi at Wakelins

	TN	TAM	NNN	NO_3-N	DIN	DIN (cal.)	TP	DRP	TSS	Turbidity	Clarity	DO	*E. coli*
Count	104	104	104	68	9	104	104	104	9	104	104	59	176
Mean	0.442	0.016	0.194	0.196	0.205	0.209	0.034	0.010	3.20	7.1	1.27	8.54	733.8
Minimum	0.110	0.002	0.001	0.002	0.012	0.003	0.010	0.001	1.00	0.5	0.09	3.10	10.0
Maximum	1.020	0.067	0.510	0.510	0.510	0.549	0.231	0.063	8.10	70.6	3.03	12.00	46110.0
Q5	0.166	0.004	0.002	0.002	0.014	0.005	0.012	0.002	1.08	1.1	0.22	4.89	51.8
Q10	0.197	0.005	0.002	0.002	0.015	0.007	0.014	0.003	1.16	1.2	0.39	5.80	74.5
Q20	0.236	0.005	0.003	0.005	0.019	0.014	0.018	0.004	1.38	2.0	0.60	6.78	96.0
Q25	0.269	0.006	0.010	0.011	0.021	0.021	0.019	0.005	1.50	2.6	0.65	7.00	107.8
Q50 Median	0.430	0.011	0.205	0.210	0.200	0.216	0.023	0.010	1.80	3.7	1.30	8.80	170.0
Q75	0.558	0.020	0.336	0.351	0.310	0.354	0.039	0.013	4.30	7.7	1.68	10.35	347.5
Q80	0.600	0.023	0.360	0.360	0.350	0.382	0.045	0.014	5.54	8.9	1.75	10.44	393.0
Q95	0.853	0.048	0.449	0.447	0.470	0.481	0.080	0.022	7.82	19.7	2.80	11.26	2419.2
Waitaua at Vinegar Hill Road													
Count	60	60	60	60	10	60	60	60	10	60	49	59	60
Mean	0.671	0.017	0.480	0.477	0.409	0.497	0.027	0.011	3.51	4.7	1.50	7.69	872.5
Minimum	0.300	0.005	0.130	0.130	0.170	0.148	0.009	0.004	1.20	0.9	0.12	2.50	146.0
Maximum	1.100	0.061	0.740	0.740	0.600	0.757	0.110	0.015	12.00	50.0	3.12	11.40	4000.0
Q5	0.340	0.005	0.210	0.210	0.242	0.223	0.014	0.007	1.20	1.4	0.54	4.09	225.5
Q10	0.419	0.007	0.248	0.248	0.314	0.264	0.014	0.007	1.20	1.5	0.64	5.30	278.1
Q20	0.508	0.009	0.318	0.310	0.330	0.331	0.018	0.008	1.36	1.9	0.81	5.60	364.2
Q25	0.520	0.009	0.328	0.320	0.330	0.337	0.018	0.009	1.45	2.1	0.90	5.90	413.3
Q50 Median	0.675	0.015	0.510	0.510	0.390	0.519	0.023	0.011	1.70	2.9	1.52	8.10	605.0
Q75	0.823	0.020	0.620	0.620	0.510	0.634	0.030	0.013	3.93	4.2	1.91	9.15	1059.5
Q80	0.852	0.022	0.632	0.630	0.514	0.658	0.036	0.013	4.88	4.5	2.06	9.48	1102.4
Q95	0.931	0.041	0.710	0.701	0.569	0.730	0.053	0.014	9.84	13.0	2.80	10.74	2082.7
Watercress at SH1													
Count	60	60	60	60	10	60	60	60	10	60	60	58	60

	TN	TAM	NNN	NO_3-N	DIN	DIN (cal.)	TP	DRP	TSS	Turbidity	Clarity	DO	*E. coli*
Mean	0.909	0.013	0.758	0.756	0.625	0.771	0.076	0.032	4.10	9.8	1.67	7.87	752.8
Minimum	0.460	0.005	0.400	0.390	0.500	0.470	0.028	0.015	1.00	0.4	0.20	4.70	22.0
Maximum	3.800	0.080	1.200	1.200	0.840	1.206	1.500	0.048	16.00	450.0	3.00	9.80	11199.0
Q5	0.500	0.005	0.489	0.489	0.505	0.494	0.033	0.020	1.09	0.6	0.79	5.77	86.0
Q10	0.547	0.005	0.499	0.490	0.509	0.511	0.039	0.024	1.18	0.7	1.09	6.54	107.2
Q20	0.588	0.006	0.570	0.570	0.518	0.577	0.043	0.027	1.36	0.9	1.18	6.94	193.4
Q25	0.645	0.008	0.580	0.570	0.533	0.592	0.044	0.028	1.40	1.1	1.30	7.10	220.0
Q50 Median	0.855	0.010	0.715	0.715	0.600	0.725	0.050	0.033	2.70	2.1	1.70	7.90	328.5
Q75	1.100	0.015	0.930	0.930	0.708	0.939	0.060	0.036	3.73	3.0	1.95	8.70	650.0
Q80	1.100	0.016	0.960	0.960	0.720	0.971	0.061	0.038	4.62	3.2	2.13	8.86	877.2
Q95	1.205	0.027	1.100	1.100	0.786	1.116	0.078	0.046	12.18	6.0	2.81	9.45	2018.9
Whakapara at Cableway													
Count	60	60	60	60	10	60	60	60	13	60	57	60	60
Mean	0.524	0.025	0.256	0.254	0.269	0.281	0.061	0.028	3.54	10.7	1.42	9.40	2524.7
Minimum	0.100	0.005	0.002	0.002	0.022	0.007	0.027	0.003	1.00	2.4	0.14	7.10	63.0
Maximum	1.500	0.150	0.820	0.810	0.710	0.904	0.260	0.073	10.00	110.0	2.80	11.50	54750.0
Q5	0.100	0.005	0.004	0.004	0.026	0.015	0.031	0.018	1.42	2.5	0.32	7.69	74.0
Q10	0.170	0.005	0.009	0.009	0.030	0.019	0.034	0.019	1.76	2.8	0.68	7.80	97.9
Q20	0.198	0.007	0.023	0.022	0.043	0.034	0.037	0.020	2.00	3.1	0.94	8.30	134.0
Q25	0.210	0.007	0.038	0.037	0.065	0.058	0.039	0.021	2.00	3.4	1.09	8.40	170.0
Q50 Median	0.440	0.011	0.240	0.240	0.215	0.292	0.052	0.027	2.60	4.9	1.48	9.55	275.5
Q75	0.680	0.027	0.423	0.420	0.415	0.444	0.063	0.034	5.20	6.3	1.69	10.40	394.3
Q80	0.802	0.042	0.442	0.440	0.462	0.507	0.067	0.035	5.32	7.3	1.78	10.40	552.6
Q95	1.305	0.084	0.595	0.595	0.638	0.646	0.116	0.041	7.24	34.3	2.35	11.01	17455.7

Appendix C: Water Quality Models and Response

Table C.1. Median water quality functions.

Search function	f(PPT, NRCD, GANC, ESC, TC, GRP, SRP, SWIR, NDWI, OLF, EWT, HYD, DD, ARTD, NBP, LUI, LUM, SLOPE, AREA_ha)	R^2	Complexity	Machine defined function
TN	TN = 8.014 + 0.9326*LUI + 1.069*NBP*NRCD + 0.2141*sgn(19.98*NDWI + 3.514*TC + 2.39*PPT - 8.238) - 0.3136*NBP - 0.3773*NRCD - 0.6597*LUM - 2.636*PPT	0.86	35	f(LUI, PPT, TC, NDWI, LUM, NBP, NRCD)
NO_3-N	NO3 = 66.23 + 149.3*NDWI + 1.833*SWIR + step(284.4 + 11.7*SWIR + 5.391*TC + 212.7*PPT*GANC - 3.796*LUM - 91.52*PPT - 681.2*GANC)*gauss(2.305e4*LUM + 6787*PPT + 6.395e4*LUM*SWIR + 1.883e4*PPT*SWIR + 2248*LUM*PPT2 + 6235*LUM*SWIR*PPT2 - 1.087e4 - 3.015e4*SWIR - 1.44e4*PPT*LUM - 1060*PPT2 - 3.994e4*PPT*LUM*SWIR - 2940*SWIR*PPT2) - 20.96*PPT - 46.63*PPT*NDWI	0.83	46	f(SWIR, TC, PPT,GANC, LUM, NDWI)
DIN	DIN = 18.02 + 4.218*logistic(7.497*GRP - 1.291) + 11.7*SWIR*logistic(7.497*GRP - 1.291) + 0.5205*sgn(15.39*TC + 11.7*SWIR - 37.36) + 408.3*NBP*logistic(2.596*NRCD - 0.7616)*gauss(4.813 + 13.35*SWIR) + 44.99*PPT*logistic(2.596*NRCD - 0.7616)*gauss(4.813 + 13.35*SWIR) - 2.596*NRCD - 5.744*PPT - 144.1*logistic(2.596*NRCD - 0.7616)*gauss(4.813 + 13.35*SWIR) - 127.5*PPT*NBP*logistic(2.596*NRCD - 0.7616)*gauss(4.813 + 13.35*SWIR)	0.84	51	f(SWIR, TC, NRCD, PPT, NBP, GRP)
NNN	NNN = 0.6373 + 2.494*NDWI + 7.671*gauss(10.18 + 19.98*NDWI) + 17.06*NDWI*gauss(10.18 + 19.98*NDWI) - logistic(7.497*GRP - 0.5862)*step(537.4*GRP + 1.207*EWT + 2540*GRP*NDWI + 2992*GRP*NDWI2 - 44.62 - 5.391*TC - 273.6*NDWI - 322.2*NDWI2)	0.83	55	f(NDWI, GRP, TC, EWT)
TKN	TKN = 0.1723 + 2.868*GRP + 1.27*NDWI + 0.65*ARTD + 0.1077*sin(6.175 + 210.6*ARTD + 468.5*ARTD*NDWI + 214.4*DD*NDWI + 122.4*SLOPE*DD - 23.3*DD - 67.34*SLOPE - 118*NDWI - 382.8*DD*ARTD - 851.5*DD*ARTD*NDWI) - 0.8703*DD - 5.212*DD*GRP	0.75	38	f(DD, ARTD, NDWI, SLOPE, GRP)
TAM	TAM = 29.99*DD + 7.359*ESC2 + 1.927*HYD + 1.125*ARTD + 0.8043*NDWI + 23.82*ESC22 + 2.282*HYD2 + -0.0001255/(ESC2 - 0.3884) + 85.43*ESC2*DD2 - 7.982 - 60.38*DD*ESC2 - 33.18*DD2 - 43.29*DD*ESC22	0.76	36	f(ESC2, ARTD, HYD, DD, NDWI)
TP	TP = 6.835 + 0.1754*TC + 26.8*PPT*cos(1.579 + 38.49*OLF*GRP - 6.629*OLF - 45.65*GRP) + 59.62*PPT*NDWI*cos(1.579 + 38.49*OLF*GRP - 6.629*OLF - 45.65*GRP) + logistic(241*DD + 48.71*TC + 6.33*ARTD + -0.002979/(7.862 + 38.49*OLF*GRP - 6.629*OLF - 45.65*GRP) - 136.2 - 88.52*DD*TC) - 2.821*PPT - 85.84*cos(1.579 + 38.49*OLF*GRP - 6.629*OLF - 45.65*GRP) - 190.9*NDWI*cos(1.579 + 38.49*OLF*GRP - 6.629*OLF - 45.65*GRP)	0.67	41	f(OLF, ARTD, PPT, TC, DD, GRP, NDWI)

DRP	DRP = 7.993 + 11.92*cos(3.109 + 1.64*TC - 7.497*GRP)2 + 12.25*SRP*TC*cos(3.109 + 1.64*TC - 7.497*GRP)2 + 1.926*ARTD*gauss(15.62*TC + 36.99*HYD*TC + tan(tan(5.031*NBP - 1.776)) - 42.52 - 100.7*HYD) - 3.084*PPT - 4.379*TC*cos(3.109 + 1.64*TC - 7.497*GRP)2 - 33.34*SRP*cos(3.109 + 1.64*TC - 7.497*GRP)2 - 0.485*gauss(15.62*TC + 36.99*HYD*TC + tan(tan(5.031*NBP - 1.776)) - 42.52 - 100.7*HYD)	0.69	108	f(NBP, PPT, ARTD, GRP, SRP, TC, HYD)
TSS	TSS = 31.41 + 1.414*NDWI + 1.092*LUM + 2.585*HYD*LUM + 13.69*AREA_ha2 + 0.1733*AREA_ha4 + 0.0008631*tan(16.42*DD - 9.035)/(NBP - 0.3529) - 1.219*HYD - 1.686*DD - 33.12*AREA_ha - 2.515*AREA_ha3	0.7	98	f(DD, AREA_ha, NDWI, NBP, LUM, HYD)
Turbidity	Turb = 25.71 + 1.405*NBP + 11*AREA_ha2 + 0.1392*AREA_ha4 + -0.001638/(NBP - 0.3529) + 4.11*OLF*sgn(13.43*GANC - 5.776) + 9.142*OLF*NDWI*sgn(13.43*GANC - 5.776) - 2.127*DD - 26.62*AREA_ha - 1.99*NBP2 - 2.021*AREA_ha3 - 4.874*sgn(13.43*GANC - 5.776) - 10.84*NDWI*sgn(13.43*GANC - 5.776)	0.79	38	f(NBP, DD, GANC, AREA_ha, OLF, NDWI)
Clarity	Clarity = 0.2353 + 2.785*DD*gauss(5.355*NBP - 1.682) + 21.05*DD*gauss(53.79*ESC2 + tan(6.12*DD + 5.629*LUI*sin(4.393 + 5.355*NBP) - 3.537 - 2.257*sin(4.393 + 5.355*NBP)) - 10.45 - 69.23*ESC22) - 1.533*gauss(5.355*NBP - 1.682) - 5.955*gauss(53.79*ESC2 + tan(6.12*DD + 5.629*LUI*sin(4.393 + 5.355*NBP) - 3.537 - 2.257*sin(4.393 + 5.355*NBP)) - 10.45 - 69.23*ESC22) - 19.13*DD2*gauss(53.79*ESC2 + tan(6.12*DD + 5.629*LUI*sin(4.393 + 5.355*NBP) - 3.537 - 2.257*sin(4.393 + 5.355*NBP)) - 10.45 - 69.23*ESC22)	0.65	98	f(DD, ESC2, NBP,LUI)
E.coli	Ecoli = 8.525 + 3.846*DD + 2.118*SWIR + 0.5654*TC + 9.107*DD*HYD + tan(0.02168*tan(16.42*DD - 9.035)) - 0.1919*AREA_ha - 1.904*LUI - 2.54*PPT - 5.011*HYD - 5.283*LUI*SWIR	0.61	33	f(DD,PPT, AREA_ha, TC, LUI, SWIR, HYD)
DO	DO = 177.2 + 2.124*GANC + 290.6*PPT*NBP + 3.392*PPT*OLF + 16.01*PPT2 - 0.07589*NRCD - 10.09*OLF - 106.6*PPT - 465.2*NBP - 0.2739*NBP*NRCD - 1.791*OLF*GANC - 45.36*NBP*PPT2	0.5	37	f(NRCD, NBP, PPT, GANC, OLF)

Table C.2. Q95, TAM_{MAX}, and $Clarity_{Q5}$ water quality functions.

Search function	f(PPT, NRCD, GANC, ESC, TC, GRP, SRP, SWIR, NDWI, OLF, EWT, HYD, DD, ARTD, NBP, LUI, LUM, SLOPE, AREA_ha)	R^2	Complexity	Machine defined function
TN_{Q95}	TN_Q95 = 1.904 + 4.002*NDWI + 1.767*ARTD + 0.2641*sin(4.992 + 7.497*GRP) + (0.05786*NBP - 0.02042)/(7.666*NRCD - 2.975) - 1.165*LUM - 3.687*LUI - 8.201*LUI*NDWI - 0.6798*ESC2*sin(4.992 + 7.497*GRP)	0.82	35	f(ARTD, LUM, NDWI, ESC2, NBP, NRCD, LUI, GRP)
NO_3-N_{Q95}	NO3_Q95 = 1.276*NBP + 1.159*ESC2 + 0.0001832/(OLF - 1.186) - 0.6092 - logistic(7.497*GRP - 49.53 - 101.8*NDWI) - sin(4.034 + 7.666*NRCD)*tan(69.48*NBP + 48.68*ARTD + 31.56*ESC2 + 22.28*DD + 710.2*ARTD*NBP*ESC2 + 501.4*DD*ARTD*NBP + 325.1*DD*NBP*ESC2 + 227.8*DD*ARTD*ESC2 + 390.8*ARTD*NBP2 + 253.4*ESC2*NBP2 + 178.9*DD*NBP2 + 1828*DD*ARTD*ESC2*NBP2 - 12.26 - 57.36*DD*ESC2 - 88.47*DD*ARTD - 125.3*ARTD*ESC2 - 126.3*DD*NBP - 178.9*NBP*ESC2 - 275.9*ARTD*NBP - 98.43*NBP2 - 1291*DD*ARTD*NBP*ESC2 - 460.5*DD*ESC2*NBP2 - 710.3*DD*ARTD*NBP2 - 1006*ARTD*ESC2*NBP2) - 3.285*NBP*ESC2	0.82	45	f(OLF, DD, NDWI, GRP, ESC2, NRCD, NBP, ARTD)
DIN_{Q95}	DIN_Cal_Q95 = 0.4804 + 4.977*SWIR + 3.311*ESC2 + 3.027*NRCD + 8.158*OLF*gauss(1.794 + 4.977*SWIR) + 18.15*OLF*NDWI*gauss(1.794 + 4.977*SWIR) + 0.1398*cos(4.171 + 5.391*TC)*cos(4.034 + 7.666*NRCD) - 11.28*NRCD*ESC2 - 9.676*gauss(1.794 + 4.977*SWIR) - 21.52*NDWI*gauss(1.794 + 4.977*SWIR) - 0.2448*sin(4.992 + 7.497*GRP)*cos(4.171 + 5.391*TC)*cos(4.034 + 7.666*NRCD)	0.71	58	f(SWIR, NRCD, GRP, TC, OLF, ESC2, NDWI)
TAM_{MAX}	TAM_MAX = 6.33*ARTD + 0.2064*TC + -0.02362/(6.33*ARTD - 1.441) + step(13.2 + 19.98*NDWI + 11.7*SWIR)*step(0.3033 + 7.497*GRP - 6.33*ARTD) - 3.135 - sin(5.084 + 6.33*ARTD)	0.78	37	f(ARTD, SWIR, NDWI, GRP, TC)
TP_{Q95}	TP_Q95 = 15.83*GRP + 8.304*ESC2 + 0.9315*AREA_ha + 11.23*AREA_ha*GRP*ESC2 + 5.629*LUI*sin(2.452 + 136.2*PPT2 - 872.7*PPT) + (0.5468 + 0.4396*PPT*ESC2 - 0.1708*PPT - 1.408*ESC2)/(GRP - 0.1722) - 4.157 - 0.3409*TC - 1.934*AREA_ha*ESC2 - 4.363*AREA_ha*GRP - 40.76*GRP*ESC2 - 2.257*sin(2.452 + 136.2*PPT2 - 872.7*PPT)	0.69	41	f(GRP, LUI, ESC2, AREA_ha, TC, PPT)
DRP_{Q95}	DRP_Q95 = 30.04 + 0.6451*NBP + 49.44*PPT*LUI + 197.4*LUI2 + gauss(16.42*ARTD + 9.615*GRP2 - 7.762 - 3.312*GRP) - 9.911*PPT - 158.9*LUI - 61.65*PPT*LUI2	0.62	33	f(ARTD, NBP,LUI, PPT, GRP)

TSS_{Q95}	TSS_Q95 = 54.48*OLF + 38.9*LUM + 33.85*NDWI + 23.49*PPT + 5.054*AREA_ha + 137.5*ARTD*GRP + 92.13*HYD*LUM + 11.97*AREA_ha*HYD + 22.89*NDWI2 + 305.9*ARTD*GRP*NDWI + exp(78.71*GRP + 11.43*OLF + 3.735*AREA_ha + 18.29*AREA_ha*OLF*GRP - 13.56 - 3.149*AREA_ha*OLF - 21.69*AREA_ha*GRP - 66.36*OLF*GRP) - 83.02 - 23.69*ARTD - 34.64*GRP - 43.44*HYD - 10.72*AREA_ha*LUM - 17.01*PPT*OLF - 52.69*ARTD*NDWI - 77.05*GRP*NDWI - 25.39*AREA_ha*HYD*LUM	0.65	45	f(GRP, PPT, AREA_ha, NDWI, OLF,LUM, ARTD,HYD)
$Turb_{Q95}$	Turb_Q95 = 0.2981 + 1.327*SRP + 0.9*ESC2 + 0.872*LUI + 0.6348*gauss(32.93*LUI + 28*LUM + 5.795*PPT + 83.86*OLF*NRCD + (0.26*ESC2 - 0.101)/(LUM - 0.4715) - 2.576 - 24.61*OLF - 99.46*NRCD - 69.84*LUI*LUM) - 2.245*ESC2*LUI	0.64	40	f(LUM, SRP, OLF, LUI, NRCD, ESC2, PPT)
$Clarity_{Q5}$	Clarity_Q5 = 0.552 + tanh(184.4*NBP + 10.16*PPT + -7.903e-5/(OLF - 1.186) + 81.56*PPT*NBP2 + (4.001*ESC2 + 2.145*LUI + 0.1397*OLF + 11.1*ESC2*SWIR + 10.75*LUI*SWIR + 3.635*OLF*SWIR + 0.4935*OLF2 + 8.413*OLF*ESC2*LUI + 23.34*OLF*ESC2*LUI*SWIR - 0.8598 - 4.311*SWIR - 0.3483*OLF*LUI - 3.373*OLF*ESC2 - 9.978*ESC2*LUI - 9.065*OLF*LUI*SWIR - 9.357*OLF*ESC2*SWIR - 27.68*ESC2*LUI*SWIR - 1.231*LUI*OLF2)/(NBP - 0.3529) - 32.49 - 57.57*PPT*NBP - 261.2*NBP2) - 0.2897*AREA_ha	0.72	45	f(OLF, AREA_ha, PPT, NBP, ESC2, SWIR, LUI)
$Ecoli_{Q95}$	Ecoli_Q95 = 134.1 + 1.697*ESC2 + 1.488*ARTD + 0.3351*AREA_ha + 871.8*NBP*GANC + 117.1*PPT*NBP + 96.08*PPT*GANC + (0.01469 - 0.03116*LUM)/(SRP - 0.3575) - 0.3819*OLF - 41.33*PPT - 307.7*GANC - 375.1*NBP - 272.2*PPT*NBP*GANC	0.82	32	f(ARTD, ESC2, AREA_ha, OLF, NBP, PPT, LUM, GANC, SRP)
DO_{Q5}	DO_Q5 = 0.981 - 0.04299*EWT - 0.144*NBP - 0.003622*exp(7.789*LUM) - 0.008058*NDWI*exp(7.789*LUM) - 1.5*gauss(24.31 - 52.83*DD)*gauss(48.38*NBP + 31.03*DD + 13.43*GANC - 22.85 - 87.92*DD*NBP)	0.45	37	f(DD, NBP, NDWI, EWT,GANC, LUM)

Table C.3. Table of sensitivity and magnitude of response for median nitrogen species.

	Variable	Sensitivity	% Positive	Positive Magnitude	% Negative	Negative Magnitude
TN	LUI	0.535	100%	0.53	0	0.00
	PPT	0.441	3%	2.83	0.97	0.36
	TC	0.406	100%	0.41	0	0.00
	NDWI	0.389	100%	0.39	0	0.00
	LUM	0.276	0%	0.00	1	0.28
	NBP	0.001	100%	0.00	0	0.00
	NRCD	0.001	0%	0.00	1	0.00
NO_3-N	SWIR	0.924	100%	0.92	0%	0.00
	TC	0.496	100%	0.50	0%	0.00
	PPT	0.386	48%	0.18	52%	0.58
	GANC	0.284	38%	0.12	62%	0.23
	LUM	0.191	30%	0.03	70%	0.26
	NDWI	0.003	100%	0.00	0%	0.00
NNN	NDWI	0.830	80%	0.91	20%	0.51
	GRP	0.396	3%	0.28	97%	0.40
	TC	0.323	100%	0.32	0%	0.00
	EWT	0.086	0%	0.00	100%	0.09
DIN	SWIR	0.843	100%	0.84	0%	0.00
	TC	0.656	100%	0.66	0%	0.00
	NRCD	0.557	0%	0.00	100%	0.56
	PPT	0.405	0%	0.00	100%	0.40
	NBP	0.115	100%	0.12	0%	0.00
	GRP	0.010	100%	0.01	0%	0.00
TAM	ESC2	2.169	98%	0.91	2%	81.31
	ARTD	0.897	100%	0.90	0%	0.00
	HYD	0.316	58%	0.27	42%	0.38
	DD	0.185	0%	0.00	100%	0.18
	NDWI	0.172	100%	0.17	0%	0.00
TKN	DD	0.573	0%	0.00	100%	0.57
	ARTD	0.563	100%	0.56	0%	0.00
	NDWI	0.346	100%	0.35	0%	0.00
	SLOPE	0.077	26%	0.09	74%	0.07
	GRP	0.002	0%	0.00	100%	0.00

Table C.4. Table of sensitivity and magnitude of response for high flow (Q95) nitrogen species and TAM maximum.

	Variable	Sensitivity	% Positive	Positive Magnitude	% Negative	Negative Magnitude
TN_{Q95}	ARTD	1.411	100%	1.41	0%	0.00
	LUM	0.692	0%	0.00	100%	0.69
	NDWI	0.145	100%	0.14	0%	0.00
	ESC2	0.041	100%	0.04	0%	0.00
	NBP	0.039	0%	0.00	100%	0.04
	NRCD	0.010	98%	0.01	2%	0.21
	LUI	0.010	0%	0.00	100%	0.01
	GRP	0.003	87%	0.00	13%	0.00
NO_3-N_{Q95}	OLF	3.924	2%	123.37	98%	2.06
	DD	1.275	97%	0.74	3%	18.05
	NDWI	0.800	100%	0.80	0%	0.00
	GRP	0.172	0%	0.00	100%	0.17
	ESC2	0.118	2%	3.81	98%	0.06
	NRCD	0.078	95%	0.08	5%	0.05
	NBP	0.044	48%	0.05	52%	0.04
	ARTD	0.018	98%	0.02	2%	0.00
DIN_{Q95}	SWIR	1.036	100%	1.04	0%	0.00
	NRCD	0.472	0%	0.00	100%	0.47
	GRP	0.197	13%	0.11	87%	0.21
	TC	0.119	38%	0.12	62%	0.12
	OLF	0.040	100%	0.04	0%	0.00
	ESC2	0.006	0%	0.00	100%	0.01
	NDWI	0.002	0%	0.00	100%	0.00
TAM_{MAX}	ARTD	1.86	85%	1.91	15%	1.55
	SWIR	0.35	100%	0.35	0%	0.00
	NDWI	0.33	100%	0.33	0%	0.00
	GRP	0.22	100%	0.22	0%	0.00
	TC	0.10	100%	0.10	0%	0.00

Table C.5. Table of sensitivity and magnitude of response for median and high flow (Q95) phosphorus species.

	Variable	Sensitivity	% Positive	Positive Magnitude	% Negative	Negative Magnitude
TP	OLF	0.785	48%	1.14	52%	0.46
	ARTD	0.610	100%	0.61	0%	0.00
	PPT	0.556	0%	0.00	100%	0.56
	TC	0.276	85%	0.30	15%	0.15
	DD	0.195	35%	0.18	65%	0.20
	GRP	0.169	70%	0.16	30%	0.20
	NDWI	0.004	100%	0.00	0%	0.00
DRP	NBP	1.098	41%	1.50	59%	0.75
	PPT	0.645	0%	0.00	100%	0.64
	ARTD	0.576	100%	0.58	0%	0.00
	GRP	0.145	43%	0.10	57%	0.18
	SRP	0.133	0%	0.00	100%	0.13
	TC	0.078	77%	0.08	23%	0.08
	HYD	0.052	25%	0.04	75%	0.06
TP_{Q95}	GRP	3.871	80%	1.75	20%	12.54
	LUI	0.998	100%	1.00	0%	0.00
	ESC2	0.854	100%	0.85	0%	0.00
	AREA_ha	0.471	100%	0.47	0%	0.00
	TC	0.287	0%	0.00	100%	0.29
	PPT	0.083	6%	0.00	94%	0.09
DRP_{Q95}	ARTD	1.883	96%	1.82	4%	0.57
	NBP	0.509	100%	0.51	0%	0.00
	LUI	0.405	0%	0.00	100%	0.40
	PPT	0.319	0%	0.00	100%	0.32
	GRP	0.152	41%	0.21	59%	0.11

Table C.6. Table of sensitivity and magnitude of response for median and high flow (Q95, Q5 for clarity) sediment indicators.

	Variable	Sensitivity	% Positive	Positive Magnitude	% Negative	Negative Magnitude
TSS	DD	0.749	6%	0.77	94%	0.75
	AREA_ha	0.477	48%	0.57	52%	0.39
	NDWI	0.414	100%	0.41	0%	0.00
	NBP	0.104	98%	0.09	2%	0.73
	LUM	0.013	100%	0.01	0%	0.00
	HYD	0.010	100%	0.01	0%	0.00
Turbidity	NBP	0.777	53%	0.89	47%	0.65
	DD	0.678	0%	0.00	100%	0.68
	GANC	0.350	0%	0.00	100%	0.35
	AREA_ha	0.285	48%	0.35	52%	0.23
	OLF	0.112	0%	0.00	100%	0.11
	NDWI	0.074	100%	0.07	0%	0.00
Clarity	DD	0.621	97%	0.64	3%	0.07
	ESC2	0.464	53%	0.53	47%	0.39
	NBP	0.255	48%	0.21	52%	0.30
	LUI	0.224	57%	0.22	43%	0.22
TSS_{Q95}	NDWI	0.542	100%	0.54	0%	0.00
	EWT	0.434	100%	0.43	0%	0.00
	PPT	0.423	69%	0.53	31%	0.20
	GRP	0.318	100%	0.32	0%	0.00
	ESC2	0.318	100%	0.32	0%	0.00
$Turbidity_{Q95}$	LUM	0.850	44%	0.50	56%	1.12
	SRP	0.458	100%	0.46	0%	0.00
	OLF	0.333	55%	0.35	45%	0.31
	LUI	0.333	42%	0.31	58%	0.35
	NRCD	0.203	27%	0.26	73%	0.18
	ESC2	0.189	51%	0.20	49%	0.18
	PPT	0.063	100%	0.06	0%	0.00
$Clarity_{Q5}$	OLF	4.226	75%	2.92	25%	8.16
	AREA_ha	0.948	0%	0.00	100%	0.95
	PPT	0.698	100%	0.70	0%	0.00
	NBP	0.130	22%	0.14	78%	0.13
	ESC2	0.101	100%	0.10	0%	0.00
	SWIR	0.062	0%	0.00	100%	0.06
	LUI	0.021	0%	0.00	100%	0.02

Table C.7. Table of sensitivity and magnitude of response for median and high flow (Q95) E. coli.

	Variable	Sensitivity	% Positive	Positive Magnitude	% Negative	Negative Magnitude
E. coli	DD	2.308	97%	1.53	3%	26.91
	PPT	0.493	0%	0.00	100%	0.49
	AREA_ha	0.459	0%	0.00	100%	0.46
	TC	0.451	100%	0.45	0%	0.00
	LUI	0.011	0%	0.00	100%	0.01
	SWIR	0.009	0%	0.00	100%	0.01
	HYD	0.003	100%	0.00	0%	0.00
E. coli$_{Q95}$	ARTD	0.718	100%	0.72	0%	0.00
	ESC	0.559	100%	0.56	0%	0.00
	AREA_ha	0.516	100%	0.52	0%	0.00
	OLF	0.198	0%	0.00	100%	0.20
	NBP	0.132	0%	0.00	100%	0.13
	PPT	0.128	0%	0.00	100%	0.13
	LUM	0.085	0%	0.00	100%	0.09
	GANC	0.049	0%	0.00	100%	0.05
	SRP	0.037	98%	0.03	2%	0.48

Table C.8. Table of sensitivity and magnitude of response for median and low flow (Q5) dissolved oxygen.

	Variable	Sensitivity	% Positive	Positive Magnitude	% Negative	Negative Magnitude
DO	NRCD	0.590	0%	0.00	100%	0.59
	NBP	0.417	0%	0.00	100%	0.42
	PPT	0.010	0%	0.00	100%	0.01
	GANC	0.009	100%	0.01	0%	0.00
	OLF	0.007	0%	0.00	100%	0.01
DO$_{Q5}$	DD	3.526	89%	2.52	11%	2.32
	NBP	0.960	9%	0.53	91%	1.00
	NDWI	0.402	0%	0.00	100%	0.40
	EWT	0.247	0%	0.00	100%	0.25
	GANC	0.242	42%	0.14	58%	0.31
	LUM	0.082	100%	0.08	0%	0.00